PSDF

Power Systems Development Facility

Technical Progress Report
Gasification Test Run TC06

July 4, 2001 -
September 24, 2001

DOE Cooperative Agreement Number
DE-FC21-90MC25140

SOUTHERN COMPANY

Energy to Serve Your World®

POWER SYSTEMS DEVELOPMENT FACILITY TECHNICAL PROGRESS REPORT

GASIFICATION TEST RUN TC06

JULY 4 – SEPTEMBER 24, 2001

DOE Cooperative Agreement Number
DE-FC21-90MC25140

Prepared by:
Southern Company Services, Inc.
Power Systems Development Facility
P.O. Box 1069
Wilsonville, AL 35186
Tel: 205-670-5840
Fax: 205-670-5843
http://psdf.southernco.com

August 2003

POWER SYSTEMS DEVELOPMENT FACILITY

DISCLAIMER

This report was prepared as an account of work sponsored by an agency of the United States Government. Neither the United States Government nor any agency thereof, nor any of their employees, nor Southern Company Services, Inc., nor any of its employees, nor any of its subcontractors, nor any of its sponsors or cofunders, makes any warranty, expressed or implied, or assumes any legal liability or responsibility for the accuracy, completeness, or usefulness of any information, apparatus, product, or process disclosed, or represents that its use would not infringe privately owned rights. Reference herein to any specific commercial product, process, or service by trade name, trademark, manufacturer or otherwise, does not necessarily constitute or imply its endorsement, recommendation, or favoring by the United States Government or any agency thereof. The views and opinions of authors expressed herein do not necessarily state or reflect those of the United States Government or any agency thereof.

Available to the public from the National Technical Information Service, U.S. Department of Commerce, 5285 Port Royal Road, Springfield, VA 22161. Phone orders accepted at (703) 487-4650.

ABSTRACT

This report discusses test campaign TC06 of the Kellogg Brown & Root, Inc. (KBR) Transport Reactor train with a Siemens Westinghouse Power Corporation (Siemens Westinghouse) particle filter system at the Power Systems Development Facility (PSDF) located in Wilsonville, Alabama. The Transport Reactor is an advanced circulating fluidized-bed reactor designed to operate as either a combustor or a gasifier using a particulate control device (PCD). The Transport Reactor was operated as a pressurized gasifier during TC06.

Test run TC06 was started on July 4, 2001, and completed on September 24, 2001, with an interruption in service between July 25, 2001, and August 19, 2001, due to a filter element failure in the PCD caused by abnormal operating conditions while tuning the main air compressor. The reactor temperature was varied between 1,725 and 1,825°F at pressures from 190 to 230 psig. In TC06, 1,214 hours of solid circulation and 1,025 hours of coal feed were attained with 797 hours of coal feed after the filter element failure. Both reactor and PCD operations were stable during the test run with a stable baseline pressure drop. Due to its length and stability, the TC06 test run provided valuable data necessary to analyze long-term reactor operations and to identify necessary modifications to improve equipment and process performance as well as progressing the goal of many thousands of hours of filter element exposure.

ACKNOWLEDGEMENT

The authors wish to acknowledge the contributions and support provided by various project managers: Jim Longanbach (DOE), Neville Holt (EPRI), Cheryl Chartier (KBR), Zal Sanjana (Siemens Westinghouse), and Vann Bush (SRI). Also, the enterprising solutions to problems and the untiring endeavors of many personnel at the site during commissioning of the Transport Reactor train in gasification mode of operation are greatly appreciated. The project was sponsored by the U.S. Department of Energy National Energy Technology Laboratory under contract DE-FC21-90MC25140.

CONTENTS

Section Page

Listing of Tables

Listing of Figures

1.0 EXECUTIVE SUMMARY

1.1 SUMMARY

This report discusses test campaign TC06 of the Kellogg Brown & Root, Inc. (KBR) Transport Reactor train with a Siemens Westinghouse Power Corporation (Siemens Westinghouse) particle filter system at the Power Systems Development Facility (PSDF) located in Wilsonville, Alabama. The Transport Reactor is an advanced circulating fluidized-bed reactor designed to operate as either a combustor or a gasifier using a particulate control device (PCD). The Transport Reactor was operated as a pressurized gasifier during TC06.

TC06 was planned as a 1,000-hour test run to perform long-term tests of the Transport Reactor using a blend of several Powder River Basin (PRB) coals and Bucyrus limestone from Ohio. The primary test objectives were as follows:

- Evaluate reactor loop and PCD operations for commercial performance by conducting long-term tests at near-constant coal-feed rate, air/coal ratio, riser velocity, solids-circulation rate, system pressure, and air distribution.

- Continue the evaluation of effects of the reactor modifications on PCD operations, especially regarding controlling PCD pressure drop through maintaining stable baseline and peak pressure drop.

- Test the effects of varying back-pulse parameters upon the particle filter system.

- Continue to test the use of metallic filter elements in the PCD.

Secondary objectives included the continuation of the following reactor characterizations:

- Reactor Operations – Study the devolatilization and tar cracking effects from transient conditions during the transition from start-up burner to coal. Evaluate the effect of process operations on heat release, heat transfer, and accelerated fuel particle heatup rates. Study the effect of changes in reactor conditions on transient temperature profiles, pressure balance, and product gas composition. Observe performance of new reactor temperature and coal-feed rate controllers.

- Effects of Reactor Conditions on Synthesis Gas Composition – Evaluate the effect of air distribution, steam/coal ratio, solids-circulation rate, and reactor temperature on CO/CO_2 ratio, synthesis gas Lower Heating Valve (LHV), carbon conversion, and cold and hot gas efficiencies.

- Recycle Gas Compressor Commissioning in Gasification Mode – Run the recycle gas compressor in bypass mode and evaluate the performance of the new moisture removal systems.

- Loop Seal Operations – Optimize loop seal operations and investigate increases to previously achieved maximum solids-circulation rate.

Test run TC06 was started on July 4, 2001, and completed on September 24, 2001, with an interruption in service between July 25, 2001, and August 19, 2001, due to a filter element failure in the PCD caused by abnormal operating conditions while tuning the main air compressor. The reactor temperature was varied between 1,725 and 1,825°F at pressures from 190 to 230 psig. In TC06, 1,214 hours of solid circulation and 1,025 hours of coal feed were attained with 797 hours of coal feed after the filter element failure. Both reactor and PCD operations were stable during the test run with a stable baseline pressure drop. Due to its length and stability, the TC06 test run provided valuable data necessary to analyze long-term reactor operations and to identify necessary modifications to improve equipment and process performance as well as progressing the goal of many thousands of hours of filter element exposure.

1.2 PSDF ACCOMPLISHMENTS

The PSDF has achieved over 4,985 hours of operation on coal feed and about 6,470 hours of solids circulation in combustion mode, and 2,505 hours of solid circulation and 1,902 hours of coal feed in gasification mode of operation. The major accomplishments in GCT1 through TC06 are summarized below. For combustion-related accomplishments see the technical progress report for the TC05 test campaign.

1.2.1 Transport Reactor Train

The major accomplishments and observations in GCT1 through TC06 include:

Commercial:

- With subbituminous coal, more than 95-percent carbon conversion and 110 Btu/scf nitrogen-corrected syngas heating value can be attained. The nitrogen-corrected syngas characteristics were sufficient to support existing pressurized syngas burners.

- Transport Reactor-generated syngas can be combusted without propane enrichment. The thermal oxidizer (atmospheric syngas burner) operated well using syngas with different heating values and was run for short periods of time without propane addition while maintaining an exit temperature near 2,000°F.

- The corrected cold gas efficiency (syngas latent heat to coal latent heat) and hot gas efficiency (syngas latent + sensible heat to coal latent heat) ranged from 65 to 75 percent and from 90 to 95 percent, respectively. These efficiencies can be obtained with subbituminous coals at coal-feed rates in terms of riser energy flux exceeding 100 MBtu/hr/ft^2.

Process:

- In GCT1, the reactor was operated using two bituminous coals and a PRB coal with different sorbents. Gasifier operations were stable, but carbon conversions were low due to disengager and cyclone inefficiencies.

- During GCT2, the longest continuous run of 184 hours at this point in gasification mode of operation was achieved with PRB coal. Reactor operations were smooth without any incident of oxygen breakthrough, temperature excursions, deposits, clinkers, or any other operational problem. The reactor loop was run consistently at about 50 percent of the design circulation rate. For the most part, the cyclone dipleg operated well with high solids flow due to the inefficiency of the disengager. However, there were brief cyclone dipleg upsets.

- In GCT3, stable gasification reactor operation was achieved at a range of coal-feed rates and solids-circulation rates, with reactor pressures ranging as high as 240 psig on PRB coal. The modification of the Y-type cyclone dipleg to a loop seal performed

well, needing little attention and promoted much higher solids-circulation rates and higher coal-feed rates that resulted in lower relative solids loading to the PCD and higher gasification ash (g-ash, formerly referred to as char) retention in the reactor. The level in the disengager standpipe reached its highest levels, attaining heights beyond expectations without difficulties. The coal-feed rate in this run was the highest to date, with much higher carbon conversions achieved. The high coal-feed rate produced the highest syngas heating value to date. Tar generation was also lower, and could be completely eliminated by varying reactor-operating parameters. It was also demonstrated that coal feed can safely be restarted after more than 30 minutes of down time without lighting the reactor start-up burner.

- In GCT4, stable gasification reactor operation was achieved at a range of coal-feed rates, solids-circulation rates, and reactor pressures ranging as high as 240 psig on PRB coal. The coal-feed rate was increased further exceeding 5,500 pph. The reactor experienced some of the highest circulation rates (more than double the design rate) and riser densities ever observed in the Transport Reactor. These characteristics improved the temperature distribution in both the mixing zone and the riser and likely resulted in higher coal particle heat-up rates. Lower coal-feed rates of about 2,500 pph were also tested because of grinding problems in the coal mill. Carbon conversions as high as 98 percent were achieved.

- TC06 consisted of very long, steady-state periods with few changes in operating parameters. The long steady periods provided data for reactor and PCD performance evaluation and general steady-state system parameter calculations.

- During TC06, a new coal grinding and feeding procedure was successfully implemented to prevent particle segregation and improve coal feeder performance. The new technique allowed the coal feeder to run continuously without any problems for over 278 hours, which was now the longest continuous run in gasification mode of operation.

- Using coke breeze as a start-up fuel to increase reactor temperatures to 1,600°F before starting coal feed drastically improved the performance of the gas analyzers and prevented tar from accumulating in the sample lines. Coke breeze was also used as an alternate fuel feed during coal feeder trips, decreasing outage time to address coal feeder problems.

- Steam injection during TC06 was much lower than in previous test runs, often less than 300 pph. Although the steam-feed rate was much lower, the overall syngas quality remained high. Lowering the moisture content in the syngas by reducing steam flow improved sulfur capture by the sorbent.

- The ammonia (NH_3) and hydrogen cyanide (HCN) concentrations in the syngas were measured for the first time. The NH_3 varied from 1,400 to 1,800 ppm and the HCN varied between 40 and 80 ppm depending on the reactor operating conditions. Fuel

nitrogen conversion to NH_3 and HCN varied between 55 to 65 percent and 1 to 3 percent, respectively.

- The gas analyzers were online for the majority of TC06, providing the best gas composition data from the Transport Reactor to date.

- Limestone calcination of 60 to 90 percent was achieved in the Transport Gasifier.

- The overall mass and energy balance was excellent with only ±5-percent error. The hydrogen and oxygen element balances illustrated marginal results with ±20-percent error. The hydrogen and oxygen balances were off due to a steam leak in the primary gas cooler. The calcium balance yielded marginal results with ±25 percent, and the silica balance error was very poor at ±100 percent.

- With PRB coal, the corrected fuel gas heating values ranged from 105 to 125 Btu/scf depending on the coal-feed rate. The air-to-coal ratio was between 3.2 and 3.6 lb/lb coal. In the test range, the solids-circulation rates, gas and solids residence times, and reactor temperatures do not show much effect on the fuel gas heating values. The devolatilization products evolution on unit coal feed basis was invariant to increases in PRB coal-feed rate. The observed increase in syngas heating value at high coal-feed rates is mainly due to the reduced effect of added nitrogen (dilution and relatively less energy consumption for heatup).

- Steam plays a major role in the performance of the Transport Gasifier. When the ratio of total steam (steam fed and coal moisture) to feed PRB carbon varied from 0.42 to 0.54, the gas H_2 to feed carbon ratio varied from 0.25 to 0.3. Based on gas analysis, test data show that for each mole of carbon converted about 0.35 moles of steam react. Calculations indicate that about 75 percent (50- to 90- percent range) of the H_2 in the gas originates from gasification reactions and 25 percent from devolatilization reactions. High steam-feed rates enhance H_2 production and reduce CO concentration in the gas phase.

- The mean particle size, in terms of mean mass diameter (mmd), of the PCD fines varied from 15 to 20 μm and the carbon content varied from 10 to 50 percent. The average higher heating value of PCD fines was about 4,200 Btu/lb at about 30-percent carbon content.

- The long test run enabled the displacement of initial start-up bed material with process-derived solids from coal minerals and sorbent. Reactor solids composition reached a steady-state condition in about 500 hours. No significant change in reactor performance was observed after reaching the steady-state.

- The particle-size distributions, in terms of mean mass diameter (mmd), were as follows: standpipe solids – 140 to 180 μm, sand – 122 μm, sorbent – 5 to 20 μm, coal – 200 to 350 μm. The standpipe solids were composed mainly of coal minerals.

Equipment:

- The recycle gas compressor was operated for about 20 hours using syngas with the discharge sent to the atmospheric syngas burner. The recycle gas moisture removal system needs additional modifications to improve its performance.

- The automatic reactor temperature control performed remarkably well, controlling air to maintain a steady reactor temperature at varied coal-feed rates.

- At the end of the test run the primary gas cooler experienced a tube failure, causing water to enter the refractory-lined pipe downstream between the cooler and the filter vessel.

- The HTF system modifications and new reactor shut-down procedure successfully prevented heat transfer fluid from leaking from the standpipe screw cooler into the reactor.

- The PCD and its solids removal system operated well without any major problems. The pressure drop was stable with a mild increase throughout the entire run. The peak pressure drop was well controlled with a 5- to 20-minute back-pulse timer. Due to the coke breeze feeding during on-coal transition, tar formation was significantly reduced, and therefore the PCD operation was much smoother, especially during the start-up phase. The inlet particulate loading averaged at about 15,000 ppmw. The outlet particulate loading was less than the detectable level of the sampling system (<0.1 ppmw) for the entire run. However, g-ash bridging was found after the shutdown.

- The gasifier g-ash removal system (FD0510) operated well without any line plugging during gasification.

- The gas coolers upstream and downstream of the PCD operated well without fouling.

- Since the high carbon conversion in the Transport Gasifier significantly reduced the amount of remaining g-ash the sulfator did not receive enough g-ash to maintain a high temperature. Thus, the sulfator required additional heating from its start-up burner and fuel oil injection system. Overall, the sulfator performed well.

1.2.2 Particulate Control Device

The highlights of PCD operation for TC06 include:

- During TC06, a 1,025-hour run, a relatively stable baseline pressure drop was maintained in the PCD. The baseline pressure drop ranged from about 80 to 120 in H_2O, a much smaller range than that seen in GCT3 or GCT4. An increase in the baseline pressure drop near the end of TC06 was largely attributable to g-ash bridging. Stable PCD inlet temperature and solids loading were maintained.

- Throughout the run SRI samples indicated that the measured PCD outlet solids loading was consistently below the minimum requirements for gas turbine operation, with the exception of one sample taken after a filter failure. There was no indication of leakage through PCD seals.

- SRI also successfully took samples at the PCD inlet, and these samples affirmed the relatively low solids loading resulting from the loop seal modifications completed after GCT2.

- The one filter element failure that occurred was caused by a thermal transient resulting from operating conditions that were well beyond normal, and the consequent leakage precipitated the first major system shutdown. The failure and leakage emphasized the need of a reliable failsafe. Several other less extreme thermal transients occurred during the run, and it was found that back-pulsing during a rapid temperature increase is very effective in stopping the temperature rise.

- As in GCT4, all metal filter elements, both new and previously exposed, were tested during the run and many of these filter elements have accumulated 1,450 hours of on-coal exposure. These filter elements will continue to be tested to assess material properties.

- After the first major shutdown in July there was no g-ash bridging found. However, operational data indicates that g-ash bridging may have been present but combusted during an extended thermal transient. After the final shutdown in September g-ash bridging was found. Addressing the issue of g-ash bridging will continue to be a major focus of PCD operations.

- Four iron aluminide filter elements and one Hastelloy X element were removed after TC06 for property testing, and the results will be presented in a subsequent run report. Property test results for elements removed after GCT3 and GCT4 are presented in this report.

1.3 FUTURE PLANS

During the outage following TC06, the Transport Reactor will be modified by adding a lower mixing zone (LMZ) to enable operations as an oxygen-blown gasifier. A 500-hour air blown test campaign (TC07) will begin in December 2001 to commission the LMZ and test a bituminous coal. A 250-hour test campaign (TC08) to commission the Transport Gasifier in oxygen-blown mode operation is scheduled for June 2002. A 250-hour test campaign (TC09) with bituminous coal in air-blown mode is scheduled for September 2002. Another oxygen-blown mode operation is scheduled for late 2002.

2.0 INTRODUCTION

This report provides an account of test campaign TC06 with the Kellogg Brown & Root, Inc. (KBR) Transport Reactor and the Siemens Westinghouse Power Corporation (Siemens Westinghouse) filter vessel at the Power Systems Development Facility (PSDF) located in Wilsonville, Alabama, 40 miles southeast of Birmingham. The PSDF is sponsored by the U. S. Department of Energy (DOE) and is an engineering-scale demonstration of advanced coal-fired power systems. In addition to DOE, Southern Company Services, Inc., (SCS), Electric Power Research Institute (EPRI), and Peabody Energy are cofunders. Other cofunding participants supplying services or equipment currently include KBR and Siemens Westinghouse. SCS is responsible for constructing, commissioning, and operating the PSDF.

2.1 THE POWER SYSTEMS DEVELOPMENT FACILITY

SCS entered into an agreement with DOE/National Energy Technology Laboratory (NETL) for the design, construction, and operation of a hot-gas, clean-up test facility for pressurized gasification and combustion. The purpose of the PSDF is to provide a flexible test facility that can be used to develop advanced power system components and assess the integration and control issues of these advanced power systems. The facility was designed as a resource for rigorous, long-term testing and performance assessment of hot stream clean-up devices and other components in an integrated environment.

The PSDF now consists of the following modules for systems and component testing:

- A Transport Reactor module.
- A hot-gas, clean-up module.
- A compressor/turbine module.

The Transport Reactor module includes KBR Transport Reactor technology for pressurized combustion and gasification to provide either an oxidizing or reducing gas for parametric testing of hot particulate control devices. The filter system tested to date at the PSDF is the particulate control device (PCD) supplied by Siemens Westinghouse.

2.2 TRANSPORT REACTOR SYSTEM DESCRIPTION

The Transport Reactor is an advanced circulating fluidized-bed reactor operating as either a combustor or as a gasifier, using a hot-gas, clean-up filter technology (particulate control devices or PCDs) at a component size readily scaleable to commercial systems. The Transport Reactor train operating in gasification modes is shown schematically in Figure 2.2-1. A taglist of all major equipment in the process train and associated balance-of-plant is provided in Tables 2.2-1 and -2.

The Transport Reactor consists of a mixing zone, a riser, a disengager, a cyclone, a standpipe, a loopseal, a solids cooler, and J-legs. The fuel, sorbent, and air are mixed together in the mixing zone along with the solids from the standpipe and solids cooler J-legs. The mixing zone, located below the riser, has a slightly larger diameter compared to the riser. Provision is made to inject air at several different points along the riser to control the formation of NO_X during combustion mode of operation. The gas and solids move up the riser together, make two turns and enter the disengager. The disengager removes larger particles by gravity separation. The gas and remaining solids then move to the cyclone, which removes most of the particles not collected by the disengager. The gas then exits the Transport Reactor and goes to the primary gas cooler and the PCD for final particulate clean-up. The solids collected by the disengager and cyclone are recycled back to the reactor mixing zone through the standpipe and a J-leg. In the combustion mode of operation, the solids cooler (not shown) controls the reactor temperature by generating steam and provides solids surge volume. A part of the solids stream from the standpipe flows through the solids cooler. The solids from the solids cooler then return to the bottom of the reactor mixing zone through another J-leg. The solids cooler is not used in gasification. The nominal Transport Reactor operating temperatures are 1,800 and 1,600°F for gasification and combustion modes, respectively. The reactor system is designed to have a maximum operation pressure of 294 psig with a thermal capacity of about 21 MBtu/hr for combustion mode and 41 MBtu/hr for gasification mode.

For start-up purposes, a burner (BR0201) is provided at the reactor mixing zone. Liquefied propane gas (LPG) is used as start-up fuel. The fuel and sorbent are separately fed into the Transport Reactor through lockhoppers. Coal is ground to a nominal average particle diameter between 250 and 400 μm. Sorbent is ground to a nominal average particle diameter of 10 to 30 μm. Limestone or dolomitic sorbents are fed into the reactor for sulfur capture. The gas leaves the Transport Reactor cyclone and goes to the primary gas cooler which cools the gas prior to entering the Siemens Westinghouse PCD barrier filter. The PCD uses ceramic or metal elements to filter out dust from the reactor. The filters remove almost all the dust from the gas stream to prevent erosion of a downstream gas turbine in a commercial plant. The operating temperature of the PCD is controlled both by the reactor temperature and by an upstream gas cooler. For test purposes, 0 to 100 percent of the gas from the Transport Reactor can flow through the gas cooler. The PCD gas temperature can range from 700 to 1,600°F. The filter elements are back-pulsed by high-pressure nitrogen or air in a desired time interval or at a given maximum pressure difference across the elements. There is a secondary gas cooler after the filter vessel to cool the gas before discharging to the stack or thermal oxidizer (atmospheric syngas combustor). In a commercial process the gas from the PCD would be sent to a gas turbine in a combined cycle package. The flue gas or fuel gas is sampled for on-line analysis after traveling through the secondary gas cooler.

After exiting the secondary gas cooler the gas is then let down to about 2 psig through a pressure control valve. In gasification the fuel gas is then sent to the thermal oxidizer to burn the gas and oxidize all reduced sulfur compounds (H_2S, COS, CS_2) and reduced nitrogen compounds (NH_3, HCN). The thermal oxidizer uses propane as a supplemental fuel. In combustion, the thermal oxidizer can be bypassed and fired on propane to make start-up steam. The gas from the thermal oxidizer goes to the baghouse and then to the stack.

The Transport Reactor produces both fine ash collected by the PCD and coarse ash extracted from the Transport Reactor standpipe. The two solid streams are cooled using screw coolers, reduced in pressure in lock hoppers, and then combined together. The combustion solids are suitable for commercial use or landfill as produced. In gasification, any fuel sulfur captured by sorbent should be present as calcium sulfide (CaS). The gasification solids are processed in the sulfator to oxidize the CaS to calcium sulfate ($CaSO_4$) and burn any residual carbon on the ash. The waste solids are then suitable for commercial use or disposal. Neither the sulfator nor the thermal oxidizer would be part of a commercial process. In a commercial process, the gasification solids could be burned in an atmospheric or pressurized fluidized bed combustor to recover the solids heat value.

Table 2.2-1

Major Equipment in the Transport Reactor Train

TAG NAME	DESCRIPTION
BR0201	Reactor Start-Up Burner
BR0401	Thermal Oxidizer
BR0602	Sulfator Start-Up/PCD Preheat Burner
CO0201	Main Air Compressor
CO0401	Recycle Gas Booster Compressor
CO0601	Sulfator Air Compressor
CY0201	Primary Cyclone in the Reactor Loop
CY0207	Disengager in the Reactor Loop
CY0601	Sulfator Cyclone
DR0402	Steam Drum
DY0201	Feeder System Air Dryer
FD0206	Spent Solids Screw Cooler
FD0210	Coal Feeder System
FD0220	Sorbent Feeder System
FD0502	Fines Screw Cooler
FD0510	Spent Solids Transporter System
FD0520	Fines Transporter System
FD0530	Spent Solids Feeder System
FD0602	Sulfator Solids Screw Cooler
FD0610	Sulfator Sorbent Feeder System
FL0301	PCD — Siemens Westinghouse
FL0302	PCD — Combustion Power
FL0401	Compressor Intake Filter
HX0202	Primary Gas Cooler
HX0203	Combustor Heat Exchanger
HX0204	Transport Air Cooler
HX0402	Secondary Gas Cooler
HX0405	Compressor Feed Cooler
HX0601	Sulfator Heat Recovery Exchanger
ME0540	Heat Transfer Fluid System
RX0201	Transport Reactor
SI0602	Spent Solids Silo
SU0601	Sulfator

Table 2.2-2 (Page 1 of 3)

Major Equipment in the Balance-of-Plant

TAG NAME	DESCRIPTION
BO2920	Auxiliary Boiler
BO2921	Auxiliary Boiler – Superheater
CL2100	Cooling Tower
CO2201A-D	Service Air Compressor A-D
CO2202	Air-Cooled Service Air Compressor
CO2203	High-Pressure Air Compressor
CO2601A-C	Reciprocating N_2 Compressor A-C
CR0104	Coal and Sorbent Crusher
CV0100	Crushed Feed Conveyor
CV0101	Crushed Material Conveyor
DP2301	Baghouse Bypass Damper
DP2303	Inlet Damper on Dilution Air Blower
DP2304	Outlet Damper on Dilution Air Blower
DY2201A-D	Service Air Dryer A-D
DY2202	Air-Cooled Service Air Compressor Air Dryer
DY2203	High-Pressure Air Compressor Air Dryer
FD0104	MWK Coal Transport System
FD0111	MWK Coal Mill Feeder
FD0113	Sorbent Mill Feeder
FD0140	Coke Breeze and Bed Material Transport System
FD0154	MWK Limestone Transport System
FD0810	Ash Unloading System
FD0820	Baghouse Ash Transport System
FL0700	Baghouse
FN0700	Dilution Air Blower
HO0100	Reclaim Hopper
HO0105	Crushed Material Surge Hopper
HO0252	Coal Surge Hopper
HO0253	Sorbent Surge Hopper
HT2101	MWK Equipment Cooling Water Head Tank
HT2103	SCS Equipment Cooling Water Head Tank
HT0399	60-Ton Bridge Crane
HX2002	MWK Steam Condenser
HX2003	MWK Feed Water Heater

Table 2.2-2 (Page 2 of 3)

Major Equipment in the Balance-of-Plant

TAG NAME	DESCRIPTION
HX2004	MWK Subcooler
HX2103A	SCS Cooling Water Heat Exchanger
HX2103C	MWK Cooling Water Heat Exchanger
LF0300	Propane Vaporizer
MC3001-3017	MCCs for Various Equipment
ME0700	MWK Stack
ME0701	Flare
ME0814	Dry Ash Unloader for MWK Train
ML0111	Coal Mill for MWK Train
ML0113	Sorbent Mill for Both Trains
PG2600	Nitrogen Plant
PU2000A-B	MWK Feed Water Pump A-B
PU2100A-B	Raw Water Pump A-B
PU2101A-B	Service Water Pump A-B
PU2102A-B	Cooling Tower Make-Up Pump A-B
PU2103A-D	Circulating Water Pump A-D
PU2107	SCS Cooling Water Make-Up Pump
PU2109A-B	SCS Cooling Water Pump A-B
PU2111A-B	MWK Cooling Water Pump A-B
PU2300	Propane Pump
PU2301	Diesel Rolling Stock Pump
PU2302	Diesel Generator Transfer Pump
PU2303	Diesel Tank Sump Pump
PU2400	Fire Protection Jockey Pump
PU2401	Diesel Fire Water Pump #1
PU2402	Diesel Fire Water Pump #2
PU2504A-B	Waste Water Sump Pump A-B
PU2507	Coal and Limestone Storage Sump Pump
PU2700A-B	Demineralizer Forwarding Pump A-B

Table 2.2-2 (Page 3 of 3)

Major Equipment in the Balance-of-Plant

TAG NAME	DESCRIPTION
PU2920A-B	Auxiliary Boiler Feed Water Pump A-B
SB3001	125-V DC Station Battery
SB3002	UPS
SC0700	Baghouse Screw Conveyor
SG3000-3005	4,160-V, 480-V Switchgear Buses
SI0101	MWK Crushed Coal Storage Silo
SI0103	Crushed Sorbent Storage Silo
SI0111	MWK Pulverized Coal Storage Silo
SI0113	MWK Limestone Silo
SI0114	FW Limestone Silo
SI0810	Ash Silo
ST2601	N_2 Storage Tube Bank
TK2000	MWK Condensate Storage Tank
TK2001	FW Condensate Tank
TK2100	Raw Water Storage Tank
TK2300A-D	Propane Storage Tank A-D
TK2301	Diesel Storage Tank
TK2401	Fire Water Tank
XF3000A	230/4.16-kV Main Power Transformer
XF3001B-5B	4,160/480-V Station Service Transformer No. 1-5
XF3001G	480/120-V Miscellaneous Transformer
XF3010G	120/208 Distribution Transformer
XF3012G	UPS Isolation Transformer
VS2203	High-Pressure Air Receiver

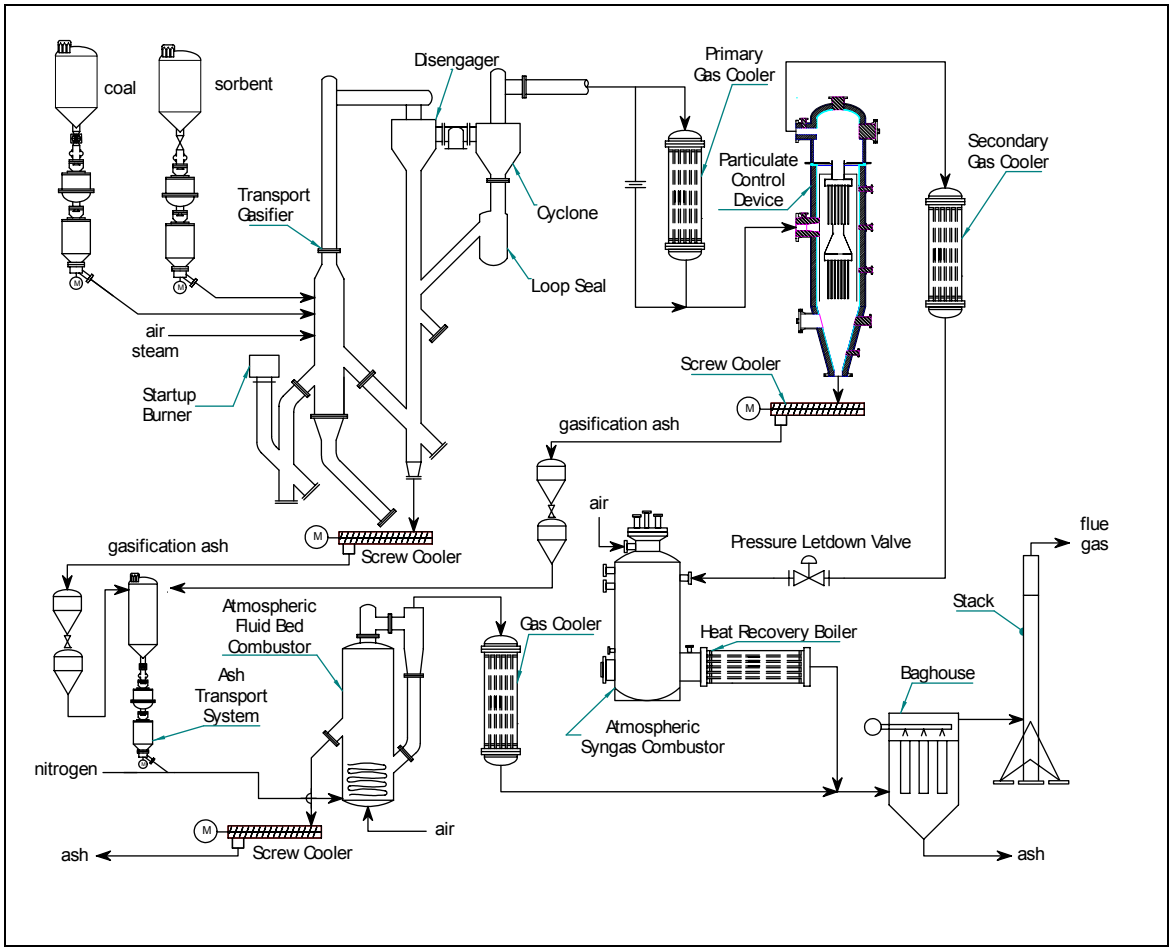

Figure 2.2-1 Flow Diagram of the Transport Reactor Train in Gasification Mode of Operation

2.3 SIEMENS WESTINGHOUSE PARTICULATE CONTROL DEVICE

Different PCDs will be evaluated on the Transport Reactor train. The first PCD that was commissioned in 1996 and has been used in all of the testing to date was the filter system designed by Siemens Westinghouse. The dirty gas enters the PCD below the tubesheet, flows through the filter elements, and the ash collects on the outside of the filter. The clean gas passes from the plenum/filter element assembly through the plenum pipe to the outlet pipe. As the ash collects on the outside surface of the filter elements, the pressure drop across the filter system gradually increases. The filter cake is periodically dislodged by injecting a high-pressure gas pulse to the clean side of the filter elements. The cake then falls to the discharge hopper.

Until the first gasification run in late 1999, the Transport Reactor had been operated only in the combustion mode. Initially, high-pressure air was used as the pulse gas for the PCD; however, the pulse gas was changed to nitrogen early in 1997. The pulse gas was routed individually to the two-plenum/filter element assemblies via injection tubes mounted on the top head of the PCD vessel. The pulse duration was typically 0.1 to 0.5 seconds.

A sketch of the Siemens Westinghouse PCD is shown in Figure 2.3-1.

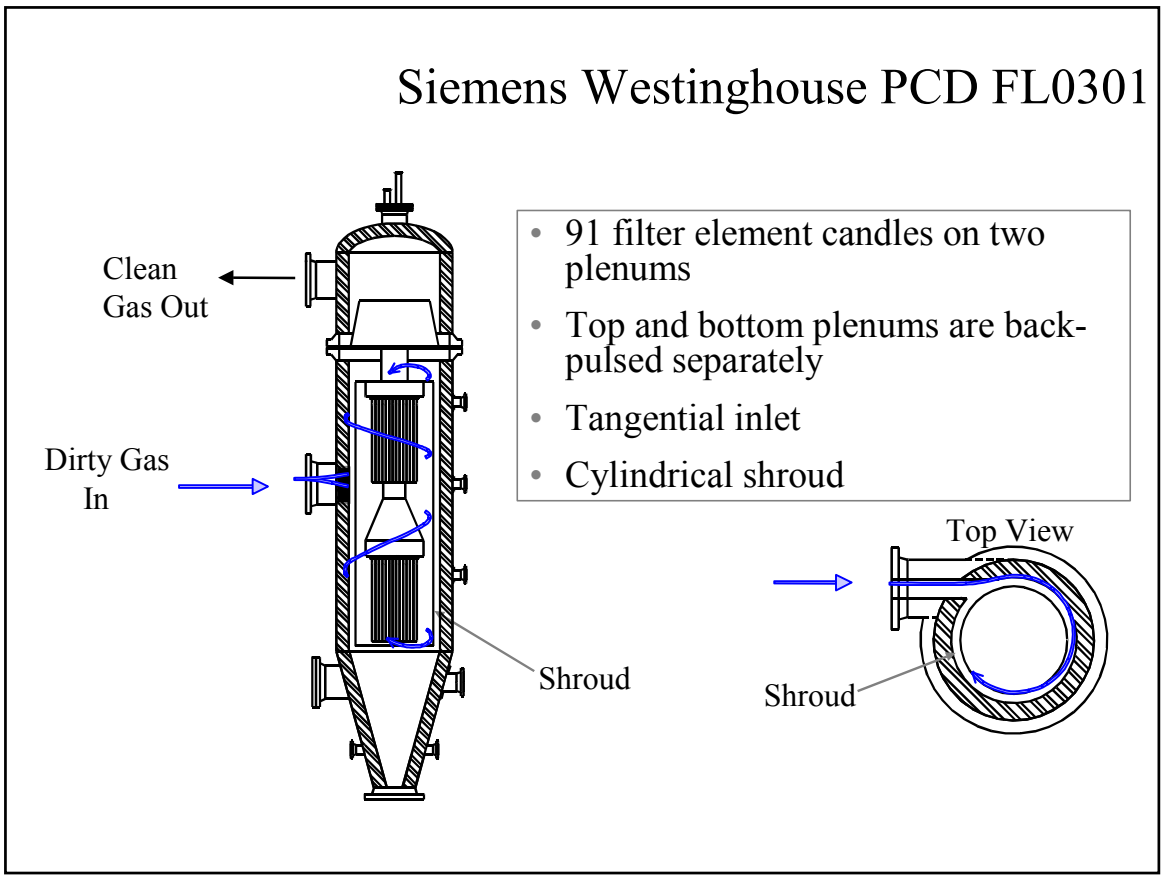

Figure 2.3-1 Siemens Westinghouse PCD

2.4 OPERATION STATUS

Commissioning activities began in September 1995 and proceeded in parallel with construction activities. Design and construction of the Transport Reactor and associated equipment was completed in early summer of 1996. All separate components and subsystems were fully operational by midsummer and commissioning work was focused on integration issues for the entire Transport Reactor train. The first coal fire in combustion mode of operation was achieved on August 18, 1996. A series of characterization tests was initiated to develop an understanding of reactor system operations. Test runs CCT1, CCT2, and CCT3 were completed by December 1996. Solids carryover from the reactor to the PCD was found to be excessive during these test runs. A number of startup and design problems associated with various equipment were successfully addressed.

During 1997, three additional sets of characterization test runs (CCT4, CCT5, and CCT6) and one major test campaign (TC01) were undertaken. TC01 focused on exposing the PCD filter elements to process gas for 1,000 hours at temperatures from 1,350 to 1,400°F and achieving stable reactor operations. An Alabama bituminous coal from the Calumet mine in the Mary Lee seam and Plum Run dolomite were used in these test runs.

Two test campaigns (TC02 and TC03) were successfully completed during 1998. TC02 was planned for reactor parametric testing to better quantify the effect of different variables on reactor and filter element operation. test run TC02 was started on April 5, 1998, and completed on May 11, 1998. Based on TC02 observations, TC03 was planned for additional reactor parametric testing to better quantify the effect of different variables on reactor and PCD operation and to evaluate operation with an Eastern Kentucky bituminous coal and a Gregg Mine limestone from Florida. The third major test campaign, TC03, was performed from May 31, 1998, to August 10, 1998. Stable operations were demonstrated using the Eastern Kentucky coal and Plum Run dolomite, Bucyrus limestone, and Longview limestone during TC03. There were, however, circulation problems using the Eastern Kentucky coal and Florida Gregg Mine limestone because of deposits resulting from excessive fines (segregated) in the Eastern Kentucky feed. One additional test run, TC04, was started on October 14, 1998, but was prematurely ended due to a temperature excursion in the PCD during the initial heat-up of the Transport Reactor system.

The final combustion test campaign was started on January 10, 1999, in combustion mode of operation and was completed May 2, 1999. During TC05 steady-state operations with a variety of fuel and sorbent feed materials was demonstrated (including petroleum coke with two different sorbents) and reactor parametric testing with different feed combinations was performed. Overall, TC05 was a successful test run with 10 different feed combinations tested.

Conversion of the Transport Reactor train to gasification mode of operation was performed from May to September 1999. The first gasification test run, GCT1, was planned as a 250-hour test run to commission the Transport Reactor train in gasification mode of operation and to characterize the limits of operational parameter variations. GCT1 was started on September 9, 1999, with the first part completed on September 15, 1999 (GCT1A). The second part of GCT1 was started on December 7, 1999, and completed on December 15, 1999 (GCT1B-D). This test run provided the data necessary for preliminary analysis of reactor

operations and for identification of necessary modifications to improve equipment and process performance. Five different feed combinations of coal and sorbent were tested to gain a better understanding of the reactor solids collection system efficiency.

GCT2, planned as a 250-hour characterization test run, was started on April 10, 2000, and completed on April 27, 2000. Additional data was taken to analyze effect of different operating conditions on reactor performance and operability. A blend of several PRB coals was used with Longview limestone from Alabama. In the outage following GCT2, the Transport Reactor underwent a major modification to improve the operation and performance of the reactor solids collection system. The most fundamental change was the addition of the loop seal underneath the primary cyclone.

GCT3 was planned as a 250-hour characterization test with the primary objective to commission the loop seal. A hot solids-circulation test (GCT3A) was started on December 1, 2000, and completed December 15, 2000. After a 1-month outage to address maintenance issues with the main air compressor, GCT3 was continued. The second part of GCT3 (GCT3B) was started on January 20, 2001, and completed on February 1, 2001. During GCT3B a blend of several PRB coals was used with Bucyrus limestone from Ohio. The loop seal performed well, needing little attention and promoting much higher solids-circulation rates and higher coal-feed rates that resulted in lower relative solids loading to the PCD and higher gasification ash (g-ash) retention in the reactor.

GCT4, planned as a 250-hour characterization test run, was started on March 7, 2001, and completed on March 30, 2001. A blend of several PRB coals with Bucyrus limestone from Ohio was used. More experience was gained with the loop seal operations and additional data was collected to better understand reactor performance. Also during GCT4, RTI began commissioning of the DSRP achieving conversions as high as 80 percent.

TC06, the subject of this report, was planned as a 1,000-hour test campaign. TC06 started on July 4, 2001, and was completed on September 24, 2001. A blend of several PRB coals with Bucyrus limestone from Ohio was used. Both reactor and PCD operations were stable during the test run, with a stable baseline pressure drop. Due to its length and stability, the TC06 test run provided valuable data necessary to analyze long-term reactor operations and to identify necessary modifications to improve equipment and process performance as well as progress toward the goal of many thousands of hours of filter element exposure. Figure 2.4-1 shows a summary of operating test hours achieved with the Transport Reactor at the PSDF.

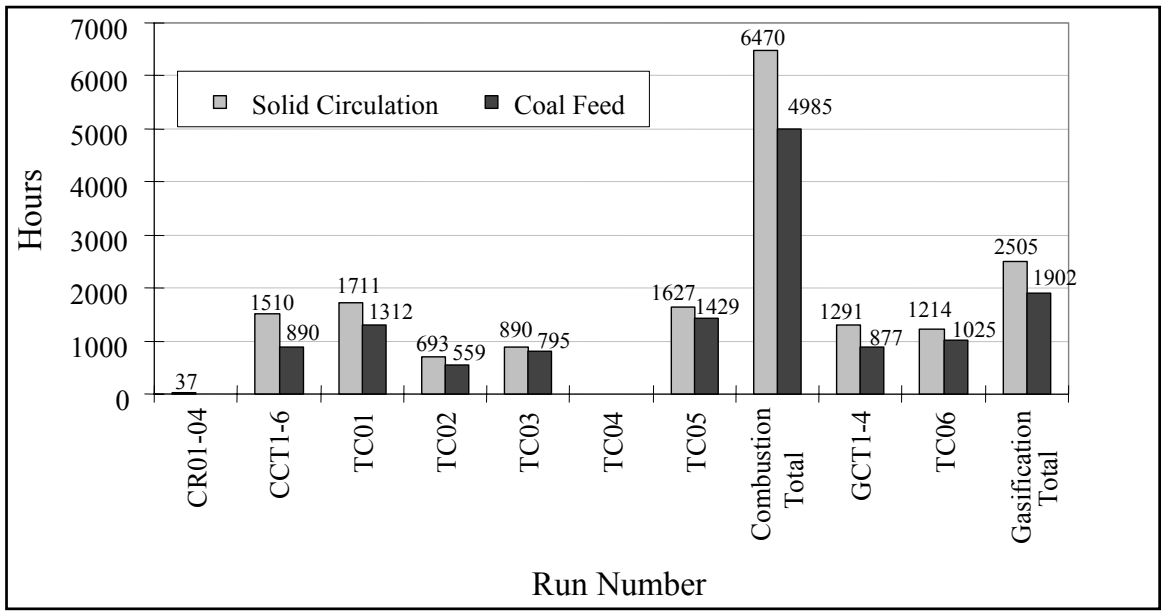

Figure 2.4-1 Operating Hours Summary for the Transport Reactor Train

3.0 PARTICLE FILTER SYSTEM

3.1 TC06 RUN OVERVIEW

TC06 was the first major gasification test campaign following four gasification characterization tests of the Halliburton KBR Transport Reactor train at the PSDF. It was the first gasification run since the reactor loop seal modifications were completed in which a stable baseline pressure drop was maintained in the particulate control device (PCD). Much of the success in attaining stable PCD operation was attributable to the reduction in tar formation during startups and periods of coal feed loss. The addition of a coke breeze feed line to the Transport Reactor allowed reactor heat-up to 1,600°F, the temperature below which excessive tar formation from coal is believed to occur, before coal feed. This change also allowed higher system pressure during the introduction of coal feed, since the start-up burner, which cannot operate at normal system pressure of 200 to 240 psig, was not required after the establishment of coke breeze feed. Because of the higher allowable system pressure at startups the PCD face velocity and subsequently the pressure drop generally did not reach unsustainable levels as it had in startups during previous runs.

TC06 consisted of two major periods of operation, including 228 on-coal hours in July 2001, and 797 on-coal hours during August and September 2001. Baseline pressure drops during both of these periods ranged from about 80 to 120 inH_2O. Only in GCT2, a 217-hour run which occurred before the reactor loop seal modifications, was the baseline pressure drop range smaller, only 50 to 80 inH_2O. The other two coal runs occurring after the reactor modifications, GCT3 and GCT4, consisted of only 183 and 242 on-coal hours, respectively. However, in GCT3 the baseline pressure drop ranged from 50 to 120 inH_2O; in GCT4, the range was 80 to 200 inH_2O. Near the end of TC06, an upward trend in baseline pressure drop occurred which corresponded to an increase in coal-feed rate. This increase may have been largely attributable to the growth of gasification ash (g-ash, formerly called char) bridging which was found during the September inspection.

The major operational concern during TC06 was the occurrence of thermal transients in the PCD caused by oxygen breakthrough. A major thermal transient occurred in July during a period when coal feed was stopped so that tuning of the main air compressor could be performed. During this time the oxygen level in the PCD exceeded 12 percent, and filter element surface thermocouples showed a rapid and sustained temperature increase. This resulted in a broken filter element, particulate leaking through the PCD, and eventually the first system shutdown after stable operation had been achieved.

This was the only time that particulate leaking was detected in TC06; all other PCD outlet samples indicated solids concentration below the sampling system limit of detection (0.1 to 0.4 ppmw). Other than the filter failure that occurred as a result of conditions that were beyond normal operating parameters, PCD operation was successful. The run provided the opportunity to expose filter elements to relatively long-term operation, advancing the goal of accumulating several thousand hours of individual filter element operation. TC06 also demonstrated the need for increased knowledge about the cause of g-ash bridging, as g-ash bridging had previously

been attributed mainly to tar deposition on the filter surfaces. In addition, the run emphasized the need for a reliable failsafe device.

This report contains the following information:

- Run Report, Section 3.2—This section describes the main events and operating parameters affecting PCD operation. Operation of the fines removal system is also included in this section.

- Inspection Report, Section 3.3—The two inspections performed during TC06 are discussed in this section, including details of the post-run conditions of various PCD components and of the fines removal system.

- G-ash Characteristics and PCD Performance, Section 3.4—This is a detailed discussion of g-ash physical and chemical properties, as well as the effects of these g-ash characteristics on PCD performance. The results of PCD inlet and outlet solids concentration sampling is presented in this section.

- Filter Material Testing, Section 3.5—This section presents results of ongoing testing of various types of filter element media in an effort to characterize material properties such as corrosion resistance and useful filter life in gasification operation.

3.2 TC06 RUN REPORT

3.2.1 Introduction

For the filter system, TC06 was a demonstration of relatively long-term stable operation. Baseline pressure drop did not show as marked an increase throughout the run as it had in the two previous gasification runs. Although the baseline pressure drop did increase slightly near the end of the run, this increase was likely due to gasification ash (g-ash) bridging and to an increase in the coal-feed rate. Also, the filter system was successful in controlling outlet solids loading below the sampling system limit of detection, except in the one instance of a filter element failure caused by conditions that were well outside normal operations.

The fines removal system operated reliably during the majority of the run, although there were some occasions when the fines removal system interfered with reactor train operation. The major problems associated with the fines removal system were the FD0520 outlet line plugging and a leaking spheri valve on FD0520. Also, although not hindering system operations, the FD0502 screw cooler required almost daily maintenance to control leaking seals. There was concern that eventually seal adjustments would become impossible. After TC06 the FD0502 seals were redesigned, providing improved purge gas distribution and more room for necessary adjustments during future operation.

Run statistics for TC06 are shown in Table 3.2-1 and the two filter element layouts implemented are shown in Figures 3.2-1 and 3.2-2. Filter element layout 20 was used during the first part of TC06 in July. This layout was modified to become layout 21 after the major thermal event in the PCD, which required the removal of and repositioning of several filter elements.

3.2.2 Test Objectives

The primary objectives of TC06 for the filter system were:

- Maintain stable baseline and peak pressure drop. In the previous two gasification runs since the reactor loop seal modifications, controlling PCD pressure drop had been a major operational challenge. The major factor in the increasing baseline pressure drop during these runs is thought to have been excessive tar formation which contributed to a thick residual g-ash cake and to g-ash bridging. TC06 was the first run in which a coke breeze feeder was used during the heat-up period prior to coal feed and during periods of unstable coal feeder operation. The addition of the coke breeze feeder significantly reduced tar formation and tar deposition in the PCD. Also, since the start-up burner was no longer needed during the transition to coal, system pressure at the introduction of coal could be much higher. Therefore, PCD face velocity was lower and the extremely high face velocities previously seen at startups were no longer inevitable.
- Test the effects of varying back-pulse parameters. The back-pulse frequency and back-pulse pressure were changed during steady-state operations so that the effect on baseline pressure drop could be compared.

- Continue to test metal filter elements. As in the GCT3 and GCT4 coal runs, all metallic filter elements were used in TC06 because of the potential for thermal transients on the filter element surfaces, which can damage ceramic filter elements. For TC06, new and previously exposed Pall Iron Aluminide (Fe_3Al) filter elements were installed as well as Pall Hastelloy-X and USF-Schumacher metallic filter elements. Exposing the metallic filter elements to the gasification environment for extended periods of time will help determine material properties such as corrosion resistance and structural integrity.

3.2.3 Observations/Events – July 6, 2001, Through September 25, 2001

Refer to Figures 3.2-3 through -26 for operating data trends corresponding to the following list of events.

A. At 07:50 on July 6, 2001, after a final pressure test, the system was pressurized to 60 psig.

B. At 15:20 on July 6, 2001, back-pulsing began with a pressure of 250 psid (250 psi above system pressure) and the frequency was set at 30 minutes. At 15:35, the main air compressor was started and at 15:50, the start-up burner was lit. The start-up burner tripped at 16:30.

C. At 14:40 on July 7, 2001, the start-up burner was again lit. Beginning at 18:30, multiple burner trips occurred, and the burner operation was unstable over the next 2 days.

D. At 08:45 on July 9, 2001, the main air compressor control response was tested and caused a momentary surge in flow to the PCD. At 09:20, back-pulsing was stopped and the system was depressurized so that repairs could be made to the start-up burner.

E. Back-pulsing began again at 17:12 on July 9, 2001, with pressure set at 250 psid and timer set at 30 minutes. The system was pressurized to 60 psig. At 17:50, the main air compressor was started. At 20:30, lighting of the start-up burner was attempted. The start-up burner tripped several times over the next day and at 00:08 on July 10, 2001, the system pressure was reduced to 40 psig to improve burner performance. At 03:38, system pressure was increased to 60 psig but was reduced again to 40 psig at 04:13 after the burner tripped. After difficulty relighting the burner, system pressure was reduced to 24 psig at 08:45, and the burner was lit successfully at this time.

F. At 08:53 on July 10, 2001, system pressure was increased to 60 psig. At 13:35, the main air compressor tripped, and was restarted at 14:45. The start-up burner was relit at 14:50. Also on July 10, 2001, at 15:20, system pressure was incrementally increased to 120 psig.

G. At 16:53 on July 10, 2001, coke breeze feed started and at 17:00 back-pulse pressure was increased to 400 psid and the back-pulse frequency was increased to 5 minutes.

H. At 01:10 on July 11, 2001, coal feed began and at 01:40, system pressure was increased to 110 psig. Propane flow to the start-up burner was reduced. At 01:45, the FD0502 screw cooler tripped because of high outlet temperature and was restarted at 01:48. At 01:55, system pressure was increased to 135 psig and coke breeze feeding stopped. During this period of coal feed PCD pressure drop was the highest of the run, exceeding 500 inH_2O at one point. For most of this period the pressure drop exceeded the back-pulsing trigger point of 275 inH_2O before the time required by logic for a back-pulse cycle (about 3 minutes, 14 seconds).

I. At 01:57 on July 11, 2001, FD0520 system plugged and the coal-feed rate was reduced. At 02:40, coal feed was stopped because FD0520 could not be cleared. At 05:20, FD0520 was cleared, cycled, and immediately plugged again. Back-pulse pressure was reduced to 250 psid and frequency was reduced at 06:20 to 30 minutes. At 08:30, coke breeze feed was discontinued until the fines removal system could be restored.

J. At 08:45 on July 11, 2001, system pressure was reduced to 110 psig because of operating problems with the start-up burner. At 18:40 back-pulse pressure was increased to 360 psid. System pressure was increased to 120 psig at 06:50 on July 12, 2001.

K. At 09:25 on July 12, 2001, back-pulse pressure was increased to 400 psid and the timer was reduced to 5 minutes. At 09:30, coal feed started and at 09:33, system pressure was increased to 212 psig. A surge in the main air compressor occurred at 10:25, which caused it to unload, so coal feed was stopped and coke breeze feed was attempted. Coke breeze feed could not be started because the system pressure was too high for the feeder operation. At 10:40, the system pressure was reduced to 190 psig and coke breeze was successfully fed.

L. At 12:30 on July 12, 2001, coal feed was attempted. The feeder motor would not operate and the feeder was taken off-line for repairs. Back-pulse pressure was decreased to 250 psid and at 12:36 the timer was increased to 30 minutes. After unsuccessfully attempting coke breeze feed, system pressure was reduced to 110 psig at 18:30 so the start-up burner could be lit. Because of problems with start-up burner operation, system pressure was reduced to 40 psig so that repairs could be made on the burner. Back-pulsing was stopped at 01:00 and the system was depressurized at 07:10 on July 13, 2001.

M. After repairs were made on the start-up burner, back-pulsing was resumed at 14:45 on July 13, 2001, with back-pulse pressure set to 250 psid and timer set to 30 minutes. The system was pressurized and reached 60 psig at 16:05. After several unsuccessful attempts to light the start-up burner, the system was depressurized at 19:26 and back-pulsing ended at 20:27 on July 13, 2001.

N. At 00:00 on July 14, 2001, the system was pressurized and reached 100 psig at 05:50. Back-pulsing was resumed with the pressure set to 250 psid and timer set to 30 minutes. The start-up burner was lit at 01:25. Coke breeze feed began at 10:15 and was fed intermittently over the next few hours. System pressure was slowly increased to 130 psig.

O. At 15:58 on July 14, 2001, back-pulse pressure was increased to 400 psid and the timer was decreased to 5 minutes. Coal feed began at 16:00 and system pressure was slowly increased over the next few hours and held at 210 psig.

P. At 16:40 on July 14, 2001, the main air compressor unloaded and tripped the coal feeder. The thermal oxidizer also tripped at this time. Coal feed was resumed at 17:18.

Q. Multiple coal feeder trips occurred from 18:43 through 19:15 on July 14, 2001. A coal feeder trip occurred at 19:59 and coke breeze feed began until coal feed could be stabilized. The coal feeder was taken off-line so that the feed line could be cleared of obstructions which were blocking coal flow. Back-pulse pressure was reduced to 250 psid and back-pulse frequency was reduced to 30 minutes at 20:12 on July 14, 2001.

R. After the coal-feed line was cleared, coal feed began at 00:44 on July 15. Back-pulse pressure was increased to 400 psid and the frequency increased to 5 minutes. Coal feed was unsteady until about 01:00 when adjustments were made on the coal feeder fluidization nozzles and gate valve.

S. At 23:06 on July 18, 2001, after about an hour of coal feeding difficulty, the coal feeder tripped. At 23:08, a thermal excursion occurred in the PCD. As filter element surface temperatures began rapidly increasing, back-pulsing was manually initiated, and as each plenum received a back-pulse, filter element surface temperatures immediately dropped. The top plenum filter element surface temperatures rose about 70°F in 1 minute, and the bottom plenum, which was back-pulsed 1 minute after the top plenum, showed a rise in filter element surface temperature of about 170°F in 2 minutes.

Coke breeze feed was started at 23:11 on July 18, 2001. After a few more minutes of coal feeding difficulty, coal feed was restored and coke breeze feed was discontinued.

T. At 13:05 on July 19, 2001, coke breeze feed was started after another period of coal feeding difficulty. The coal feeder tripped at 13:15 but was quickly restored. At 18:18, the back-pulse timer was increased from 5 to 10 minutes, but was reduced back to 5 minutes at 19:04 because back-pulsing was being triggered by high peak pressure drop.

U. At 14:34 on July 20, 2001, back-pulse pressure was reduced to 200 psid to observe the effect of back-pulse pressure on baseline pressure drop for a few hours. Back-pulse pressure was increased back to 400 psid at 20:53.

V. At 07:13 on July 21, 2001, the back-pulse timer was increased to 7.5 minutes.

W. At 14:34 on July 21, 2001, back-pulse pressure was increased to 400 psid to observe the effect of back-pulse pressure on baseline pressure drop.

X. At 18:00 on July 21, 2001, system pressure was gradually reduced from 210 to 180 psig because of coal feeding difficulty. At 18:38, back-pulse pressure was decreased to 400 psid to end the testing of back-pulse effect, and at 18:59 the back-pulse timer was reduced to 5 minutes. Coal feed stabilized and system pressure of 210 psig was resumed at 20:10.

Y. At 00:00 on July 22, 2001, after coal feeding difficulty began again, system pressure was gradually reduced to 175 psig, and at 00:10 coke breeze feed was started. As coal feed became steadier, coke breeze feed was stopped at 02:12 and system pressure was increased to 210 psig. Coal feeding became unsteady again, and after a coal feed trip at 03:40, system pressure was reduced to 194 psig and coke breeze feed resumed.

Z. At 06:41 on July 22, 2001, coal feed was started and coke breeze feed was discontinued at 07:03. At 08:06, system pressure was slowly increased to 210 psig.

AA. At 21:15 on July 23, 2001, coal feeder problems reoccurred. At 21:26, system pressure was reduced to 197 psig and coke breeze feed started. Coal feeding improved and system pressure was increased to 210 psig on July 24, 2001, at 00:27. Coke breeze feed stopped at 00:49.

BB. At 11:50 on July 24, 2001, coal feed was discontinued so that the main air compressor could be tuned. System pressure was reduced to 190 psig and coke breeze was attempted. Coke breeze would not convey, so system temperature dropped. At 14:25, back-pulse pressure was reduced to 250 psid (differential, that is, 250 psi above reactor pressure), and the timer was increased to 30 minutes.

At 16:12 on July 24, 2001, as the air compressor was being tuned, oxygen levels in the PCD increased to about 12 percent, and two filter element surface thermocouples indicated combustion on the bottom plenum. One thermocouple reading increased from about 480 to 800°F in less than 5 minutes. Back-pulsing frequency was increased to 5 minutes at this time. The temperatures did not return to their previous values for about 20 minutes. At 16:25, the on-line particulate monitor on the PCD outlet duct detected particle leakage.

The back-pulse timer was increased to 30 minutes at 20:00 on July 24, 2001, and at 20:20 system pressure was reduced to 60 psig.

CC. At 06:36 on July 25, 2001, the start-up burner was lit and circulation was reestablished. A Southern Research Institute (SRI) sample taken at 09:55 showed a PCD outlet solids concentration of 23 ppmw, indicating a possible filter element

failure. The system was therefore shut down. The start-up burner was shut off at 13:23 and the system was depressurized at 15:05. During this outage the PCD was inspected, a crack was found in one filter, and several filter elements were removed.

DD. After a final pressure test the system was pressurized to 60 psig on August 18, 2001, at 21:20. At 13:50 on August 19, 2001, the start-up burner was lit, and at 15:50 the back-pulsing sequence was started with back-pulse pressure set to 250 psid and timer set at 30 minutes. At 21:47 on August 19, 2001, system pressure was slowly increased to 100 psig. The start-up burner tripped a few times beginning at 03:30 on August 20, but operation continued. Coke breeze feed started at 08:40. At 08:55, back-pulse pressure was increased to 400 psid.

EE. Coal feed was started at 15:55 on August 20, 2001. The back-pulse timer was decreased to 5 minutes. Coke breeze feed was discontinued at 16:10 on August 20.

FF. At 01:22 on August 21, 2001, the back-pulse timer was increased from 5 to 10 minutes.

GG. At 21:43 on August 21, 2001, the back-pulse timer was decreased to 7.5 minutes because back-pulsing was being triggered by high peak pressure drop.

HH. At 22:30 on August 21, 2001, the coal feeder operation became unsteady. Coke breeze feed was started at 22:50 and the coal feeder tripped at 22:56. Coke breeze would not feed, apparently because of a plugged feed line. At 23:35 on August 21, system pressure was reduced gradually to 70 psig so that the start-up burner could be lit. The start-up burner was successfully lit at 01:30 on August 22.

II. At 02:26 on August 22, 2001, the back-pulse timer was increased to 10 minutes. At 04:48, FD0520 tripped, apparently due to a plugged line resulting from a large amount of solids carryover from the reactor. Operations personnel cleared the line and FD0520 operation resumed at 05:34 on August 22. Coke breeze was successfully fed beginning at 10:35 on August 22.

JJ. At 16:37 on August 22, 2001, coal feed was resumed and system pressure was incrementally increased to 190 psig.

KK. At 02:38 on August 23, 2001, the back-pulse timer was decreased to 7.5 minutes.

LL. At 09:12 on August 23, 2001, the coal feeder tripped, coke breeze feed was started, and FD0520 also tripped due to a momentary drop in control nitrogen pressure. FD0520 operation resumed at 09:38 and coal feed was resumed at 10:02.

MM. At 23:21 on August 23, 2001, the coal feeder tripped and coke breeze feed was started. Adequate air flow could not be maintained due to a logic problem, so system pressure was reduced to 60 psig at 23:37. The start-up burner was lit at 01:12 on August 24, 2001. System pressure was then increased to 80 psig. The back-pulse timer was increased to 10 minutes at 04:25 on August 24.

At 08:10 on August 24, 2001, coke breeze feed began and at 10:55 system pressure was increased to 115 psig.

NN. At 11:30 on August 24, 2001, the back-pulse timer was reduced to 5 minutes, coal feed resumed at 12:32, and system pressure was gradually increased to 200 psig.

OO. At 17:10 on August 24, the back-pulse timer was increased to 10 minutes. At 22:50, system pressure was reduced to 190 psig because the coal feeder operation was unsteady. System pressure was increased to 195 psig at 23:15 on August 25.

PP. At 11:50 on August 27, 2001, the fines removal system (including FD0502, FD0520, and FD0530) was taken off-line so that a g-ash leak on the FD0530 spheri valve could be repaired. The coal- and sorbent-feed rates were reduced to minimize solids carryover to the PCD. As the PCD cone thermocouples indicated that the cone was filling up; coke breeze was started at 13:32 and coal feed was discontinued at 13:47. Operation of the fines removal system resumed at 14:40 after the leak was repaired.

QQ. At 17:15 on August 27, 2001, the back-pulse timer was increased to 15 minutes.

RR. After the PCD cone was cleared of all solids, coal feed was resumed at 17:45. The back-pulse timer was decreased to 5 minutes. At 00:55 on August 28, 2001, system pressure was increased to 200 psig.

SS. Coal feeding became unsteady, so coke breeze feed was started and system pressure was reduced to 190 psig at 21:05 on September 2, 2001. The coal feeder tripped at 21:17. Coal feed quickly resumed at 21:22 and coke breeze feed was discontinued at 21:30. System pressure was increased to 200 psig at 21:42 on September 2, 2001.

TT. The coal feeder tripped at 12:43 on September 3, 2001, due to low control nitrogen pressure. Coke breeze feed started at 12:45, and system pressure was lowered to 190 psig. Coal feed was resumed at 13:21 and coke breeze feed was stopped at 14:43. At 15:07 on September 3, 2001, system pressure was increased to 200 psig.

UU. At 01:10 on September 4, 2001, the coal feeder tripped and coke breeze feed was started at 01:12. Coal feed was resumed at 01:14 and coke breeze feed was discontinued at 01:17.

VV. At 06:40 on September 5, 2001, the bottom plenum back-pulse pressure was increased to 600 psid while the top plenum back-pulse pressure was kept at 400 psid. Earlier, on September 4, at 17:00, one of the seven filter element surface thermocouples on the bottom plenum began reading a higher temperature than the other six thermocouples. Based on operational experience, such a deviation in temperature is caused by g-ash bridging. The bottom plenum back-pulse pressure was increased in an effort to dislodge the bridging. There was no effect on the thermocouple readings and the back-pulse pressure was set back to 400 psid at 12:50 on September 5, 2001.

WW. At 11:30 on September 6, 2001, the back-pulse valve open time was increased from 0.2 to 0.5 seconds in an effort to dislodge the apparent g-ash bridging. The valve-open time was then increased to 0.8 seconds and then to 1.2 seconds before eventually changing the timer back to 0.2 seconds on September 8, 2001.

XX. At 12:58 on September 6, 2001, the back-pulse timer was decreased to 5 minutes.

YY. At 14:25 on September 6, 2001, the bottom plenum back-pulse pressure was again increased to 600 psid. Despite this change and the longer back-pulse valve-open time, the deviating thermocouple remained at a higher reading than the other thermocouples, although it did show an increased response to back-pulsing while the valve-open time was increased. The bottom plenum back-pulse pressure was decreased to 400 psid at 21:55 on September 7, 2001.

ZZ. At 08:00 on September 7, 2001, the coal feeder tripped due to a high-oxygen-level alarm, which had been set off during gas analyzer calibrations. Coke breeze feed was started at 08:03, coal feed was reestablished at 08:07, and coke breeze feed was discontinued at 08:14.

AAA. At 18:13 on September 7, 2001, the back-pulse timer was increased from 5 to 10 minutes.

BBB. At 22:59 on September 7, 2001, coke breeze feed was started after coal feeding became unsteady. The coal feeder tripped at 23:38, and coal feed was resumed at 01:43 on September 8.

CCC. At 03:03 on September 10, 2001, coke breeze feed was started after coal feeding became unsteady. The coal feeder tripped at 03:05 and resumed operation at 03:17. Coke breeze feed was discontinued at 04:31 on September 10.

DDD. The next coal feeder trip occurred on September 10, at 23:00, and coal feed was quickly reestablished at 23:19.

EEE. There were several times over the next few days when the coal feed tripped but was quickly back on-line. This occurred on September 11, 2001, at 10:18; on September 11, at 19:01; on September 12, at 01:02; and on September 12, at 23:21. The coal feeding problems were attributed to coal particle-size segregation in the coal silos. Changing the coal grinding schedule from grinding coal 12 hours per day to continuous coal grinding seemed to negate the size segregation and solve the coal feeding problem.

FFF. At 18:57 on September 16, 2001, system pressure was increased to 220 psig.

GGG. At 13:48 on September 17, 2001, air- and coal-feed rates were increased.

HHH. At 12:48 on September 18, 2001, air- and coal-feed rates were again increased. At 13:46, the back-pulse timer was reduced from 20 to 10 minutes.

III. At 18:47 on September 19, 2001, system pressure was increased to 230 psig.

JJJ. At 00:10 on September 21, 2001, air- and coal-feed rates were increased.

KKK. At 00:05 on September 22, 2001, the back-pulse timer was decreased to 7.5 from 10 minutes.

LLL. At 13:38 on September 22, 2001, the coal feeder tripped and coke breeze feed was started. Coal feed resumed at 13:47, and coke breeze feed was stopped at that time.

MMM. At 11:26 on September 24, 2001, system pressure was increased to 240 psig.

NNN. At 14:27 on September 24, 2001, the back-pulse sequence was disabled for a dirty shutdown. Coal feed was stopped at 14:33 on September 24, 2001.

3.2.4 Run Summary and Analysis

For the PCD, TC06 began as the system was pressurized and the back-pulsing sequence was first started on July 6, 2001. After solving some initial operational problems (primarily involving the start-up burner) coal feed first began on July 11, 2001, at 01:10 but was discontinued at 02:40. During this period of coal feed, the PCD pressure drop was the highest of the run. Back-pulsing exceeded the trigger point of 275 inH_2O before back-pulsing could be initiated by the logic sequence, and the peak pressure drop reached 515 inH_2O at one point. Coke breeze had been fed to bring the reactor temperature above 1,500°F and both coke breeze feed and start-up burner operation were continued over the duration of coal feed. Apparently, there was a tremendous amount of solids entering the PCD when coal feed was introduced, because the screw cooler FD0502 outlet temperature quickly reached 400°F (the high-high alarm set point). The face velocity in the PCD was also extremely high, exceeding 8 ft/min several times. One reason for the high face velocity was that system pressure was kept low, between 119 and 134 psig, during this time so that the start-up burner could operate. Coal feed was ended after FD0502 tripped on high outlet temperature and the FD0520 outlet line plugged and could not be cleared. This was the first time coke breeze had been used in the transition to coal feed and it was a learning experience. After this experience, the start-up burner was no longer used during the transition to coal and coke breeze feed was discontinued quickly after coal feed was established.

The next time coal feed was introduced was on July 12, 2001. However, this period of coal feed lasted less than one hour due to operational problems with the main air compressor. Over the next few days, coal feed was attempted several times, but due to various problems coal feed was not established again until 00:44 on July 15, 2001. At 23:08 on July 18, 2001, after a coal feeder trip, oxygen breakthrough caused a thermal excursion in the PCD. As filter element surface temperatures began rapidly increasing, back-pulsing was manually initiated, and as each plenum

received a back-pulse, filter element surface temperatures immediately dropped. The top plenum filter element surface temperatures rose about 70ºF in 1 minute, and the bottom plenum, which was back-pulsed 1 minute after the top plenum, showed a filter element surface temperature increase of about 170ºF in 2 minutes. This was useful operational experience, supporting the action of back-pulsing during a thermal excursion as an effective method of stopping combustion on the filter element surfaces.

Coal feed was quickly reestablished at 23:42 on July 18, 2001, and coal feed was maintained except for short periods of coal-feed loss occurring over the next few days. During these periods of coal-feed loss, reactor temperatures were kept fairly stable with coke breeze feed, and system pressure was also fairly constant. There were other minor thermal excursions occurring during unstable coal feeder operation causing oxygen breakthrough.

At 11:50 on July 24, 2001, coal feed was stopped so that the main air compressor could be tuned. At 16:12, during the compressor tuning, oxygen levels in the PCD exceeded 12 percent, and two filter element surface thermocouples indicated combustion in the PCD. The temperature of the filter element surfaces had been about 480ºF, but during this thermal excursion one thermocouple increased to about 800ºF. The air compressor tuning continued and the PCD oxygen level remained elevated. The filter element surface thermocouple readings did not return to their previous temperatures until about 16:47 on July 24, 2001. At this time, no coal or coke breeze had been fed for over 4 hours, although back-pulsing had continued. Therefore, most g-ash in the form of a transient filter cake should have been removed, and the extended thermal transient was likely caused by the combustion of g-ash bridging. The two thermocouples that showed significant response during the thermal excursion had previously begun deviating a few degrees from the nearby thermocouples, indicating that they were covered with g-ash bridging. The on-line PCME PCD outlet particulate monitor began indicating particle leakage at 16:23, showing a peak reading of 100 percent at 16:30 on July 24, 2001. On July 25, 2001, at 10:45, an SRI outlet sample affirmed particulate leakage through the PCD with a solids concentration of 23 ppmw. Therefore, the system was shut down so that the PCD could be opened for inspection. When the PCD was inspected, one broken filter element was found. This filter element was removed (as well as several nearby filter elements) because of the potential damage incurred by the thermal excursion.

System operation resumed in August. The system was pressurized on August 18, 2001, and back-pulsing and system heat-up started on August 19, 2001. Coal feed began on August 20, 2001, at 15:55, and this period of coal feed lasted until August 21, 2001, at 22:56, when the coal feeder tripped. At this time, the coke breeze feeding system would not convey solids, so the system pressure was reduced so that the start-up burner could be lit to reheat the reactor. On August 22, 2001, at 16:37, coal feed began again, but after a coal feeder trip on August 23, 2001, at 23:21, a logic problem caused inadequate air flow to the reactor, and system pressure had to be reduced again to light the start-up burner. The next time coal feed began was on August 24, 2001, at 11:30. This period of coal feed lasted until the end of the run on September 24, 2001, and was interrupted by only short periods of coal-feed loss. During unsteady coal feeder operation, coke breeze was successfully fed, so system temperature and pressure were generally kept constant. Unsteady coal feeder operation was attributed to particle-size segregation in the silos which could result in periods of coal feeding with finer particles that are more difficult to convey. This problem was apparently alleviated by constantly filling the

silos with coal instead of only grinding coal and filling the silos 12 hours per day as had been previously done. The run ended in a controlled dirty shutdown on September 24, 2001. The back-pulsing sequence was disabled at 14:27 at the end of a back-pulsing cycle, and coal feed was discontinued at 14:33 on September 24, 2001.

The baseline pressure drop was much more stable in TC06 than it was in the two preceding gasification runs (GCT3 and GCT4). As discussed in Section 3.4, the fairly stable baseline was largely attributable to the reduction in tar deposition on the filter element surfaces. Near the end of the run, the baseline did show a noticeable increase. This increase corresponded to an increase in the coal-feed rate and the apparent presence of g-ash bridging. Because baseline pressure drop is only a small function of coal-feed rate, g-ash bridging growth likely contributed most to the increasing baseline.

Figure 3.2-27 shows the normalized baseline pressure drop throughout TC06, a filter surface temperature difference indicating g-ash bridging, and the coal feeder speed. The normalized baseline pressure drop is the baseline pressure drop corrected for constant face velocity and temperature. The filter surface temperature difference is the difference between one thermocouple reading (TI3025J), which began reading higher than the other nearby thermocouples on the bottom plenum, and another thermocouple (TI3025H), which showed no such deviation throughout the run. In addition, on inspection, g-ash bridging was extensive in the area where TI3025J was located and was not found near TI3025H. Also seen in Figure 3.2-27 is the coal feeder speed, which gives an estimate of the relative coal-feed rate. As seen in the figure, the baseline pressure drop changes correspond well to the indications of g-ash bridging. PCD operations will continue to focus on maintaining a stable baseline; therefore, eliminating g-ash bridging will remain a priority.

Table 3.2-1

TC06 Run Statistics and Steady-State PCD Operating Parameters
July 6, 2001 Through September 24, 2001

Start Time:	07/06/00 15:20 (for back-pulse system)
End Time:	09/24/00 14:27
Coal Type:	Powder River Basin
Hours on Coal:	Approximately 1,025 hr
Sorbent Type:	Ohio limestone
Number of Filter Elements:	90
Filter Element Layout No.:	20 and 21 (Figure 3.2-1 and 3.2-2)
Filtration Area:	261.3 ft^2 (24.3 m^2)
Pulse-Valve-Open Time:	0.2 sec
Pulse-Time Trigger:	5 to 20 min
Pulse Pressure, Top Plenum	250 to 400 psi above System Pressure
Pulse Pressure, Bottom Plenum:	250 to 600 psi above System Pressure
Pulse-dP Trigger:	275 inH_2O
Inlet Gas Temperature:	675 to 750°F
Face Velocity:	3 to 4 ft/min
Inlet Loading Concentration:	9,200 to 18,800 ppmw
Outlet Loading Concentration:	Below 0.4 ppmw*
Baseline Pressure Drop:	80 to 120 inH_2O
Peak Pressure Drop:	150 to 250 inH_2O

* Except for outlet loading concentration of 22.9 ppmw detected on July 25, 2001, during an off-coal period resulting from a broken filter element.

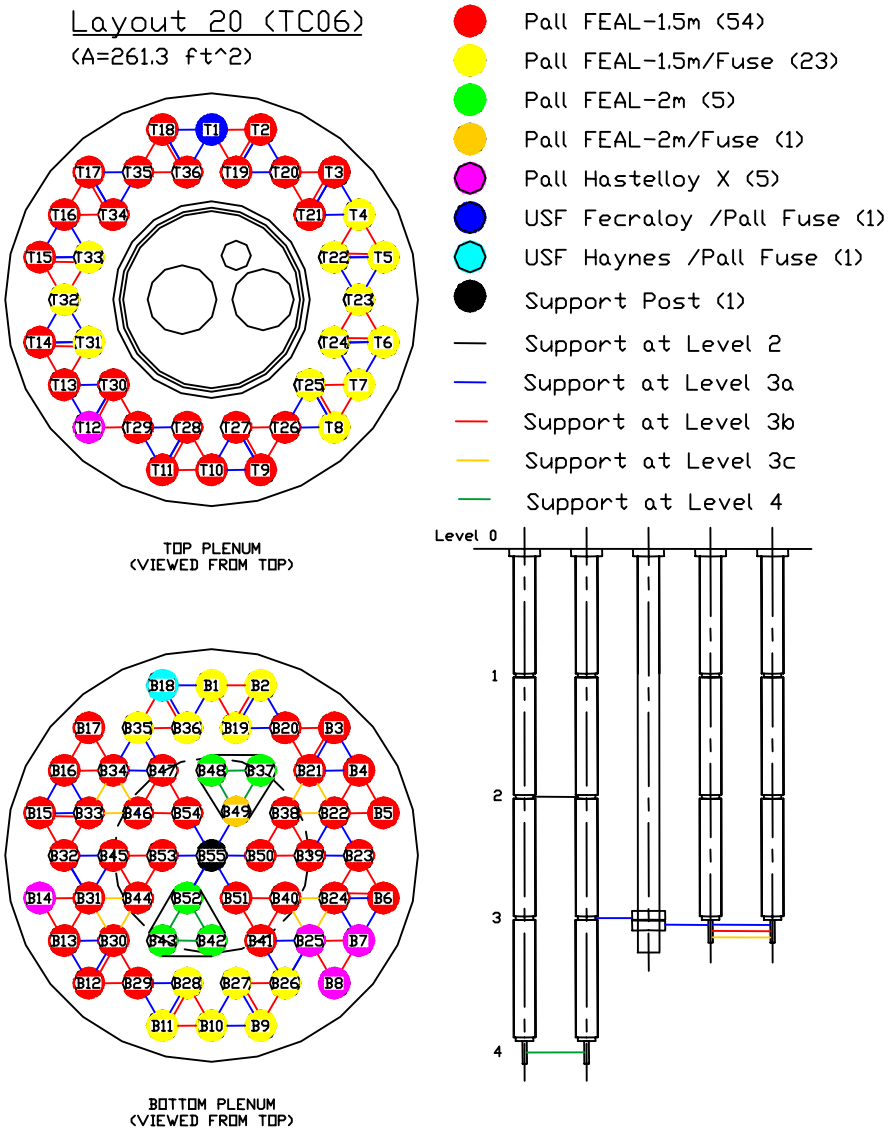

Figure 3.2-1 Filter Element Layout for TC06, July 2001

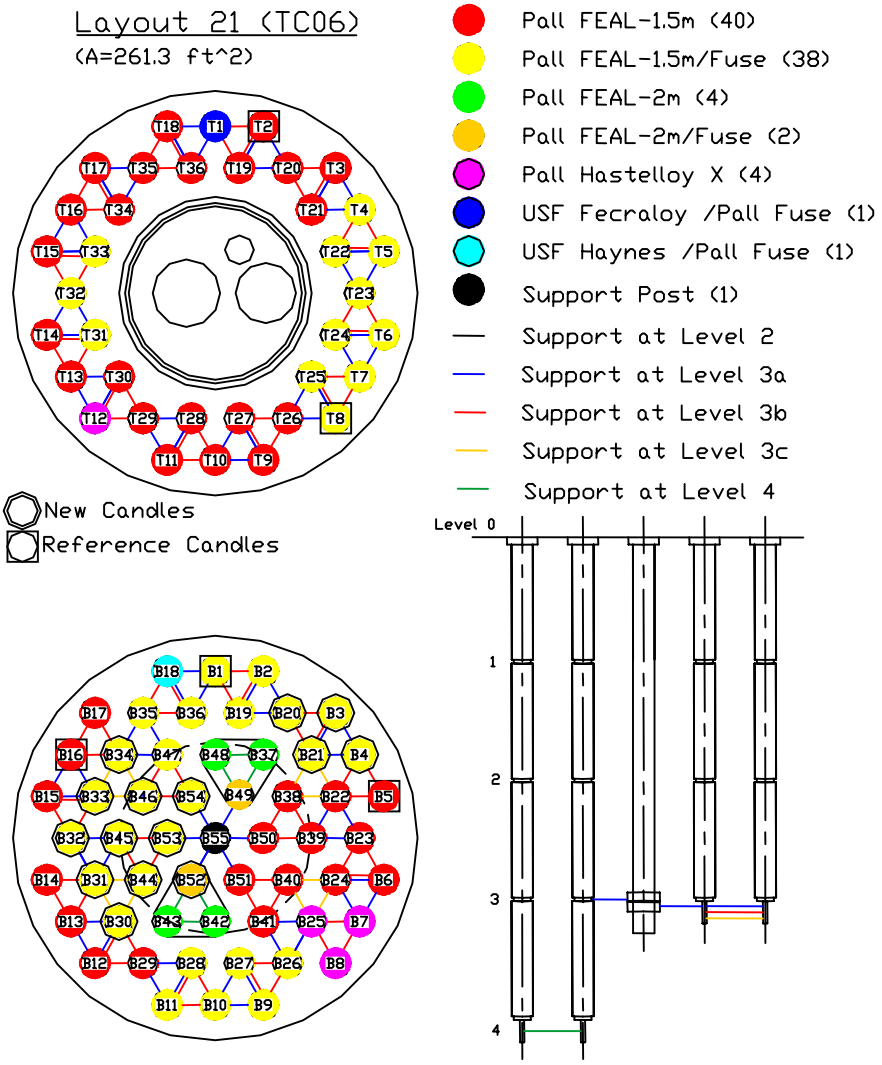

Figure 3.2-2 Filter Element Layout for TC06, August and September 2001

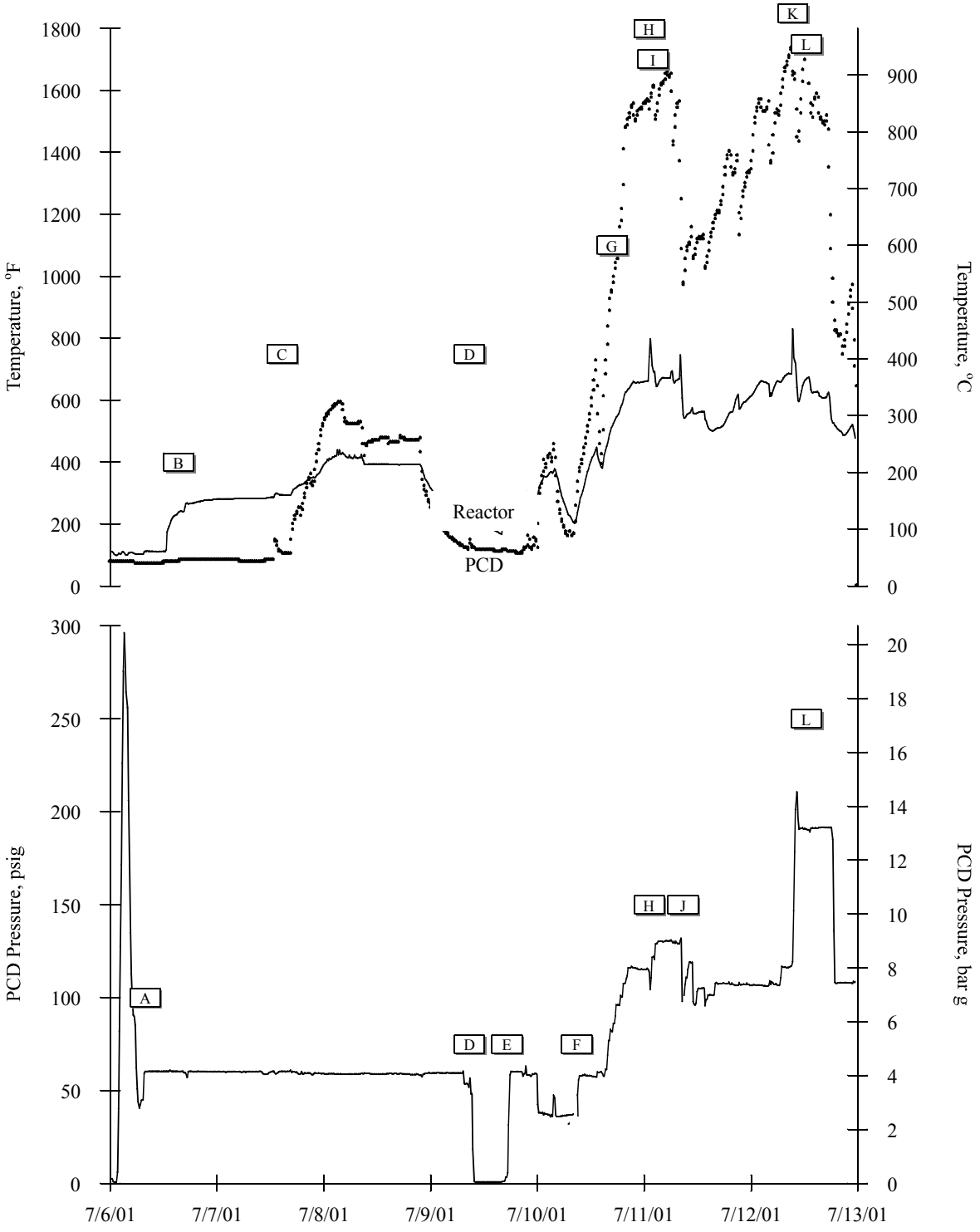

Figure 3.2-3 Reactor and PCD Temperatures and PCD Pressure, July 6, 2001 Through July 13, 2001

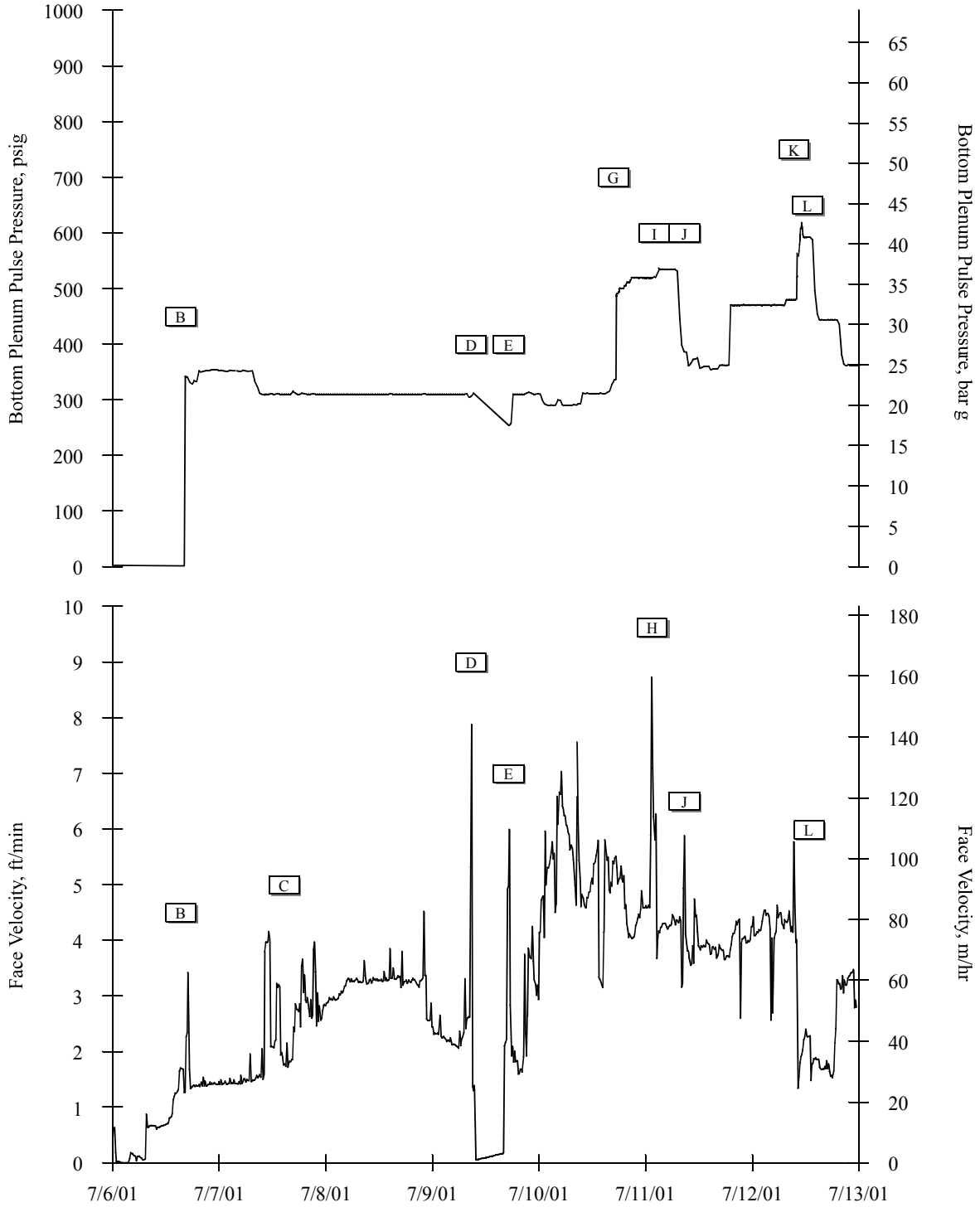

Figure 3.2-4 PCD Pulse Pressure and Face Velocity, July 6, 2001 Through July 13, 2001

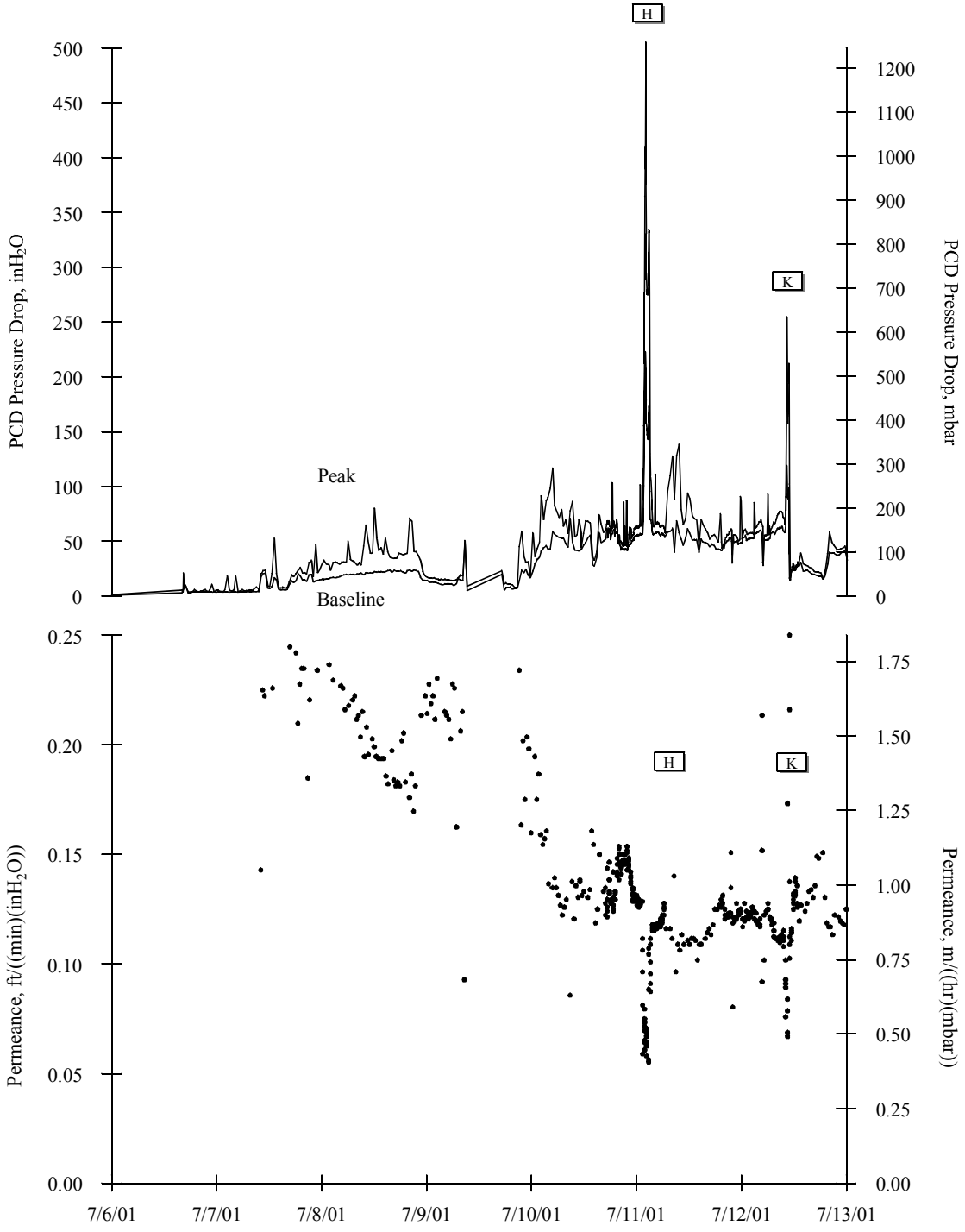

Figure 3.2-5 PCD Pressure Drop and Permeance, July 6, 2001 Through July 13, 2001

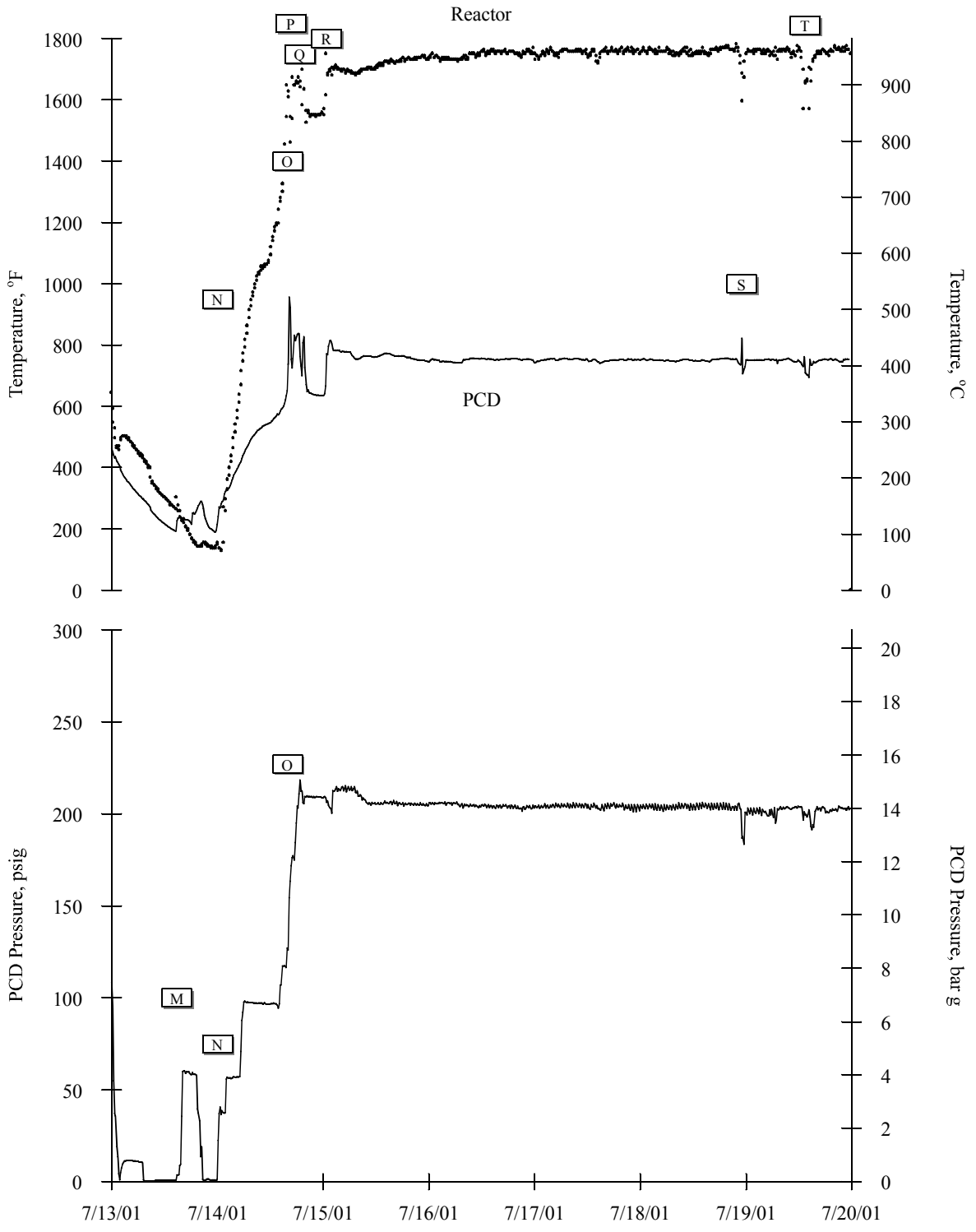

Figure 3.2-6 Reactor and PCD Temperatures and PCD Pressure, July 13, 2001 Through July 20, 2001

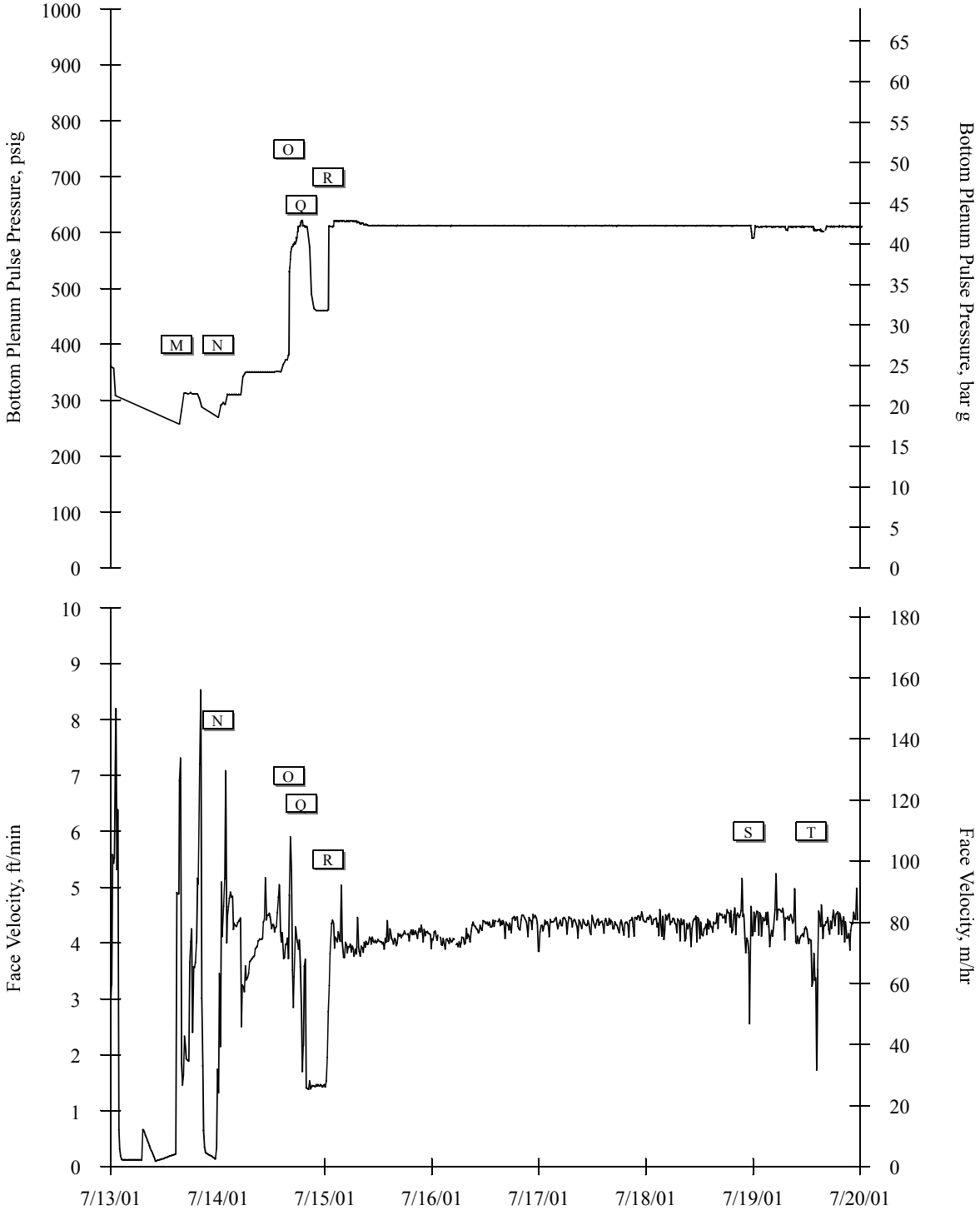

Figure 3.2-7 PCD Pulse Pressure and Face Velocity, July 13, 2001 Through July 20, 2001

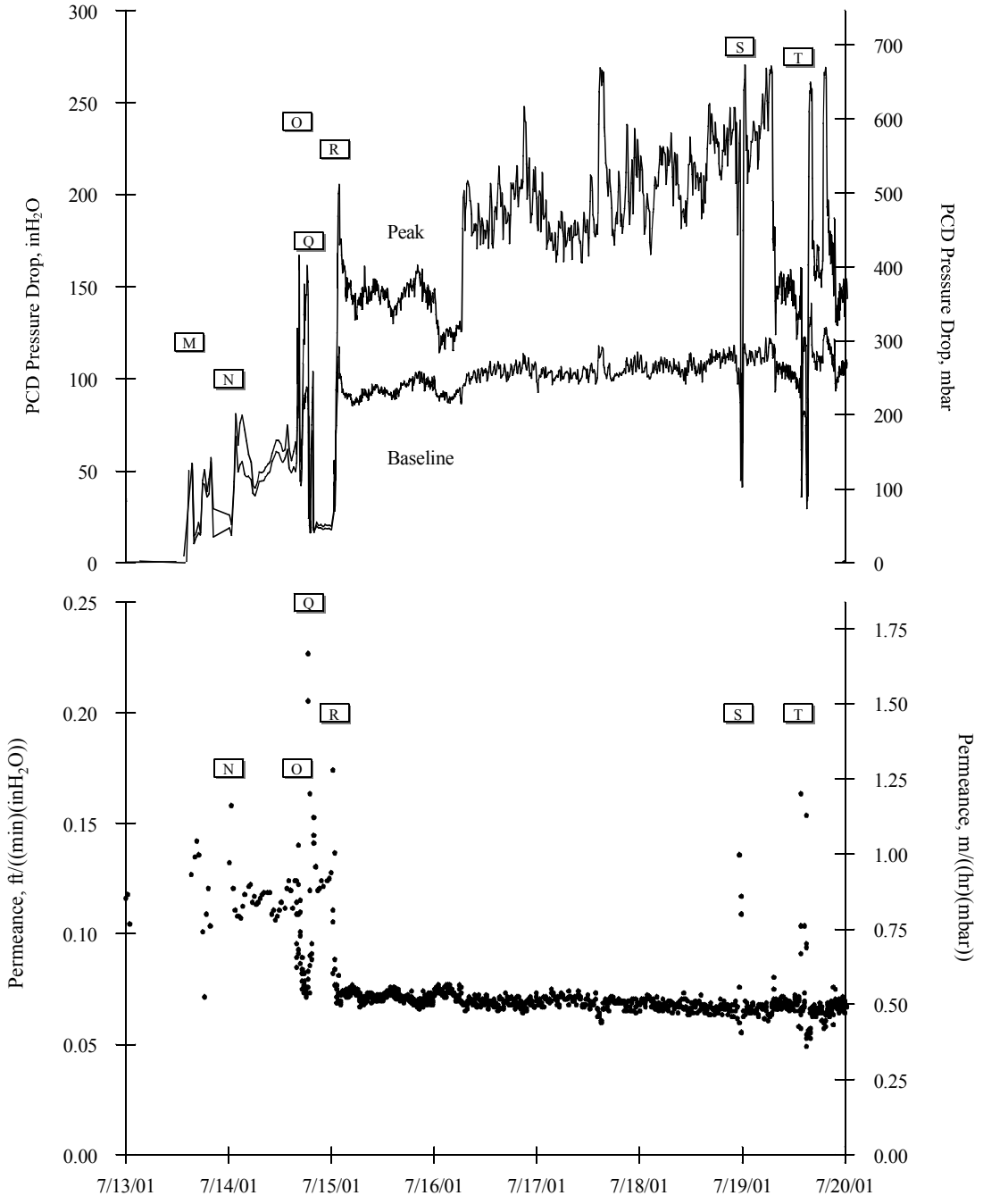

Figure 3.2-8 PCD Pressure Drop and Permeance, July 13, 2001 Through July 20, 2001

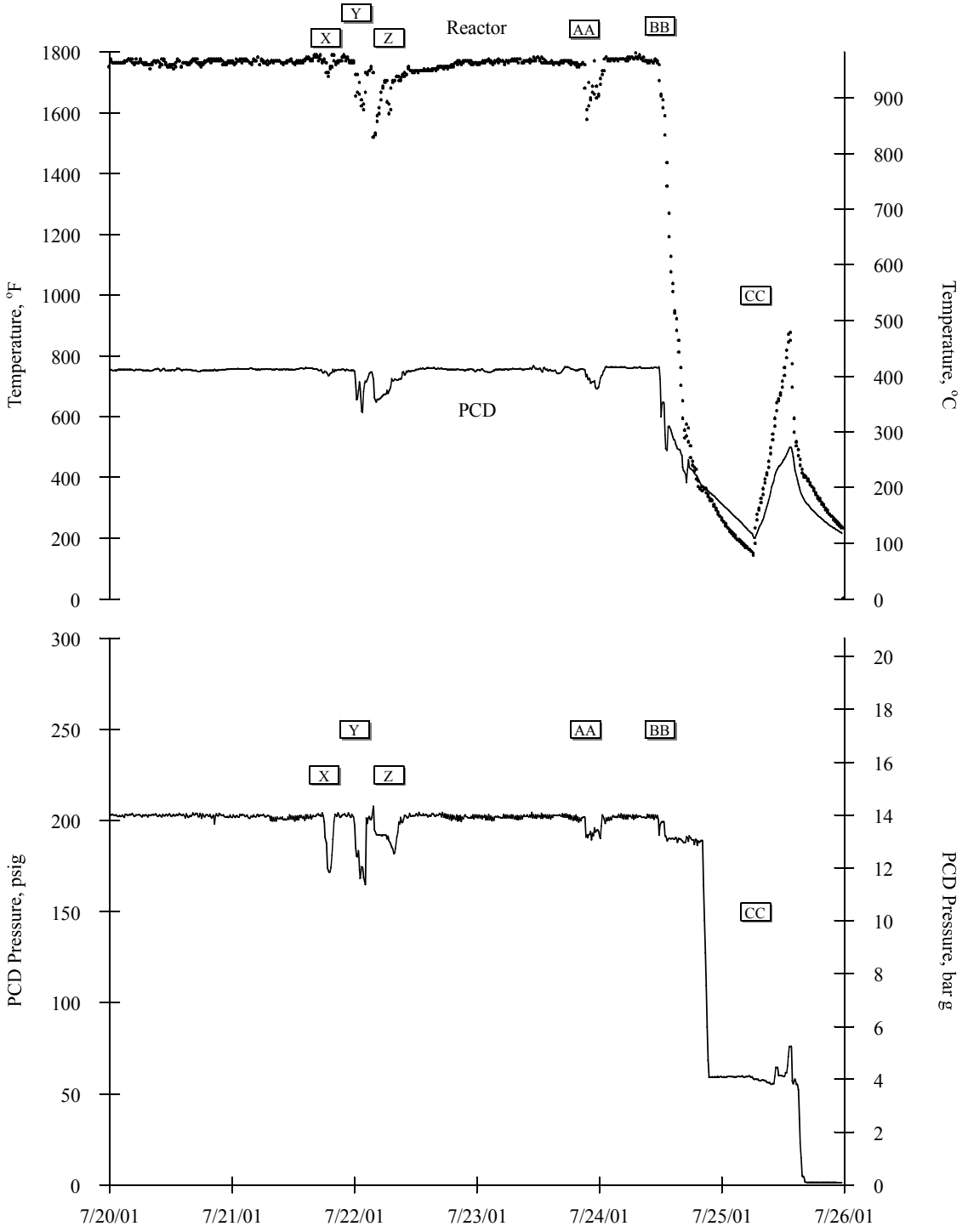

Figure 3.2-9 Reactor and PCD Temperatures and PCD Pressure, July 20, 2001 Through July 26, 2001

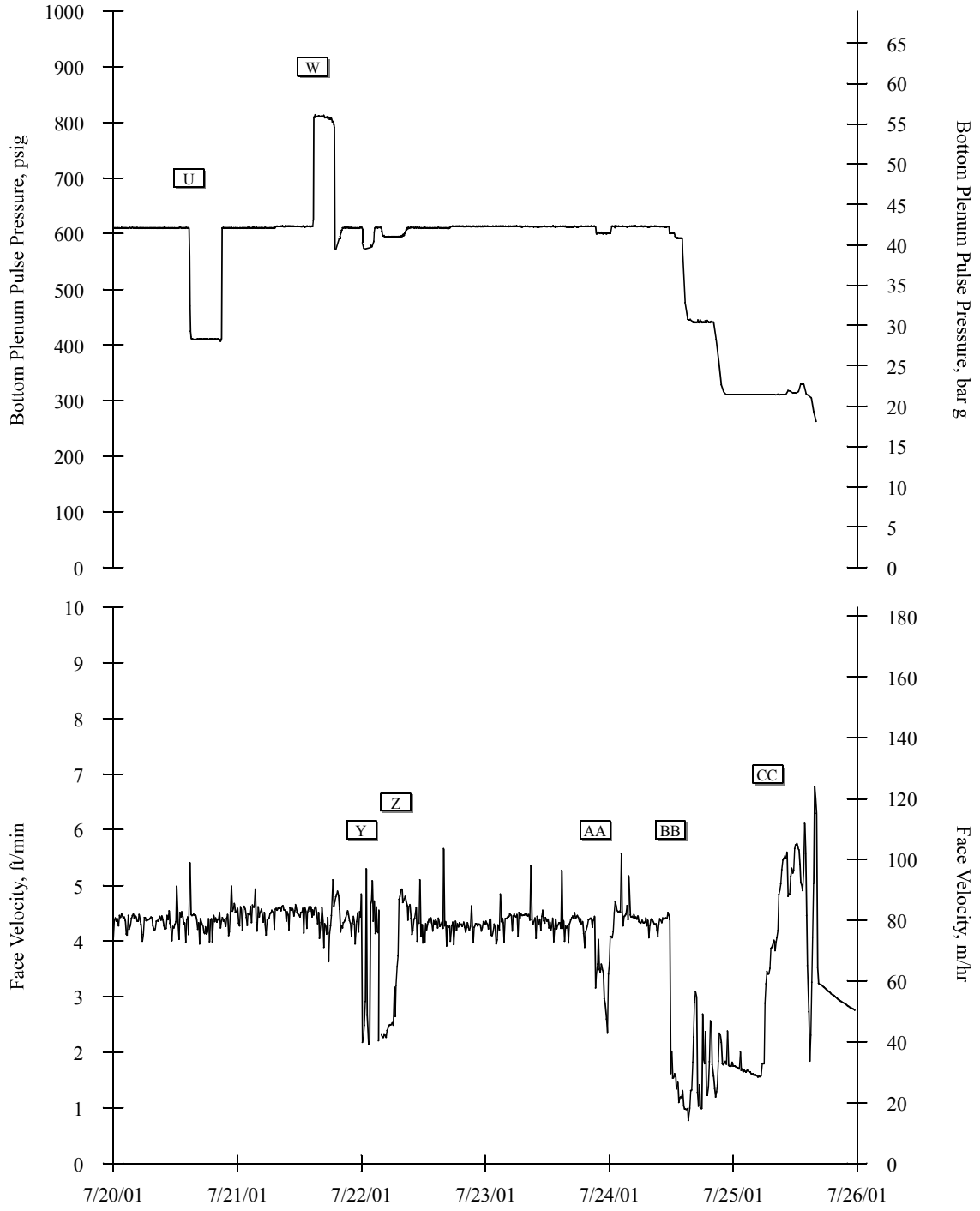

Figure 3.2-10 PCD Pulse Pressure and Face Velocity, July 20, 2001 Through July 26, 2001

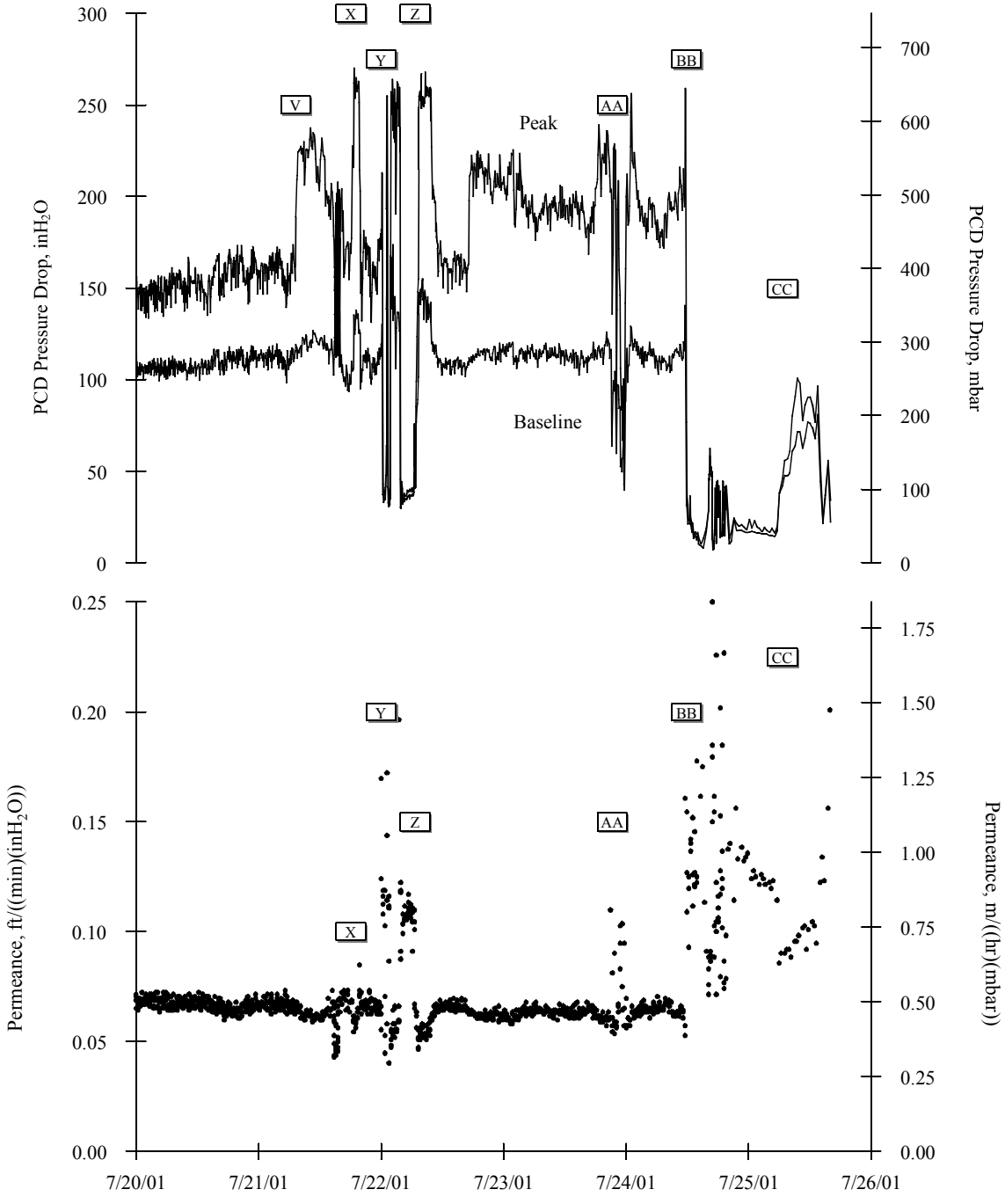

Figure 3.2-11 PCD Pressure Drop and Permeance, July 20, 2001 Through July 26, 2001

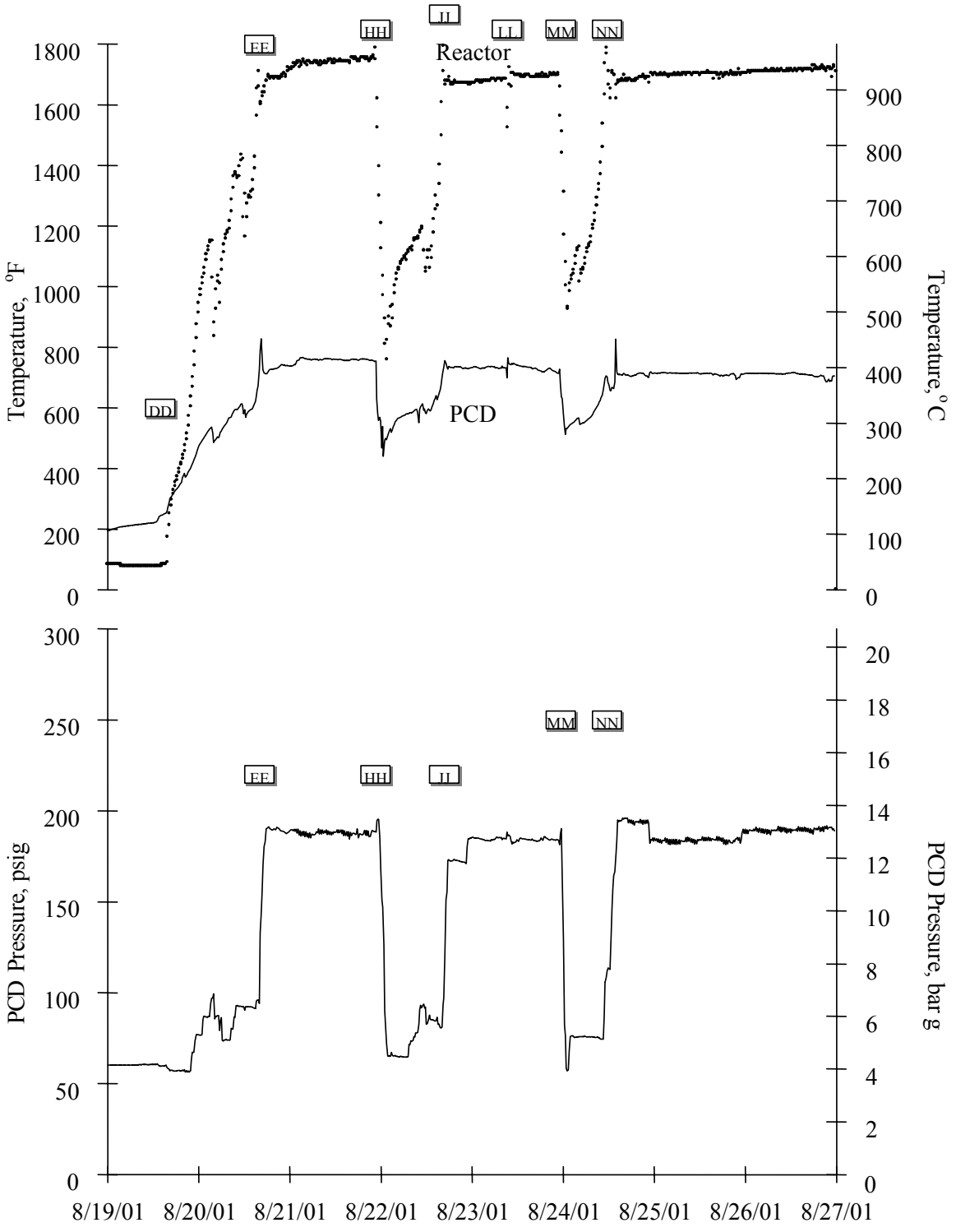

Figure 3.2-12 Reactor and PCD Temperatures and PCD Pressure, August 19, 2001 Through August 27, 2001

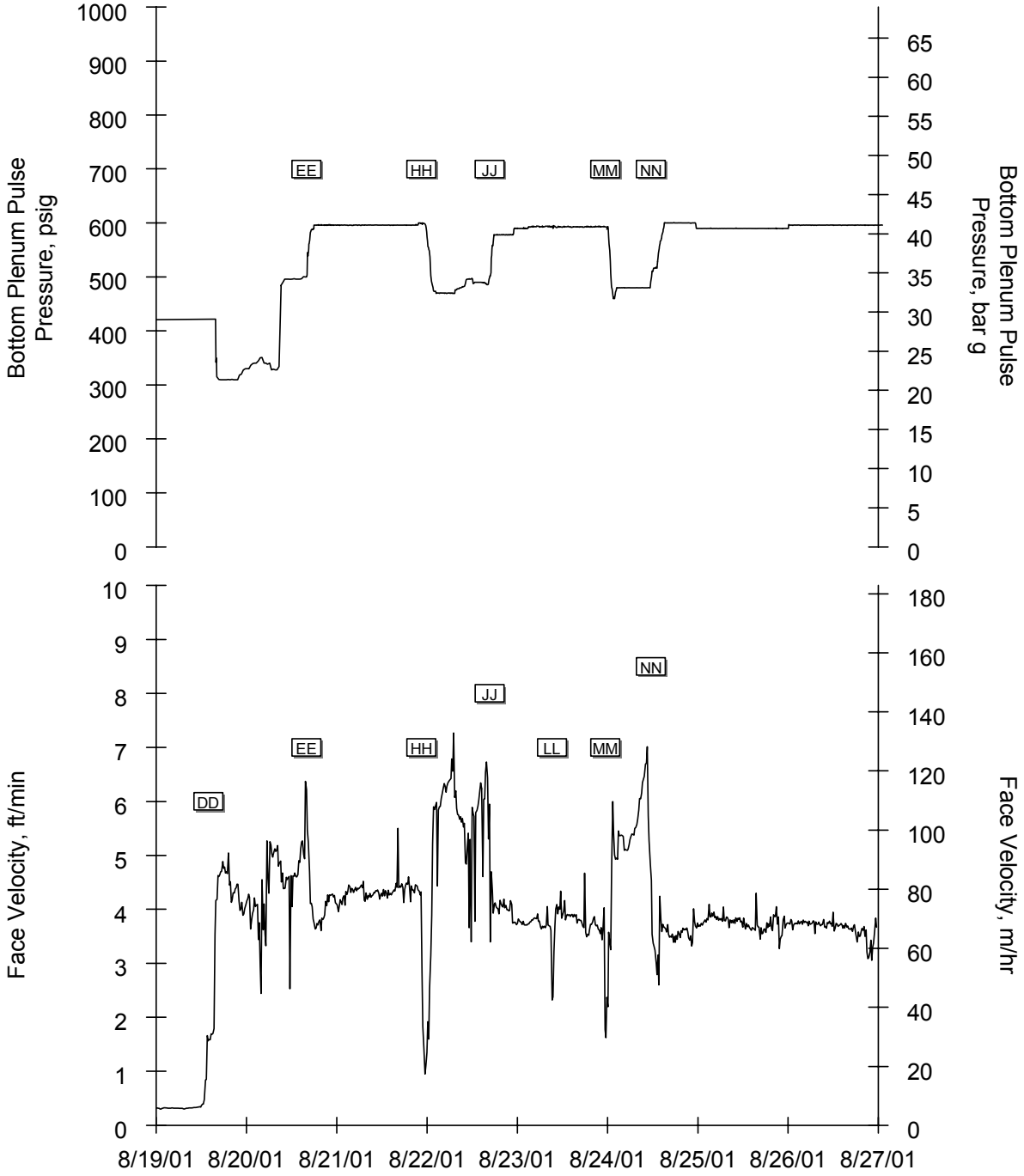

Figure 3.2-13 PCD Pulse Pressure and Face Velocity, August 19, 2001 Through August 27, 2001

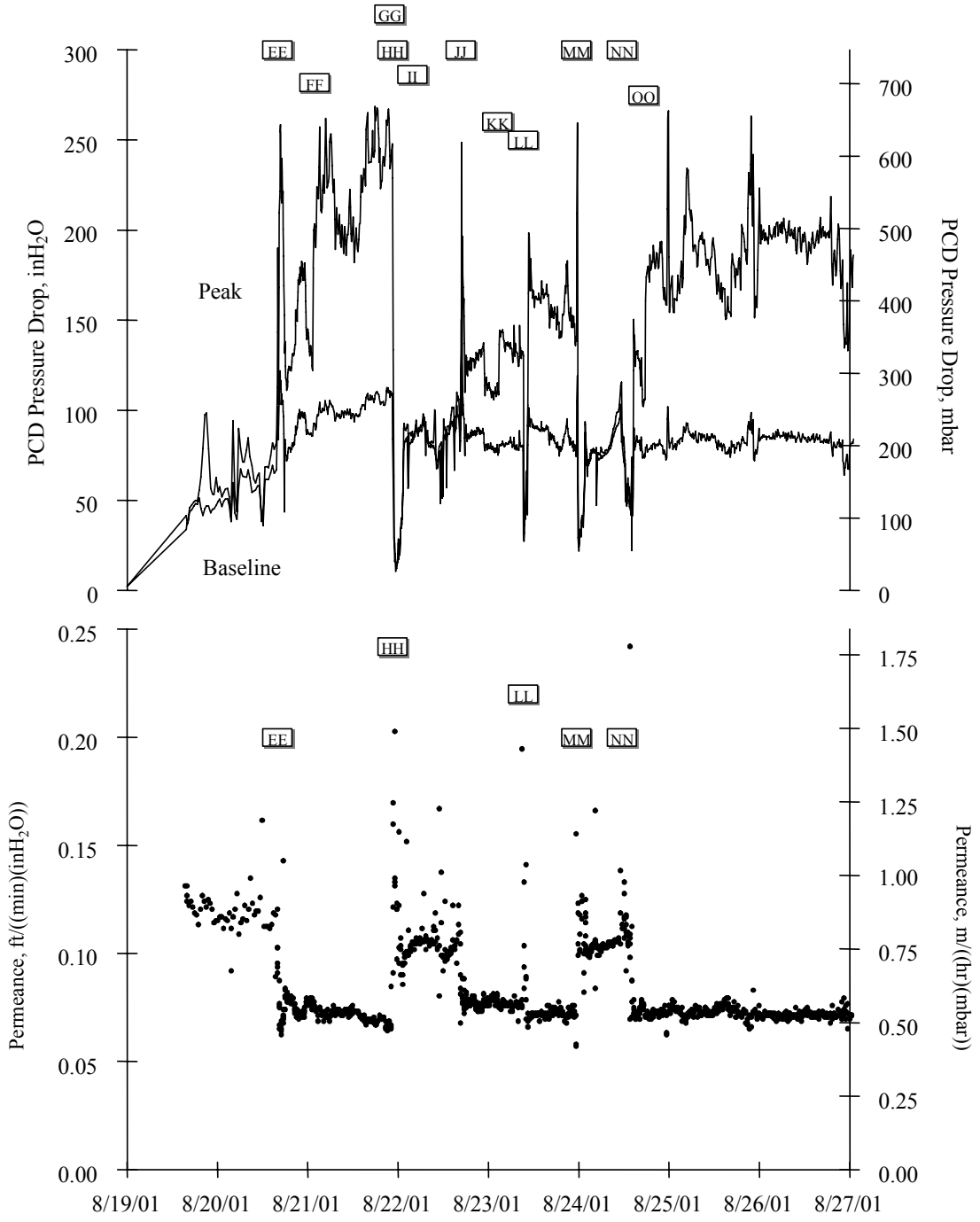

Figure 3.2-14 PCD Pressure Drop and Permeance, August 19, 2001 Through August 27, 2001

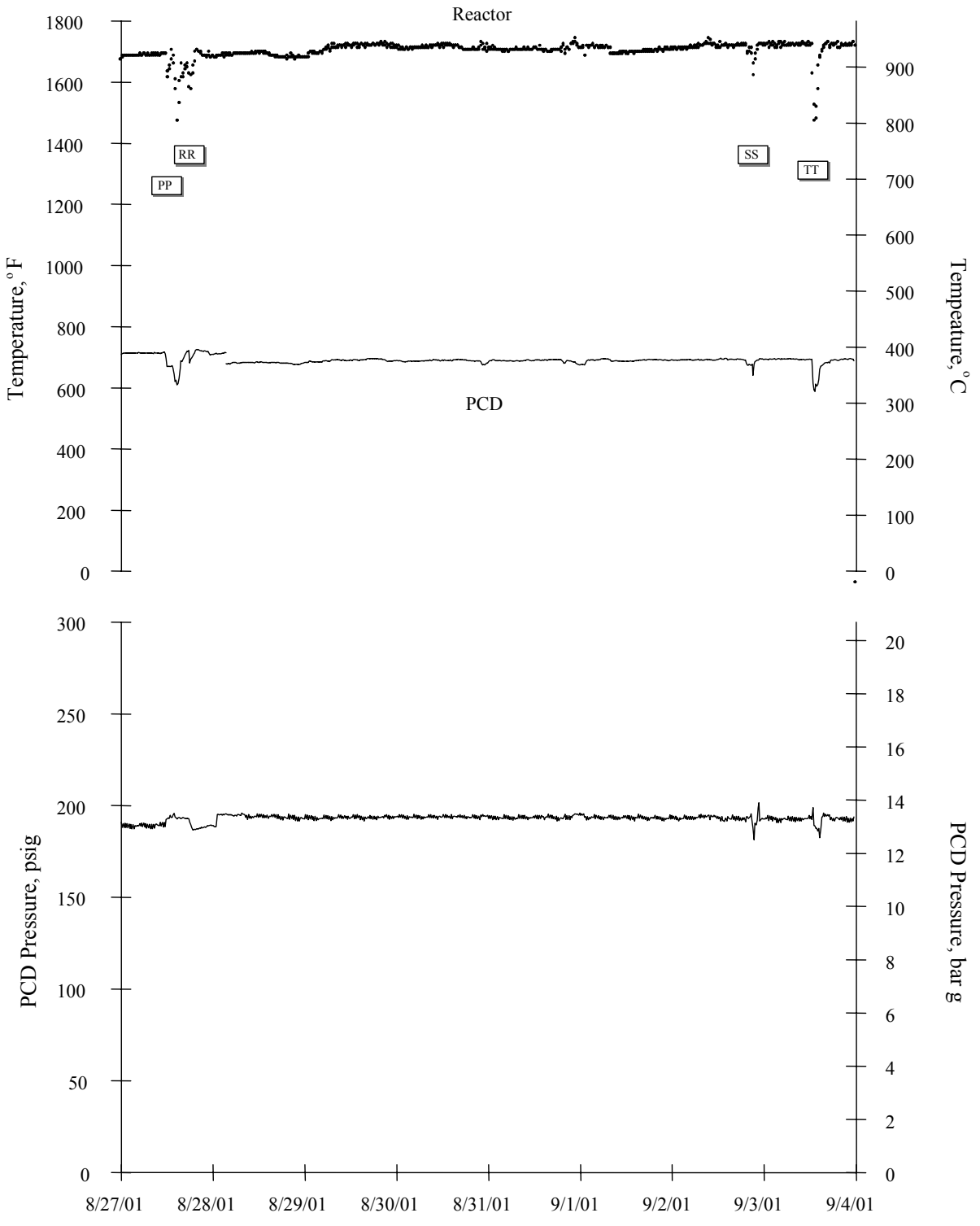

Figure 3.2-15 Reactor and PCD Temperatures and PCD Pressure, August 27, 2001 Through September 4, 2001

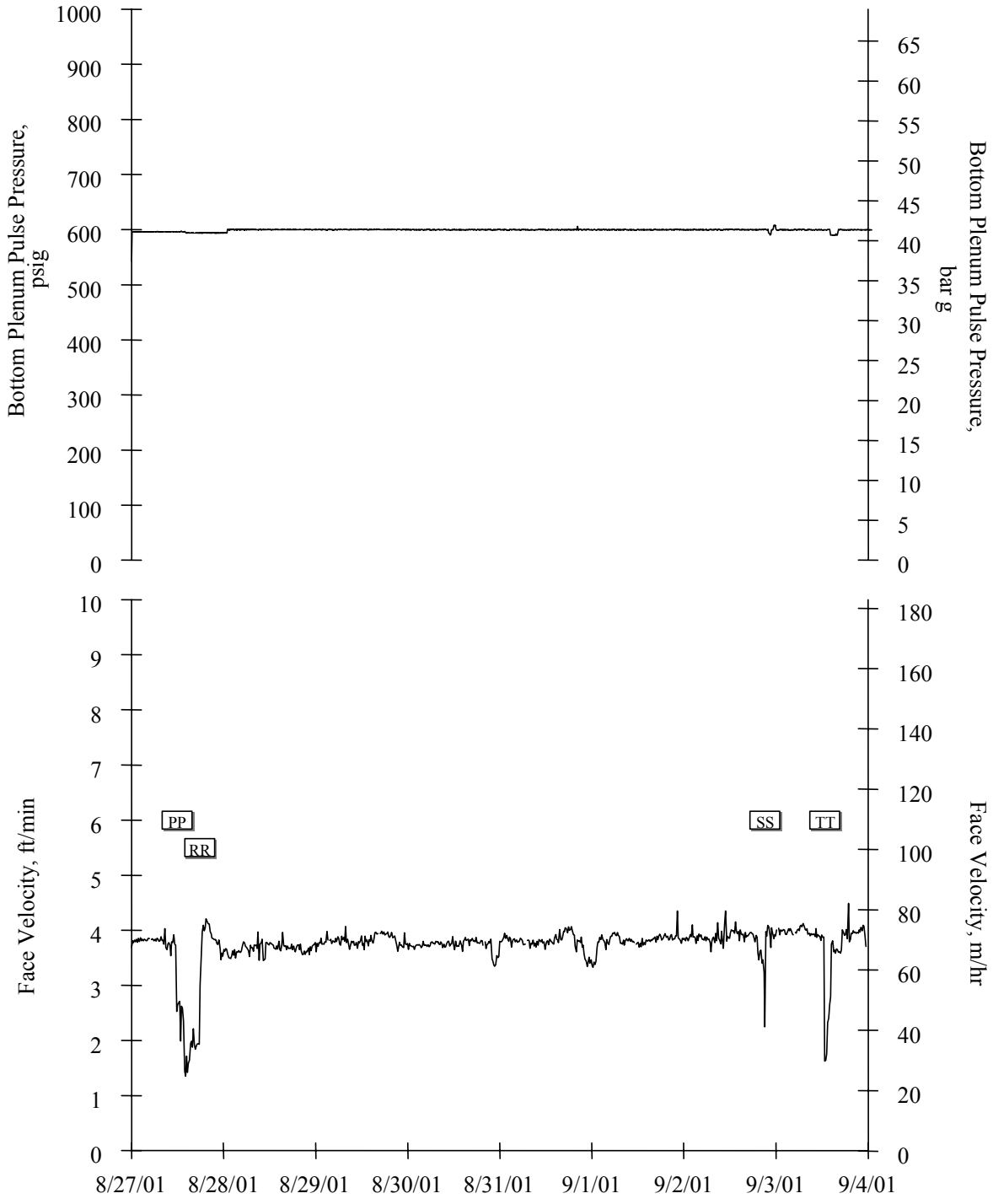

Figure 3.2-16 PCD Pulse Pressure and Face Velocity, August 27, 2001 Through September 4, 2001

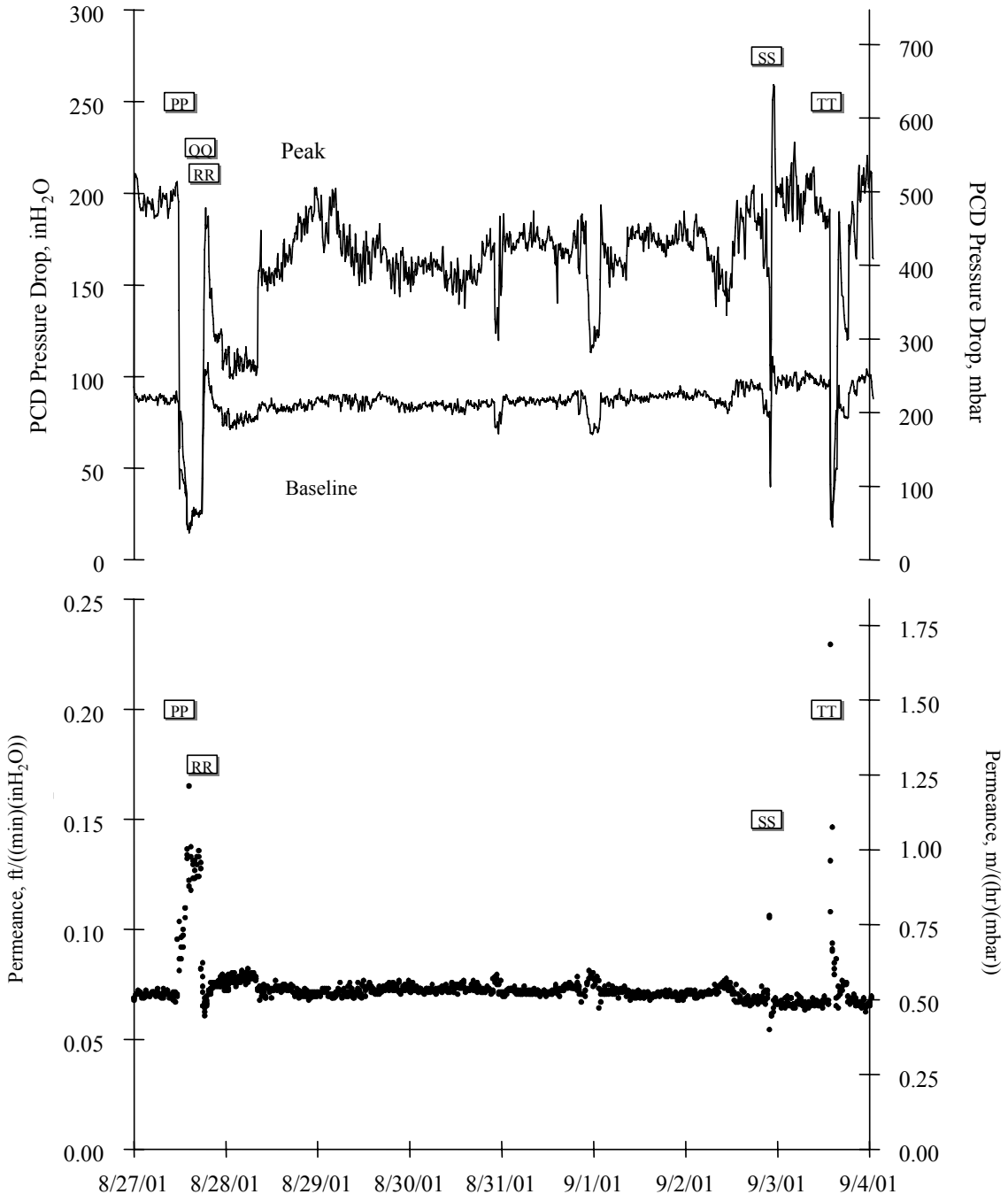

Figure 3.2-17 PCD Pressure Drop and Permeance, August 27, 2001 Through September 4, 2001

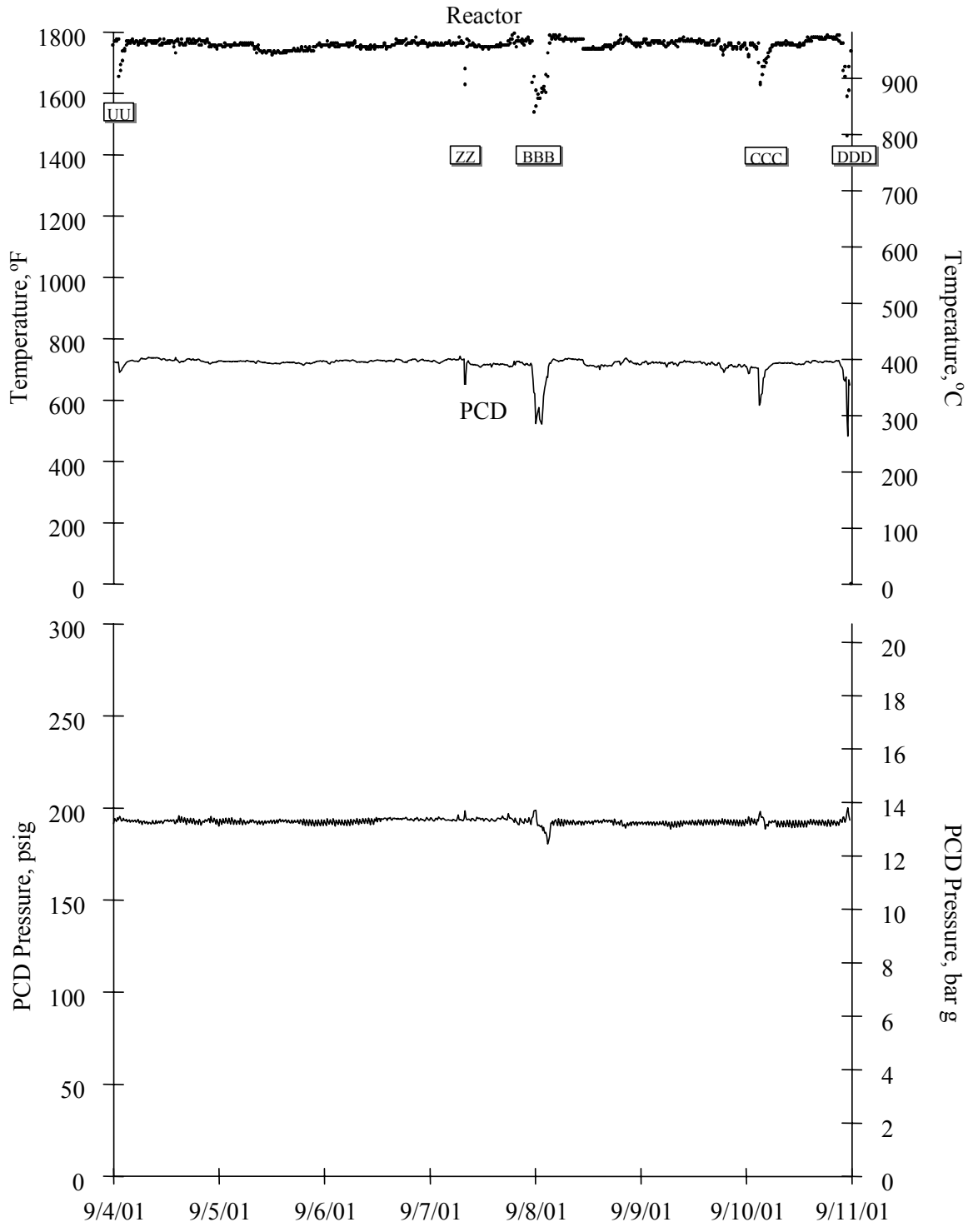

Figure 3.2-18 Reactor and PCD Temperatures and PCD Pressure, September 4, 2001 Through September 11, 2001

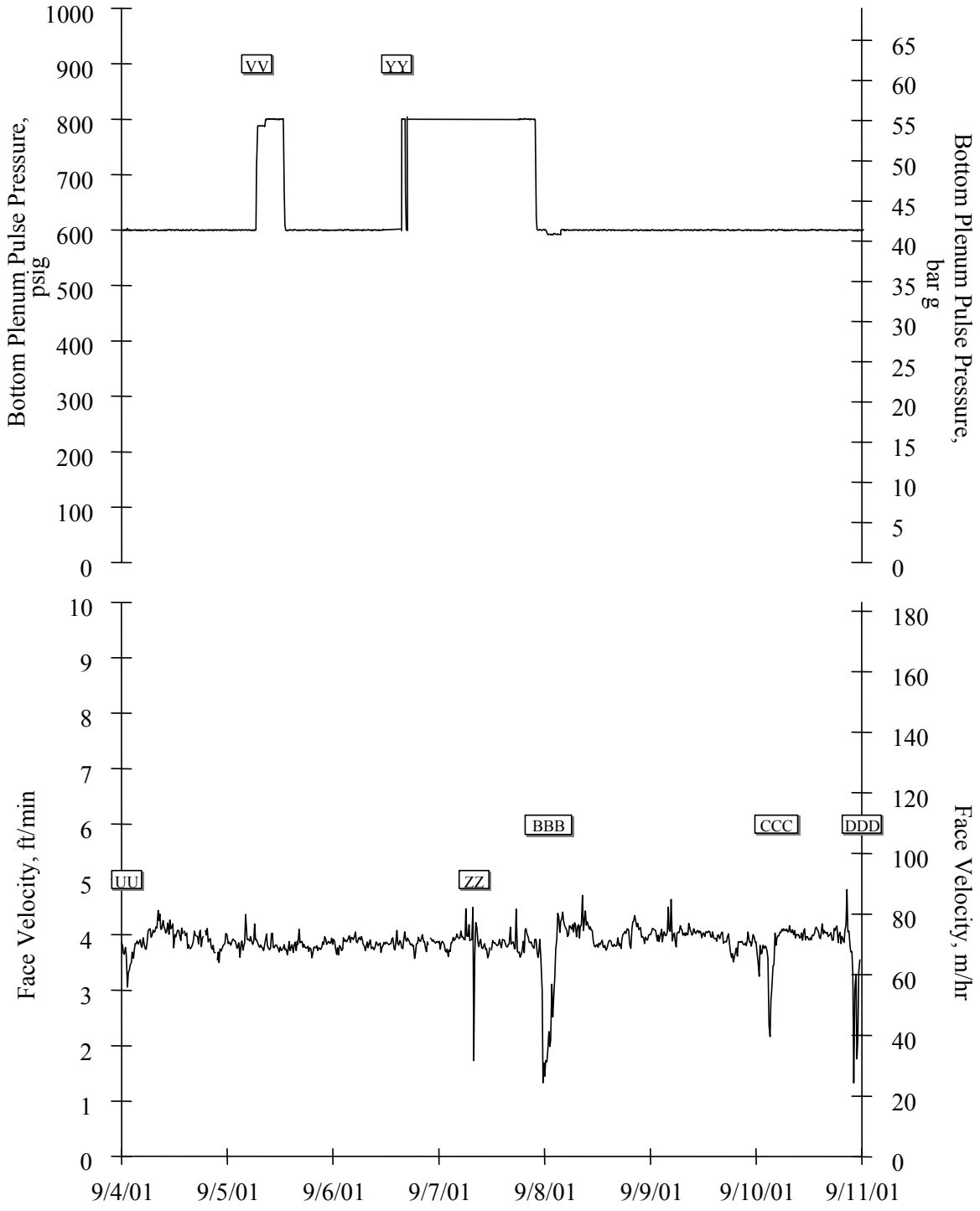

Figure 3.2-19 PCD Pulse Pressure and Face Velocity, September 4, 2001 Through September 11, 2001

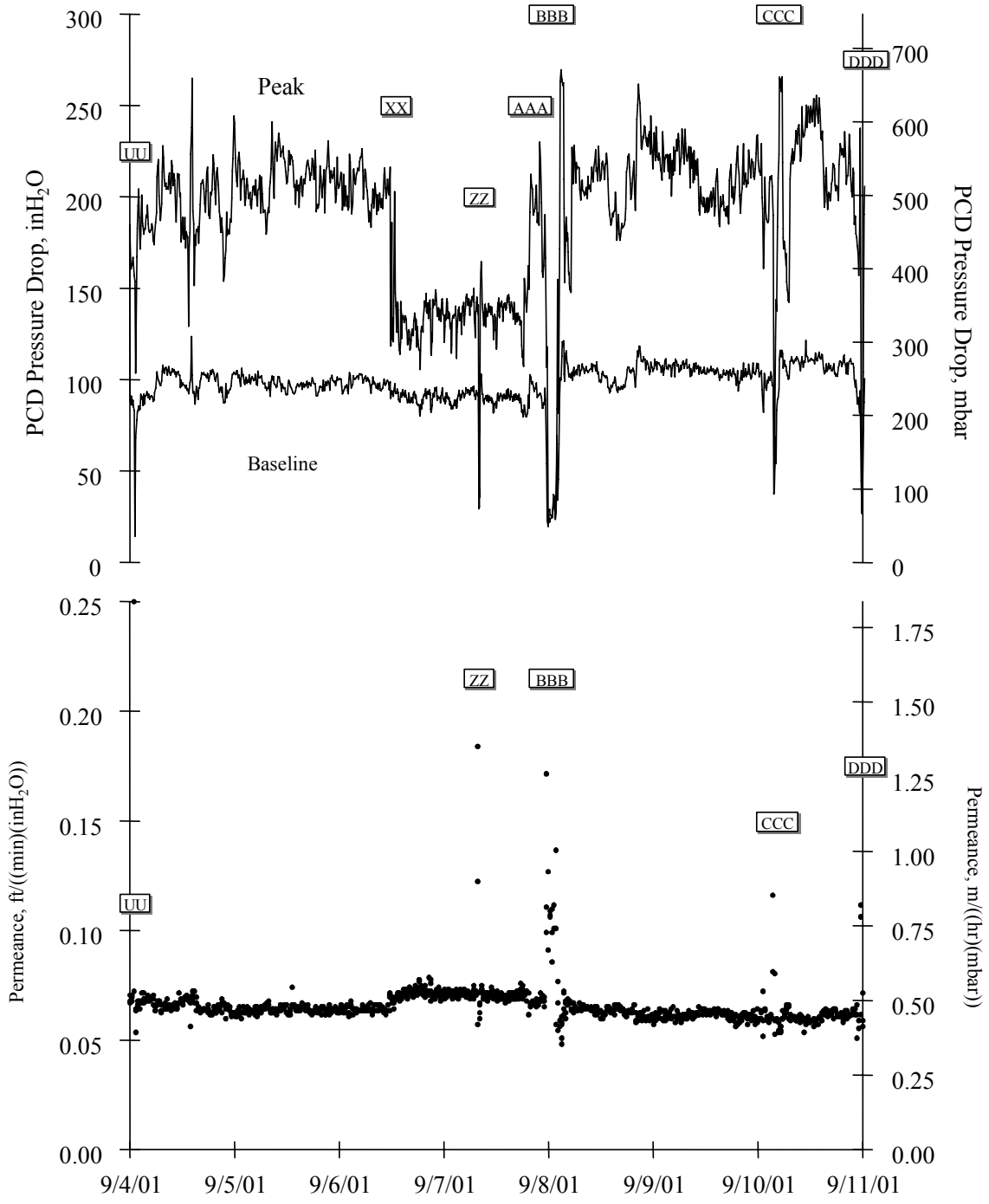

Figure 3.2-20 PCD Pressure Drop and Permeance, September 4, 2001 Through September 11, 2001

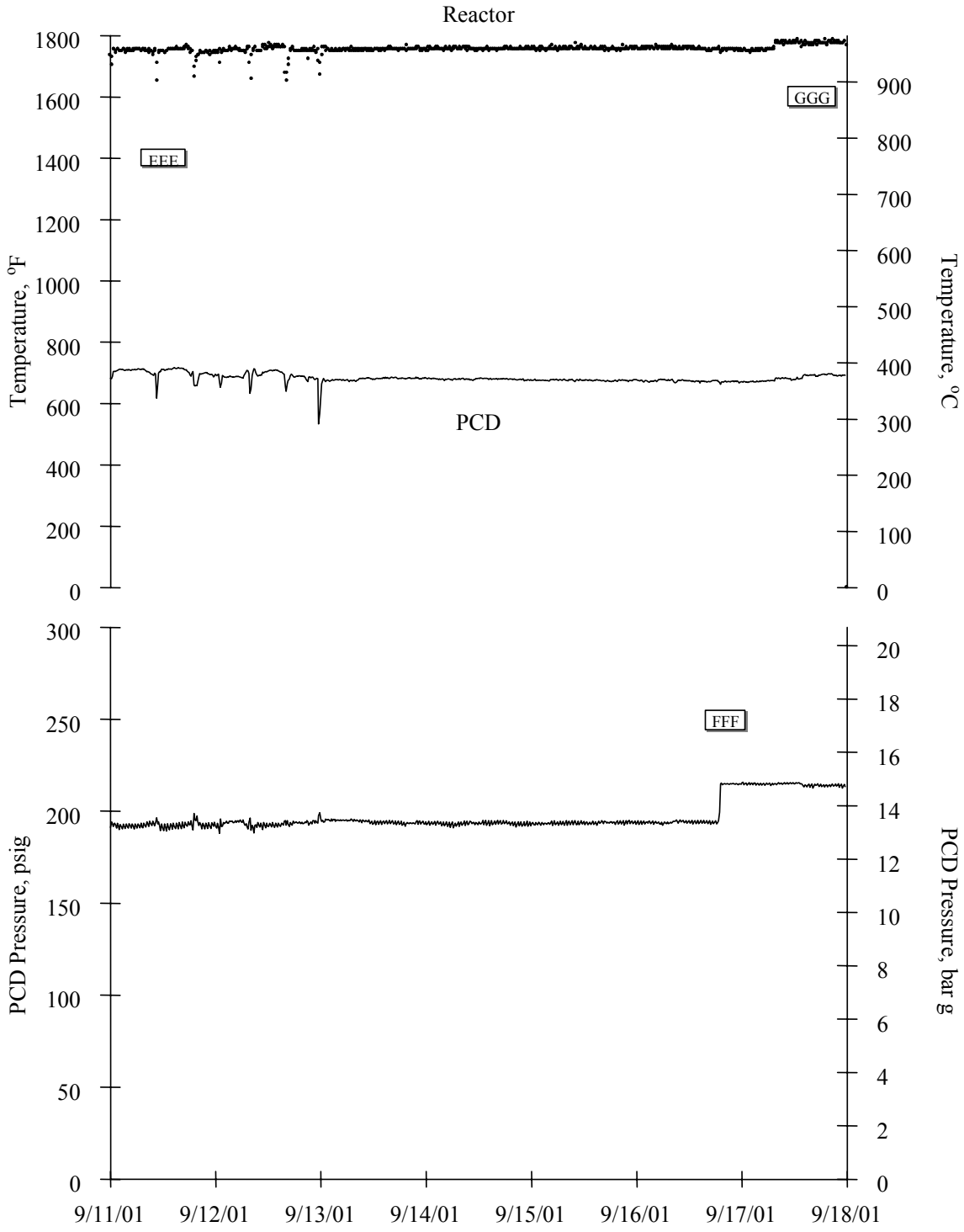

Figure 3.2-21 Reactor and PCD Temperatures and PCD Pressure, September 11, 2001 Through September 18, 2001

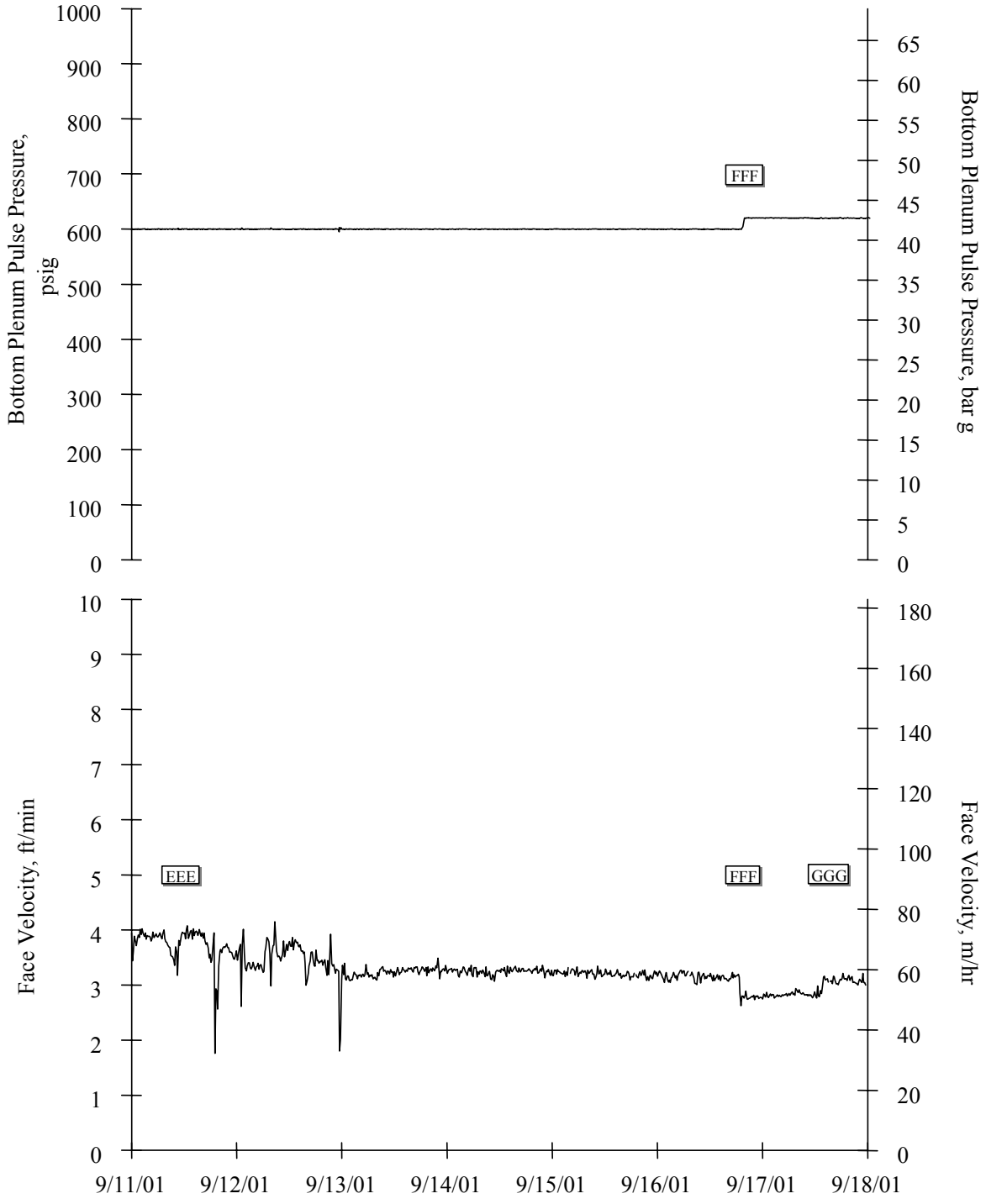

Figure 3.2-22 PCD Pulse Pressure and Face Velocity, September 11, 2001 Through September 18, 2001

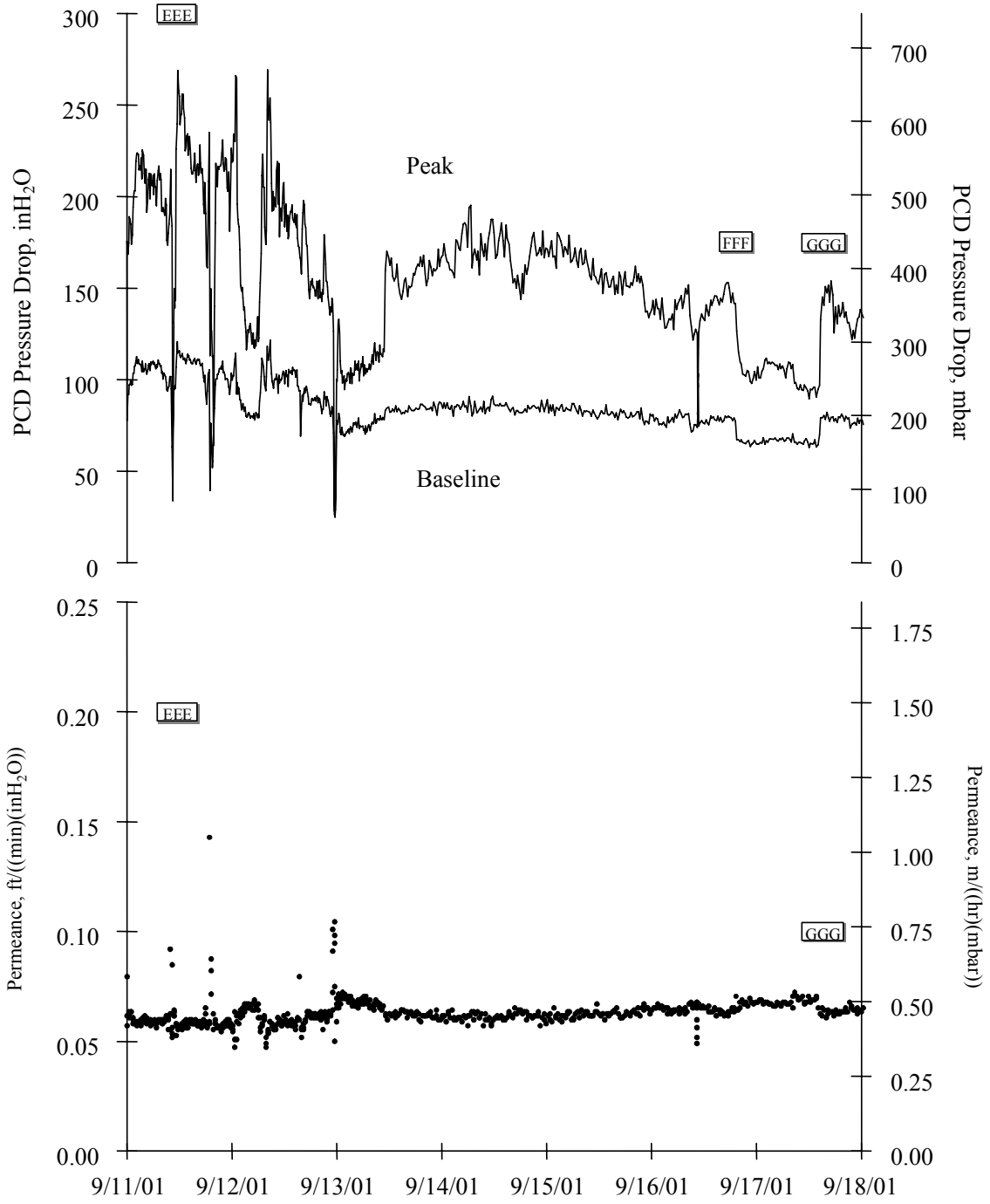

Figure 3.2-23 PCD Pressure Drop and Permeance, September 11, 2001 Through September 18, 2001

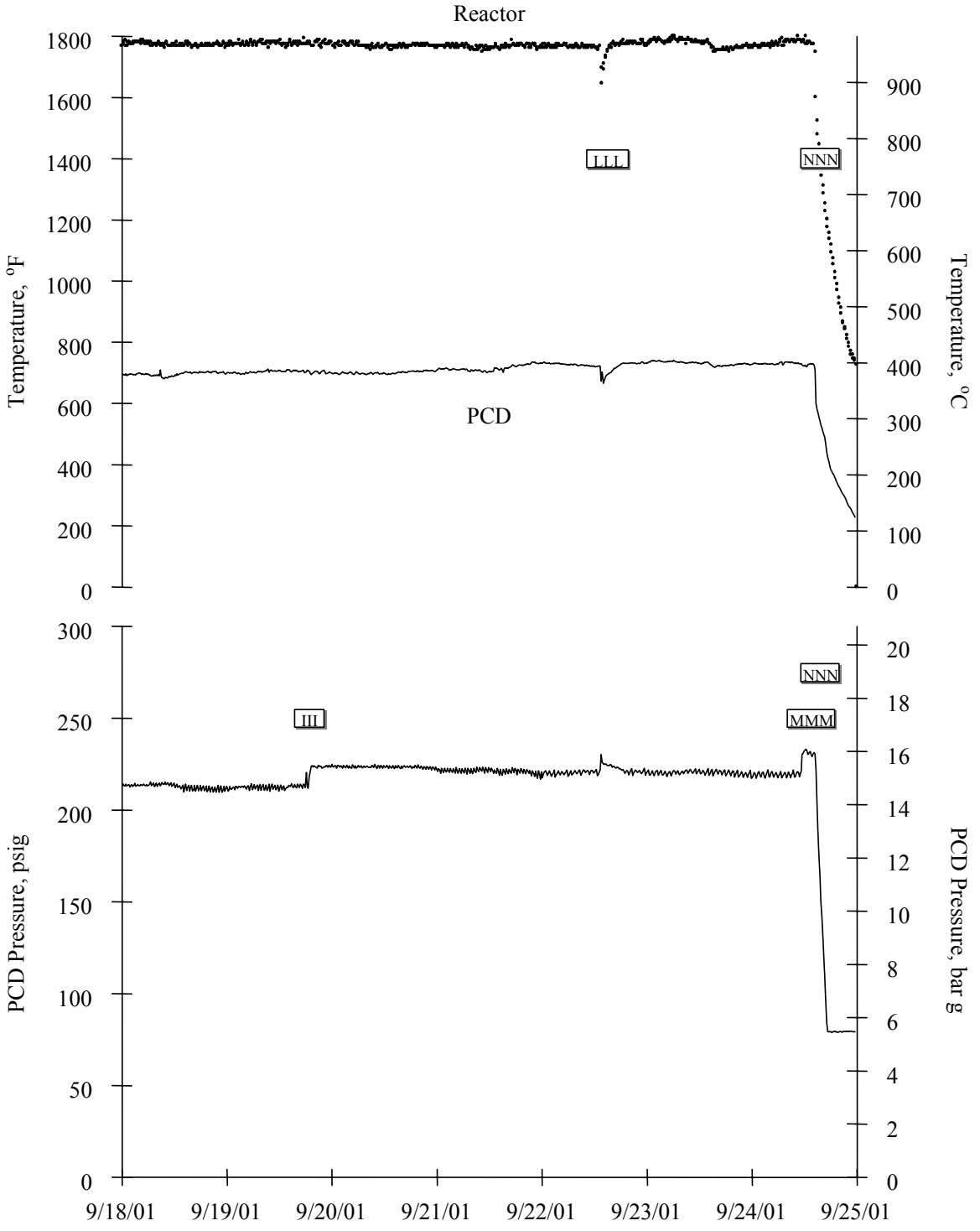

Figure 3.2-24 Reactor and PCD Temperatures and PCD Pressure, September 18, 2001 Through September 25, 2001

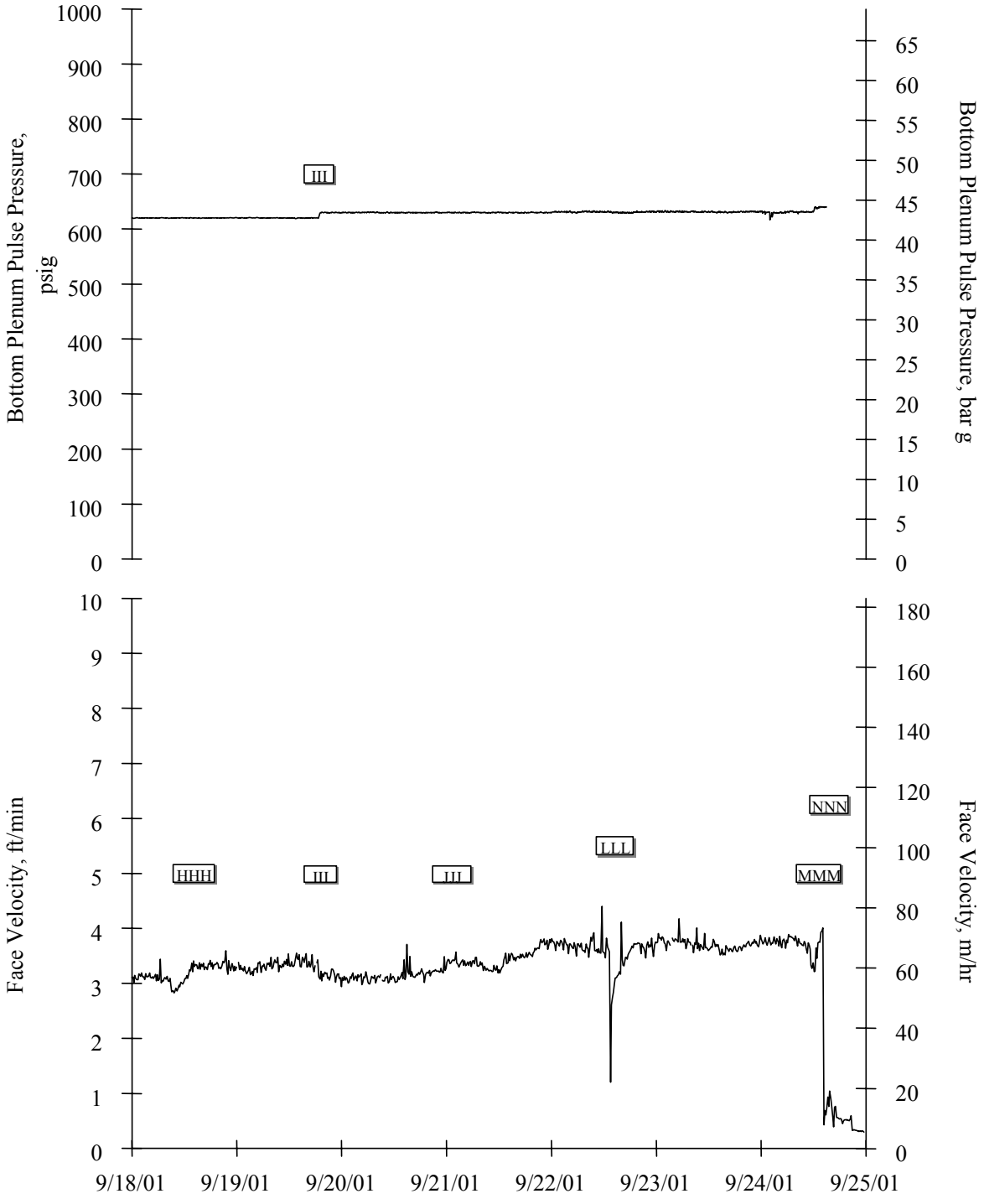

Figure 3.2-25 PCD Pulse Pressure and Face Velocity, September 18, 2001 Through September 25, 2001

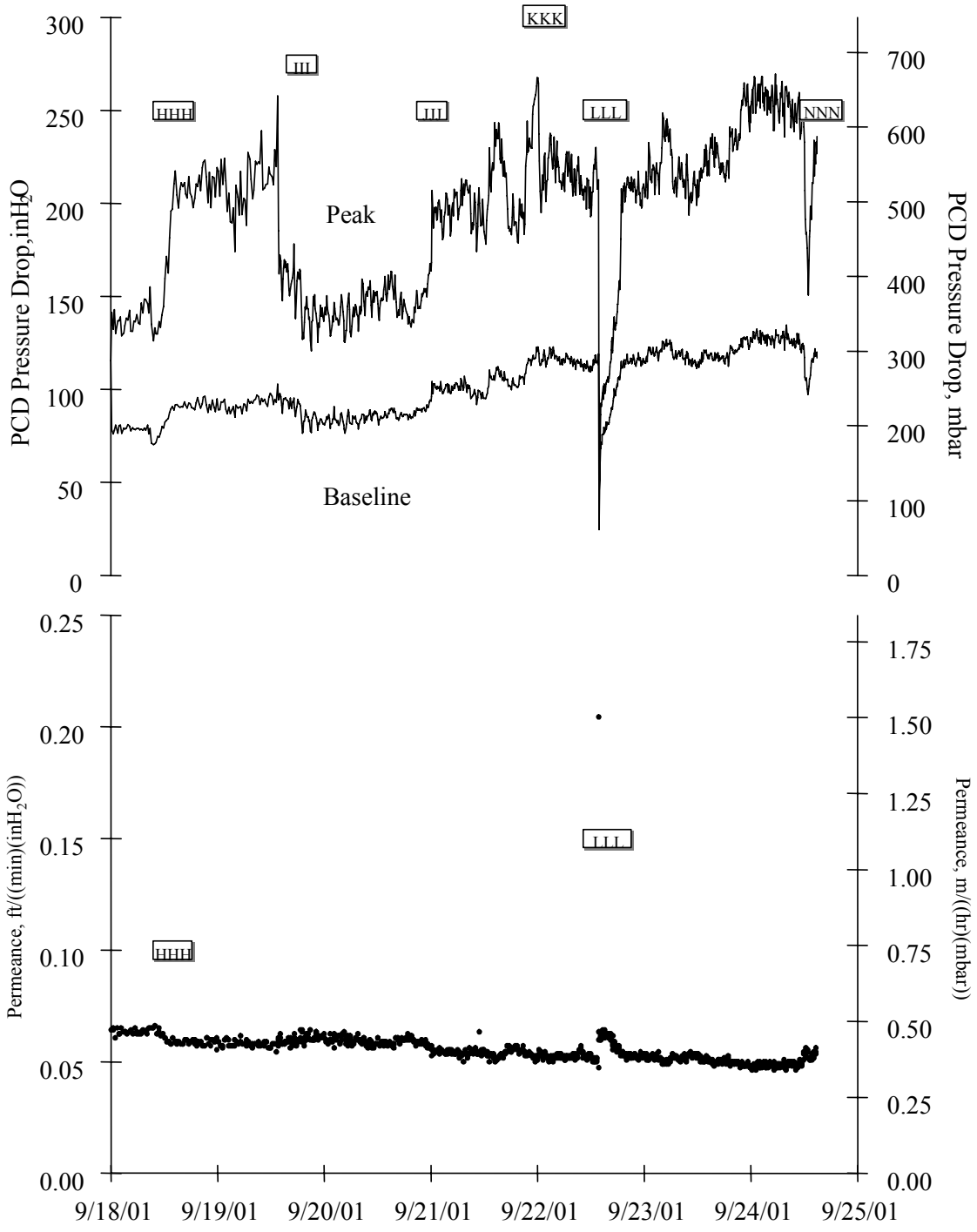

Figure 3.2-26 PCD Pressure Drop and Permeance, September 18, 2001 Through September 25, 2001

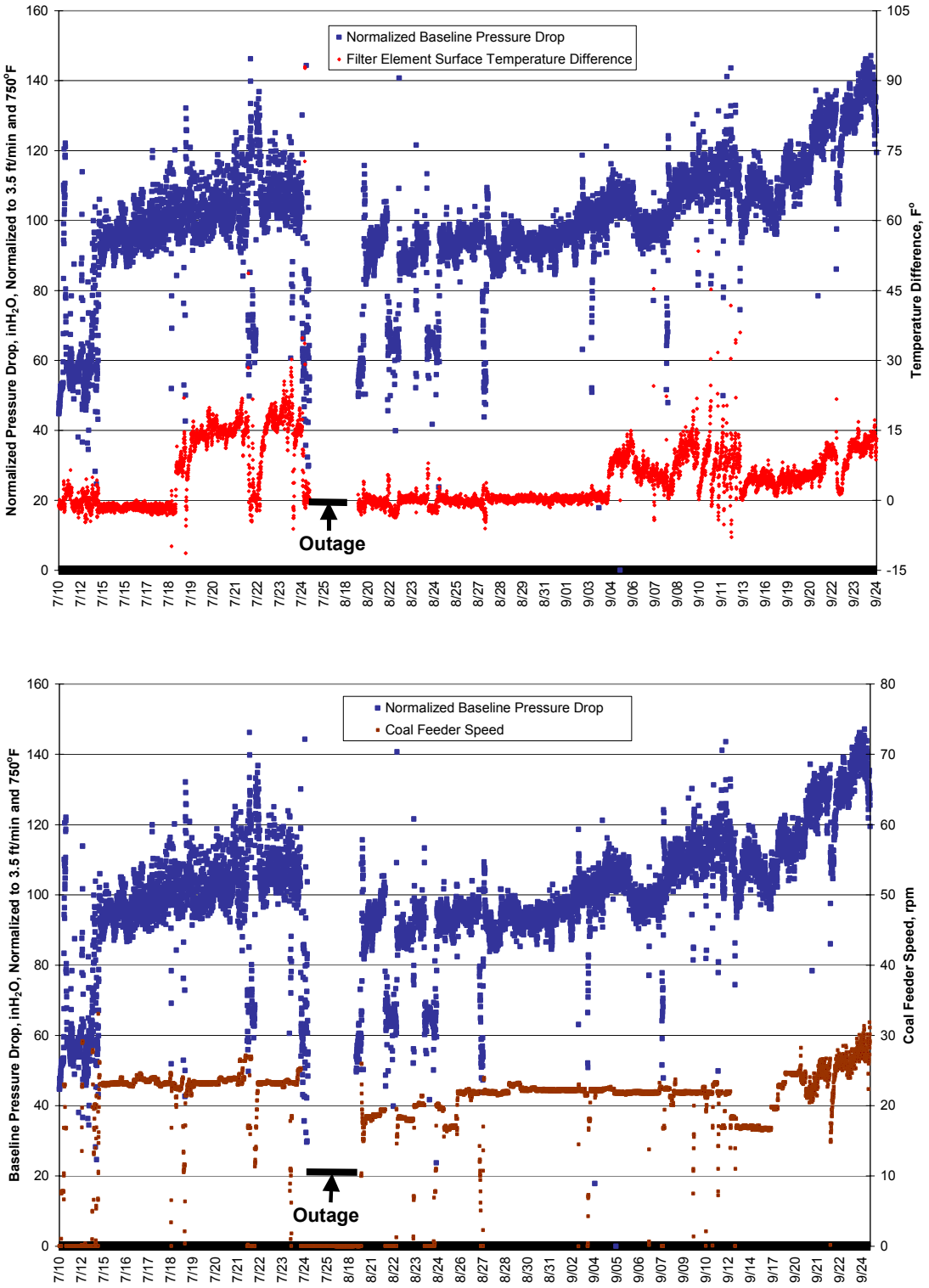

Figure 3.2-27 Normalized Pressure Drop, Filter Surface Temperature Difference, and Coal Feeder Speed

3.3 TC06 INSPECTION REPORT

3.3.1 Introduction

The TC06 test run was divided into two components, TC06A and TC06B. For the PCD, TC06A started on July 6, 2001, and ended on July 25, 2001. During TC06A, the PCD operated approximately 228 on-coal hours. TC06B started on August 18, 2001, and ended on September 24, 2001. During TC06B, the PCD operated approximately 797 on-coal hours. During the TC06 test run, the PCD was exposed to a total of 1,025 on-coal hours. Outage inspections were conducted after both TC06A and TC06B and included examinations of the filter elements, their fixtures to the plenums, solids deposition, filter element gaskets, and auxiliary equipment. This inspection report is divided in two sections. The first section addresses the outage activity after TC06A; while the second section addresses the outage activity after TC06B.

3.3.2 TC06A Inspection

The PCD operated in gasification mode for approximately 228 on-coal hours during TC06A. The PCD operating parameters for TC06A are shown in Table 3.3-1. The outlet loading from the PCD, as measured by SRI, was below 1 ppmw before July 25, 2001. On July 25 SRI measured an outlet loading of approximately 23 ppmw in an off-coal period. The main air compressor was tuned online on July 24, 2001. Oxygen broke through to the PCD and ignited the gasification ash (g-ash) while the air compressor was being tuned. It was believed that one or more filters had failed; therefore, the run was terminated to prevent contamination of unaffected filters by backside blinding. The purpose of this shutdown was to replace the broken filter or filters and start the run again as quickly as possible; therefore, the solids removal system was not inspected.

The PCD was shut down clean, which means the back-pulse system continued to cycle after the coal feed was stopped. The PCD vessel was opened on July 27, 2001. Upon inspection, one filter element was discovered cracked and several were bowed. Based on these findings it was decided to remove 15 filters from the affected area.

3.3.2.1 TC06A Filter Elements

The following filter elements were installed for TC06A: 54 Pall 1.5-meter Fe_3Al; 23 Pall 1.5-meter Fe_3Al with fuse; 5 Pall 2-meter Fe_3Al; 1 Pall 2-meter Fe_3Al with fuse; 5 Pall 1.5-meter Hastelloy X; and 2 U.S. Filter 1.5-meter sintered metal fiber filters (See Figure 3.3-1). The fuse is a safeguard device inserted into the clean side of the filter. In the event of a filter failure the fuse acts as a backup filter.

As mentioned in the Section 3.2, TC06A was ended due to a filter leak. On July 24, 2001, the main air compressor was tuned while online; however, the coal feed was stopped. Originally, it was believed that oxygen would not ignite the g-ash at low temperature. The temperature in the PCD during this time was below 500°F. Around 16:20 on July 24, 2001, the temperature measured by thermocouple TI3025N (B-53) began to increase rapidly after the air compressor tuning began (See Figure 3.3-2). Figure 3.3-2 shows that the temperature measured by this

thermocouple reached approximately 810°F, significantly higher than the inlet gas temperature; therefore, localized combustion was suspected. Figures 3.3-2 and -3 show that TI3025N (B-53) and TI3025J (B-15) were the only two thermocouples that showed a significant response. These thermocouples show the temperature at a single point but it is suspected that the elements reached higher temperatures. Figure 3.3-1 shows that these two filters (B-53 and B-15) were in the same area; therefore, g-ash bridging in that area was suspected. G-ash bridging has been noticed in this area in past run inspections. Also, starting on July 19, 2001, TI3025N and TI3025J began reading temperatures that were different from the other thermocouples on the lower plenum. It is believed that this indicated that these two thermocouples were covered with g-ash; however, the mechanism to explain the different temperatures is not fully understood. After this thermal event the on-line particulate monitor (PCME) indicated a possible leak. SRI verified that there was a leak by taking an outlet sample. The sample revealed that the outlet loading was ~ 23 ppmw. At this point the run was terminated to prevent filter contamination from the backside.

On July 27, 2001, the PCD plenum was removed for inspection. Upon inspection a crack was found near the weld between the top and middle sections of Pall Fe_3Al Element 21076, location B-32 (See Figure 3.3-4). This filter was located in the area where the temperature spike was detected by thermocouples TI3025N and TI3025J. When the support brackets were removed from the bottom of this element and the ones around it, as required for its removal, it became apparent that several elements were bowed (See Figure 3.3-5). The support brackets were then removed from all elements on the bottom plenum to determine how many elements were bowed. Five bowed elements were found, all in the same area and all of the bowed elements were apparently exposed to the temperature spike (See Figure 3.3-6). These five elements were removed and replaced for TC06B. Since the extent of the suspected g-ash bridging and subsequent damage to the filters was not known, 15 filters were removed during this outage. The locations of the elements that were removed are shown in Figure 3.3-6.

After removal, the elements were cleaned by water washing and then inspected. On inspection, a dramatic color pattern was seen. The elements were light colored on one side and bowed toward that side (See Figures 3.3-7 and -8). The light color resulted from combustion of bridged g-ash on the surface of the elements; therefore, these regions reached the highest temperature during the thermal transient. The bowing of the Fe_3Al elements and the failure of the element at location B-32 can be understood from the thermal expansion of this material measured in the SRI lab. Thermal expansion up to 2,100°F, measured during heating up from room temperature and then cooling down, is shown in Figure 3.3-9. In this plot, the change in length divided by original length (that is, the unit thermal expansion) is plotted on the y-axis and temperature on the x-axis. The slope of this curve is the familiar coefficient of thermal expansion. At approximately 1,800°F, the curve measured during heating begins to "roll over." This behavior in thermal expansion is usually an indication of a change in the material such as a phase change. In fact, the Al-Fe phase diagram indicates that a phase change occurs at approximately 1,800°F, the exact temperature depending on the composition. The thermal expansion curve obtained during cooling (Figure 3.3-9) is offset below the curve obtained during heatup. The implication of this is that after the material underwent the phase change at 1,800°F the length was permanently decreased. During the thermal transient of TC06A, one side of the elements (the light-colored side) got hot enough to go through the phase change and the length was permanently changed. The other side did not. Therefore, on cool down after thermal transient,

the elements tended to bow to accommodate the different lengths resulting from one side of the elements undergoing a phase change but not the other side. Since the bottom supports restrained the elements from bowing, one of them failed.

Other than the one failed element and the bowed elements, the Pall Fe_3Al filters performed well during the TC06A gasification run. The remaining Fe_3Al elements were inspected and no obvious damage was found. At this point some of the filters had accumulated 669 on-coal hours while being exposed during GCT3, GCT4, and TC06A.

Five Pall Hastelloy X filters were tested for the first time since GCT1A. During GCT1A the PCD was operating at higher temperatures (> 900ºF). There was concern that the nickel in the filter material would react with the sulfur in the gas at these temperatures and form nickel-sulfide, which would ultimately blind the filter. Since the temperatures were constantly below 800ºF during GCT3 and GCT4 it was decided to start testing the Pall Hastelloy X filters again. Each filter was visually inspected and no obvious damage was found.

Currently, the PSDF is working with U.S. Filter to test new sintered metal fiber filter element materials. Based on their experience with filtration media, U.S. Filter suggested that the following materials be tested:

Fecralloy-M (FeCrAlY).
Haynes Alloy 214.
Haynes Alloy 160.
Haynes Alloy 230.

Sintered metal fiber elements have lower pressure drops than sintered metal powder elements. Only two filters from U.S. Filter were installed for this run. Each filter was constructed from three separate filter sections. These sections were connected to each other by welding the porous media to solid metal rings. One filter was constructed from Fecralloy-M, while the other filter was constructed with the other three remaining alloys (Haynes 214, 160, and 230). In other words, each section was made from a different alloy. This offered the advantage of screening three different filter materials, while using only one filter position. Each filter was visually inspected and no obvious damage was found; therefore, it was decided to continue testing these filters during TC06B.

3.3.2.2 TC06A G-ash Deposition

G-ash bridging was believed to have contributed to the temperature excursion in the PCD; however, upon inspection g-ash bridging was not observed. Figure 3.3-10 shows the bottom plenum being lifted out of the PCD vessel and into the maintenance bay. This figure shows that the filters were relatively clean compared to past gasification runs. During the temperature excursion the bridged material may have dislodged and fallen out or burned out. The material that was left on the filters had a relatively high ash content indicating partial combustion.

The g-ash buildup on the filter element fixtures was light compared to past gasification runs. The g-ash buildup on the top and bottom plenums was not severe. Figure 3.3-11 shows the

accumulated g-ash on the top ash shed. Figure 3.3-12 shows very little g-ash buildup on the inside wall of the shroud. Also, there was very little buildup on the liner sections. The clean side of the tubesheet appeared to be in good shape despite the filter failure. Figure 3.3-13 shows that the insulation on the clean side of the tubesheet was relatively clean. Figure 3.3-14 shows the condition of the insulation in the PCD head. The insulation reveals the g-ash penetration in that area was not significant. The shiny scale material detected in GCT3 and GCT4 was not found after this run. Before this run a coke breeze feeder system was installed to help prevent tar formation. The existing start-up burner on the Transport Reactor can raise the reactor temperature to around 1,000°F. In the past, coal has been fed after the reactor temperature exceeded 1,000°F. While the reactor was heating up to 1,600 from 1,000°F on coal, tars were produced because there was not enough energy to crack them. It is suspected that these tars condense during the back-pulse, leaving the shiny scale that has been noted. The coke breeze is fed to the reactor once the reactor reaches 1,000°F. When the reactor reaches 1,600°F coal is introduced to the reactor and the coke breeze system is shut down. The coke breeze feeder addition appears to have solved the tar formation problem.

3.3.2.3 TC06A Filter Element Gaskets

One of the test objectives for the PCD during TC06A was to continue evaluating the Siemens Westinghouse lapped construction gaskets. These gaskets have performed very well since testing began during GCT1B. The gasket types used during TC06A are:

Gasket Type	Gasket Location	Function
Lapped construction	Plenum-to-failsafe	Sealing
Top donut	Failsafe-to-failsafe holder	Sealing
Bottom donut (No.1)	Failsafe holder-to-element	Sealing
Bottom donut (No.2)	Filter nut-to-element	Nonsealing
Sock gasket	Element-to-bottom donut gasket	Nonsealing

During this outage only 17 filter elements were inspected. Therefore, the inspection of the gaskets was not extensive. However, the following observations were made based on the gaskets that were examined:

- There were no leak paths in the area of the failsafe holder flanges that would indicate a leak past the primary gasket.
- Some lapped construction gaskets had broken fibers. This did not appear to affect the sealing capability of the gasket. It is possible that the fibers were damaged during removal.
- Some of the gaskets were cut to inspect the extent of g-ash penetration. The inside of the sealing gaskets were relatively clean.
- The gaskets above the failed filter were dirty, which was expected.

3.3.2.4 TC06A Failsafes

Thirteen failsafe devices were removed during this outage. Several screens on top of the Siemens Westinghouse designed failsafes were found damaged. The failsafe device that was in the B-52 position had the most damage. There were large holes in the top and bottom screens. There was a large amount of rust on top of the failsafe device. It is believed that the rust came from the carbon steel back-pulse pipes used before the carbon steel pipe was replaced with stainless steel for TC06. The mechanism that caused damage to the failsafe device screens is not understood; therefore, the failsafe above B-52 was sent to Siemens Westinghouse for further inspection.

The failsafe device above the Fe_3Al filter that failed was removed and flow tested. This failsafe was a standard Siemens Westinghouse design. The flow coefficient was 11.2 $lb/(hr\text{-}(lb/ft^3)\text{-}inH_20)^{0.5}$ compared to an average of 133.7 $lb/(hr\text{-}(lb/ft^3)\text{-}inH_20)^{0.5}$ for a clean failsafe device; therefore, the flow coefficient of the plugged failsafe was about 8 percent of the clean failsafe value. Based on the flow test values, the Siemens Westinghouse failsafe device appeared to have at least partially plugged; however, as mentioned above the outlet loading after the thermal event was ~23 ppmw. These results imply that failsafe research is still necessary.

3.3.2.5 TC06A Auxiliary Equipment

Prior to TC06, 14 thermocouples were installed on individual filter elements to monitor local temperatures. During this outage all of the thermocouples were tested to check for damage. No damage was detected; therefore, all of the thermocouples were reused. Starting with GCT2 all the thermocouple wires were routed from the dirty side of the PCD directly to atmosphere through a nitrogen purged flange on the PCD. The thermocouple wires were sealed using Conax fittings with Teflon sealant. This arrangement has been successful in all the gasification runs since GCT2. During the outage, the Conax fittings were inspected. They appeared to be in good condition and were reused.

The back-pulse pipes inside the PCD head were also inspected. There was a slight discoloration on the back-pulse pipes; however, there was no tar buildup. The inner line of the back-pulse pipes appeared to be in good condition.

3.3.2.6 TC06A Solids Removal Equipment

Since the solids removal equipment performed well during the first 228 hours of TC06, it was decided to postpone any inspection. During TC06A the screw cooler required very little attention. Periodically, maintenance personnel would tighten down the packing follower to seal minor leaks. Also, the lock-vessel (FD0520) system was not disassembled because it performed well during TC06A with one exception. During startup at the beginning of TC06A the conveying line between FD0520 and FD0530 plugged. During this outage the seal on the spheri valve was tested and it checked out; therefore, it was decided to keep running FD0520 without disassembling the system.

3.3.3 TC06B Inspection

The PCD operated in gasification mode for approximately 797 on-coal hours during TC06B. The PCD parameters for TC06B are shown in Table 3.3-2. The outlet loading from the PCD, as measured by SRI, was less than 1 ppmw throughout TC06B. The PCD was shut down dirty after the coal feed was stopped. This allowed SRI to collect transient dustcake samples. The PCD vessel was opened on September 27, 2001. The initial inspection revealed a large amount of g-ash bridging on the lower plenum. During this outage 34 filter elements were removed.

3.3.3.1 TC06B G-ash Deposition

Figure 3.3-15 shows the severity of the g-ash bridging as the plenum was lifted out of the PCD vessel. Once the plenum was set in the maintenance bay, inspection of the PCD internals continued. The g-ash bridging was isolated to the lower plenum. Figure 3.3-16 is a filter layout that shows where the g-ash bridging was found on the lower plenum. The numbers around the layout designate how far down the length of the filter the g-ash penetrated. Figure 3.3-17 shows the extent of the g-ash bridging in the area of TI3025J. On September 4, 2001, the temperature from this thermocouple began to deviate from the other thermocouples. This relationship between temperature deviation and g-ash bridging has been noticed, but no satisfactory explanation for the temperature deviation has been found.

Since this was the fourth time that g-ash bridging was either detected or suspected during a gasification run, several suggestions to address the g-ash bridging issue were explored. These suggestions included:

- Install a soot blower: A soot blower would involve blowing high-pressure nitrogen through nozzles strategically placed immediately below the tubesheet to remove g-ash bridging. A feasibility test was conducted on the g-ash bridging material that was found on the lower plenum after shutdown. A soot blower lance was constructed with a 1/8-inch diameter nozzle that could be directed downward from the top of the g-ash bridge. The high-pressure air (100-psig service air) did not remove the g-ash bridging. It was found that the soot blower was effective in removing the deposit only within about 1 foot of the nozzle exit. Therefore, it was determined that once the g-ash bridging forms it will be difficult to remove with a soot blower. Based on these results it was suggested that the soot blower should be used to prevent the g-ash bridging from ever forming. In other words, a soot blower should be installed and cycled periodically (or continuously) to keep the material from consolidating. However, it was concluded that by preventing the formation of g-ash bridging, a learning opportunity would be missed since the g-ash bridging mechanism is not understood.

- Remove all 2-meter filter elements: One possible mechanism that has been suggested for the formation of the g-ash bridge was that the back-pulse gas intensity was not evenly distributed due to the 2-meter filter elements. All six 2-meter filter elements from TC06 will be replaced with 1.5-meter elements for TC07.

- Remove tie wire: Tie wire is currently used to secure the metal filter elements in the event of a filter failure. Originally, there were some concerns that a failed metal filter element would damage the screw cooler (FD0502). Since the filter elements are secured at the bottom by the support pins, the relative risk of filters failing and falling into the screw cooler is low; therefore, the tie wires will be removed for TC07. The thought behind removing the tie wire is to remove any object that would possibly facilitate g-ash bridging.

- Determine how the g-ash bridge forms: Instrumentation to measure the pressure inside the filter elements during TC07 will be installed. Since bridging has consistently been seen in certain areas, test measurements will be made in an area where g-ash bridging has not been detected and an area where g-ash bridging is normally seen. The pressure measurements will be made inside the filter element to test this theory of preferential flow during a back-pulse. In addition to pressure measurements, thermocouples will be inserted into the filter elements to monitor the temperature. Also, before TC07, 12 additional thermocouples will be installed. Currently, the PCD divides 14 thermocouples evenly between the top and bottom plenums. For TC07, 3 thermocouples will be installed on the top plenum and the remaining 23 thermocouples will be installed on the bottom plenum. The purpose for these thermocouples is to determine where the g-ash bridging originates.

- Maintain constant back-pulse timer and test higher back-pulse pressures: During the next run the back-pulse time interval will be set and maintained at 5 minutes. Also, higher bottom plenum back-pulse pressure will be used to account for the 55-to-36 filter element ratio on the bottom and top plenums.

Hopefully, the changes made during this outage, such as removing the 2-meter filter elements and tie wires, will prevent g-ash bridging during TC07; however, if the g-ash bridging occurs, then the addition of pressure and temperature measurements will produce some understanding behind the g-ash formation mechanism.

Upon inspection of the filter elements, the g-ash was noticed to be very fluffy. According to SRI this was the first time that they were able to take dustcake samples by simply brushing the samples off. In the past the g-ash has been very adherent to the filter elements. It is believed that in the past tar condensation in the PCD made the dustcake on the filter elements very sticky. Figure 3.3-18 shows the filter elements after they were cleaned off with an air cannon. In the past the only method to clean the filter elements with a dustcake that was very adherent was pressure washing. It appears that the addition of the coke breeze feeder helped reduce tar, which resulted in this less adherent g-ash. See Section 3.4 for more details concerning dustcake properties.

Figure 3.3-19 shows a large amount of g-ash buildup on the filter element on the lower plenum. Figure 3.3-20 shows very little g-ash buildup on the lower support brackets. The g-ash buildup on the top plenum was relatively small. Figures 3.3-21 and -22 show the accumulated g-ash on the top and bottom ash shed, respectively. Figure 3.3-23 shows that there was very little g-ash buildup on the inside wall of the shroud. Also, there was very little buildup on the liner sections.

The clean side of the tubesheet appeared to be in good condition. Figure 3.3-24 shows that there was very little g-ash penetration to the insulation on the clean side of the tubesheet. Figure 3.3-25 shows the condition of the insulation of the PCD head.

3.3.3.2 TC06B Filter Elements

Figure 3.3-26 shows the filter layout for TC06B. Upon initial inspection all the filters appeared to be intact and undamaged; however, there was a considerable amount of g-ash bridging. Once the upper and lower plenums were cleaned each filter element was visually inspected.

During TC06B, 40 Pall 1.5-meter Fe_3Al filter elements; 38 Pall 1.5-meter Fe_3Al filters with fuse; 4 Pall 2-meter Fe_3Al filters with no fuse; and 2 Pall 2-meter Fe_3Al filters with fuse were used. The filter elements were visually inspected and no obvious damage was found. During this outage, 37 Pall Fe_3Al filters were removed. All filter elements were considered clean on the inside, which means that no loose g-ash was found inside any of the elements. After TC06B some of the Fe_3Al filters had accumulated 1,450 on-coal hours. Four of the Fe_3Al filters that were removed were sent to SRI for material testing. Test results from these elements will be provided in the TC07 run report.

During TC06B, four Pall 1.5-meter Hastelloy X filters were tested. The filter elements were visually inspected and no obvious damage was found. During this outage, two Pall 1.5-meter Hastelloy X filters were removed. All the filter elements were considered to be clean on the inside. After TC06B, 3 of the 4 Pall Hastelloy X filter elements had accumulated 1,025 on-coal hours.

During TC06B, two 1.5-meter U.S. Filter filter elements were tested. PSDF is currently working with U.S. Filter to test new filter element materials. Both filter elements were sintered metal fiber filters. The material of construction for one filter was Fecralloy-M. The materials of construction for the other filter were Haynes Alloys 214, 160, and 230. Each filter was visually inspected and no damage was noticed. Since this was the first time that either of these materials were tested at the PSDF, two Pall fuse safeguard devices were modified and installed above each filter. During the inspection each failsafe was removed and inspected. Each failsafe appeared to be clean, which indicated that the new filter elements did not leak. The materials of construction were chosen based on their corrosion resistance in reducing environments. Each of these filters was sent back to U.S. Filter for further testing to see if the materials had degraded or blinded. Based on their recommendations, further material testing will be pursued.

During this outage all of the bottom support brackets were removed to inspect the filters for bowing. Five of the 1.5-meter Fe_3Al filters bowed during TC06A as a result of the thermal incident. After the support brackets were removed no bowing was observed.

3.3.3.3 TC06B Filter Element Gaskets

During this outage 44 filter elements were removed and inspected. Also, 16 failsafe devices were removed and inspected. As each filter and failsafe device was inspected the filter element

gaskets were inspected as well. The gasket types are outlined in Section 3.3.2.3. Based on the inspection of these gaskets, the following observations were made:

- There were no leak paths in the area of the failsafe holder flanges that would indicate a leak past the sealing gasket.
- Some of the gaskets were cut to inspect the extent of the g-ash penetration. The inside of the sealing gaskets were relatively clean.
- The gaskets between the failsafe and plenum were clean.

The gasket material performed well throughout the 1,025 on-coal hours. This is based on the fact that the outlet loading was below 1 ppmw.

3.3.3.4 TC06B Failsafes

During TC06B four different types of failsafe devices were tested. These failsafe devices included:

- Standard Siemens Westinghouse failsafe device.
- New prototype Siemens Westinghouse failsafe device.
- Pall fuse.
- PSDF-designed failsafe device.

During this outage 16 failsafe devices and 17 Pall Fe_3Al filters with fuses were removed and inspected.

One standard Siemens Westinghouse failsafe device was removed. It was inspected and no evidence of damage was observed. Also, several filter elements that were below the standard failsafe design were removed and from that perspective the failsafe devices appeared to be in good condition.

During this outage nine of the new prototype Siemens Westinghouse failsafe devices containing metal fiber made from a variety of alloys were removed. These failsafe devices were weighed and flow tested. All of the failsafe devices, with the exception of one, weighed between 0.1 to 0.3 grams less than they did after GCT2. The other failsafe weighed 2.3 grams less than after GCT2. All the failsafe devices, with the exception of one, had flow coefficients that were lower than the flow coefficients that were measured after GCT2 by 1 to 6 percent. The reduction in flow coefficients was thought to be due to settling of the fiber rather than fouling. These failsafe devices will be installed for further testing. The failsafe device that weighed 2.3 grams less had a flow coefficient that was 5 percent higher than that measured after GCT2. It appears that the failsafe has lost some material. This failsafe device will not be installed in the next run.

The Pall Fe_3Al filters that were removed and had a fuse were inspected. All the fuses appeared to be in good condition and intact. Inspection of the filtering side of the fuse is not possible without destroying the filter, so conclusive comments with respect to the fuses are not possible at this time.

Before TC06A, four PSDF-designed failsafe devices were installed for snygas exposure testing. The purpose of this initial test was to determine whether or not this new design would be able to handle the severe conditions of gasification environment and back-pulse events while maintaining its mechanical integrity. After TC06B, the PSDF-designed failsafe devices were removed and inspected and appeared to be in good condition with no evidence of failsafe corrosion or damage. Based on these initial test results, further testing on these failsafe devices will continue.

3.3.3.5 TC06B Auxiliary Equipment

The filter element surface thermocouples that were also used during TC06A were used during TC06B. During this outage the thermocouples were inspected and no damage was noticed. The thermocouples were installed on individual filters to monitor the local temperatures. It is believed that the thermocouples will play a key role in determining the mechanism of g-ash formation; therefore, 26 thermocouples will be installed prior to TC07.

The back-pulse pipes were removed and inspected during this outage. Inspection of the back-pulse pipes didn't reveal any significant damage. There was no significant tar buildup on the pulse pipes and the inner liner appeared to be in good condition. Figure 3.3-27 shows the condition of the back-pulse pipes after TC06B.

During the outage it was noticed that the two 4-inch carbon steel pipe studs that the pulse pipes pass through on the PCD head were badly corroded. In the past, scale has been reported on top of the failsafes; therefore, the pipe studs were replaced with 310 stainless steel during this outage. The lengths of the new pipe studs were adjusted using field measurements to maintain the specified gaps between the ends of the pulse pipes and the venturi inlets.

During the last two gasification test runs, the ball valves (SV3104A and SV3106B) upstream of the back-pulse valves (SV3111A and SV3112A) had problems closing when the back-pulse pressure was higher than 600 psid. During this outage the ball valves were replaced. The new valves should allow back-pulse testing at higher pressures during TC07.

3.3.3.6 TC06B Fine Solids Removal System Inspection

The fine solid removal system performed well during TC06. During the TC06B outage, the spent fines removal system was thoroughly inspected. The inspection included disassembling the screw cooler and the lock vessel system.

The screw cooler (FD0502) performed well during TC06 based on the fact that after 1,025 on-coal hours, FD0502 did not fail. Other than minor packing adjustments, the screw cooler required no maintenance. During the outage FD0502 was disassembled and inspected. A large

amount of g-ash was caked up in the screw cooler and in the drop pipe to the lock-vessel system. This cake was very wet and had the consistency of mud. The primary gas cooler had a leak in a couple of the tubes. It is believed that at the end of the run the steam being injected into the process through these leaks condensed once the temperature dropped during shut down. The condensation caused the g-ash to plug the screw cooler.

The packing rings appeared to be in good condition. Also, the stuffing box was inspected and no damage was noted (See Figure 3.3-28). The wear sleeve and shaft appeared to be in good condition as well (See Figures 3.3-29 and -30).

In an attempt to increase reliability, several modifications were made to the stuffing box during this outage. The lantern ring was increased to ¾ from ½ in. to allow for more adjustment room. Also, the current stuffing box had the lantern ring positioned with five packing rings on each side of it. In order to add flow resistance and keep the purge gas toward the system instead of escaping to the atmosphere, the lantern ring was moved so that there were two packing rings between the lantern ring and the system. Therefore, eight packing rings were between the lantern rings and the outside of the system. Once again, this was done to promote purge gas flow in toward the system. Finally, the packing follower and guide studs were extended to allow more room to adjust the follower.

During this outage a Teflon plate was installed internally on the shaft of FD0502 on the outlet end. It is believed that as the drop-pipe between the screw cooler and the lock-vessel fills, solids are forced by the screw cooler into the packing, which ultimately contributes to failure. The Teflon plate was installed to act as a deflector and keep the solids out of the packing. It is believed that these modifications will keep the solids out of the packing and lead to increased reliability.

The lock-vessel (FD0520) system performed well during TC06B. There was one incident where solids carryover overloaded the lock-vessel system and caused the outlet pipe to plug. Since GCT1A, the FD0520 system has cycled over 49,000 times. During the inspection the drop pipe between the screw cooler and the lock vessel was plugged with the wet g-ash. Figures 3.3-31 and -32 show how severe the solid packing was during the inspection. Once the solids were removed, the upper and lower spheri valves were inspected. The upper spheri valve appeared to be in good condition (See Figure 3.3-33). There was no scoring or sign of solid penetration past the dome valve. Also, the upper spheri valve inflatable seal was inspected and no visible damage was noticed (See Figure 3.3-34). The top ring plate was inspected and no damage was noted (See Figure 3.3-35). Next the lower spheri valve was inspected. The lower dome valve was in good condition and no damage was noted. The lower spheri valve inflatable seal was inspected and no sign of g-ash penetration was noted. The ring plate was inspected and no sign of damage was observed. Since all of the components appeared to be in good condition, they were reinstalled for TC07.

Table 3.3-1

TC06A PCD Operating Parameters

Element Layout	Layout 20 (Figure 3.3-1)
Filtration Area	261.3 ft^2
Back-pulse Pressure	200 to 400 psig Above Reactor Pressure (Approximate)
Back-pulse Timer	Set to 5 min (Varied Between 5 and 20 min)
Back-pulse High-Pressure Trigger Point	250 to 275 inH_2O
Back-pulse Valve-Open Time	0.2 sec
Inlet Gas Temperature	750 to 800°F (Approximate)
Face Velocity	3 to 4 ft/min (Approximate)
Baseline DP	80 to 140 inH_2O (Approximate)
Peak DP	140 to 270 inH_2O
Inlet Loading (SRI Sampling)	7,000 to 18,800 ppmw
Outlet Loading (SRI Sampling)	0.10 ppmw (During Normal Operation) and 22.9 ppmw (When Leaking Due to Filter Element Failure)
Coal/Sorbent	PRB/Dolomite

Table 3.3-2

TC06B PCD Operating Parameters

Element Layout	Layout 21 (Figure 3.3-26)
Filtration Area	261.3 ft^2
Back-pulse Pressure	200 to 400 psig Above Reactor Pressure (Approximate)
Back-pulse Timer	Set to 5 min (Varied Between 5 and 20 min)
Back-pulse High-Pressure Trigger Point	250 – 275 inH_2O
Back-pulse Valve-Open Time	0.2 sec
Inlet Gas Temperature	670 to 750°F (Approximate)
Face Velocity	2.3 to 4 ft/min (Approximate)
Baseline DP	80 to 125 inH_2O (Approximate)
Peak DP	140 to 275 inH_2O
Inlet Loading (SRI Sampling)	9,300 to 17,000 ppmw
Outlet Loading (SRI Sampling)	$<$ 0.1 ppmw
Coal/Sorbent	PRB/Dolomite

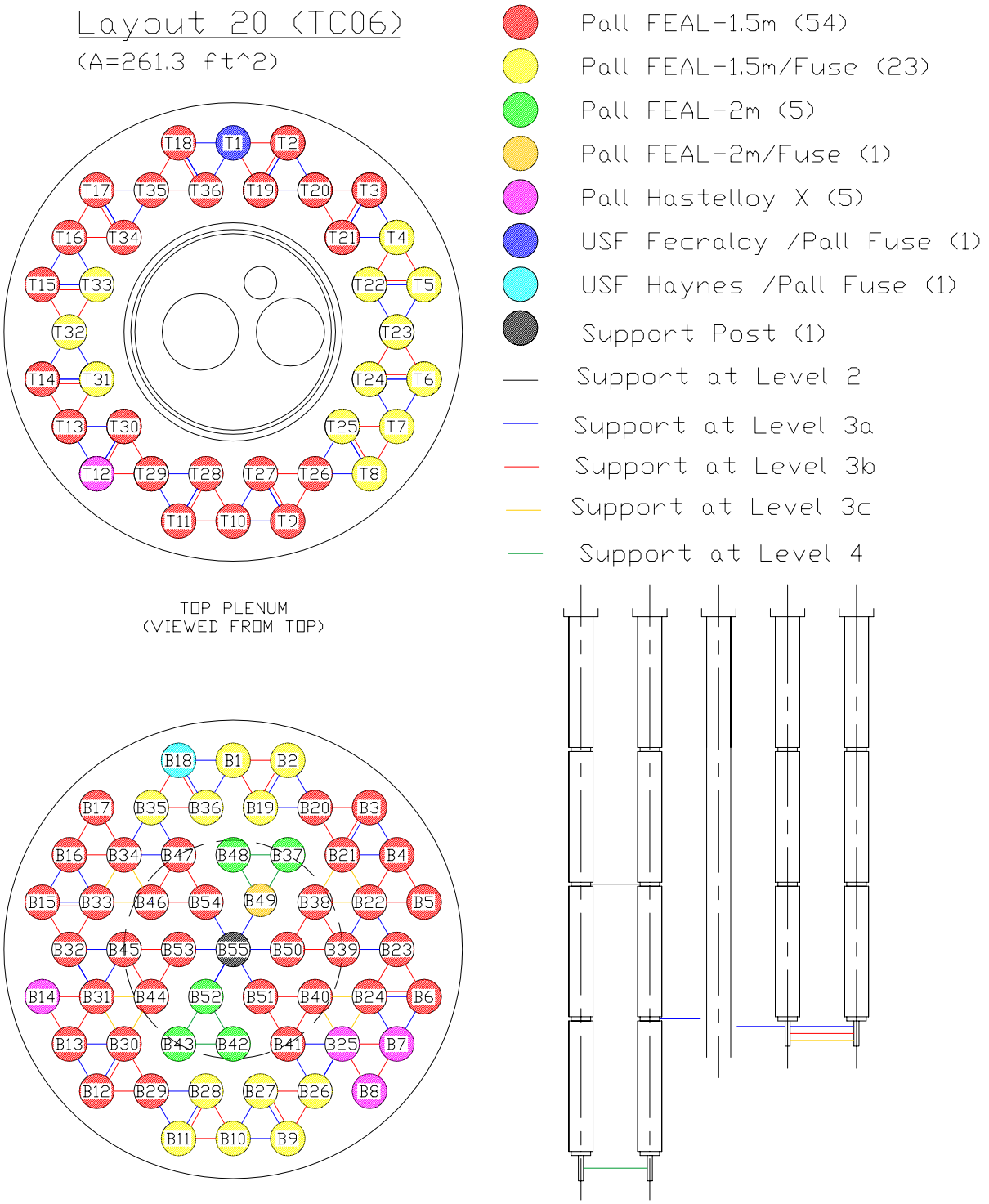

Figure 3.3-1 TC06A Tubesheet Layout

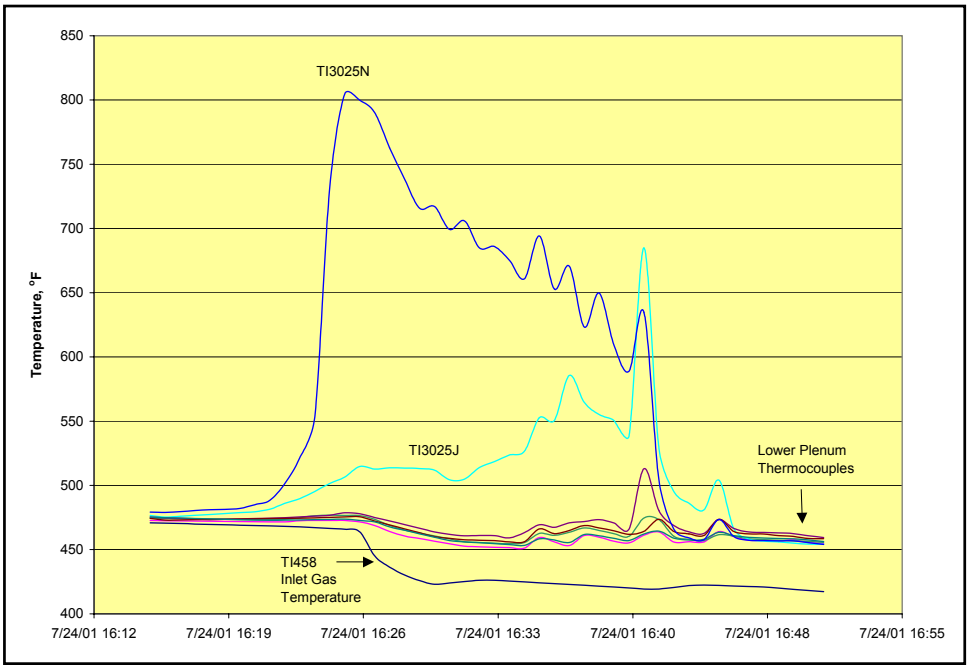

Figure 3.3-2 Temperature Excursion on the Lower Plenum

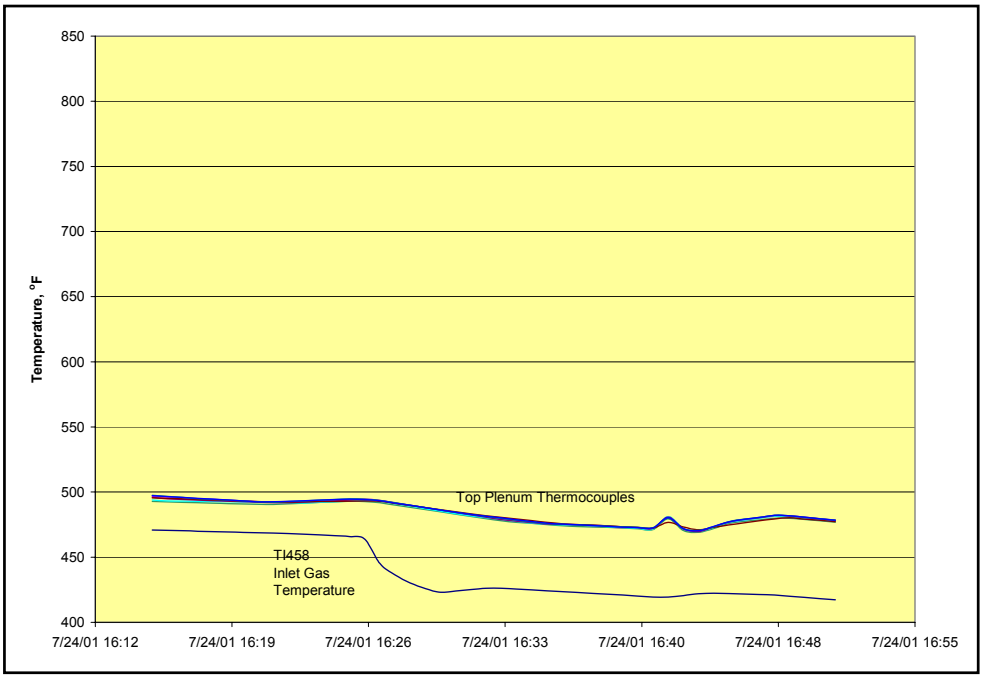

Figure 3.3-3 Top Plenum Response During the Temperature Excursion

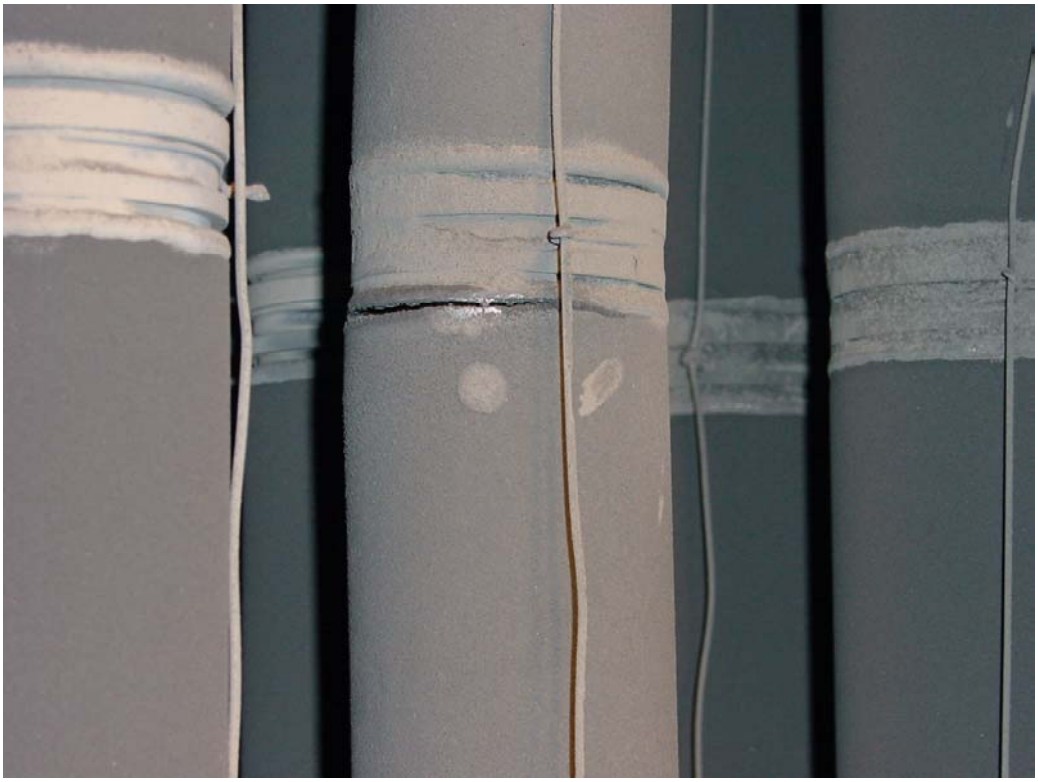

Figure 3.3-4 Failed Fe_3Al Filter (B-32)

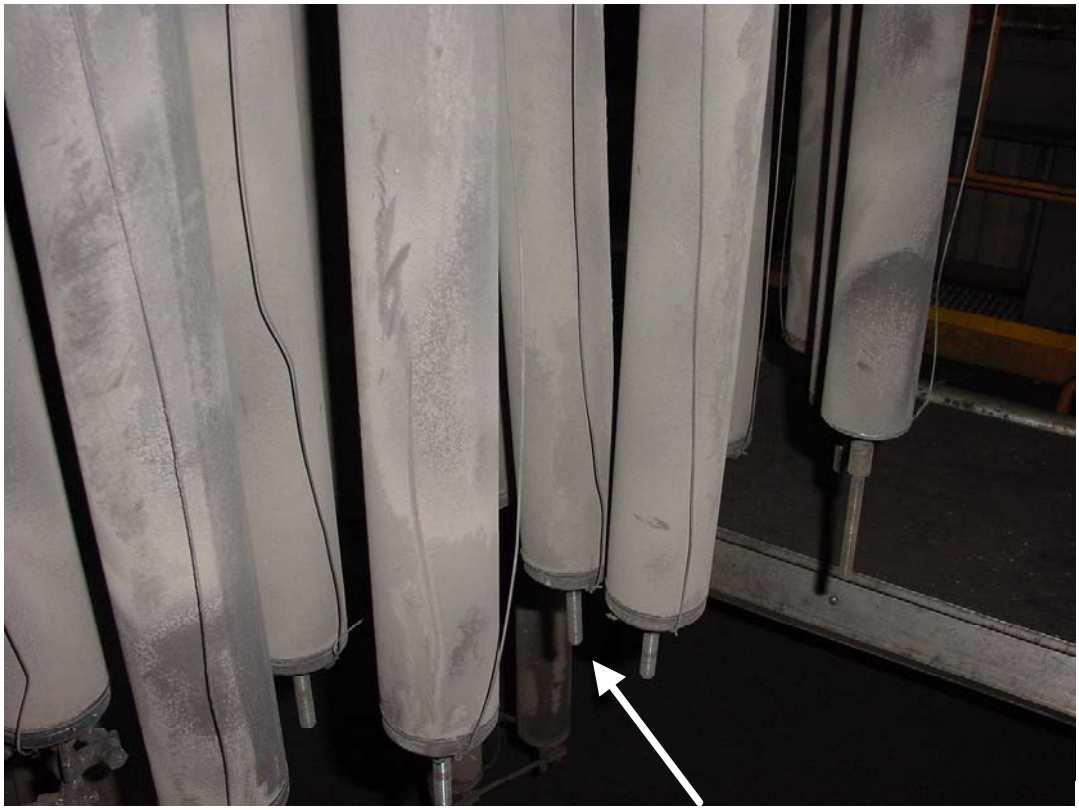

Figure 3.3-5 Bowed Fe_3Al Filters on Lower Plenum

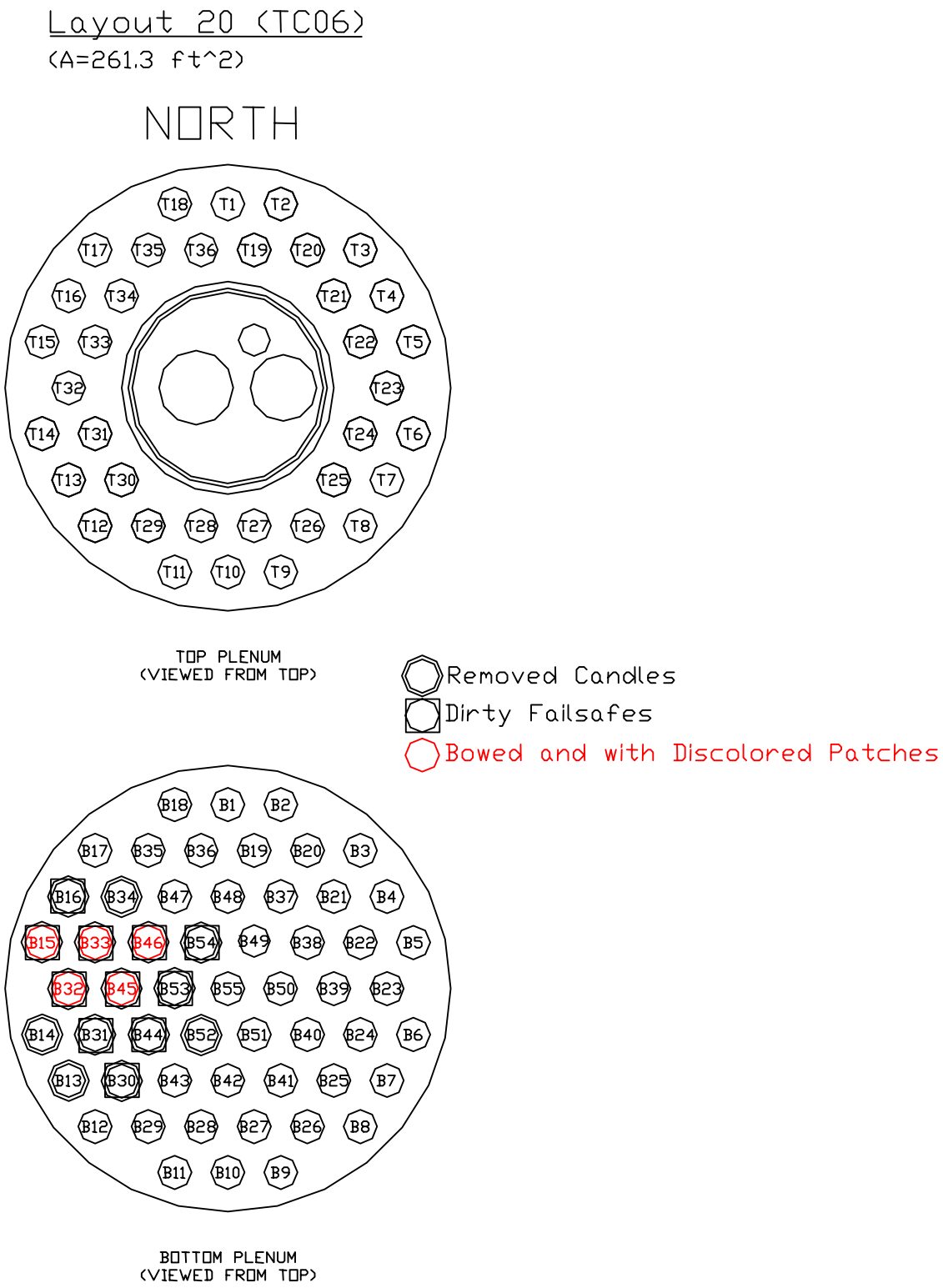

Figure 3.3-6 Filter Layout of Bowed Filters

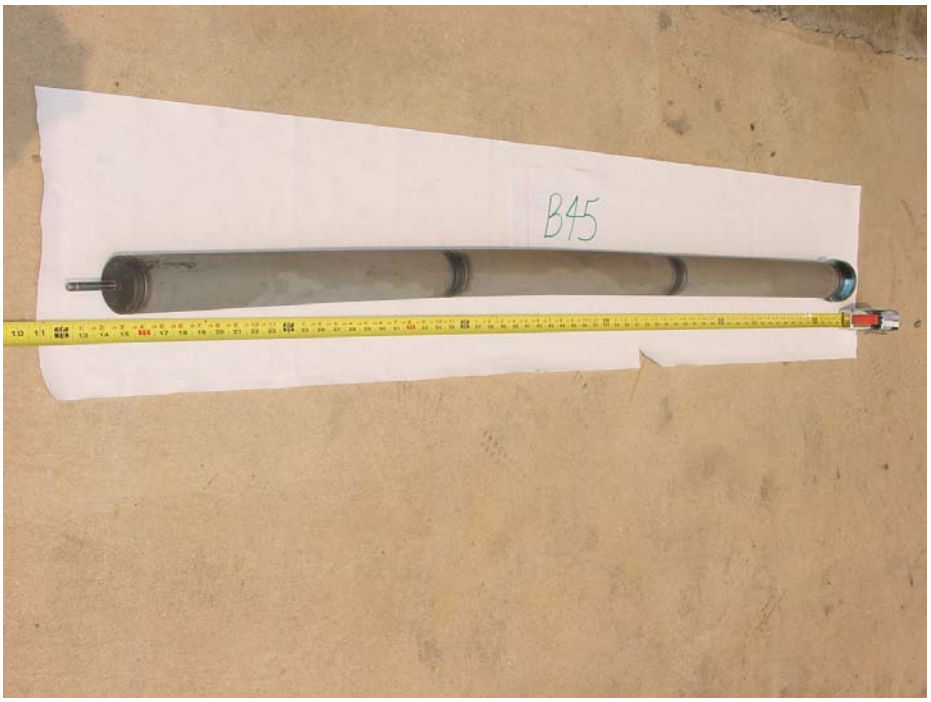

Figure 3.3-7 Abnormal Color Pattern After TC06A

Figure 3.3-8 Abnormal Color Pattern After TC06A

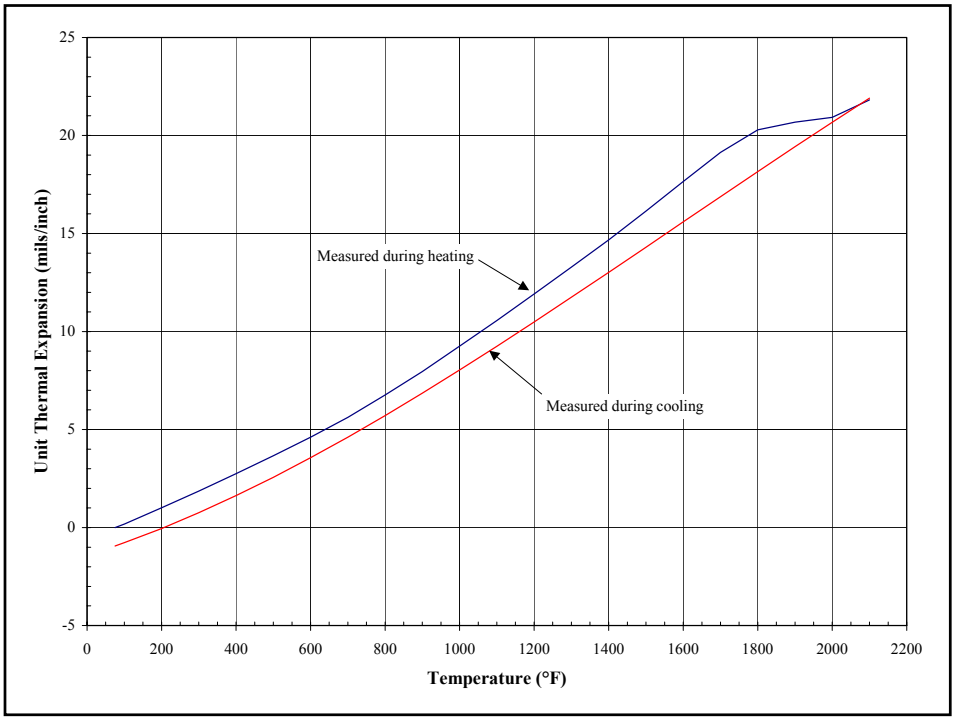

Figure 3.3-9 Thermal Expansion Test Results

Figure 3.3-10 PCD Internal Removal (Lower Plenum)

Figure 3.3-11 G-ash Accumulation on Top Ash Shed

Figure 3.3-12 PCD Internal Shroud and Liner

Figure 3.3-13 Tubesheet Insulation

Figure 3.3-14 Insulation in the Head of the PCD

Figure 3.3-15 Removal of PCD Internals After TC06B

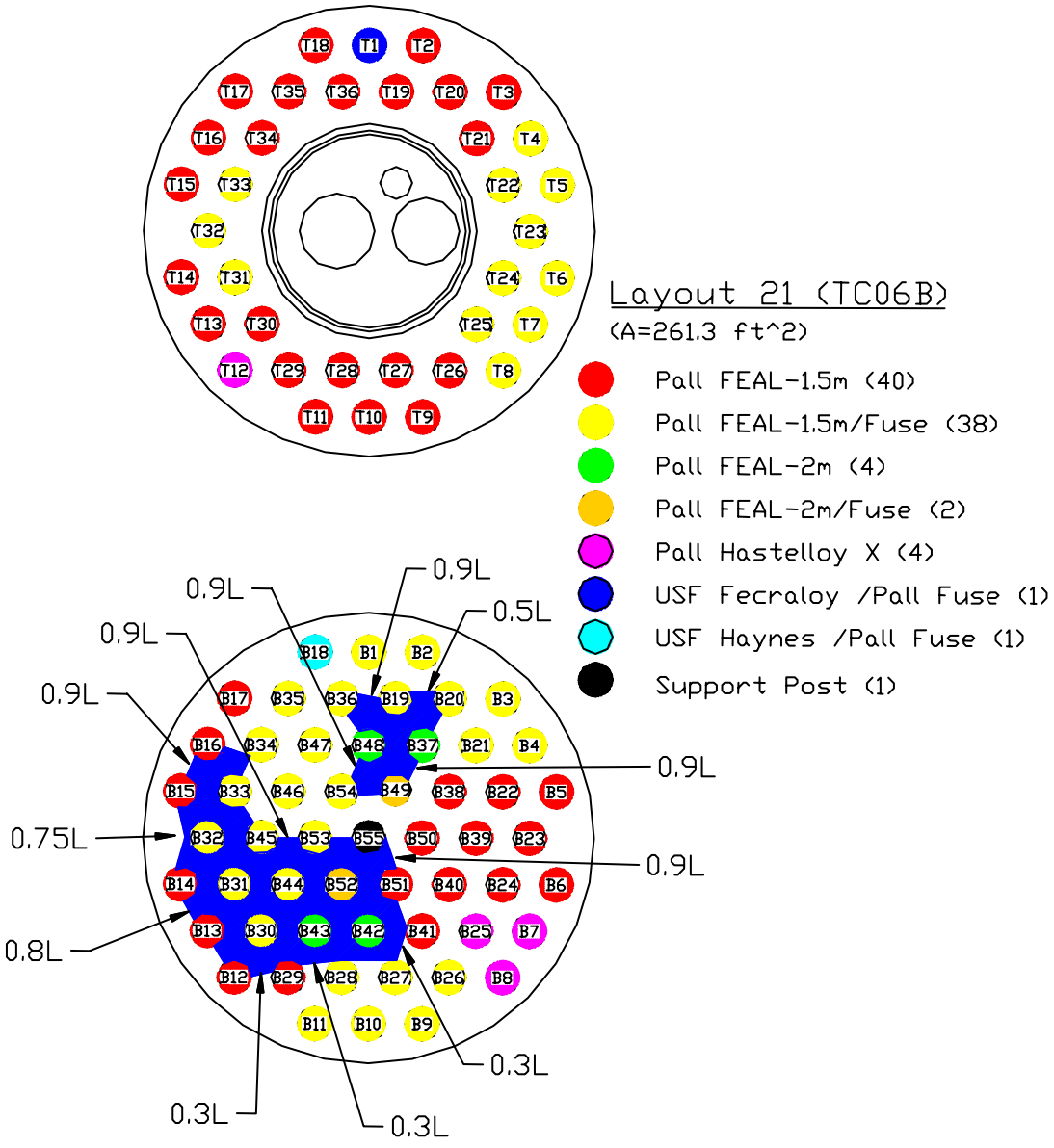

Figure 3.3-16 Location of G-ash Bridging After TC06B

Figure 3.3-17 G-ash Bridging Over TI3025J

Figure 3.3-18 Filters After Being Cleaned With Air

Figure 3.3-19 G-ash Buildup on Filter Element Fixtures

Figure 3.3-20 G-ash Buildup on Lower Support Brackets

Figure 3.3-21 G-ash Buildup on Top Ash Shed

Figure 3.3-22 G-ash Buildup on Bottom Ash Shed

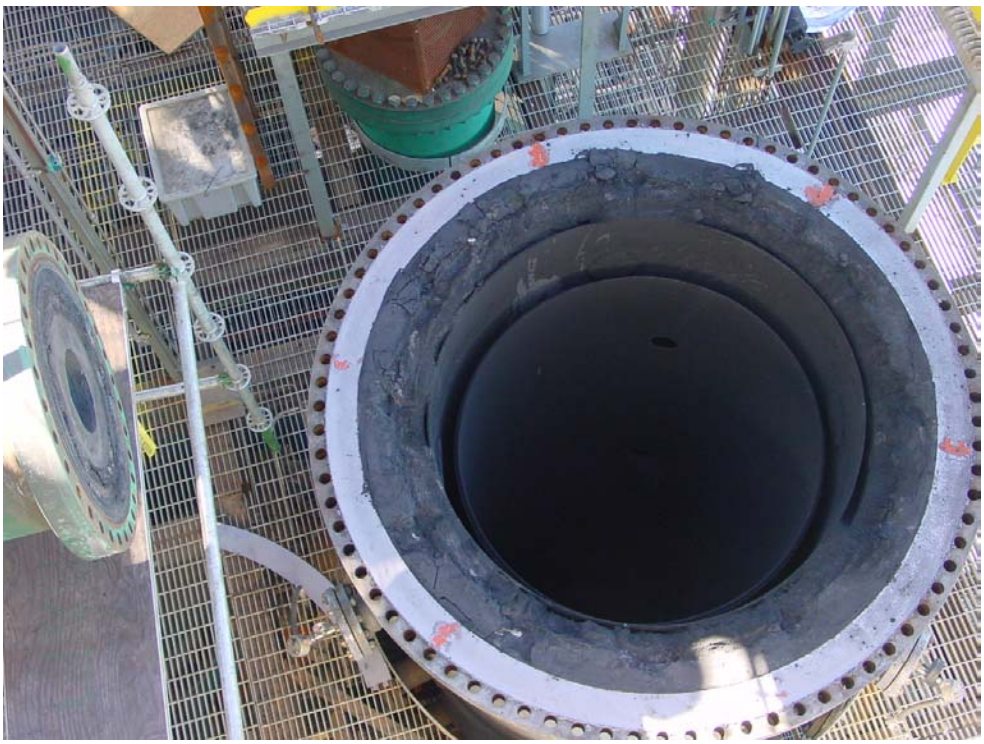

Figure 3.3-23 PCD Shroud and Liner

Figure 3.3-24 Tubesheet Insulation

Figure 3.3-25 PCD Head Insulation

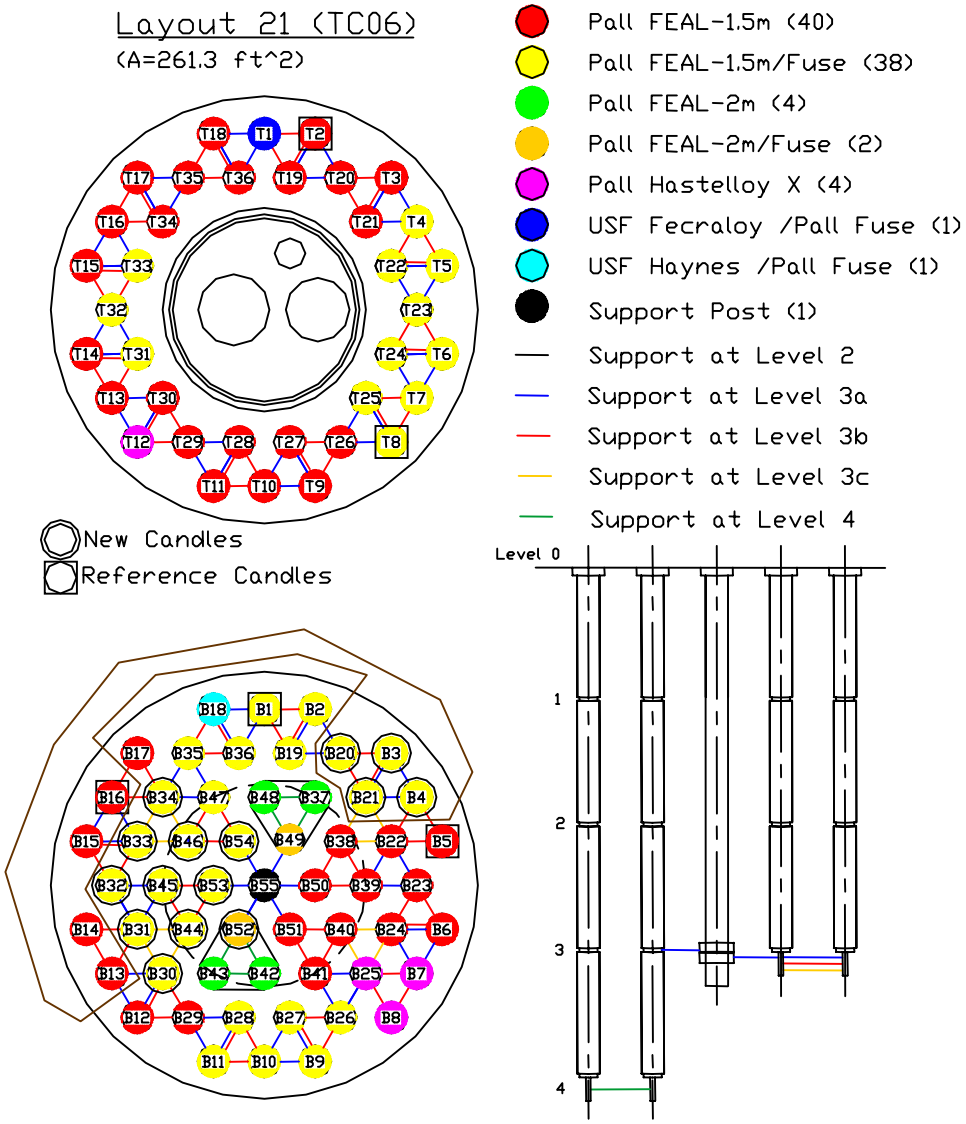

Figure 3.3-26 TC06B Filter Element Layout

Figure 3.3-27 Back-Pulse Pipes After TC06B

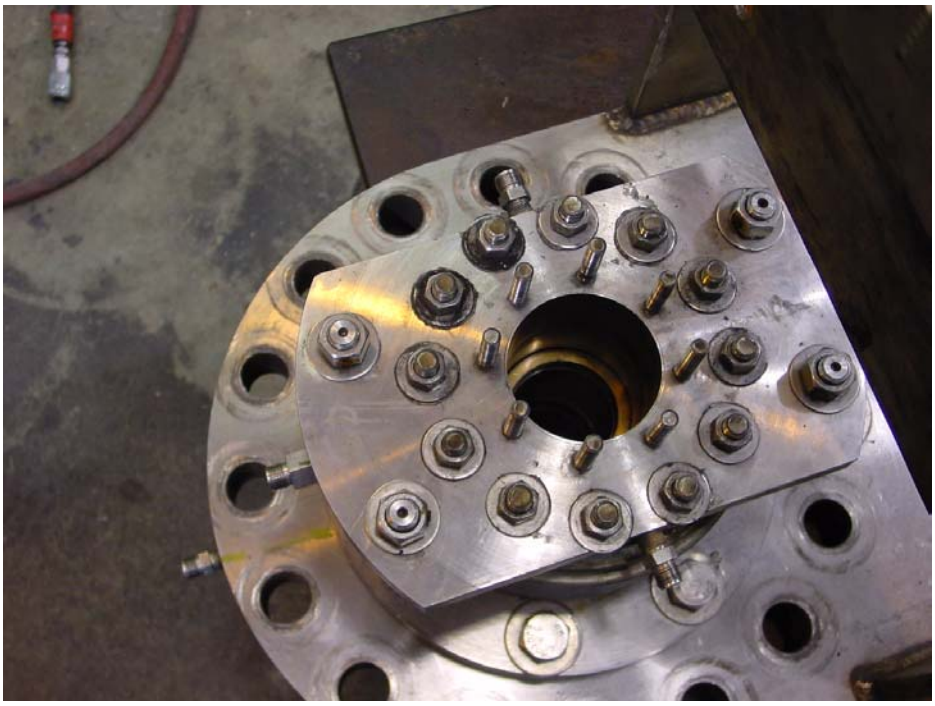

Figure 3.3-28 FD0502 Stuffing Box After TC06

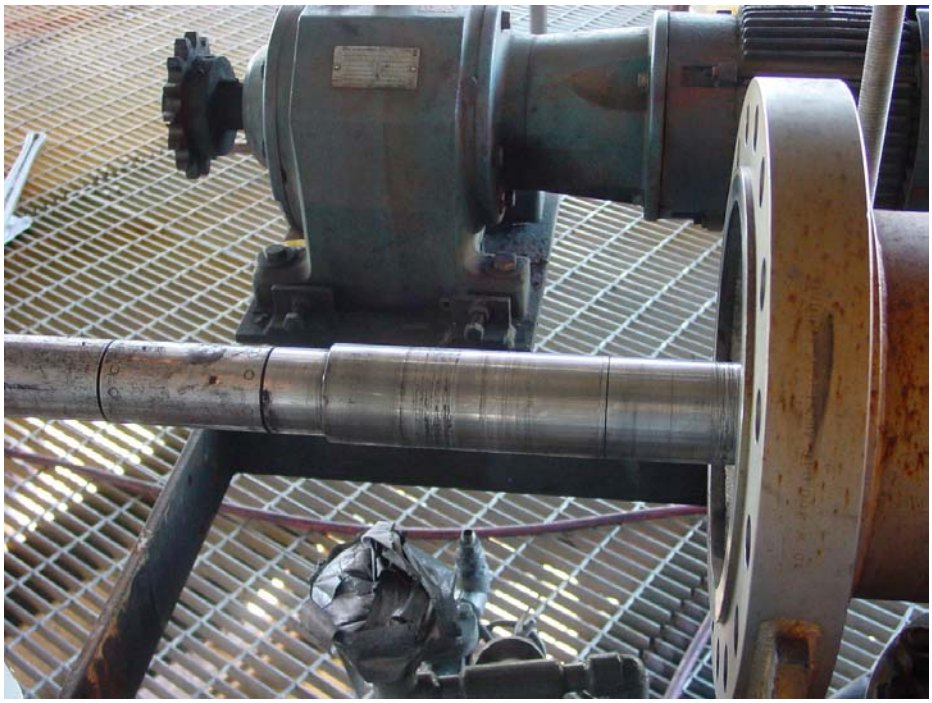

Figure 3.3-29 FD0502 Drive End Wear Sleeve and Shaft

Figure 3.3-30 FD0502 Nondrive End Wear Sleeve and Shaft

Figure 3.3-31 Drop Pipe Between FD0502 and FD0520

Figure 3.3-32 Upper Spheri Valve on FD0520

Figure 3.3-33 Upper Spheri Valve After Cleaning

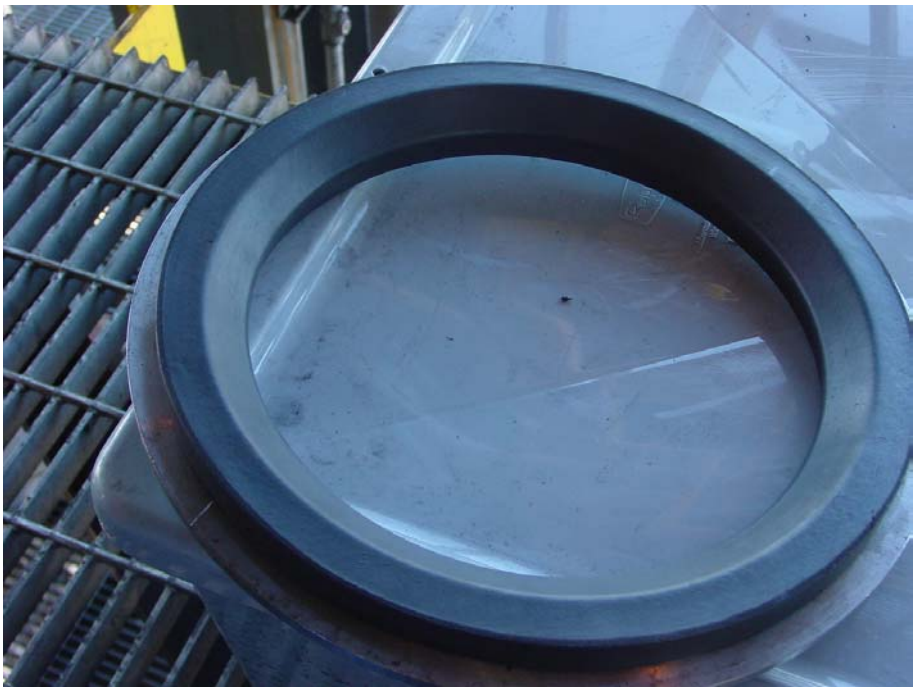

Figure 3.3-34 Upper Spheri Valve Inflatable Seal After TC06

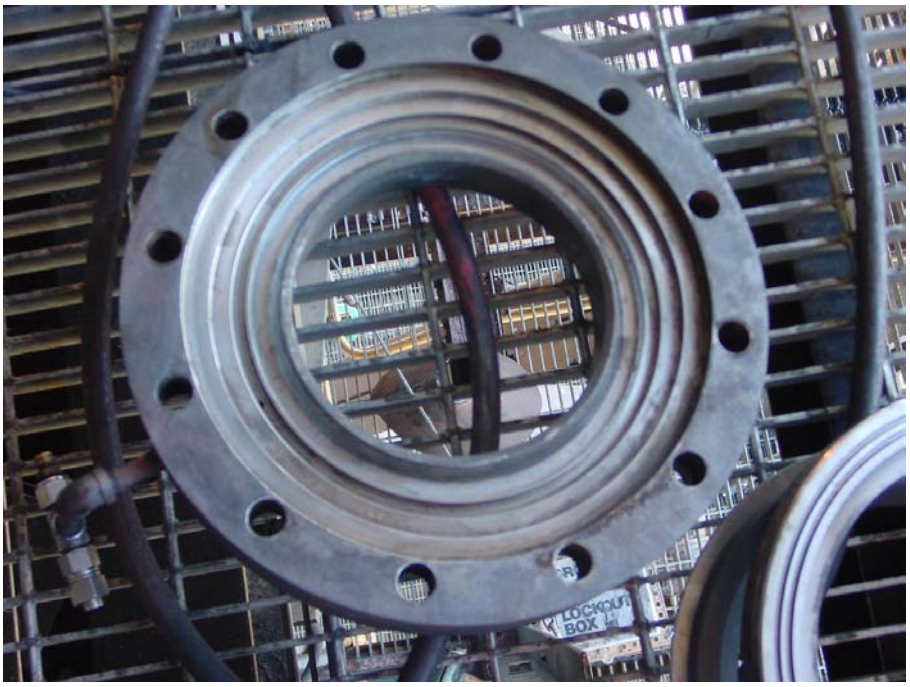

Figure 3.3-35 Top Ring Plate for FD0520 After TC06

3.4 TC06 GASIFICATION ASH (G-ASH) CHARACTERISTICS AND PCD PERFORMANCE

This section reports the characteristics of the g-ash produced during TC06 and the relationship between the g-ash characteristics and PCD performance. As in previous tests, in situ g-ash samples and dustcake samples from TC06 were thoroughly characterized in an effort to better understand the effects of the g-ash characteristics on filter pressure drop and the formation of bridged deposits. G-ash samples were collected at the PCD inlet and at the PCD outlet throughout TC06 using the SRI in situ sampling system described in previous reports. Dustcake samples were collected after both portions of the TC06 run (TC06A and TC06B) even though the samples collected after TC06A were not representative of normal operation as a result of the thermal transient that occurred in the PCD during tuning of the main air compressor. There were no such anomalies after TC06B, and representative samples of the residual dustcake, transient dustcake, and bridged deposits were obtained after that test segment. Characterization of the in situ g-ash samples, dustcake samples, and bridged deposits included: chemical analyses; particle-size analyses; laboratory drag measurements; and measurements of the true particle density, bulk density, uncompacted bulk porosity, and specific-surface area. As in the previous gasification tests, drag measurements were made using the resuspended ash permeability tester (RAPTOR) as modified to allow measurements as a function of particle size. As in previous tests, the RAPTOR drag measurements were compared to transient drag values determined from PCD performance data, and the results were used to gain a better understanding of the contribution of the dustcake to PCD ΔP and to gain insight into the effect of particle size and morphology on drag.

3.4.1 In situ Sampling

As in previous test campaigns, in situ particulate sampling runs were performed on a regular basis at the PCD inlet and the PCD outlet throughout TC06. The system and procedures used for the in situ particulate sampling have been described in previous reports. During TC06, a total of 27 particulate sampling runs were performed at the PCD inlet and 31 particulate sampling runs were performed at the PCD outlet.

3.4.1.1 PCD Inlet Particle Mass Concentrations

Table 3.4-1 is a summary of the particulate loadings measured at the PCD inlet during TC06. Excluding the two runs performed during coke feed (run Nos. 1 and 3) and the one run performed in the absence of limestone addition (run No. 4), the TC06 inlet mass loadings varied from 9,200 to 18,800 ppmw, with a mean value of 13,900 ppmw and a standard deviation of 2,900 ppmw (coefficient of variation of 0.21). The substantial variation in the inlet loading is largely attributable to the inclusion of eight runs that were performed during periods of low coal-feed rate. Excluding these runs (run Nos. 7, 12, 13, 21 through 24, and 26), the average inlet loading is increased to 15,700 ppmw with a standard deviation of 1,700 ppmw (coefficient of variation of 0.11). This average value is still somewhat lower than the average inlet loading measured during GCT3 and GCT4, which was 18,400 ppmw with a standard deviation of 6,000 ppmw (coefficient of variation of 0.33). Considering the variability of the measurements, however, the difference between the TC06 and the GCT3/GCT4 mass loadings is not statistically significant. The TC06 and GCT3/GCT4 mass loadings are, however, significantly different from those measured in GCT2, in which the mean mass loading was 31,100 ppmw

with a standard deviation of 2,600 ppmw (coefficient of variation of 0.08). This difference reflects the changes made in the Transport Reactor recycle loop between GCT2 and GCT3.

The inlet mass concentration measured during startup on coke breeze is shown by run Nos. 1 and 3. These data indicate that the PCD inlet particulate concentration during coke operation was approximately one-half the average of that obtained during coal operation. This is consistent with PCD operational data, which indicated that PCD ΔP was very low during coke startup.

3.4.1.2 PCD Outlet Particle Mass Concentrations

Table 3.4-1 shows the particle concentrations measured at the outlet of the PCD along with the PCD collection efficiency calculated from the corresponding inlet and outlet mass measurements. Except for one sampling run performed at the end of TC06A (outlet sample No. 8 in Table 3.4-1), the PCD operated with very low outlet loadings, consistent with an absence of significant leaks. The high loading for outlet sample No. 8 was obtained after the PCD thermal transient, which resulted in a cracked filter element as discussed in the section on PCD operations (see Section 3.2). Excluding this run and the runs performed during particulate monitor calibration (discussed in a later section), the outlet loading was always below the lower limit of resolution of the measurement with an average collection efficiency exceeding 99.997 percent. As indicated in the table, the lower limit of resolution of these particulate measurements varied from 0.1 to 0.4 ppmw depending on the test duration.

3.4.1.3 Tar Contamination

In previous gasification runs, particulate samples have sometimes shown evidence of tar contamination. Evidence of tar formation has also been seen in the form of sticky residual dustcakes and condensed tar components found in the gas analysis system. The tar was apparently formed when coal was introduced into the Transport Reactor system while the temperatures in the system were too low to completely crack the tar components. To address this problem, a system for feeding coke breeze was added prior to TC06. This system makes it possible to heat the Transport Reactor system to the temperatures required for tar cracking before coal is introduced. With the coke feed system in use, the TC06 particulate samples showed no evidence of tar contamination.

3.4.1.4 Syngas Moisture Content

As in previous tests, measurements of the syngas moisture content were made in conjunction with the outlet particulate sampling runs. The water vapor content of the syngas was determined by collecting the condensate from the syngas in an ice-bath condenser and calculating the vapor concentration from the volume of gas sampled and the volume of condensate collected. The values determined for individual runs are included in Table 3.4-1. Based on these data, the TC06 syngas moisture content varied from 4.6 to 10.9 percent, with a mean value of 7.6 percent and a standard deviation of 1.3 percent (coefficient of variation of 0.17). In the section on Transport Reactor operations, these measurements are compared to moisture data obtained from on-line instrumentation. Much of the variation in syngas moisture content is a result of changes in steam-injection rates.

3.4.2 PCD Dustcakes and Consolidated Deposits

Following both segments of TC06, samples were collected of the dustcakes and any bridged deposits that remained in the PCD. After TC06A, there was only a very thin residual dustcake remaining in the PCD, and the dustcake may not have been representative of normal operation as a result of the thermal transient that occurred at the end of TC06A, resulting in a cracked filter element. Chemical analysis suggests that the TC06A residual cake was partially combusted during the thermal transient. No transient dustcake and no bridged deposits were present in the PCD after TC06A.

At the conclusion of TC06B, a dirty shutdown of the PCD was performed to allow sampling of both residual and transient dustcakes as well as any bridged deposits that may have been present. Even though a dirty shutdown was performed, there were areas of the filter surfaces that were completely devoid of dustcake. Other areas were covered with what appeared to be the residual dustcake and there were several patches of what appeared to be transient dustcake. Most of the transient dustcake apparently fell off the filter elements before or during the removal of the filter internals. The remaining residual and transient dustcakes could be easily removed with a soft-bristle brush and there was no evidence of any type of stickiness or consolidation in the dustcakes. This observation suggests that the TC06B dustcakes were not substantially affected by tar deposition as the GCT4 dustcakes were.

The TC06B residual cake was extremely thin (~0.01 in. average thickness). The thickness of the transient cake varied from about 0.09 to 0.15 in. Since there were only a few patches of transient cake remaining, and since some of the residual cake had apparently fallen off also, these thickness measurements are probably not reliable for any analysis of PCD ΔP. The patches of remaining dustcake were deemed to be too small and too irregular to make reliable measurements of the areal loadings, but the thicknesses of the cakes were estimated from measurements made within the small remaining patches. The dustcake areal loadings were then estimated from the thickness measurements, assuming that the porosity of the TC06 dustcake was the same as the porosity measured for the GCT3/GCT4 dustcakes (83 percent). Based on this assumption, the areal loadings of the TC06 residual and transient dustcakes were estimated to be 0.02 and 0.2 lb/ft^2, respectively. Again, these values of areal loading are probably not reliable since much of the transient cake and perhaps some of the residual cake had fallen off prior to the thickness measurements. The information below compares the average dustcake thicknesses and areal loadings for TC06B and GCT4 based on the assumption that the TC06 dustcake porosity was the same as the GCT4 dustcake porosity (83 percent).

	Residual Dustcake		Transient Dustcake	
	TC06	GCT4	TC06	GCT4
Thickness (in.)	0.01	0.1	0.12	0.3
Areal Loading (lb/ft^2)	0.02	0.2	0.24	0.6

As discussed previously, the thickness and areal loading values for TC06 are probably too low since some of the cake appeared to have fallen off prior to the thickness measurements. On the other hand, the thickness and areal loading values for GCT4 may be too high as a result of tar

deposition. The "appropriate" values of thickness and areal loading probably lie between the TC06 and GCT4 values given in the table above. Later in this report, the dustcake areal loadings will be estimated from dustcake drag measurements and data on PCD ΔP. Because of the uncertainties in the thickness measurements it is believed that the areal loadings that are estimated from the dustcake drag and the filter ΔP are more reliable than the values given above.

As discussed in the section on PCD inspection, bridged deposits were present between some of the filter elements in the bottom plenum after TC06B. There was no bridging in the top cluster. Roughly 25 percent of the filter surface in the bottom plenum appeared to be covered by the bridged deposits. The bridged g-ash appeared to be packed between the elements but it did not appear to be consolidated. It was impossible to remove intact chunks of the bridged material without the chunks breaking apart into loose dust. This observation suggests that the bridged material was not bonded together by tar or any other chemical consolidation mechanism.

To investigate the differences between the residual and transient cakes and the bridged material, all three types of samples were thoroughly characterized. In previous tests this characterization has included evaluation of both physical properties and chemical analysis but the analytical results have not been particularly useful in the evaluation of PCD performance. Therefore, this report will focus on the physical properties of the samples.

3.4.3 Physical Properties of In situ Samples and Dustcakes

The TC06 in situ particulate samples and dustcake samples were subjected to the standard suite of physical measurements, including true (skeletal) particle density, bulk density, uncompacted bulk porosity, specific-surface area, and particle-size analysis. The instruments and procedures used for making these measurements have been described in previous reports.

3.4.3.1 In situ Particulate Samples

Physical properties of the in situ particulate samples from TC06 are presented in detail in Table 3.4-2, and the information listed below compares the average in situ physical properties for TC06 and GCT4.

	TC06	GCT4
Bulk density (g/cc)	0.29	0.27
Skeletal particle density (g/cc)	2.45	2.29
Uncompacted bulk porosity (%)	88.3	88.2
Specific surface area (m^2/g)	222	197
Mass-median diameter (μm)	15.3	15.9

Based on the above comparison, the g-ash produced in TC06 appears to be very similar to the g-ash produced in GCT4. Although the bulk density and true density of the TC06 g-ash are slightly higher than those of the GCT4 g-ash, the difference is small (about 7 percent), and in both cases the densities yield the same value of bulk porosity (88.3 percent). The differences in

surface area and mass-median diameter (MMD) are insignificant considering the variability of the data. The similarity of the TC06 and GCT4 g-ash is not surprising, since both were produced from the same Powder River Basin (PRB) coal and the same Ohio (bucyrus) limestone, and the operating conditions of the Transport Reactor system did not differ dramatically between GCT4 and TC06. The role of these physical properties in determining dustcake drag will be discussed in more detail in the section on drag measurements. A more detailed comparison of the TC06 and GCT4 particle-size distributions will be presented in the next section of this report.

Also included in Table 3.4-2 are the physical properties of in situ samples collected during coke breeze startup (inlet runs 1 and 3). The coke samples have much lower values of specific surface area than do the samples obtained during coal operation. Consistent with PCD operational data, there does not appear to be any evidence that startup with coke should negatively affect PCD operation.

3.4.3.2 Dustcake Samples

The physical properties of the residual and transient dustcake samples and bridged deposits from TC06B are compiled in Table 3.4-3, and the average properties of the various TC06B samples are compared to those from GCT4 in the listing below.

	Residual Dustcake		Transient Dustcake		Bridged G-ash	
	TC06	GCT4	TC06	GCT4	TC06	GCT4
Bulk density (g/cc)	0.25	0.34	0.25	------	0.27	0.34
Skeletal particle density (g/cc)	2.28	1.91	2.39	------	2.41	2.21
Uncompacted bulk porosity (%)	89.0	82.2	89.5	------	88.8	84.6
Specific surface area (m^2/g)	257	8.0	261	------	261	173
Mass-median diameter (μm)	9.3	8.4	9.2	------	10.8	12.7

The properties of the GCT4 transient dustcake are not included in the comparison above because these samples were not representative of normal GCT4 operations as discussed in the GCT4 report. In comparing the residual dustcakes and bridged deposits it is apparent that both types of samples from TC06 have lower bulk densities, higher true (skeletal) particle densities, higher bulk porosities, and higher surface areas than do the GCT4 dustcakes and bridged deposits. These differences in the residual dustcakes and bridged deposits are interesting because there was very little difference between the TC06 and GCT4 in situ samples. One difference between the in situ samples and the other types of samples is that the in situ sampling avoids periods of tar formation, while the residual dustcakes and bridged deposits are unavoidably exposed to any tar deposition that may occur. This result suggests that the TC06 and GCT4 g-ashes are similar in the absence of tar formation and that the observed differences in the residual dustcakes and bridged deposits may be related to the tar deposition that occurred during GCT4.

3.4.4 Particle-Size Analysis of In situ Samples and Dustcakes

The average particle-size distribution of in situ dust samples entering the PCD during TC06 coal operation is shown in Figure 3.4-1. Also shown on the figure is the average distribution from GCT4. The two distributions are nearly identical and show that no significant changes in particle size occurred between the two test programs. At least with PRB coal, Transport Reactor operation appears to have reached a stable, reproducible condition.

Startup and restart following lost coal feed during TC06 were conducted using coke breeze to reduce tar formation. The particle-size distribution measured at the PCD inlet during coke operation is compared to coal operation in Figure 3.4-2. As shown in Section 3.4.1.1, the coke produced less overall mass than the coal. Comparison of the size distribution data indicates that the reduction occurred over almost the entire size range covered by the measurements. The coke data are largely unremarkable and there is no suggestion from the particle-size data that any operational problems would be expected because of coke operation.

The size distributions of samples removed from inside the PCD after shutdown are shown in Figure 3.4-3. The solid symbols represent PCD dustcake samples while open symbols are the PCD inlet data discussed above. (The PCD dustcake samples shown here are only from TC06B because the dustcake samples of TC06A were damaged by the thermal transient at the end of the run.) The three dustcake samples (residual, transient, and bridged deposit) show almost exactly the same size distributions. This is different from previous test programs, which frequently indicated that the residual dustcake was finer than the transient dustcake or bridged deposits. The similarity of dustcakes may be attributable to the lack of tar formation during TC06, which resulted in residual dustcakes that were fluffy with low cohesivity. Unlike previous test programs, the TC06 residual dustcake was very thin and easily removed. Since the residual dustcake could be pulse cleaned more readily, there may have been less opportunity for fine-particle enrichment of a long-lived, residual dustcake that persisted throughout the run.

Comparison of the in situ and dustcake samples in Figure 3.4-3 shows that the in situ distribution contained more large particles than were found in the dustcakes although the differences are minor. This difference could indicate some cyclonic separation of large particles by the tangential entry system, although evidence of this effect has been inconsistent over a number of test programs.

3.4.5 Laboratory Drag Characteristics of G-ash

At the end of TC06B, a dirty shutdown was attempted to preserve the transient dustcake in the PCD. While a quick and uneventful shutdown was successfully accomplished, very little transient dustcake remained by the time the PCD was disassembled. The g-ash was very fluffy and loose, with low cohesivity. Most of the transient dust simply fell off the filter elements and apparently took most of the residual dustcake with it (as discussed previously). The result was that insufficient material was recovered of either dustcake for laboratory drag measurements using the RAPTOR system. Only the bridged deposit was available in sufficient quantity for RAPTOR measurements. Therefore, for this analysis, both CAPTOR and RAPTOR data will be used to understand the dustcake drag characteristics from TC06. The CAPTOR will be used

to compare the three PCD samples (transient, residual, and bridged deposit), while the RAPTOR measurements will be made only on the bridged deposit.

CAPTOR drag, as a function of porosity for the three TC06B samples are shown in Figure 3.4-4. Although there are some differences, the three curves are very similar. The solid symbols on the graph indicate the drag at the flow-compacted porosity (FCP) as determined from the CAPTOR measurement. The drag values at FCP ranged from 74 to 105 inWC/(ft/min)/(lb/ft^2), which is a typical degree of scatter for this type of data.

For comparison with the TC06 data, CAPTOR data from dustcake samples collected in GCT2 and GCT4 are shown in Figure 3.4-5. These drag curves show a substantial difference between the two GCT4 dustcakes with the transient drag comparable to the TC06 data and the tar-contaminated residual dustcake in a much lower drag range. Interestingly, the GCT2 transient and residual dustcakes are not very different despite the residual layer being contaminated with tar, with both indicating low drag. These data appear to suggest that tar contamination of a low-surface-area particulate, such as the GCT2 g-ash, does not have a significant effect on dustcake drag, while coating the high-surface-area particles from GCT4 with tar has a substantial effect on drag. This would seem to support the conclusion that the residual dustcake from TC06 was relatively free of tar and that the use of coke breeze during startup was effective in preventing residual dustcake contamination.

Figure 3.4-6 shows the results of RAPTOR measurements of drag as a function of particle size for the TC06 bridged deposit sample. The solid circles represent the TC06 data, while the solid line is a regression fit to those data ($r^2 = 0.96$). For comparison, the regression fits to the GCT2 and GCT3/GCT4 data are also shown on the figure. The TC06 data are in substantial agreement with the other data collected since the modification of the Transport Reactor recycle loop (after GCT2). The agreement of the CAPTOR data for the residual and transient dustcake samples suggests that the RAPTOR data from the bridged deposit can be reasonably applied to all of the TC06 dustcakes.

In Figure 3.4-7, specific surface areas measured on the RAPTOR samples are plotted as a function of the MMD of the sample. Also included on the graph are GCT2 and GCT4 data for comparison. In the GCT4 report, it was suggested that the large increase in surface area from GCT2 to GCT4 was caused by improved gasification and a resulting change in particle morphology. The relationships between surface area and MMD and between drag and MMD suggest that, at a given particle size, there is a definite effect of surface area on drag. However, the GCT4 hopper samples and bridged dustcake samples had similar drag characteristics despite the difference in surface area shown in Figure 3.4-7. This difference in surface area was attributed to the deposition of tar in features too small to affect drag (submicron pores). The TC06 bridged deposit has both high surface area and high drag, despite what is presumed to be long exposure inside the PCD. This is another measure of the success of coke breeze startup in eliminating tar.

3.4.6 Analysis of PCD Pressure Drop

In this section, the contributions of the transient and residual dustcakes to PCD ΔP are examined by comparing dustcake drag values calculated from the PCD ΔP to dustcake drag values measured by RAPTOR. This is a very valuable comparison because mismatches between these two methods of determining drag can indicate that other factors (i.e., tar deposition) may be influencing the PCD ΔP.

3.4.6.1 PCD Transient ΔP Analysis

This analysis was done using the same procedure described in detail in the GCT3 and GCT4 reports. For each in situ particulate sampling run, the transient PCD drag during the run was determined from the rate of ΔP rise during the run and the rate of g-ash accumulation in the transient cake. The latter was determined from the measured particulate loading and the syngas mass-flow rate during the run. To allow direct comparison of this PCD drag value with the RAPTOR drag measurements, the PCD drag was adjusted to the RAPTOR conditions using the ratio of the syngas viscosity at process temperature to the viscosity of air at laboratory room temperature. The RAPTOR drag value for each particulate sampling run was taken from the plot of drag versus MMD shown previously in Figure 3.4-6 using the MMD values determined by Microtrac analysis for each sampling run.

Table 3.4-4 summarizes the PCD transient drag calculations discussed above and compares the PCD transient drag values to the corresponding drag values measured by RAPTOR. As in the previous data analysis, the sampling runs performed during coke feed and during low coal feed have been excluded. Average values of PCD transient drag and RAPTOR drag are given below for both TC06 and GCT4. The drag values are on the viscosity basis of air at 77°F.

	TC06	GCT4
Average Drag from PCD ΔP/Δt (inWC/(lb/ft^2)/(ft/min))	83	66
Average Drag from RAPTOR Data (inWC/(lb/ft^2)/(ft/min))	94	70

This summary shows that there is good agreement between the PCD performance calculations and the RAPTOR measurements. This agreement can also be seen by plotting the individual values of PCD drag and RAPTOR drag determined for each sampling run, as shown in Figure 3.4-8. This plot shows that the RAPTOR drag values track the PCD transient drag values reasonably well. This result suggests that the flow resistance of the g-ash is high enough to account for all of the transient ΔP, and that the transient dustcake drag was not affected by tar deposition or other anomalies during the in situ particulate sampling runs.

Laboratory measurements of drag were also made with a sample collected during startup on coke breeze. The normalized drag at CAPTOR FCP was determined to be 23 inWC/(lb/ft^2)/(ft/min) on PCD inlet in situ run No. 3. This drag is much lower than the average value obtained for coal operation [94 inWC/(lb/ft^2)/(ft/min)]. The actual PCD drag (corrected to room temperature) during the period of the in situ test was 17 inWC/(lb/ft^2)/

(ft/min), which is in good agreement with the lab measurement. Thus, both the calculated transient PCD drag and the laboratory-measured drag suggest that PCD performance should not have been adversely affected by using coke breeze as the start-up fuel.

3.4.6.2 PCD Baseline ΔP Analysis

In the section on PCD operations analysis, a plot is shown of the normalized baseline ΔP as a function of time throughout TC06. As shown in the plot, the normalized baseline ΔP remained fairly stable at around 80 inWC until about September 2, 2001. At that point, the normalized baseline ΔP slowly increased, reaching a maximum value of about 100 inWC after about 10 days. Tar deposition does not appear to have been a major contributing factor in the increasing baseline ΔP, since the residual dustcake was easily removed and did not appear to be bonded together with tar. In the absence of tar-related effects on the residual dustcake, the most likely cause of the increasing baseline ΔP is the formation of bridged deposits. In order to separate the effect of the residual dustcake ΔP from the effect of the bridged deposits, the analysis of baseline ΔP will be done using the stable baseline ΔP value (80 inWC) that was recorded prior to the suspected bridging.

As shown in previous reports, the contribution of the residual dustcake to the baseline ΔP can be estimated by subtracting out the contributions of the vessel losses and any irreversible increases in the filter element ΔP and the failsafe ΔP. Vessel losses and irreversible changes in filter element and failsafe ΔP, normalized to the same conditions as the baseline ΔP, were estimated to be 30 and 3 inWC, respectively. After subtracting out these contributions, the remaining normalized ΔP that can be attributed to the residual dustcake is 47 inWC. To allow direct comparison with the laboratory drag measurements, this value of residual dustcake ΔP must be corrected to the same viscosity basis as the RAPTOR measurements (air at room temperature). In this case, the corrected residual dustcake ΔP value at room temperature is 29 inWC.

Since some of the residual dustcake apparently fell off prior to the PCD inspection, the areal loading of the residual cake is unknown. Therefore, it is not possible to calculate the PCD residual dustcake drag from the residual dustcake ΔP. However, the residual dustcake ΔP can be used in combination with the RAPTOR drag and the PCD face velocity to estimate the areal loading of the residual cake. Using an average RAPTOR drag value (at room temperature) of 100 inWC/(lb/ft^2)/(ft/min), a residual dustcake ΔP of 29 inWC (at room temperature), and a face velocity of 3.5 ft/min, the areal loading of the residual cake is estimated to be 0.08 lb/ft^2. This value of areal loading is much higher than the areal loading that was estimated from the measured thickness, confirming that much of the residual cake fell off. The calculated areal loading is somewhat lower than the areal loading that was measured for GCT4, where the residual cake was held together with tar. This result suggests that tar deposition can contribute to the formation of a thicker residual dustcake and consequently a higher baseline ΔP, but no such effect was evident in TC06.

3.4.7 Real-Time Particulate Monitor Evaluation

As discussed in the GCT3 and GCT4 reports, testing of the PCME Dustalert-90 electrodynamic particulate monitor indicated that this device might have the potential to detect PCD leaks at levels low enough for turbine protection. During GCT4, the monitor responded to injected combustion ash particles in a definite, repeatable way with ash concentrations in the range of approximately 8 to 30 ppmw. The goal of the TC06 testing was to evaluate the response of the Dustalert-90 with g-ash as the injected particulate and at lower injected concentrations. To facilitate this testing, the dust injection system that has been described in previous reports was modified to operate at lower flow rates, so that lower concentrations of g-ash could be produced in the syngas downstream from the PCD. Because g-ash is more readily fluidized than ash, it was also necessary to increase the injection system fluid-bed disengager height and improve the fluidizing nitrogen distribution system to achieve reliable operation. With the modified injection system it was possible to test the response of the PCME monitor over a range of g-ash concentrations from about 0.5 to 3 ppmw.

The Dustalert-90 results from TC06 are shown in Figure 3.4-9, which is a plot of actual particle concentration measured with the in situ sampling system as a function of the PCME monitor output. Since the Dustalert-90 does not determine particle concentration directly but instead measures the number of particles passing the probe per-unit time, and the gas flow during the measurement must be taken into account. The particle concentrations shown in the figure have been normalized to a syngas flow of 25,000 lb/hr. The five data points at the lower concentrations were obtained with injected g-ash while the one point at the highest concentration was determined during the leak that occurred at the end of TC06A. The line on the graph is a linear regression to all of the data. Although the correlation is not very good ($r^2 = 0.88$), both the injected and leaked g-ash values appear to follow the same trend. This is encouraging because of concerns that this instrument might respond differently to injected g-ash than it does to particles straight from the Transport Reactor.

The most promising result from the TC06 tests of the Dustalert-90 is that a clear indication was obtained from the instrument at injected concentrations as low as 0.5 ppmw. This is a sufficiently low concentration to provide a significant level of turbine protection. We will continue to refine our understanding of this instrument during future test programs.

3.4.8 Conclusions

The g-ash entering the PCD during TC06 was very similar to the g-ash produced during GCT4 (uncompacted bulk porosity of about 88 percent, specific-surface area of about 200 m^2/g, and mass-median diameter of about 15 μm). Despite this similarity in the inlet g-ash, the residual dustcakes and the bridged deposits from TC06 have significantly higher porosities and higher surface areas than do the same types of samples from GCT4. These differences reflect the effect of tar deposition within the GCT4 dustcakes and deposits. Since the properties of the TC06 dustcakes and deposits are also similar to the properties of the TC06 in situ samples, any effect of tar deposition within the TC06 dustcake appears to be minimal. The use of coke feed during periods of interrupted coal feed was apparently successful in minimizing tar formation.

Throughout all of TC06B and most of TC06A, the PCD operated with outlet particulate loadings below the lower limit of resolution (0.1 to 0.4 ppmw). The only exception to the excellent particulate collection performance occurred after a thermal excursion led to a cracked filter element. This thermal excursion was caused by a situation that would not occur in a commercial facility.

Drag and surface area measurements made on TC06, GCT4, and GCT2 g-ash samples suggest that tar deposition can have a significant effect on the drag of high-surface-area g-ashes and very little effect on the drag of low-surface-area g-ashes. These measurements also support the conclusion that the residual dustcake from TC06 was relatively free of tar. Laboratory drag measurements made on hopper samples and bridged deposits were in good agreement with transient drag values calculated from the rate of ΔP rise, again suggesting that the transient dustcake drag was not affected by tar deposition.

Testing of the PCME Dustalert-90 real-time particulate monitor with injected g-ash suggests that the monitor is capable of detecting g-ash concentrations as low as 0.5 ppmw in the process gas stream downstream from the PCD (based on a syngas-flow rate of 25,000 lb/hr). Based on comparisons with batch measurements, the response of the monitor appears to be directly proportional to the mass-flow rate of g-ash in the process pipe. Additional testing is needed to validate the performance of the monitor on actual PCD leaks and to determine how the response of the monitor varies with different types of g-ash.

Table 3.4-1
PCD Inlet and Outlet Particulate Measurements From TC06

Test Date	PCD Inlet				PCD Outlet					PCD Collection Efficiency, %
	SRI Run No.	Start Time	End Time	Particle Loading, ppmw	SRI Run No.	Start Time	End Time	H_2O Vapor, vol. %	Particle Loading, ppmw	
TC06A										
07/11/01	1	08:00	08:10	7,400[1]	--	--	--	--	--	--
07/12/01	3	12:45	13:15	7,000[1]	--	--	--	--	--	--
07/16/01	4	10:30	10:45	11,600[2]	1	09:45	13:45	10.9	< 0.1	> 99.999
07/17/01	5	09:45	10:00	13,100	2	09:15	13:00	10.3	--[3]	> 99.999
07/18/01	6	10:00	10:10	14,900	3	09:30	13:30	9.6	< 0.1	> 99.999
07/19/01	7	10:15	10:25	10,600	4	09:30	13:25	8.4	< 0.1	> 99.999
07/20/01	8	09:35	09:45	18,800	5	08:45	11:45	7.6	< 0.1	> 99.999
07/23/01	9	10:10	10:20	14,200	6	10:05	13:05	7.1	< 0.1	> 99.999
07/24/01	--	--	--	--	7	09:10	10:10	8.0	1.2[4]	--
07/25/01	--	--	--	--	8	09:55	10:45	--	22.9[5]	--
TC06B										
08/20/01	--	--	--	--	9	13:15	14:15	4.6	< 0.4[6]	--
08/21/01	10	09:30	09:45	14,900	10	08:30	09:33	9.2	< 0.4[6]	> 99.997
08/23/01	11	11:00	11:15	14,100	11	10:50	12:15	6.7	< 0.4[6]	> 99.997
08/27/01	12	09:00	09:14	10,400	12	08:45	11:32	5.8	< 0.1	> 99.999
08/29/01	13	08:40	08:55	11,800	13	08:15	10:52	5.8	< 0.1	> 99.999
08/30/01	14	09:45	10:00	17,000	14	09:30	13:30	5.8	< 0.1	> 99.999
08/31/01	15	10:00	10:15	13,500	15	09:30	13:00	6.3	< 0.1	> 99.999
09/04/01	16	10:00	10:15	16,300	16	09:25	13:25	6.5	< 0.1	> 99.999
09/05/01	17	09:30	09:45	16,500	17	09:15	13:15	7.0	< 0.1	> 99.999
09/06/01	18	12:25	12:40	16,600	18	10:15	13:15	7.0	< 0.1	> 99.999
09/07/01	--	--	--	--	19	10:25	11:15	7.8	2.1[4]	--
09/07/01	--	--	--	--	20	13:33	14:03	8.4	2.7[4]	--
09/10/01	19	10:00	10:15	17,000	21	09:30	13:30	7.4	< 0.1	> 99.999
09/11/01	--	--	--	--	22	09:20	12:20	8.3	0.5[4]	--

continued on next page

Table 3.4-1

PCD Inlet and Outlet Particulate Measurements From TC06 (continued)

Test Date	PCD Inlet				PCD Outlet					PCD Collection Efficiency, %
	SRI Run No.	Start Time	End Time	Particle Loading, ppmw	SRI Run No.	Start Time	End Time	H_2O Vapor, vol. %	Particle Loading, ppmw	
09/12/01	20	09:45	10:00	14,000	23	09:00	13:00	7.9	< 0.1	> 99.999
09/13/01	21	10:40	10:55	11,700	24	10:30	13:30	8.6	< 0.1	> 99.999
09/14/01	--	--	--	--	25	10:30	12:00	7.3	1.6[4]	--
09/17/01	22	10:00	10:15	9,300	26	09:45	13:45	8.5	< 0.1	> 99.999
09/18/01	23	09:30	09:55	9,700	27	09:00	13:00	8.4	< 0.1	> 99.999
09/19/01	24	09:45	10:00	9,200	28	09:20	13:20	7.3	< 0.1	> 99.999
09/20/01	25	10:00	10:15	18,100	29	09:00	13:00	7.3	< 0.1	> 99.999
09/21/01	26	09:30	09:45	11,900	30	09:00	13:00	7.7	< 0.1	> 99.999
09/24/01	27	09:00	09:15	15,800	31	08:30	11:30	7.1	< 0.1	> 99.999
Average Inlet Loading				13,900	Average Outlet Loading				< 0.1	> 99.999

1. Inlet samples 1 and 3 collected during coke feed – not included in average. Inlet sample 2 discarded because of filter leakage.
2. Inlet sample 4 collected without limestone addition.
3. Filter weight problem with outlet sample 2 – measurement not reliable.
4. Outlet sample collected during dust injection for particulate monitor calibration – no PCD leak – not included in average.
5. Outlet sample 8 collected during propane combustion – PCD leak through cracked filter element.
6. Short duration test – resolution reduced accordingly.

Table 3.4-2

Physical Properties of TC06 In situ Samples[1]

Lab ID	SRI Run No.	Date	Bulk Density, g/cm^3	True Density, g/cm^3	Uncompacted Bulk Porosity, %	Surface Area, m^2/g	Mass-Median Diameter, m
TC06A							
AB08748	TC06IMT-1	07/11/01	0.48	2.17	77.9	16.7	18.9
AB08750	TC06IMT-3	07/12/01	0.50	2.26	77.9	10.2	19.1
AB08751	TC06IMT-4	07/16/01	0.31	2.49	87.6	182	18.6
AB08752	TC06IMT-5	07/17/01	0.34	2.67	87.3	151	13.1
AB08753	TC06IMT-6	07/18/01	0.32	2.63	87.8	180	12.7
AB08754	TC06IMT-7	07/19/01	0.24	2.35	89.8	257	13.1
AB08755	TC06IMT-8	07/20/01	0.27	2.43	88.9	215	14.7
AB08756	TC06IMT-9	07/23/01	0.31	2.46	87.4	197	14.3
TC06B							
AB09219	TC06IMT-10	08/21/01	0.31	2.51	87.6	183	15.1
AB09220	TC06IMT-11	08/23/01	0.33	2.41	86.3	145	18.6
AB09221	TC06IMT-12	08/27/01	0.29	2.35	87.7	221	14.2
AB09222	TC06IMT-13	08/29/01	0.29	2.42	88.0	255	16.2
AB09223	TC06IMT-14	08/30/01	0.27	2.52	89.3	219	16.1
AB09224	TC06IMT-15	08/31/01	0.29	2.60	88.8	248	16.7
AB09225	TC06IMT-16	09/04/01	0.28	2.40	88.3	244	18.1
AB09226	TC06IMT-17	09/05/01	0.24	2.27	89.4	310	14.6
AB09227	TC06IMT-18	09/06/01	0.27	2.41	88.8	262	15.2

continued on next page

Table 3.4-2

Physical Properties of TC06 In situ Samples (continued)[1]

Lab ID	SRI Run No.	Date	Bulk Density, g/cm^3	True Density, g/cm^3	Uncompacted Bulk Porosity, %	Surface Area, m^2/g	Mass-Median Diameter, m
AB09442	TC06IMT-19	09/10/01	0.27	2.39	88.7	266	12.5
AB09443	TC06IMT-20	09/12/01	0.24	2.32	89.7	311	11.4
AB09444	TC06IMT-21	09/13/01	0.32	2.62	87.8	202	18.3
AB09445	TC06IMT-22	09/17/01	0.36	2.60	86.2	135	15.4
AB09446	TC06IMT-23	09/18/01	0.27	2.39	88.7	195	16.2
AB09447	TC06IMT-24	09/19/01	0.32	2.43	86.8	187	16.4
AB09448	TC06IMT-25	09/20/01	0.26	2.28	88.6	243	16.8
AB09449	TC06IMT-26	09/21/01	0.26	2.33	88.8	243	16.5
AB09450	TC06IMT-27	09/24/01	0.22	2.40	90.8	277	13.0
TC06 Average[1]			0.29	2.45	88.3	222	15.3

1. Sample Nos. TC06IMT-1 and -3 collected during coke feed; not included in average.

Table 3.4-3

Physical Properties of TC06 Dustcake Samples[1]

Lab ID	Type	Date	Bulk Density, g/cc	Particle Density, g/cc	Uncompacted Bulk Porosity, %	Surface Area m^2/g	Mass-Median Diameter, μm
TC06A							
AB08757	Residual	07/27/01	0.46	2.62	82.4	4.6	5.7
AB08758	Residual	07/27/01	0.46	2.50	81.6	24.9	9.9
AB08759	Residual	07/27/01	0.47	2.58	81.8	24.8	14.2
AB08760	Deposit[2]	07/27/01	0.53	2.68	80.2	24.4	11.1
TC06B							
AB09474	Bridging	09/27/01	0.27	2.41	88.8	261	10.8
AB09475	Transient	09/27/01	0.25	2.39	89.5	261	9.2
AB09476	Residual	09/27/01	0.25	2.28	89.0	257	9.3

1. TC06A dustcake samples appear to have been partially combusted as a result of fire in PCD.
2. Deposit removed from filter element support bracket.

Table 3.4-4

Transient Drag Determined From PCD ΔP and From RAPTOR

Run No.	ΔP/Δt, inWC/min	Δ(AL)/ Δt, lb/min/ft^2	FV, ft/min	MMD, μm	Drag, inWC/(lb/ft^2)/(ft/min)		
					PCD	PCD@RT	RAPTOR
5	8.46	0.02440	3.67	13.1	94	57	104
6	10.49	0.02748	3.63	12.7	105	63	107
8	14.65	0.03496	3.71	14.7	113	68	94
9	12.55	0.02604	3.67	14.3	131	79	96
10	10.48	0.02521	3.68	15.1	113	68	91
11	13.27	0.02250	3.46	18.6	171	103	76
14	7.93	0.02660	3.18	16.1	94	57	86
15	9.67	0.02142	3.22	16.7	140	86	84
16	12.04	0.02788	3.53	18.1	122	74	78
17	15.73	0.02606	3.21	14.6	188	115	94
18	11.01	0.02699	3.29	15.2	124	75	91
19	14.39	0.02828	3.39	12.5	150	92	108
20	11.33	0.02092	2.96	11.4	183	114	117
25	7.76	0.02758	2.64	16.8	107	66	83
27	19.01	0.02778	3.18	13.0	215	131	104

Nomenclature:

1. ΔP/Δt = rate of pressure drop rise during particulate sampling run (inWC/min).
2. Δ (AL)/ Δt = rate of increase in areal loading during sampling run (lb/min/ft^2).
3. FV = average PCD face velocity during particulate sampling run (ft/min).
4. MMD = mass-median diameter of in situ particulate sample (μm).
5. RT = room temperature, 77°F (25°C).
6. RAPTOR = resuspended ash permeability tester.

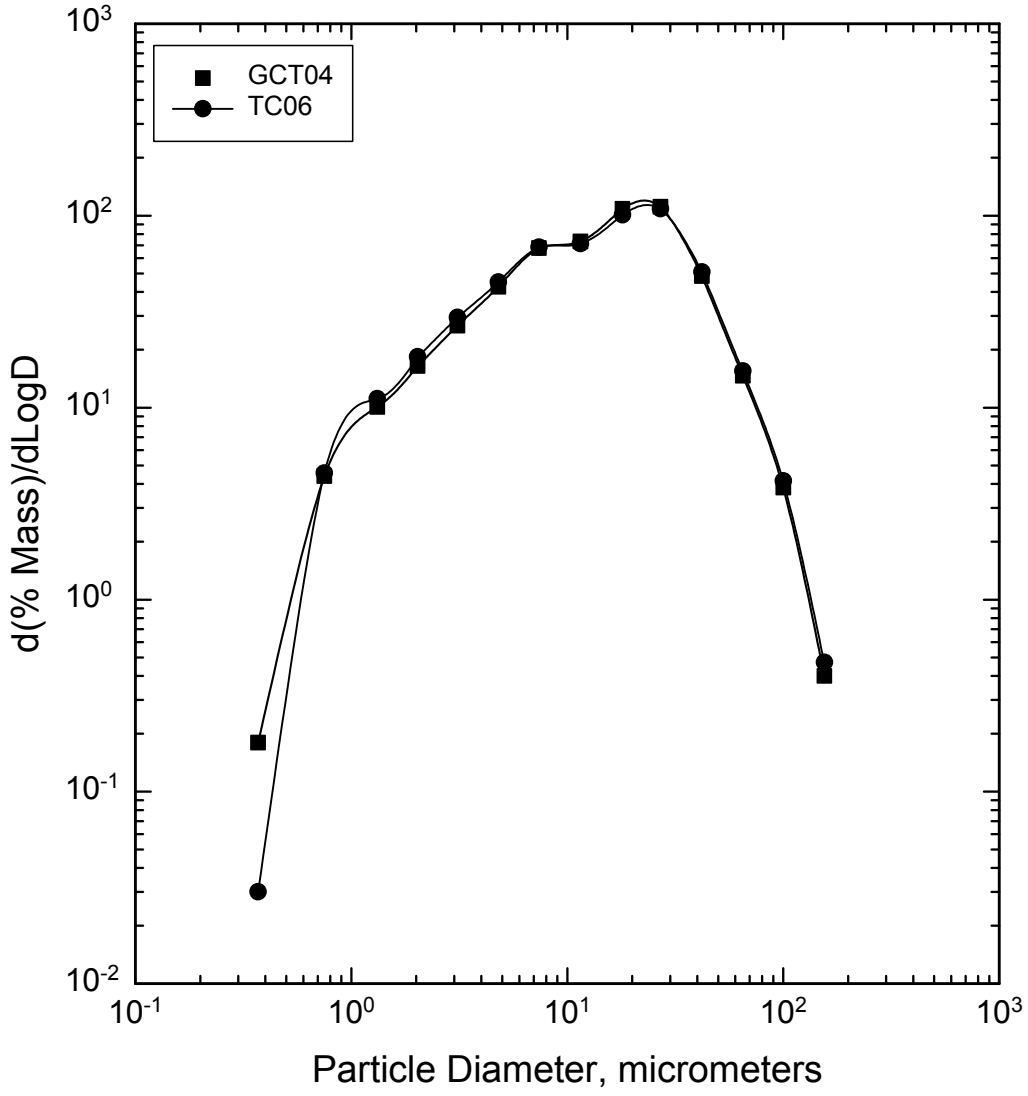

Figure 3.4-1 GCT4 and TC06 Coal G-ash Particle-Size Distributions

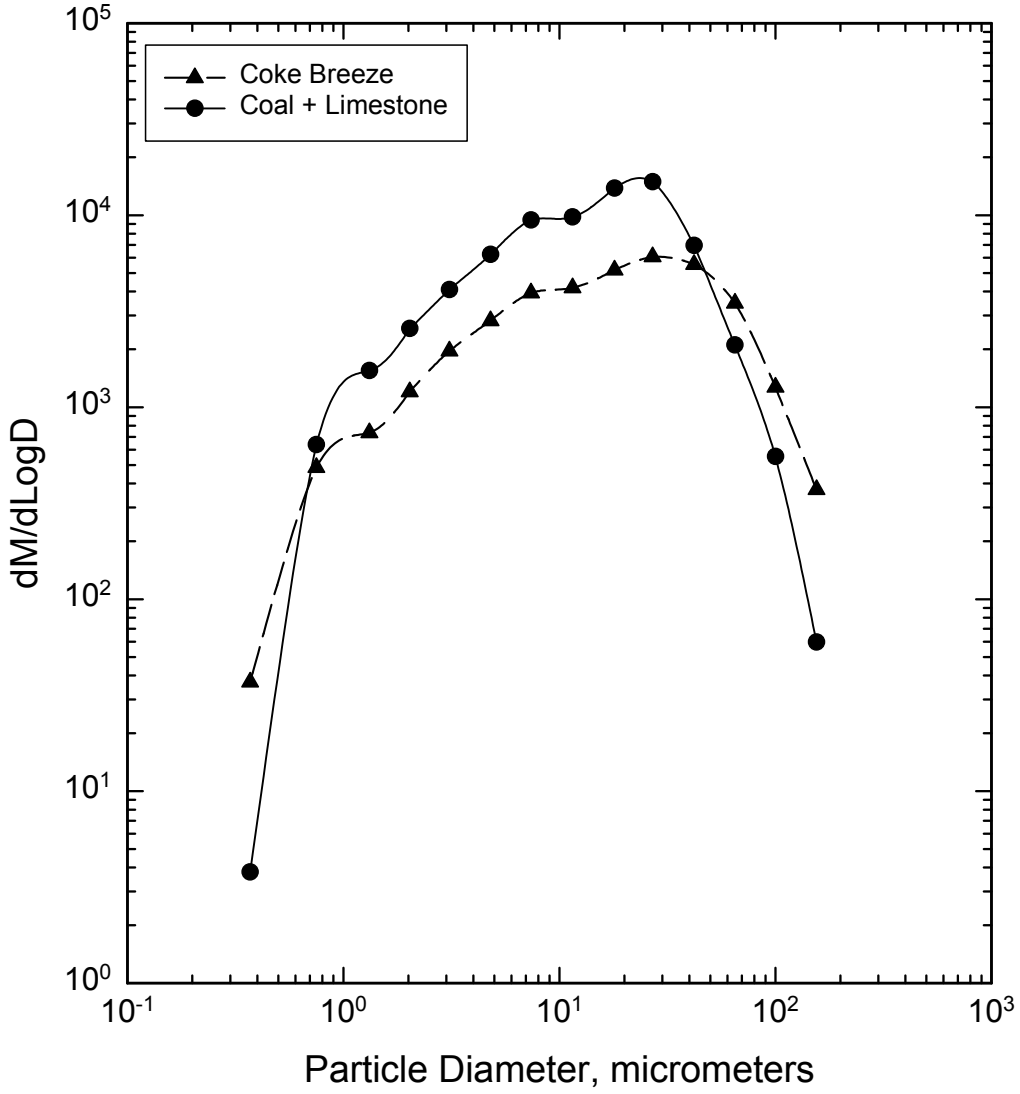

Figure 3.4-2 Particle-Size Distributions for Coal and Coke Operation

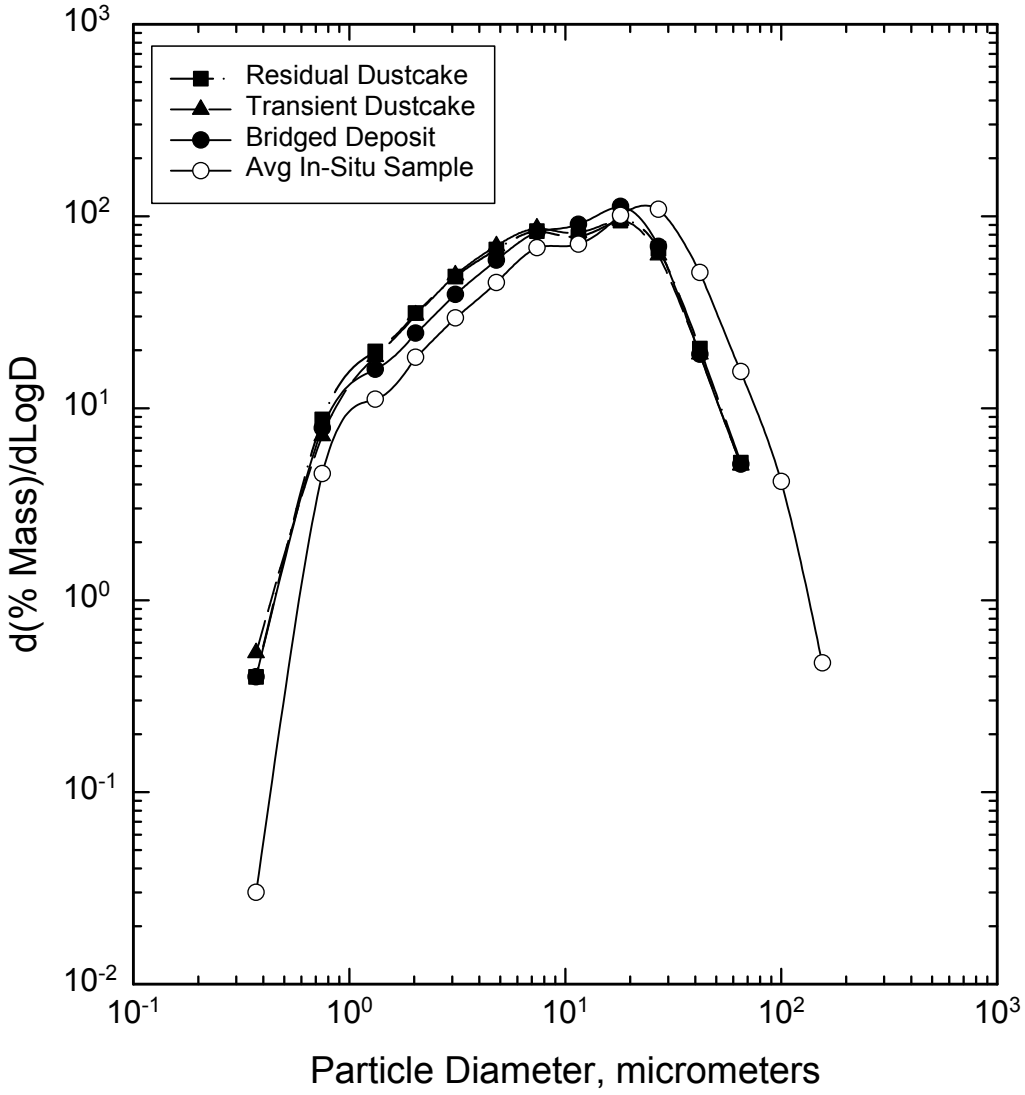

Figure 3.4-3 G-ash Particle-Size Distributions

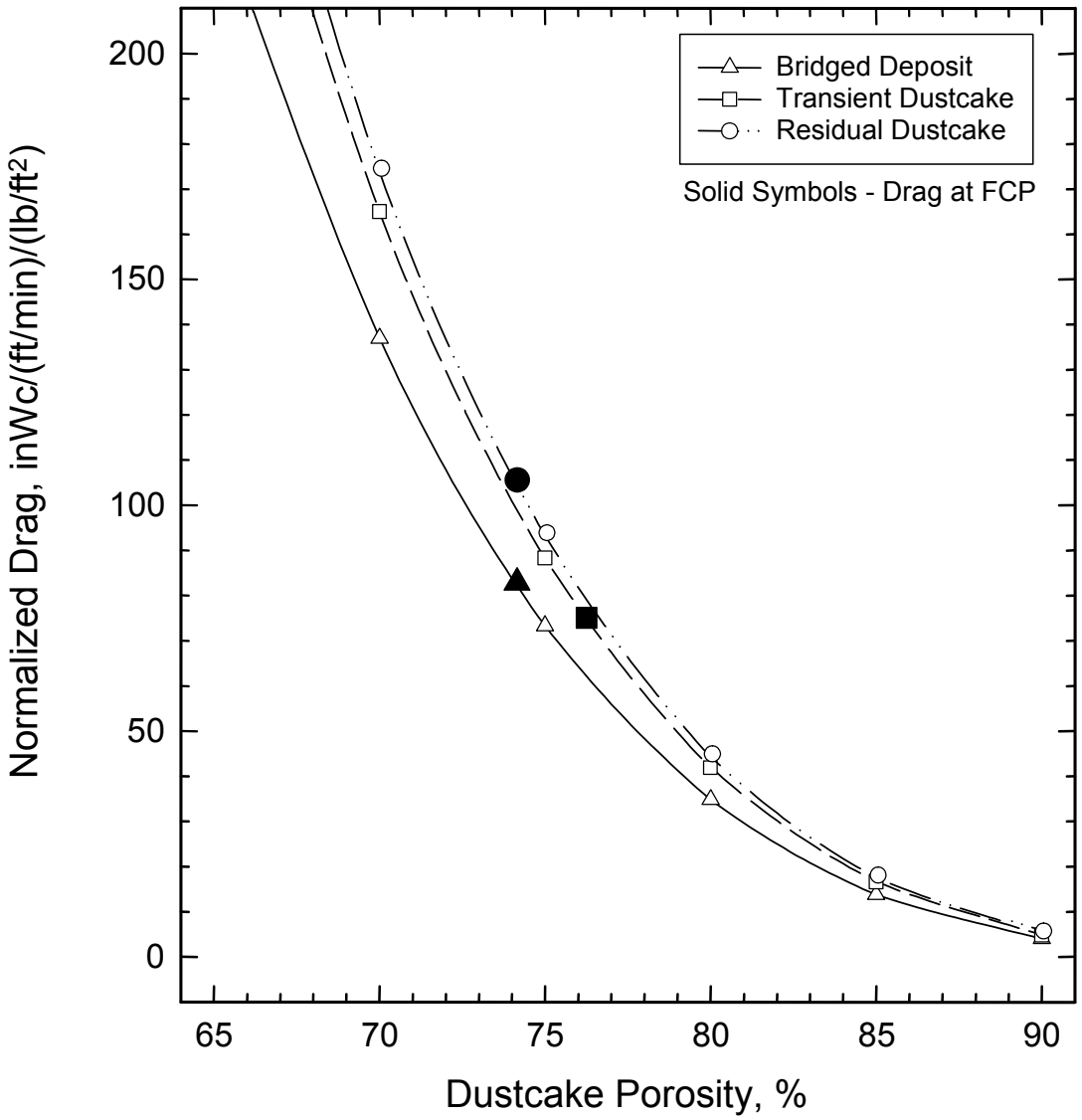

Figure 3.4-4 CAPTOR Drag of PCD Dustcake Samples (FCP Is the Flow-Compacted Porosity)

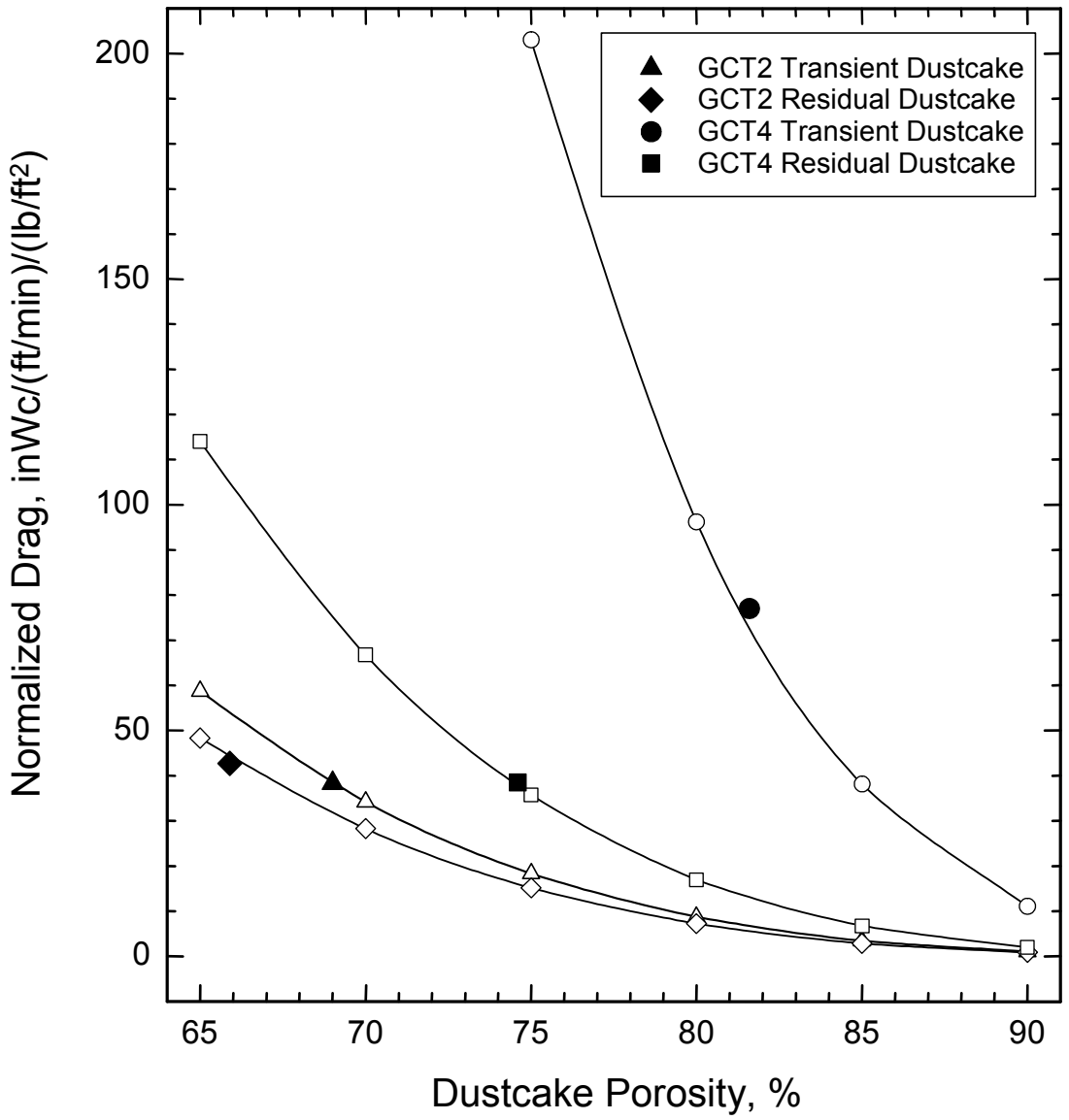

Figure 3.4-5 CAPTOR Drag During Previous Test Programs (Solid Symbols Denote Drag Measured at the Flow-Compacted Porosity)

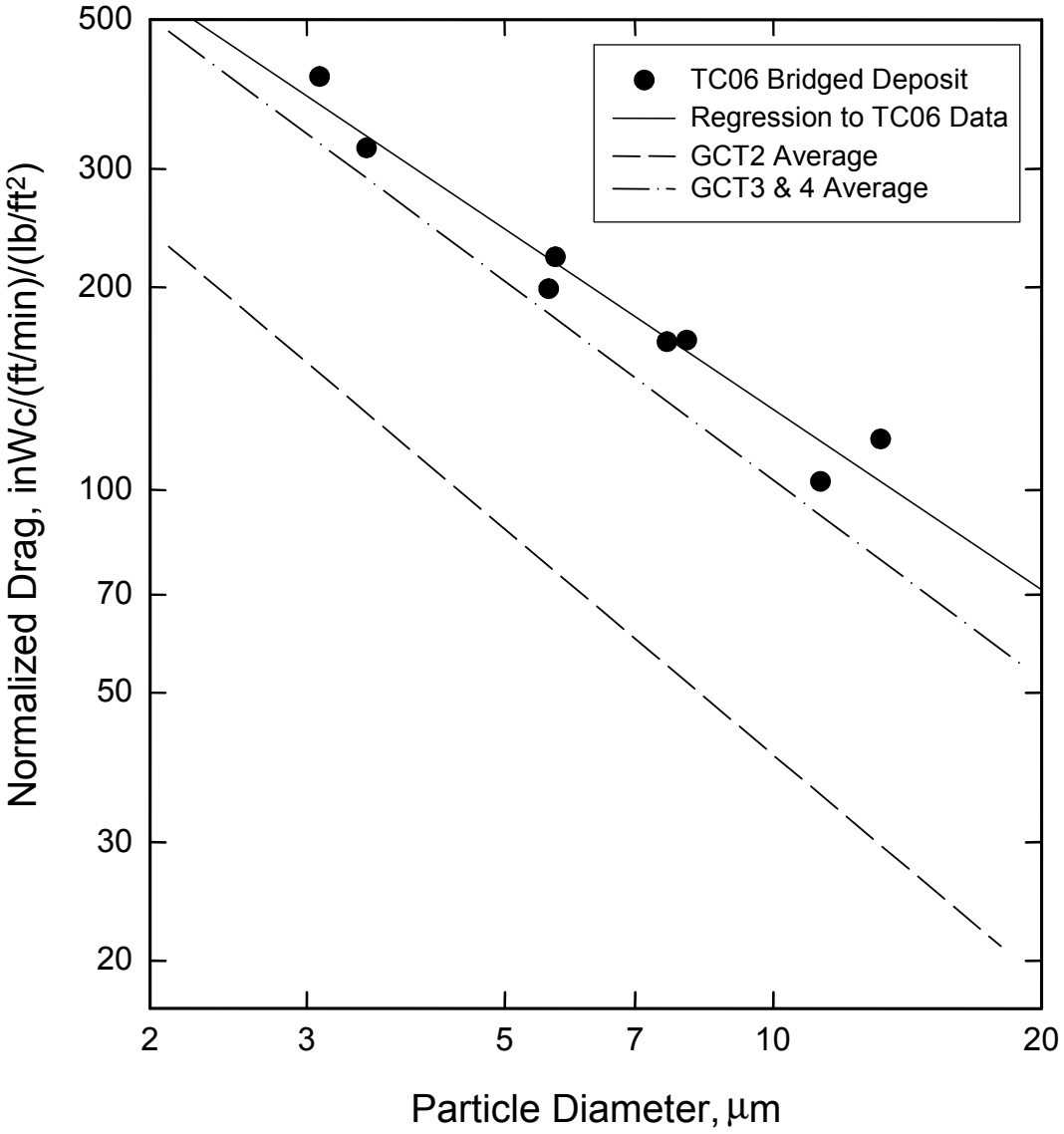

Figure 3.4-6 G-ash Drag as a Function of Particle Size

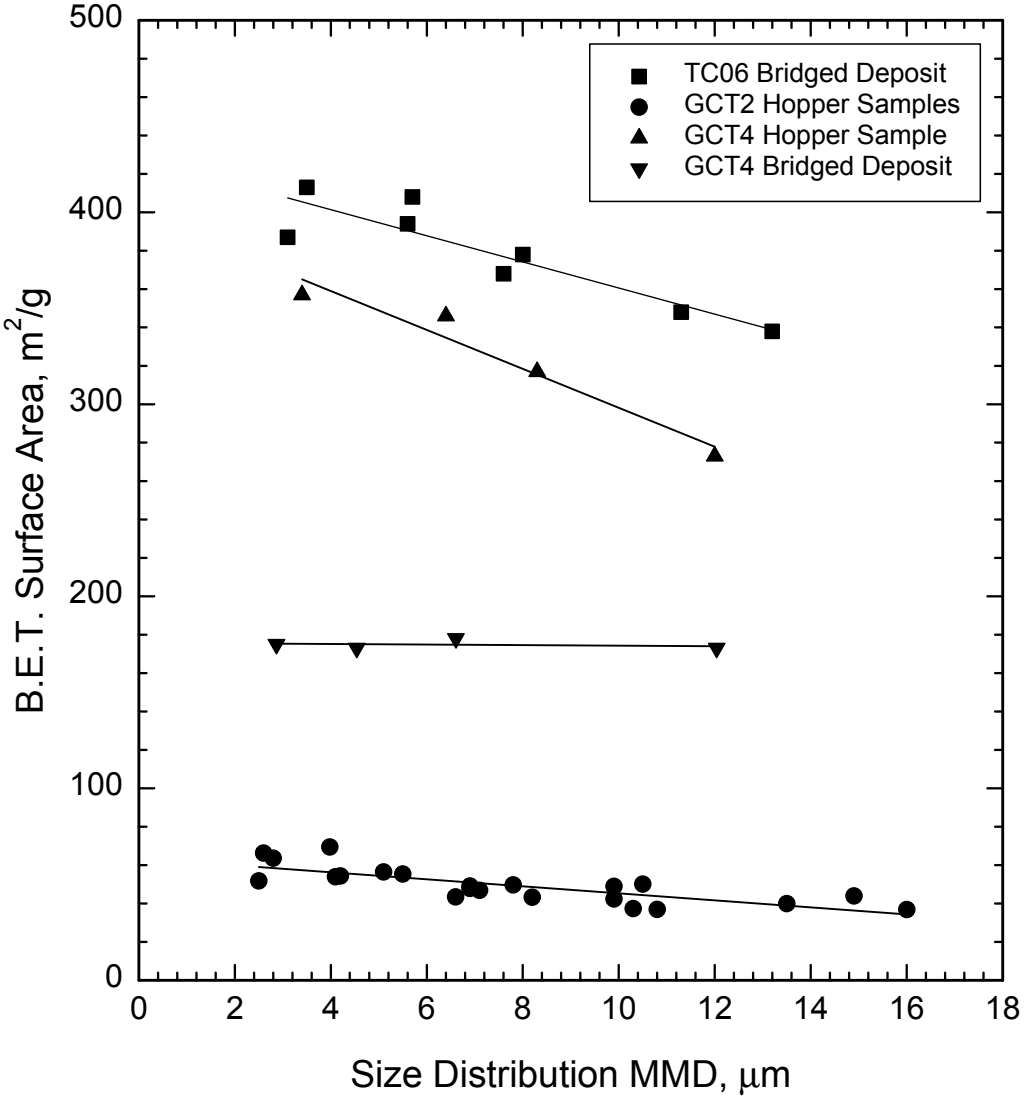

Figure 3.4-7 BET Surface Areas of G-ash Samples

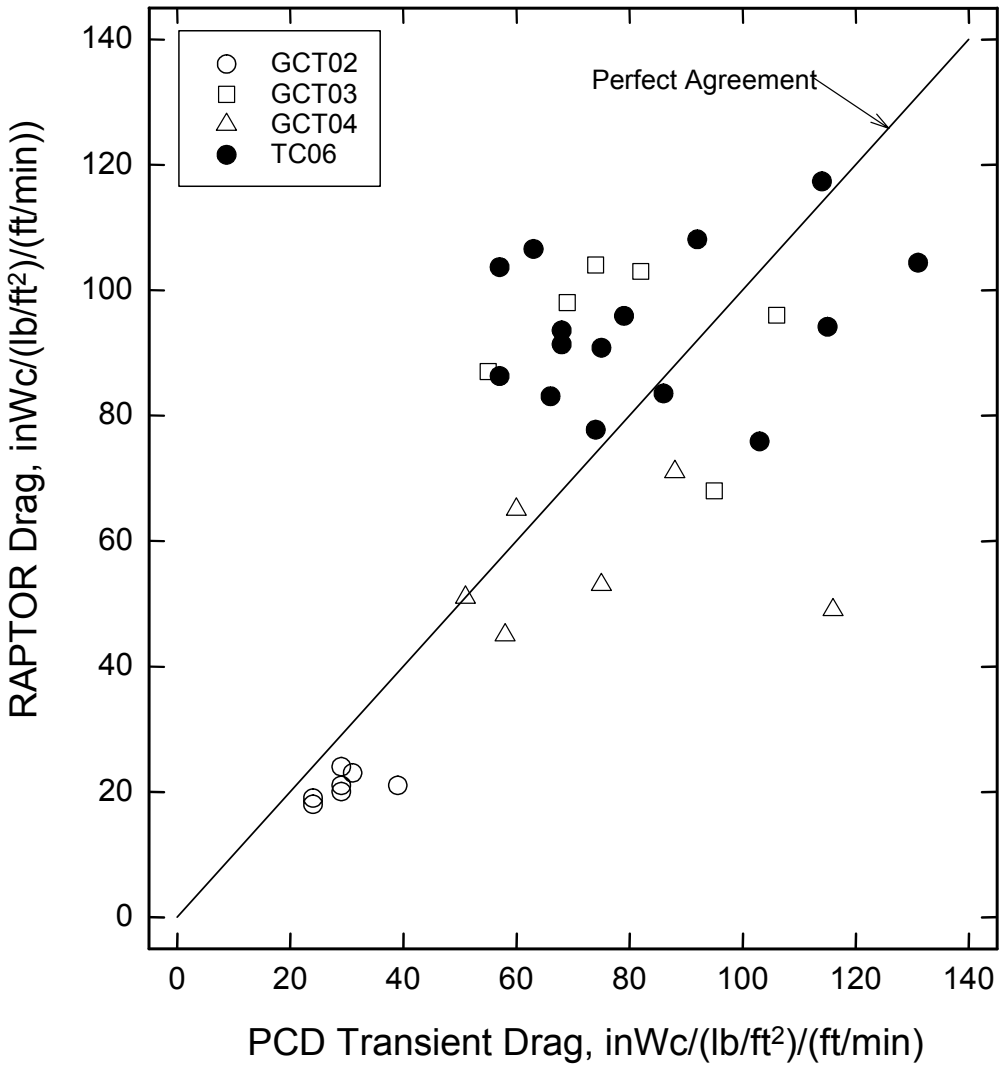

Figure 3.4-8 Comparison of Actual PCD Drag With RAPTOR Estimated Drag

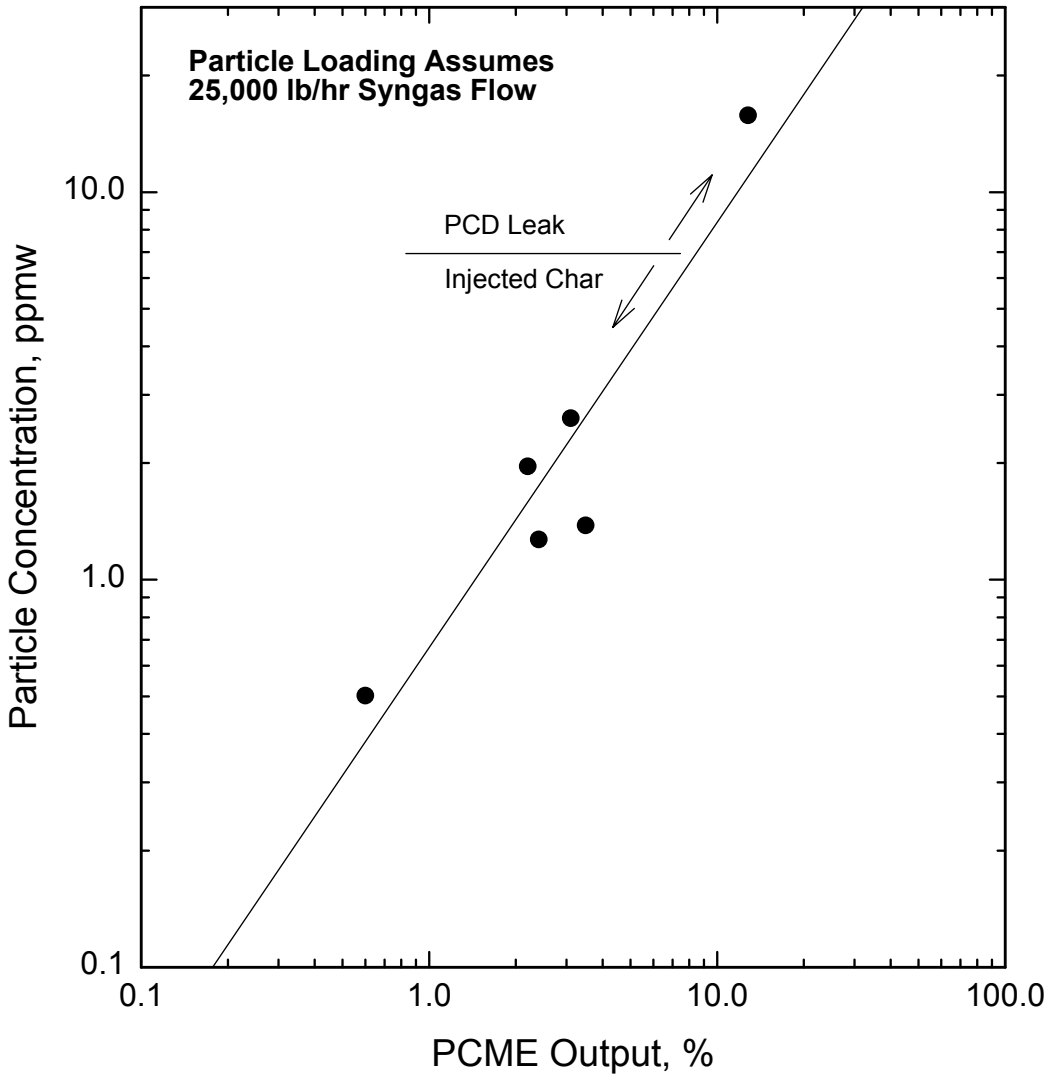

Figure 3.4-9 Calibration Tests on PCME Dustalert-90 Real-Time Monitor

3.5 TEST RESULTS FOR FILTER ELEMENTS

Property testing of filter elements continued during this test campaign. Pall iron aluminide (Fe_3Al), Schumacher T10-20, and Pall 326 elements were tested. The elements tested and their operational histories are summarized in Table 3.5-1. The test plan for each individual element is summarized in the test matrices shown in Tables 3.5-2 and -3. Specimens required to conduct the testing were removed from the elements as shown on the cutting plans in Figures 3.5-1 to -6.

The GCT3 test run was a 184-hour gasification run with a nominal operating temperature of 700°F. There was a thermal transient during this run where 14 thermocouples in the PCD vessel, which are mounted near the outside surfaces of the elements, measured a temperature increase of approximately 300°F in 1 minute. One Schumacher T10-20 element and one Pall 326 element were removed after this run and tested to determine if they suffered damage during the thermal transient. Fe_3Al element 27056 was also tested after this run. GCT4 was a 242-hour gasification run with a nominal operating temperature of 700°F. Fe_3Al Element 27060 was tested after operation in both GCT3 and GCT4, 425 total hours of on-coal operation. TC06A was a 228-hour gasification run with a nominal operating temperature of 700°F. This run ended because particulate was detected downstream of the PCD following a thermal transient. The thermal transient was severe but localized. The temperature of the elements probably exceeded 1,800°F but only 15 elements were affected. Element 21076, which was cracked after TC06A (see photograph, Figure 3.3-4), was tested and examined microscopically. This thermal transient is discussed in greater detail in Section 3.3. Finally, Fe_3Al element 034H-005, with 2,780 hours of combustion operation at a nominal temperature of 1,450°F, was tested. This is the longest exposure time on any Fe_3Al element and it was tested to determine if any degradation occurred even though the current operating mode is gasification with a nominal operating temperature of 750°F. This element was in operation during thermal transients in TC03 and TC04 that caused some ceramic element failures.

3.5.1 Pall Fe_3Al

All room-temperature tensile stress-strain responses obtained so far for Fe_3Al elements from gasification operation are shown in Figures 3.5-7 and -8 for the axial and hoop directions, respectively. Axial stress-strain responses measured at 1,400°F are shown in Figure 3.5-9. The hoop and axial tensile strengths are plotted versus hours in operation in Figure 3.5-10. All results are summarized in Tables 3.5-4 and -5. The hoop stress-strain responses (see Figure 3.5-8) represent the strains measured on the outside surface of the specimens and the corresponding stresses at the outside surface. However, for this test the specimens were loaded by hydrostatic pressure at the inside surface and the maximum stresses and strains occur at the inside surface. Therefore, the endpoints of these curves do not represent ultimate strength or strain values. The tensile strengths measured on virgin elements and after 63 hours were ~10 percent greater than the strengths measured after 180 to 650 hours; however, the hydrostatic burst pressure was nearly the same. This is because of variations in wall thickness. The elements tested in virgin condition and after 63 hours had thinner walls so the tensile stress was greater for the same hydrostatic pressure. In the axial direction, the strength was ~5 to 15 percent lower after operation than on virgin material; however, there have not been enough elements tested so far to assess element-to-element strength variation. The slightly lower

strength may be because of material variability, not a strength decrease during operation. The 0.05-percent yield strength (a line was drawn parallel to the initial slope of the stress-strain curve but offset by 0.0005 and the intersection of this line with the stress-strain curve is the 0.05-percent yield strength) also did not change after operation. Elevated temperature tensile strengths, in the axial direction only, were also slightly lower on the elements tested after operation. Again, this may be because of material variability. It is important to note that all Fe_3Al elements tested after gasification operation, with the possible exception of element 034H-004 tested after 63 hours in GCT1A, were in operation during at least one thermal transient event. As discussed in the second paragraph of Section 3.5, the severity of the thermal transients varied. There was a thermal transient during GCT1A with a temperature increase of ~135°F in 7.5 minutes measured on one element. There was no thermocouple on element 034H-004; therefore, it is not known if this element was affected by the thermal transient. The strengths may have been affected by the thermal transients as well as by normal operation. Because Fe_3Al has high thermal conductivity, thin walls, and high strain-to-failure compared to the Pall and Schumacher clay-bonded SiC, it was assumed that thermal transients survived by the clay-bonded SiC elements would have little or no effect on Fe_3Al elements. However, this has not been verified.

Hoop tensile results from element 21076, which was cracked during the thermal transient of TC06A, indicated that the tensile strength of 2 of 3 specimens was near the strength of all other specimens tested after operation. The other specimen from this element had strength ~18 percent below these two specimens. This could have been because of either material variability or damage from the transient. All specimens failed along the line separating the region of the element that was exposed to the highest temperature increase as shown in Figure 3.5-11. Results from this element indicate that there may have been local areas of damage that caused lower strength while the overall strength of the element was not affected.

Two room-temperature axial specimens, Tn-Ax-16 and 20, from element 27056, removed from operation after GCT3, had ultimate strengths and strains-to-failure significantly lower than all other axial tensile specimens. Examination of the fracture surfaces showed these two specimens had pits or voids that were barely visible unaided and easily seen with a low-powered optical microscope. SEM images of two regions on the fracture surface of specimen Tn-Ax-16 are shown in Figures 3.5-12 and -13. Similar regions were also seen on specimen Tn-Ax-20. Pitting was seen in each of these regions, both at the surface and internally. Higher magnification images of two selected pits, locations A and B in Figure 3.5-13, are shown in Figures 3.5-14 and -15. An image from a typical region of a specimen with no pits, Tn-Ax-22, is shown for comparison at the higher magnification in Figure 3.5-16. Particle size and morphology were both different in the pits than the material away from the pits. The particles inside of the pits were larger and had smoother edges. Elemental compositions were also different. Spectra obtained by energy dispersive spectroscopy (EDS) are shown in Figures 3.5-17 to -19 for the regions pictured in Figures 3.5-14 to -16, respectively. The typical composition shown in Figure 3.5-19 was iron, aluminum, and chromium. At many locations, oxygen was also seen although it does not appear in the spectra shown in Figure 3.5-19. Spectra from the pits, Figures 3.5-17 and -18, show large peaks representing the presence of chlorine. Chlorine was found in all pits but was not detected at any locations away from the pits. There were other "foreign" elements including sulfur, calcium, lead, arsenic, and titanium found in some, but not

all, pits. The source of these foreign elements (that is all elements except Fe, Al, Cr, and O) is not definitively known; however, this filter was water washed and all of these foreign elements are sometimes found in regular tap water. The cause and effect relationship between the foreign elements and the pits was not determined. They may have accumulated in preexisting pits or they may have caused the pits. If the pits already existed, it is also not known if these foreign elements changed them or made them worse. Material testing in the future will be conducted on filters that are not water washed to eliminate that possible source of contamination. Specimen Tn-Ax-18, also from element 27056, had an ultimate strength and strain-to-failure near the same as specimens from other Fe_3Al elements tested after gasification operation. Examination of the failure surface of this specimen showed pits, both internal and at the surface, but they were much smaller than those seen on Tn-Ax-16 and 20. Particle size and morphology appeared the same in the pits of this specimen as away from the pits; however, EDS analysis showed many of the same foreign elements as in the other two specimens from this filter. The pits on Tn-Ax-16 and 20 were much different than those observed on the outside surface of the elements discussed in Section 3.3.4. The material inside of and surrounding the surface pits discussed previously appeared the same in particle size and morphology as the material far away from the pits.

All axial tensile stress-strain responses measured so far at room temperature for Fe_3Al elements from combustion operation are shown in Figure 3.5-20. Responses measured at 1,400°F are shown in Figure 3.5-21. All results are summarized in Table 3.5-6. The strengths and strains-to-failure measured after operation in combustion for up to 2,780 hours were near the same as measured after gasification operation. All three of the Fe_3Al elements from combustion were in operation during at least one thermal transient. Element 034H-001, tested after 1,356 hours, was in operation during the TC03 event where a temperature increase of 320°F in 55 seconds was measured and 9 ceramic elements failed. Element 034H-004, tested after 1,424 hours, was in operation during TC04 when 6 ceramic elements (that is all ceramic elements except for IF&P REECER™) failed in a thermal transient. Element 034H-005, tested after 2,780 hours, was in operation during both of these thermal transients.

All room-temperature tensile strengths, axial and hoop, gasification, and combustion, are plotted versus hours in operation in Figure 3.5-22. This plot illustrates that the strength after 2,750 hours in combustion operation was similar to the strength after much shorter operation times. Note that the strengths compared in Figure 3.5-22 were measured on elements from different operating conditions, gasification (reducing) and combustion (oxidizing), and temperatures, 700 to 1,000°F for gasification and 1,350 to 1,450°F for combustion. The difference in operating environments and temperatures did not appear to affect the material properties, at least for the operating times tested so far.

3.5.2 Schumacher T10-20

Room-temperature hoop tensile strengths measured on Schumacher T10-20 element 323I178, removed after GCT3 with 183 hours in operation, are shown in Table 3.5-7. An average strength of 1,230 psi was measured. Hoop tensile strengths measured on all Schumacher clay-bonded SiC elements tested so far, from combustion or gasification operation, are plotted versus

hours in operation in Figure 3.5-23. The strength measured on this element was near the same as on other Schumacher clay-bonded SiC elements after operation.

3.5.3 Pall 326

Room-temperature hoop tensile strengths measured on Pall 326 element 1341-4, removed after GCT3 with 183 hours in operation, are shown in Table 3.5-8. An average strength of 1,980 psi was measured including one specimen with a strength of only 1530 psi, ~25 percent lower than the other specimens. Hoop tensile strengths measured on all Pall 326 elements tested so far, from combustion or gasification operation, are plotted versus hours in operation in Figure 3.5-24. Although there has been much variability in strengths measured so far, the values measured from this element are very near the average value. The low strength specimen could have resulted from local damage during the thermal transient; however, normal variability in strength on this material makes it impossible to determine if this low-strength value was because of variability or damage during the thermal transient.

3.5.4 Conclusions

Tensile strength measurements on Pall Fe_3Al elements from gasification operation at 700 to 1,000°F and combustion operation at 1,350 to 1,450°F indicated little or no strength decrease for at least up to 2,780 hours of operation. The strengths measured after operation were slightly lower than on virgin elements; however, because of the small number of elements tested so far, it is not possible to determine if this represents a slight strength decrease or element-to-element variability. The operating temperatures and environments within the range considered here did not appear to affect the properties measured. Thermal transients that have been encountered many times during operation at the PSDF, with a temperature increase of ~300°F measured during 1 minute, have not had an effect on the properties measured. However, exposure to temperatures above approximately 1,800°F, even for a short time during a thermal transient, may cause element failure. This is not surprising because the material was designed for operation below 1,470°F.

Internal pitting was seen on one element. The cause of the pitting is unknown. This element was water washed before testing and this must be considered as a possible cause of the pitting. Even if water washing was not the cause of the pitting, trace elements in the tap water used for washing may have collected and remained in pits, causing chemical and morphology changes. In the future, elements will not be water washed before testing.

The strengths of Schumacher T10-20 and Pall 326 tested after GCT03 were nearly the same as for other elements of these types tested after operation at the PSDF. The thermal transient experienced during this run did not cause any greater strength decrease than any previous runs. However, metal elements will be used for at least the next two gasification runs because similar thermal transients are possible and there is concern about cumulative damage caused by repeated transients.

Table 3.5-1

Filter Element Test Plan

Element Type	Run	Hours in Operation	Test Matrix
Pall Fe_3Al	GCT3	183	1
Pall Fe_3Al	GCT3 and 4	425	1
Pall Fe_3Al	GCT3 and 4 and TC06A	653	2
Pall 326	GCT3	183	2
Schumacher T10-20	GCT3	183	2
Pall Fe_3Al	Combustion	2,780	1

Table 3.5-2

Test Matrix 1

Test	Direction	Tests at	
		Room Temp.	1,400°F
Tension	Hoop	6	
Tension	Axial	3	3
Microstructure – microscopy, SEM,EDS, as req'd		Yes	

Note: Hoop tests not conducted on element 034H-005, 2,780 hours in combustion operation

Table 3.5-3

Test Matrix 2

Test	Direction	Tests at Room Temp
Tension	Hoop	6 (See Note)

Note: 3 tests for element 21076, 653 hours in gasification operation.

Table 3.5-4

Axial Tensile Results for Pall Fe_3Al Gasification Elements

Element	Specimen Number	Hours in Operation	Test Temperature (°F)	0.05% Yield Strength (psi)	Ultimate Strength (psi)	Young's Modulus (msi)	Strain-to-Failure (mils/in.)	Remarks
034H-002	Tn-Ax-1	virgin	RT[1]	13,400	20,200	5.26	10.1	
034H-002	Tn-Ax-3	virgin	RT	12,770	18,670	4.94	9.6	
034H-002	Tn-Ax-4	virgin	RT	12,160	18,400	5.38	9.0	
			Average	12,777	19,090	5.19	9.5	
034H-004	Tn-Ax-10	63	RT	11,390	17,770	5.63	10.5	Note 2
034H-004	Tn-Ax-12	63	RT	12,470	18,010	5.45	9.5	Note 2
034H-004	Tn-Ax-14	63	RT	11,460	17,950	5.70	10.1	Note 2
			Average	11,773	17,910	5.59	10.0	
27056	Tn-Ax-16	183	RT	12,190	12,680	5.69	2.9	Note 3
27056	Tn-Ax-18	183	RT	13,040	17,350	5.02	8.3	Note 3
27056	Tn-Ax-20	183	RT	12,440	12,440	5.92	2.6	Note 3
			Average	12,557		5.54		
27060	Tn-Ax-22	425	RT	12,800	16,250	5.47	5.8	Note 3
27060	Tn-Ax-24	425	RT	12,510	14,990	5.73	4.4	Note 3
27060	Tn-Ax-26	425	RT	12,700	16,800	5.71	6.7	Note 3
			Average	12,670	16,013	5.64	5.6	
034H-002	Tn-Ax-2	virgin	1,400	4,140	6,440	3.83	20	
034H-002	Tn-Ax-5	virgin	1,400	4,340	6,110	3.29	21	
			Average	4,240	6,275	3.56	20	
034H-004	Tn-Ax-11	63	1,400		5,200			Notes 2,4
034H-004	Tn-Ax-13	63	1,400	3,190	5,320	3.30	31	Note 2
034H-004	Tn-Ax-15	63	1,400	3,210	5,610	2.58	37	Note 2
			Average	3,200	5,377	2.94	34	
27056	Tn-Ax-17	183	1,400	3,330	5,250	2.29	24	Note 3
27056	Tn-Ax-19	183	1,400	3,250	5,320	2.53	34	Note 3
27056	Tn-Ax-21	183	1,400	3,250	5,850	2.79	43	Note 3
			Average	3,277	5,473	2.54	34	
27060	Tn-Ax-23	425	1,400	3,100	5,480	3.11	26	Note 3
27060	Tn-Ax-25	425	1,400	3,120	5,520	2.89	32	Note 3
27060	Tn-Ax-27	425	1,400	3,090	5,550	2.83	33	Note 3
			Average	3,103	5,517	2.94	30	

Notes:
1. RT = Room Temperature.
2. All operation at SCS - PSDF in gasification mode. Nominal operating temperature was 1,000°F.
3. All operation at SCS - PSDF in gasification mode. Nominal operating temperature was 700 - 800 °F.
4. Strain measurements were not obtained because the extensometers slipped during the test.

Table 3.5-5

Hoop Tensile Results for Pall Fe_3Al Gasification Elements

Element	Specimen Number	Hours in Operation	Maximum Hydrostatic Pressure (psig)	Ultimate Strength (psi)	Young's Modulus (msi)	Maximum Strain at O.D.[1] (mils/in.)	Remarks
034H-002	Tn-Hoop-309	virgin	1,170	18,000	6.09	5.6	
034H-002	Tn-Hoop-310	virgin	1,150	17,590	7.29	4.9	
034H-002	Tn-Hoop-311	virgin	1,160	17,460	5.84	5.2	
034H-002	Tn-Hoop-312	virgin	1,110	17,100	5.96	4.9	
034H-002	Tn-Hoop-313	virgin	1,150	17,720	5.64	5.7	
034H-002	Tn-Hoop-314	virgin	1,060	16,580	5.78	4.7	
034H-002	Tn-Hoop-315	virgin	1,080	16,750	5.84	4.8	
Average			1,126	17,314	6.06	5.1	
Standard Deviation			40	483	0.52	0.37	
Coefficient of Variation (COV)			4%	3%	9%	7%	
39185	Tn-Hoop-399	virgin	1,180	15,970	4.86	5.2	
39185	Tn-Hoop-400	virgin	1,180	16,270	5.17	5.3	
39185	Tn-Hoop-401	virgin	1,160	15,980	5.29	4.4	
39185	Tn-Hoop-402	virgin	1,120	17,090	5.29	4.6	
39185	Tn-Hoop-403	virgin	1,080	16,510	5.27	4.5	
39185	Tn-Hoop-404	virgin	1,180	16,490	4.97	5.1	
Average			1,150	16,385	5.14	4.8	
Standard Deviation			38	381	0.17	0.37	
Coefficient of Variation (COV)			3%	2%	3%	8%	
034H-004	Tn-Hoop-342	63	1,100	16,700	5.34	6.0	See Note 2
034H-004	Tn-Hoop-343	63	1,120	16,800	5.59	6.3	See Note 2
034H-004	Tn-Hoop-344	63	1,090	16,210	5.46	5.5	See Note 2
034H-004	Tn-Hoop-345	63	1,070	17,190	5.72	6.8	See Note 2
034H-004	Tn-Hoop-346	63	1,180	17,680	5.74	7.6	See Note 2
034H-004	Tn-Hoop-347	63	1,140	17,220	5.70	6.5	See Note 2
Average			1,117	16,967	5.59	6.4	
Standard Deviation			36	464	0.15	0.66	
Coefficient of Variation (COV)			3%	3%	3%	10%	
27056	Tn-Hoop-348	183	1,170	15,050	4.97	5.5	See Note 3
27056	Tn-Hoop-349	183	1,160	15,230	5.00	5.4	See Note 3
27056	Tn-Hoop-350	183	1,210	16,840	5.17	6.7	See Note 3
27056	Tn-Hoop-351	183	1,230	16,470	4.88	6.8	See Note 3
27056	Tn-Hoop-352	183	1,090	14,840	4.70	4.6	See Note 3
27056	Tn-Hoop-353	183	1,080	14,620	4.97	4.1	See Note 3
Average			1,157	15,508	4.95	5.5	
Standard Deviation			56	839	0.14	0.98	
Coefficient of Variation (COV)			5%	5%	3%	18%	
27060	Tn-Hoop-354	425	1,200	15,470	4.99	5.4	See Note 3
27060	Tn-Hoop-355	425	1,210	16,530	5.37	5.4	See Note 3
27060	Tn-Hoop-356	425	1,150	15,750	5.13	4.6	See Note 3
27060	Tn-Hoop-357	425	1,170	15,810	5.21	4.7	See Note 3
27060	Tn-Hoop-358	425	1,060	15,440	5.05	4.7	See Note 3
27060	Tn-Hoop-359	425	1,140	16,100	5.15	5.3	See Note 3
Average			1,155	15,850	5.15	5.0	
Standard Deviation			49	376	0.12	0.36	
Coefficient of Variation (COV)			4%	2%	2%	7%	
21076	Tn-Hoop-366	653	1,160	15,130	5.16	6.0	See Notes 3,4
21076	Tn-Hoop-367	653	1,150	15,300	5.25	5.9	See Notes 3,4
21076	Tn-Hoop-368	653	960	12,570	5.00	3.2	See Notes 3,4
Average			1,090	14,333	5.14	5.1	
Standard Deviation			92	1,249	0.10	1.28	
Coefficient of Variation (COV)			8%	9%	2%	25%	

Notes:
1. This value does not represent the strain-to-failure. The strain was measured at the outside surface but for this test, the maximum stress occurs at the inside surface.
2. All operation was in gasification mode at a nominal temperature of 1,000°F.
3. All operation was in gasification mode at a nominal temperature of 700°F.
4. Element exposed to much higher temperature during TC06A fire.

Table 3.5-6

Axial Tensile Results for Pall Fe_3Al Combustion Elements

Candle	Specimen Number	Hours in Operation	Test Temperature (°F)	0.05% Yield Strength (psi)	Ultimate Strength (psi)	Young's Modulus (msi)	Strain-to-Failure (mils/in.)	Remarks
034H-002	Tn-Ax-1	virgin	RT[1]	13,400	20,200	5.26	10.1	
034H-002	Tn-Ax-3	virgin	RT	12,770	18,670	4.94	9.6	
034H-002	Tn-Ax-4	virgin	RT	12,160	18,400	5.38	9.0	
			Average	12,777	19,090	5.19	9.5	
034H-001	Tn-Ax-6	1356	RT	10,820	15,680	5.36	6.71	Note 2
034H-001	Tn-Ax-7	1356	RT	10,920	15,100	5.36	5.76	Note 2
034H-001	Tn-Ax-8	1356	RT	11,040	16,440	5.28	8.32	Note 2
034H-001	Tn-Ax-9	1356	RT	11,570	16,950	4.89	8.45	Note 2
			Average	11,088	16,043	5.22	7.31	
034H-005	Tn-Ax-29	2780	RT	12,450	16,000	5.93	5.1	Note 2
034H-005	Tn-Ax-32	2780	RT	12,560	16,490	6.1	5.3	Note 2
034H-005	Tn-Ax-33	2780	RT	12,450	16,530	5.45	6.1	Note 2
			Average	12,487	16,340	5.83	5.5	
034H-002	Tn-Ax-2	virgin	1,400	4,140	6,440	3.83	20.0	
034H-002	Tn-Ax-5	virgin	1,400	4,340	6,110	3.29	21.0	
			Average	4,240	6,275	3.56		
034H-005	Tn-Ax-28	2780	1,400	3,470	5,650	2.61	26	Note 2
034H-005	Tn-Ax-30	2780	1,400	3,990	5,650	2.58	20	Note 2
034H-005	Tn-Ax-31	2780	1,400	3,950	5,410	2.78	17	Note 2
			Average	3,803	5,570	2.66	21	

Notes:
1. RT = Room Temperature.
2. All operation at SCS - PSDF in combustion mode. Nominal operating temperature was 1,350 to 1,450°F.

Table 3.5-7

Hoop Tensile Results for Schumacher T10-20 and TF20 Gasification Elements

Element	Specimen Number	Hours in Operation	Maximum Hydrostatic Pressure (psig)	Ultimate Strength (psi)	Remarks
323I178	Tn-Hoop-467	183	500	1,210	Notes 1,3
323I178	Tn-Hoop-468	183	520	1,320	Notes 1,3
323I178	Tn-Hoop-469	183	510	1,280	Notes 1,3
323I178	Tn-Hoop-470	183	470	1,210	Notes 1,3
323I178	Tn-Hoop-471	183	480	1,240	Notes 1,3
323I178	Tn-Hoop-472	183	430	1,100	Notes 1,3
Average			485	1,227	
Standard Deviation			30	69	
COV			6%	6%	
335I297	Tn-Hoop-425	218	530	1,270	Note 1
335I297	Tn-Hoop-426	218	530	1,290	Note 1
335I297	Tn-Hoop-427	218	460	1,160	Note 1
335I297	Tn-Hoop-428	218	460	1,160	Note 1
335I297	Tn-Hoop-429	218	470	1,220	Note 1
335I297	Tn-Hoop-430	218	460	1,180	Note 1
Average			485	1,213	
Standard Deviation			32	52	
COV			7%	4%	
326I121	Tn-Hoop-431	218	560	1,370	Note 1
326I121	Tn-Hoop-432	218	510	1,270	Note 1
326I121	Tn-Hoop-433	218	470	1,210	Note 1
326I121	Tn-Hoop-434	218	480	1,220	Note 1
326I121	Tn-Hoop-435	218	520	1,360	Note 1
326I121	Tn-Hoop-436	218	460	1,190	Note 1
Average			500	1,270	
Standard Deviation			34	71	
COV			7%	6%	
326I126	Tn-Hoop-455	218	510	1,230	Notes 1,2
326I126	Tn-Hoop-456	218	490	1,200	Notes 1,2
326I126	Tn-Hoop-457	218	430	1,090	Notes 1,2
326I126	Tn-Hoop-458	218	440	1,120	Notes 1,2
326I126	Tn-Hoop-459	218	410	1,050	Notes 1,2
326I126	Tn-Hoop-460	218	420	1,070	Notes 1,2
Average			450	1,127	
Standard Deviation			37	66	
COV			8%	6%	

Notes:
1. All operation at SCS - PSDF in gasification mode at a nominal operating temperature of 700 to 1,000°F.
2. Element went through cleaning process at Southern Metals Processing.
3. In operation during thermal transient.

Table 3.5-8

Hoop Tensile Results for Pall 326 Gasification Elements

Element	Specimen Number	Hours in Operation	Maximum Hydrostatic Pressure (psig)	Ultimate Strength (psi)	Remarks
1341-4	Tn-Hoop-473	183	830	2,070	Notes 2,3
1341-4	Tn-Hoop-474	183	839	2,120	Notes 2,3
1341-4	Tn-Hoop-475	183	810	2,070	Notes 2,3
1341-4	Tn-Hoop-476	183	590	1,530	Notes 2,3
1341-4	Tn-Hoop-477	183	800	2,060	Notes 2,3
1341-4	Tn-Hoop-478	183	780	2,030	Notes 2,3
Average			775	1,980	
Standard Deviation			85	203	
COV			11.0%	10.3%	
1322-2	Tn-Hoop-407	218	820	2,070	Note 2
1322-2	Tn-Hoop-408	218	840	2,120	Note 2
1322-2	Tn-Hoop-409	218	820	2,100	Note 2
1322-2	Tn-Hoop-410	218	810	2,080	Note 2
1322-2	Tn-Hoop-411	218	760	2,050	Note 2
1322-2	Tn-Hoop-412	218	740	2,010	Note 2
Average			798	2,072	
Standard Deviation			36	35	
COV			4.5%	1.7%	
1316-6	Tn-Hoop-413	218	870	2,190	Note 2
1316-6	Tn-Hoop-414	218	850	2,150	Note 2
1316-6	Tn-Hoop-415	218	790	2,030	Note 2
1316-6	Tn-Hoop-416	218	770	1,990	Note 2
1316-6	Tn-Hoop-417	218	800	2,140	Note 2
1316-6	Tn-Hoop-418	218	790	2,120	Note 2
Average			812	2,103	
Standard Deviation			36	70	
COV			4.4%	3.3%	
1339-5	Tn-Hoop-449	218	910	2,270	Notes 1,2
1339-5	Tn-Hoop-450	218	1,000	2,510	Notes 1,2
1339-5	Tn-Hoop-451	218	900	2,300	Notes 1,2
1339-5	Tn-Hoop-452	218	920	2,360	Notes 1,2
1339-5	Tn-Hoop-453	218	920	2,450	Notes 1,2
1339-5	Tn-Hoop-454	218	890	2,410	Notes 1,2
Average			923	2,383	
Standard Deviation			36	83	
COV			3.9%	3.5%	

Notes:
1. Element went through cleaning process at Southern Metals Processing.
2. All operation at SCS - PSDF in gasification mode at a nominal operating temperature of 700 to 1,000°F.
3. In operation during thermal transient.

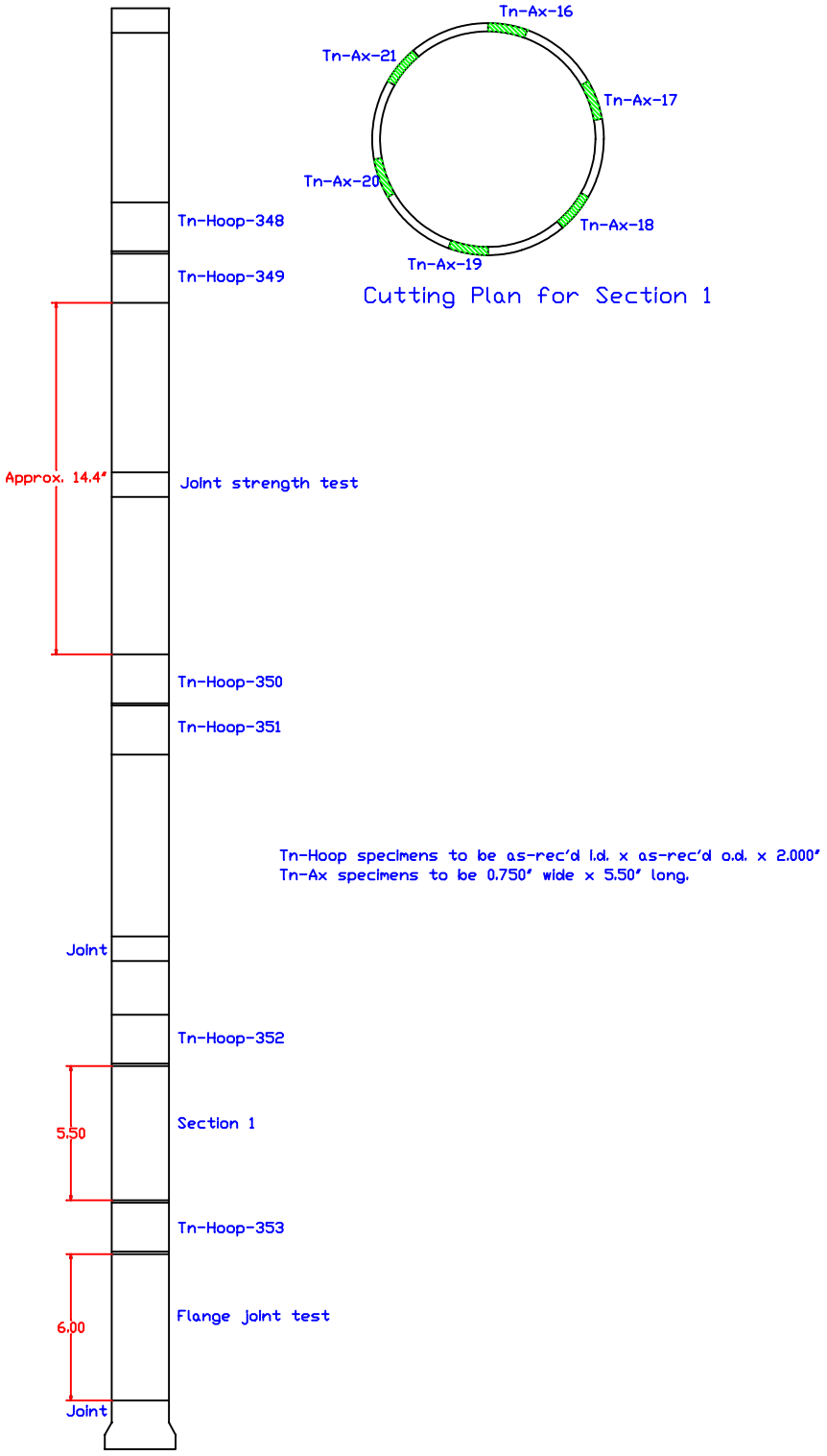

Figure 3.5-1 Cutting Plan for Pall Fe_3Al Element 27056

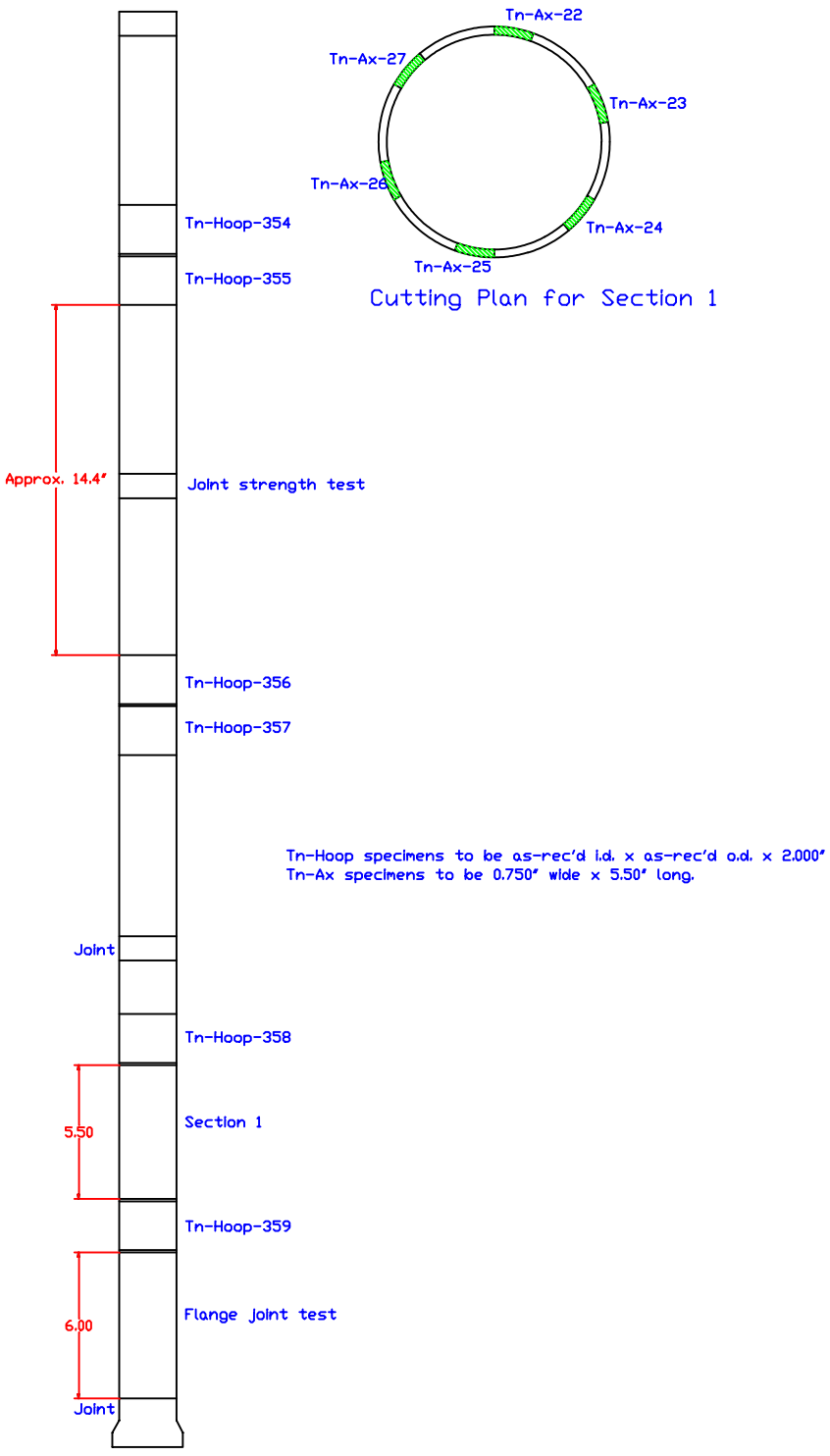

Figure 3.5-2 Cutting Plan for Pall Fe_3Al Element 27060

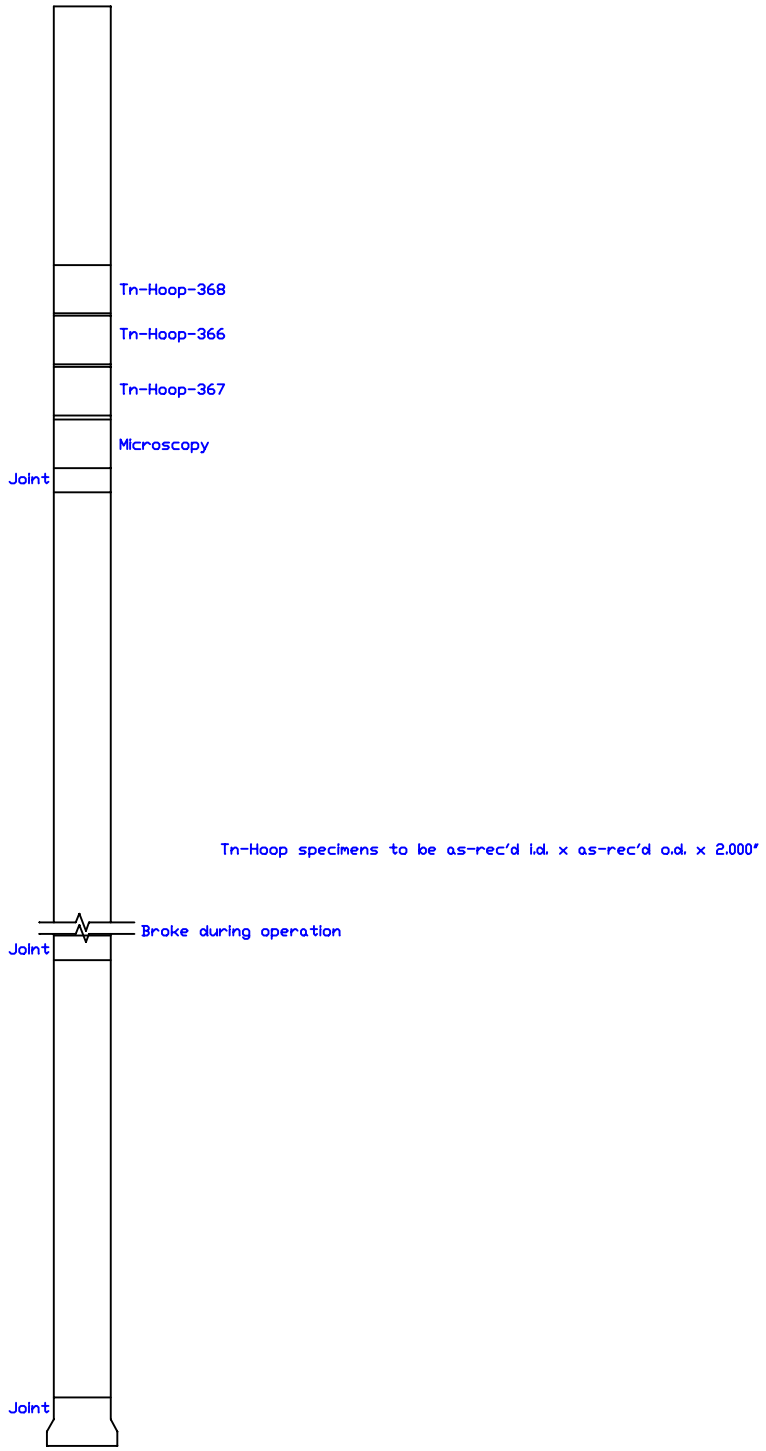

Figure 3.5-3 Cutting Plan for Pall Fe_3Al Element 21076

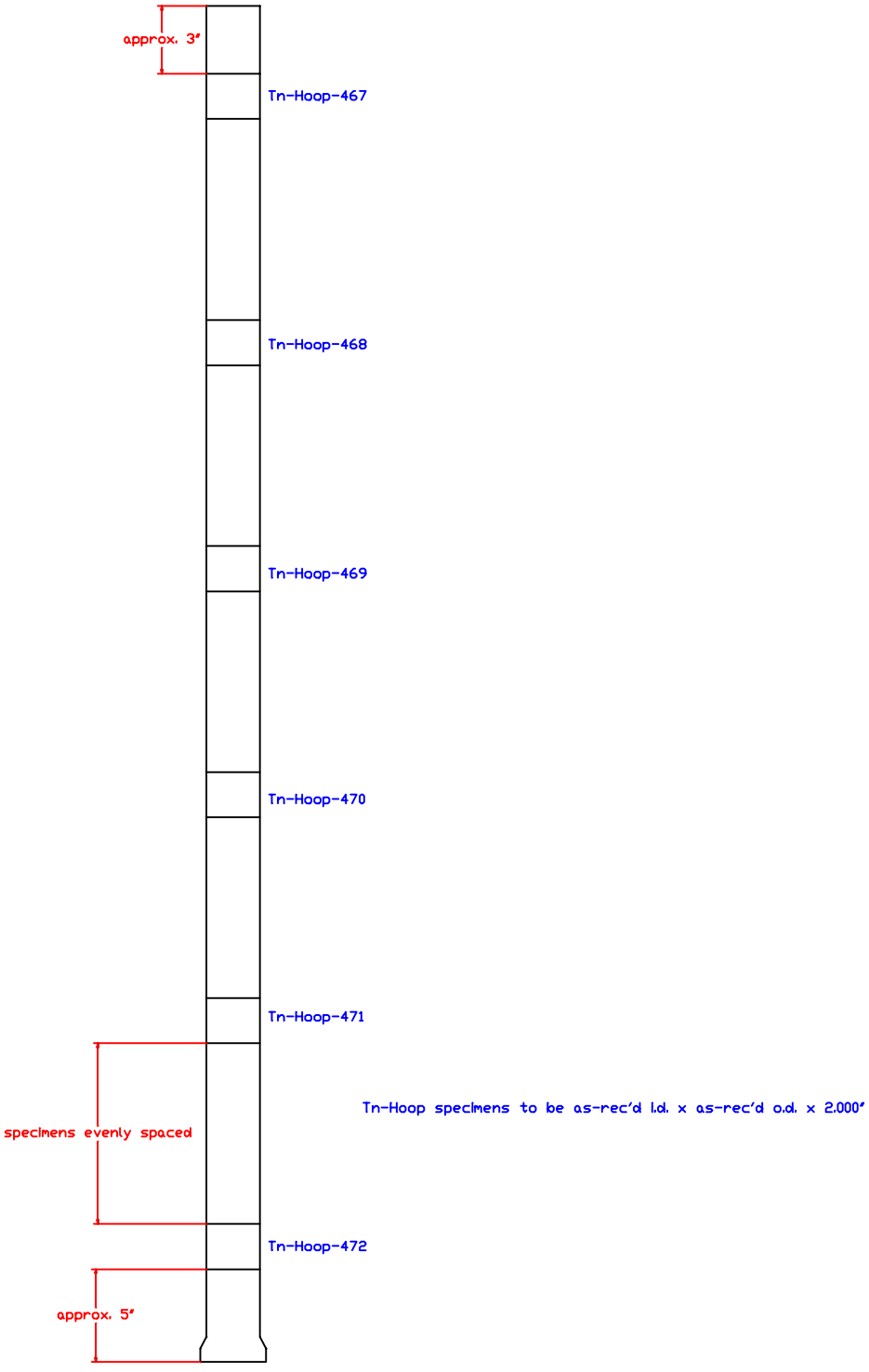

Figure 3.5-4 Cutting Plan for Schumacher T10-20 Element 323I178

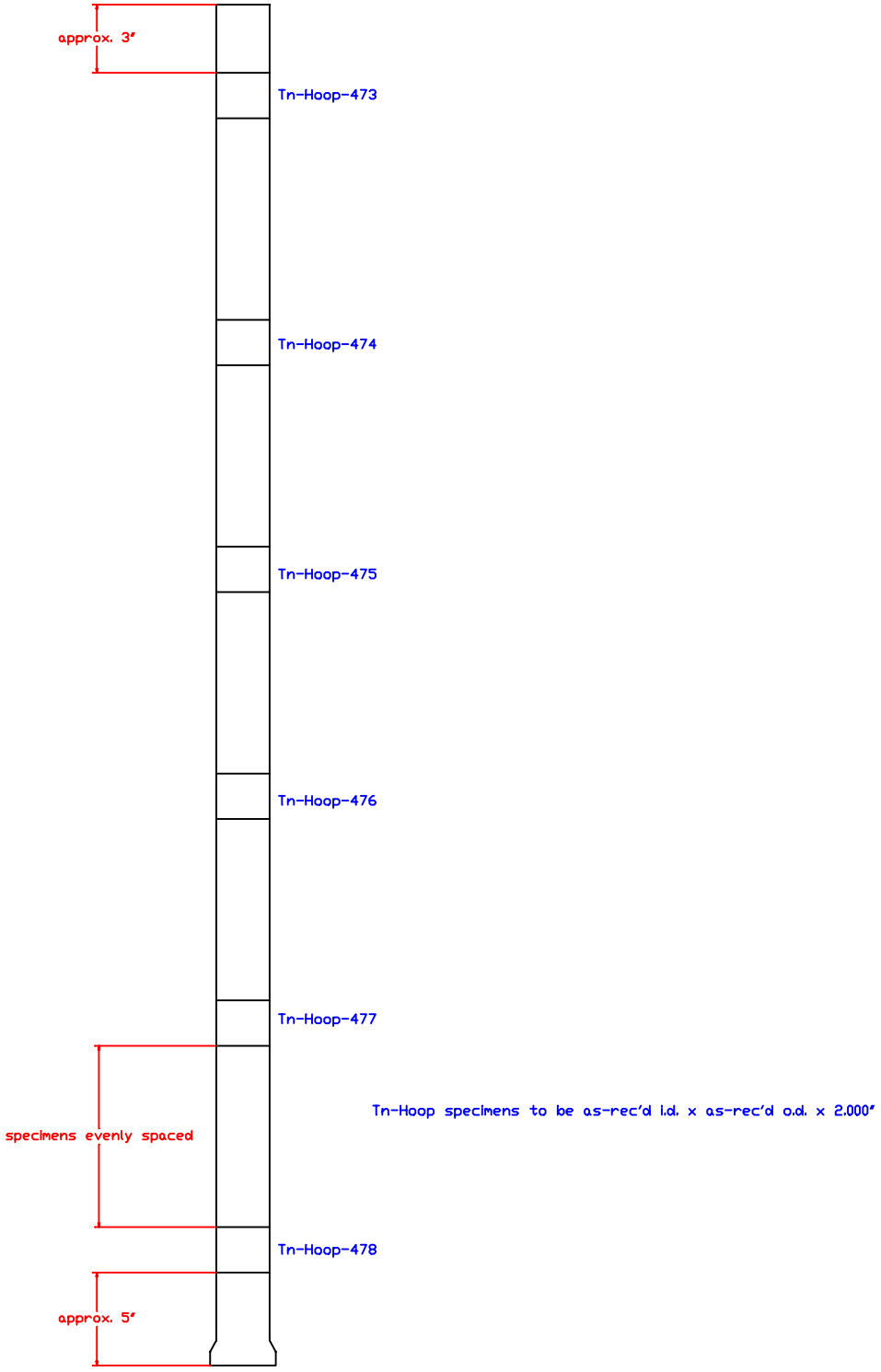

Figure 3.5-5 Cutting Plan for Pall 326 Element 1341-4

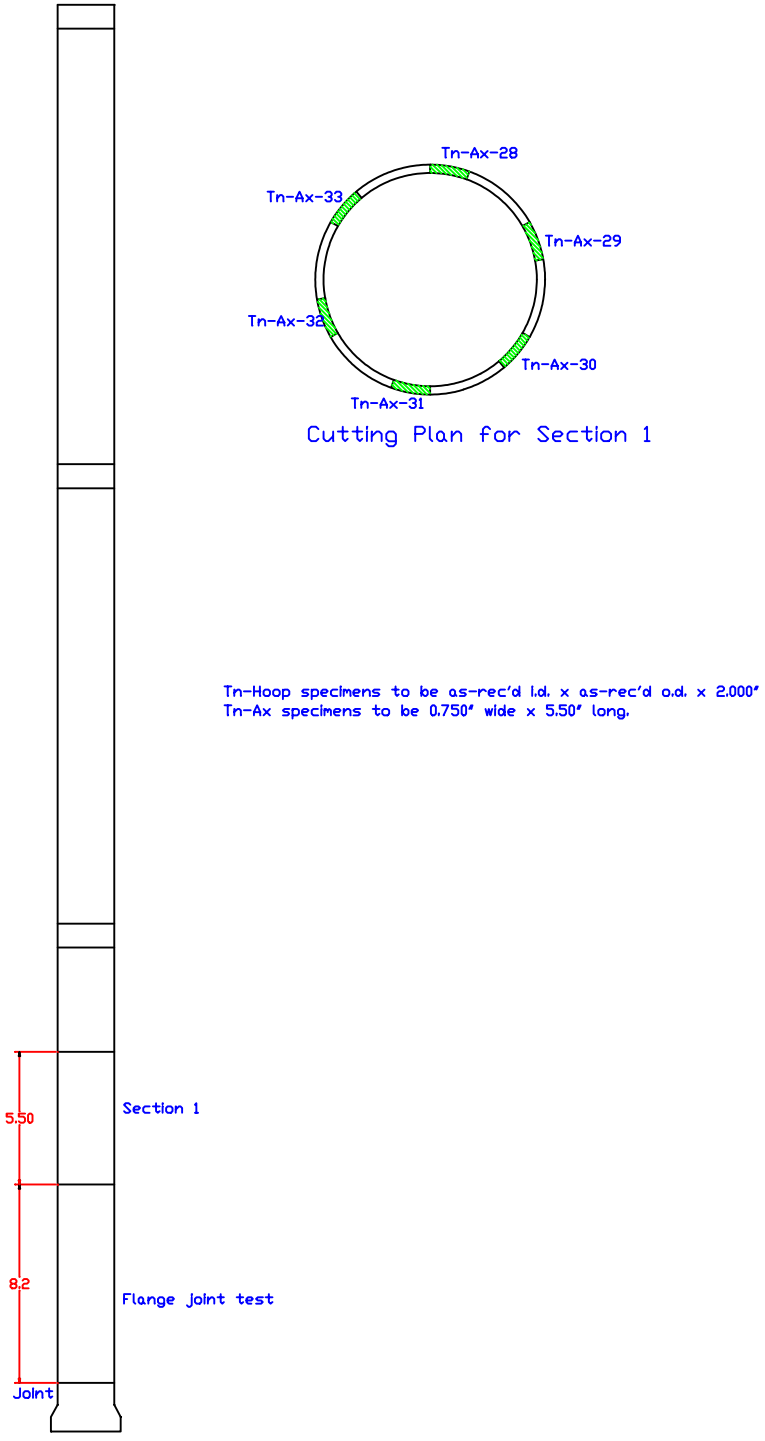

Figure 3.5-6 Cutting Plan for Pall Fe_3Al Element 034H-005

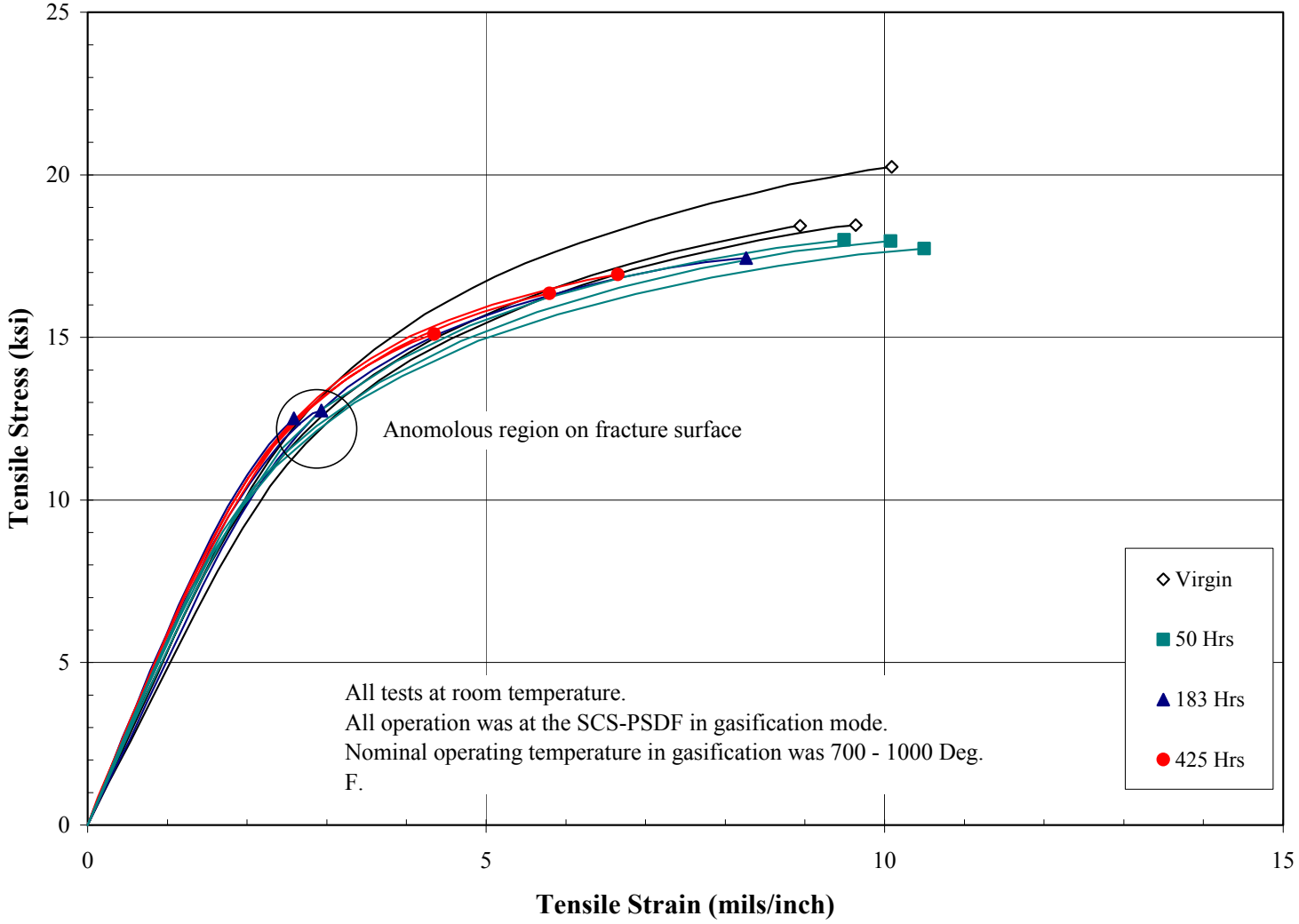

Figure 3.5-7 Axial Tensile Stress-Strain Responses for Pall Fe_3Al at Room Temperature

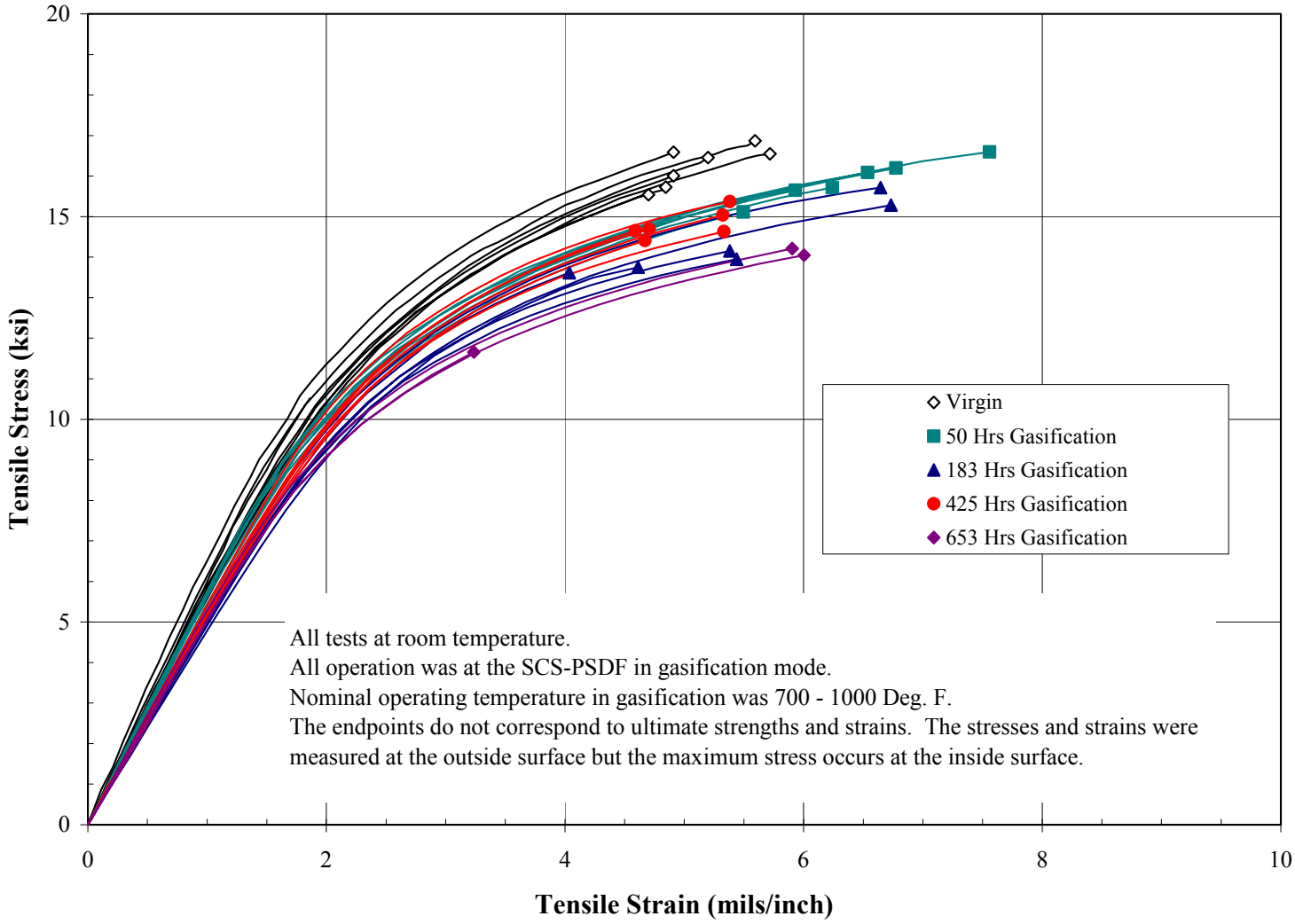

Figure 3.5-8 Hoop Tensile Stress-Strain Responses for Pall Fe_3Al at Room Temperature

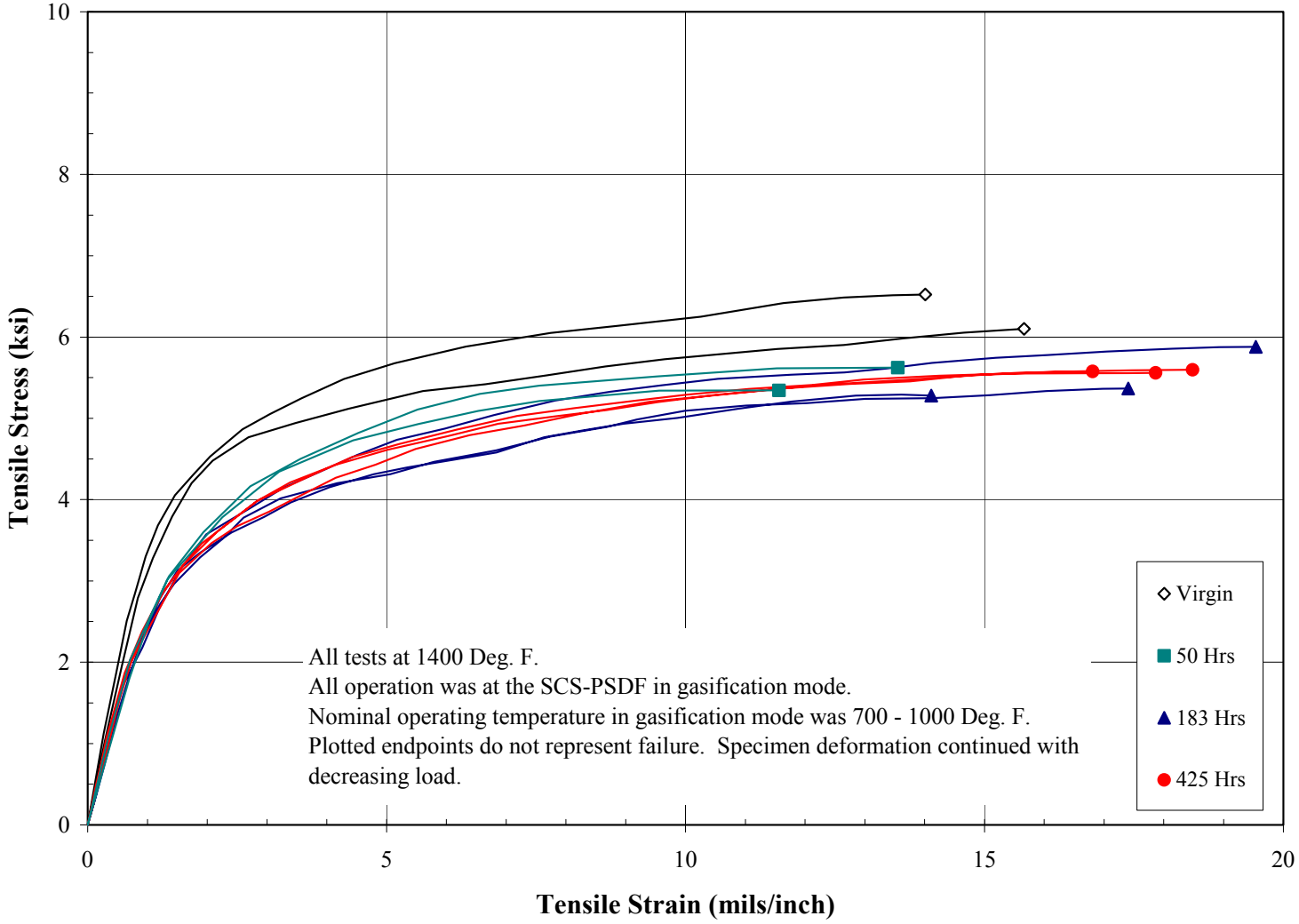

Figure 3.5-9 Axial Tensile Stress-Strain Responses for Pall Fe_3Al at 1,400°F

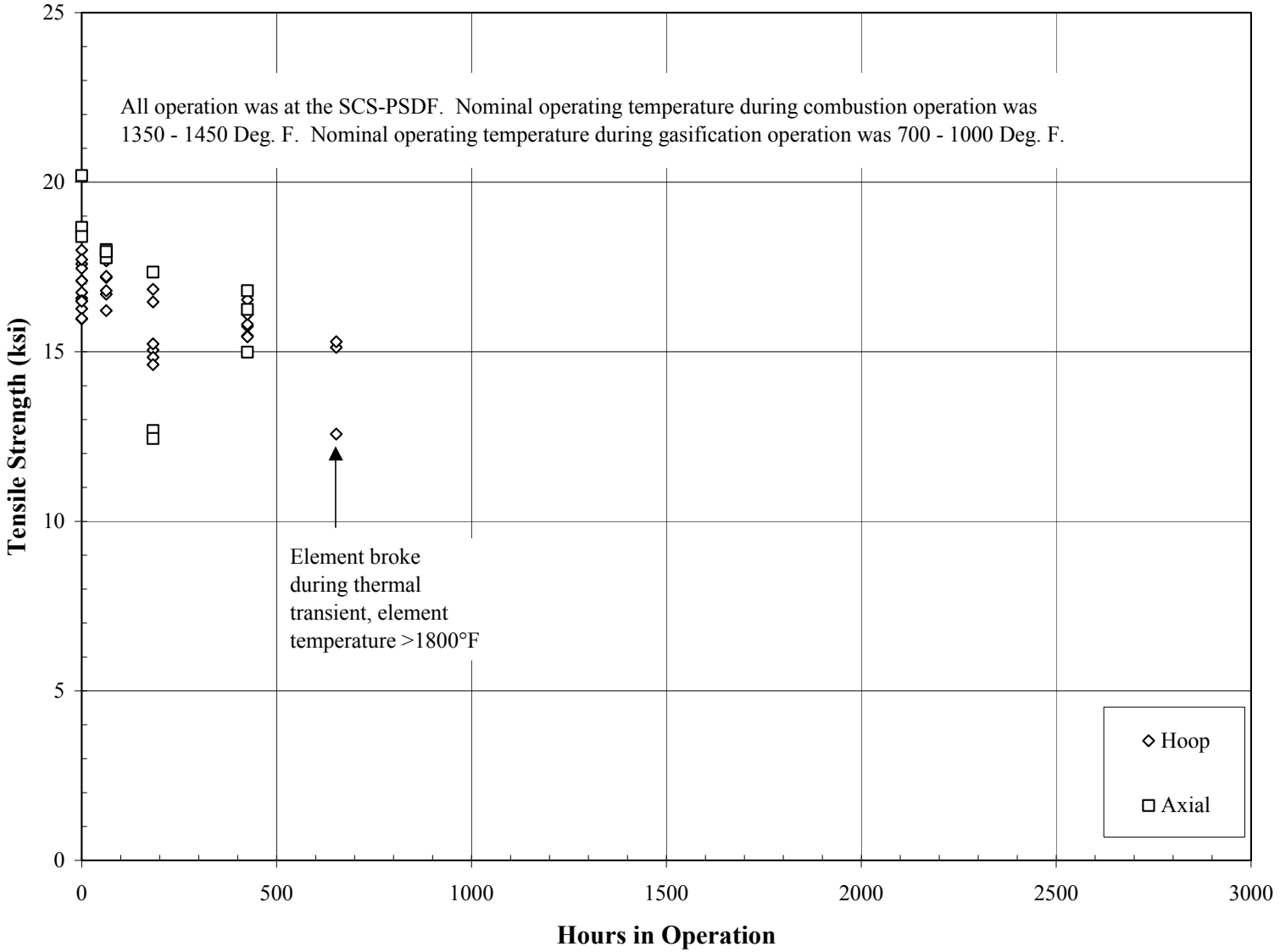

Figure 3.5-10 Tensile Strength of Pall Fe_3Al

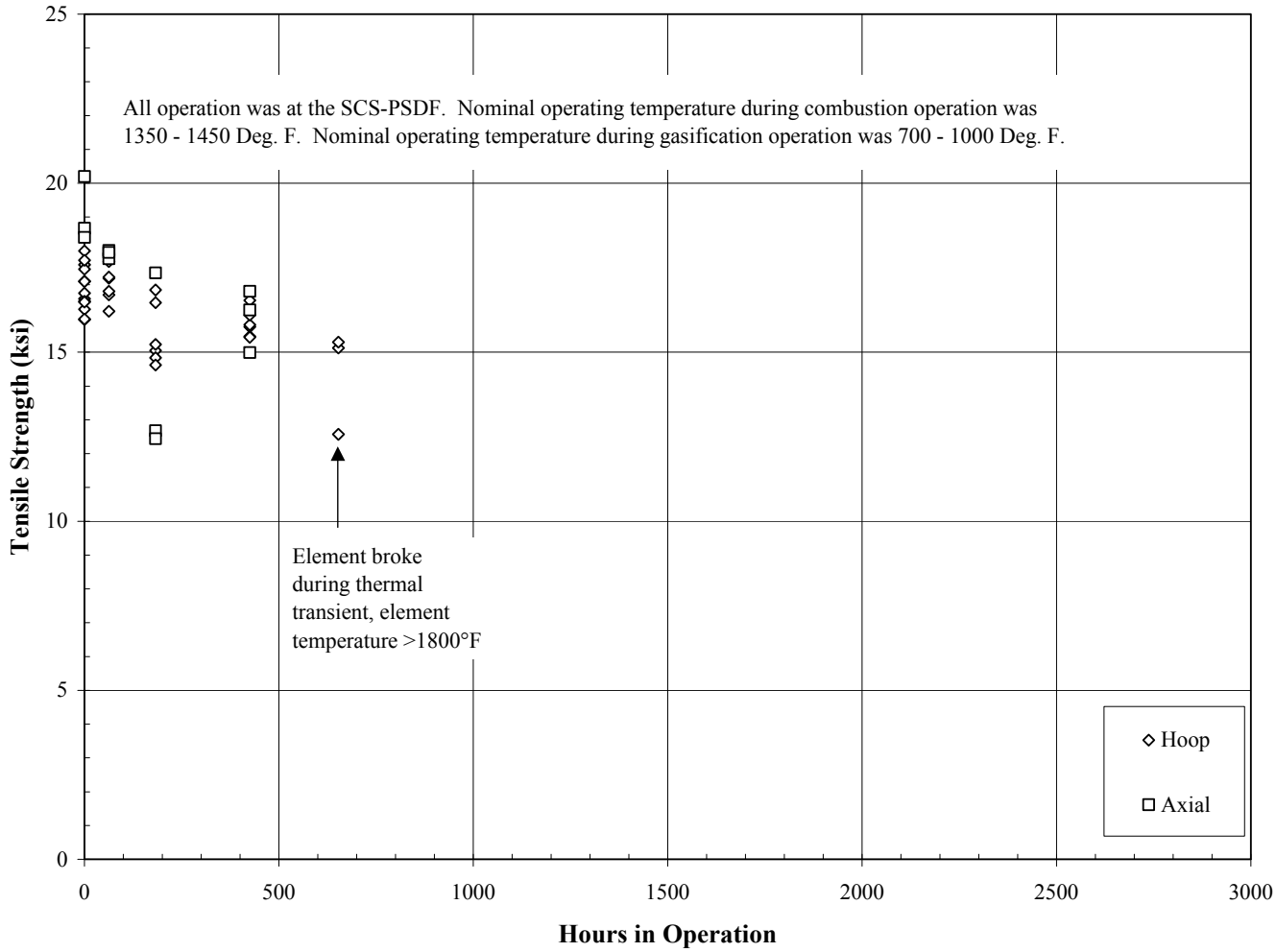

Figure 3.5-11 Failed Fe_3Al Tensile Specimen From Element 21076

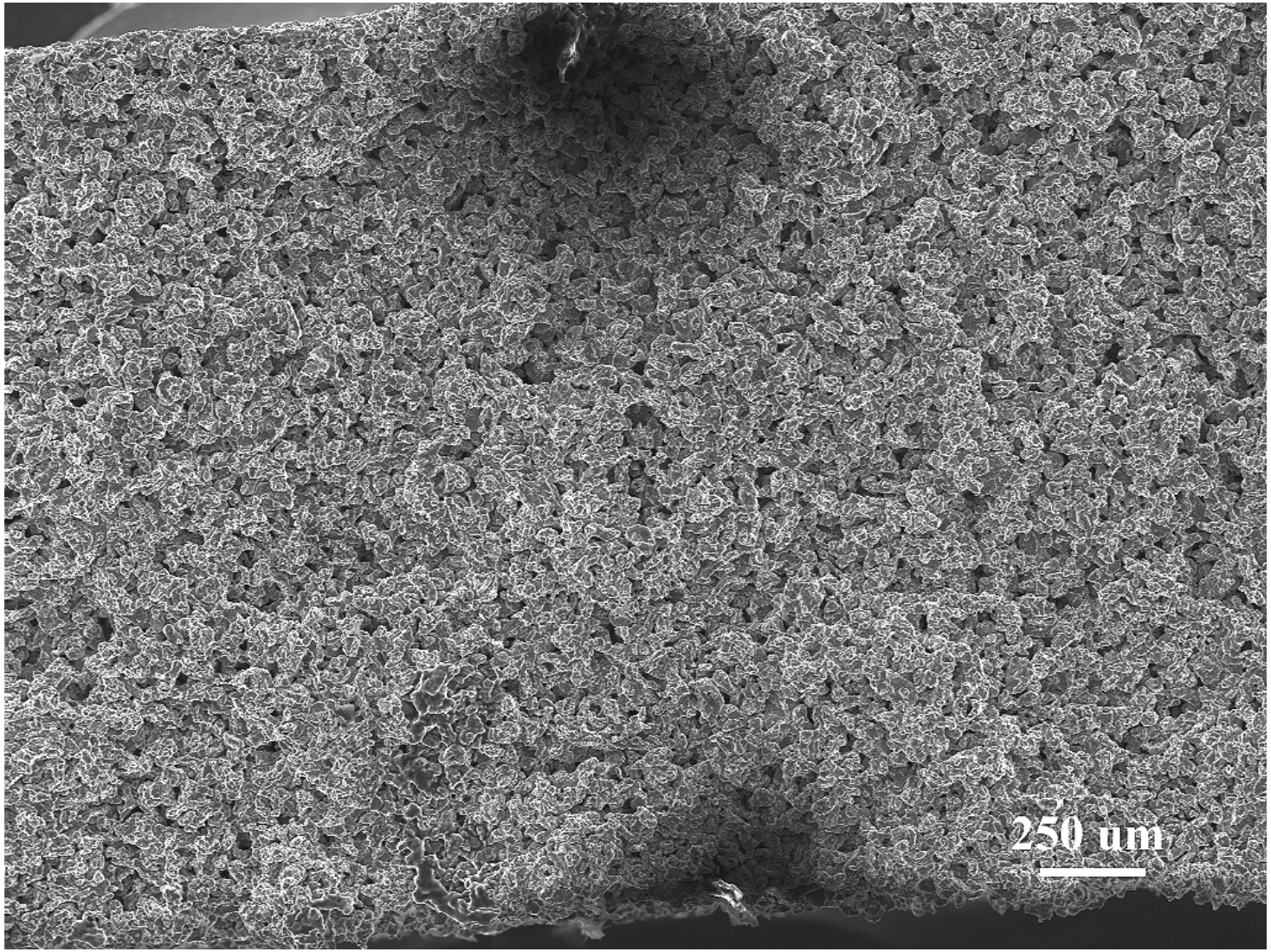

Figure 3.5-12 Fracture Surface of Fe_3Al Tensile Specimen Tn-Ax-16 – Location 1

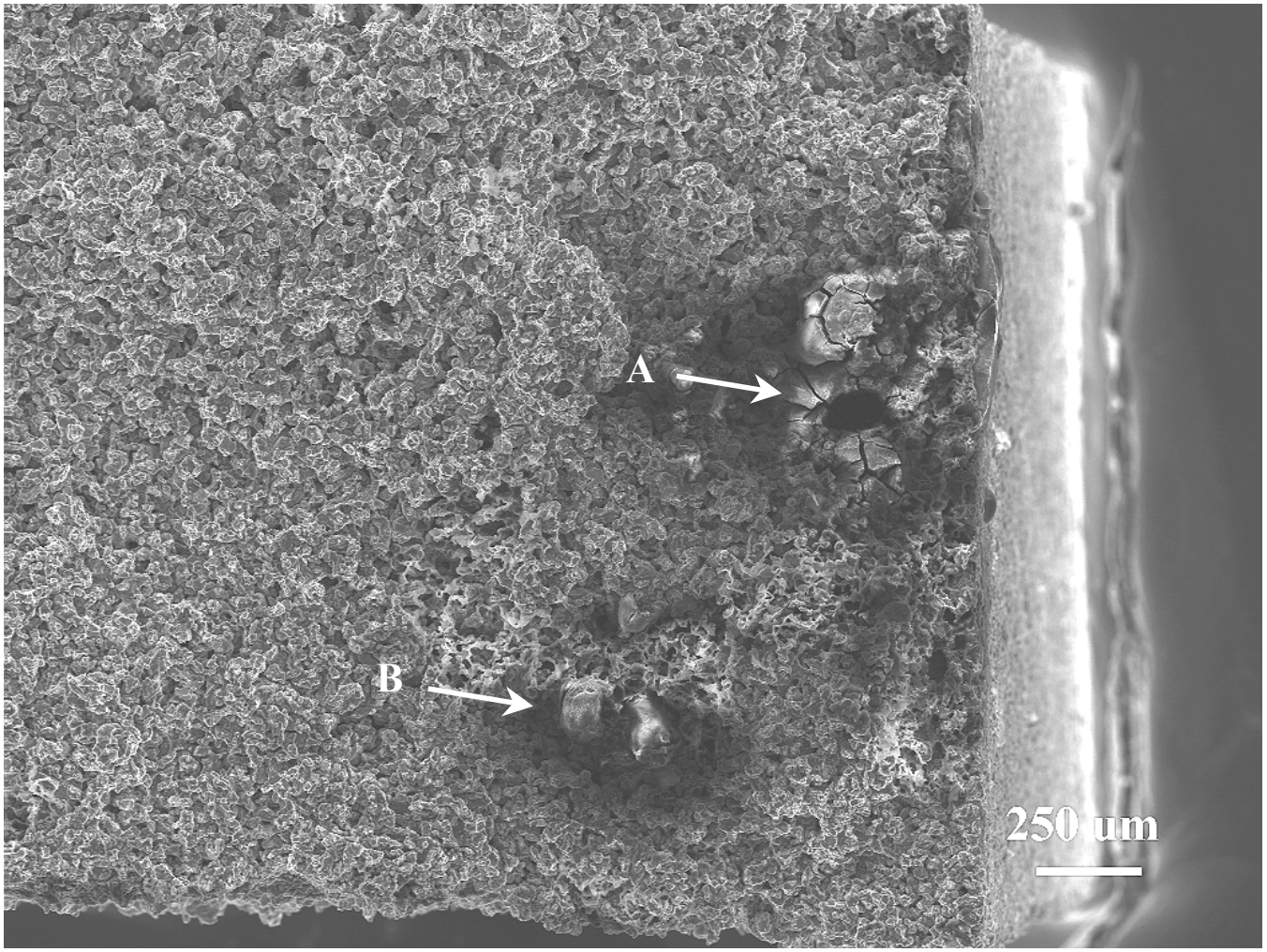

Figure 3.5-13 Fracture Surface of Fe_3Al Tensile Specimen Tn-Ax-16 – Location 2

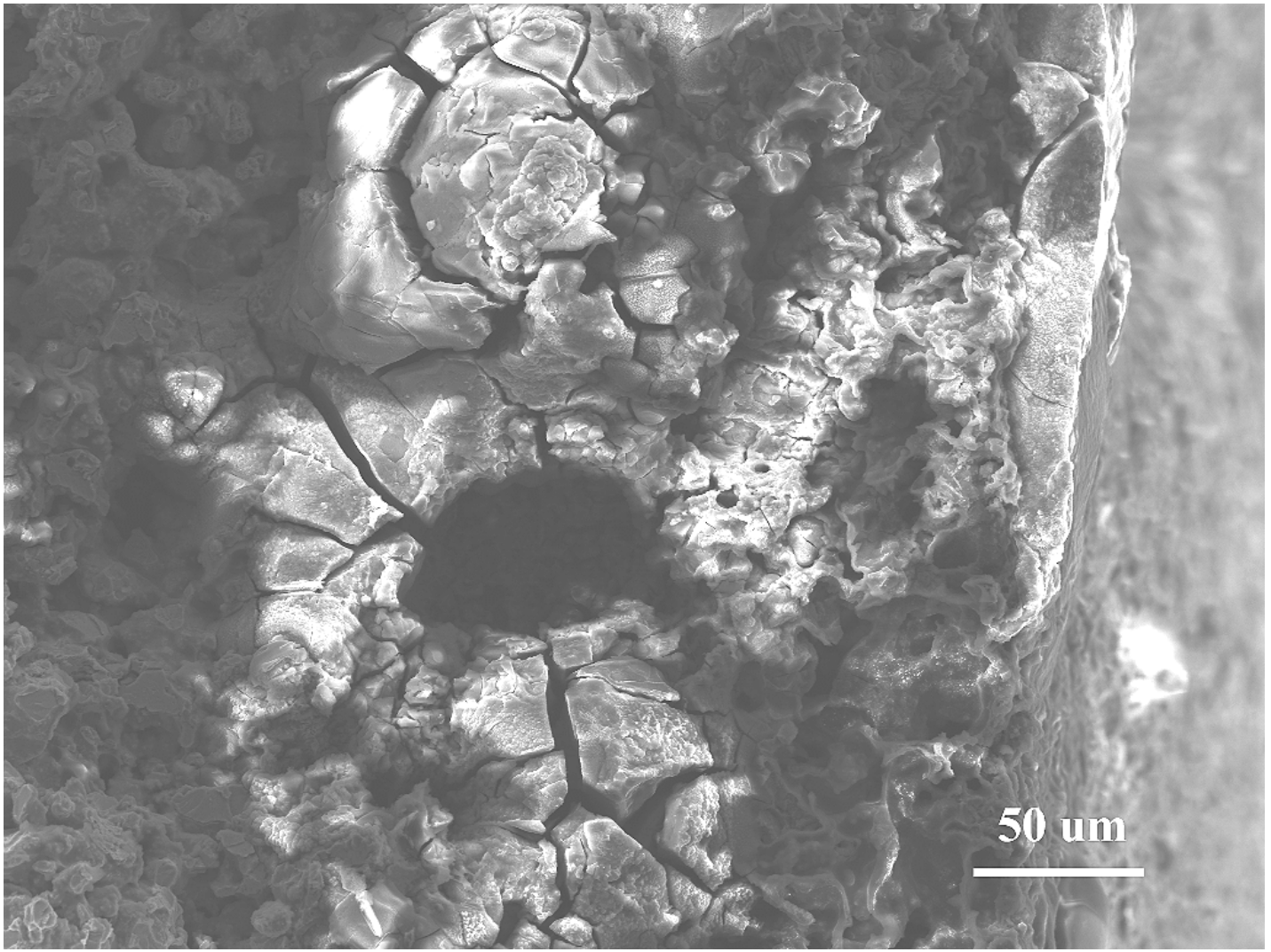

Figure 3.5-14 Area "A" of Location 2 - Fe_3Al Tensile Specimen Tn-Ax-16

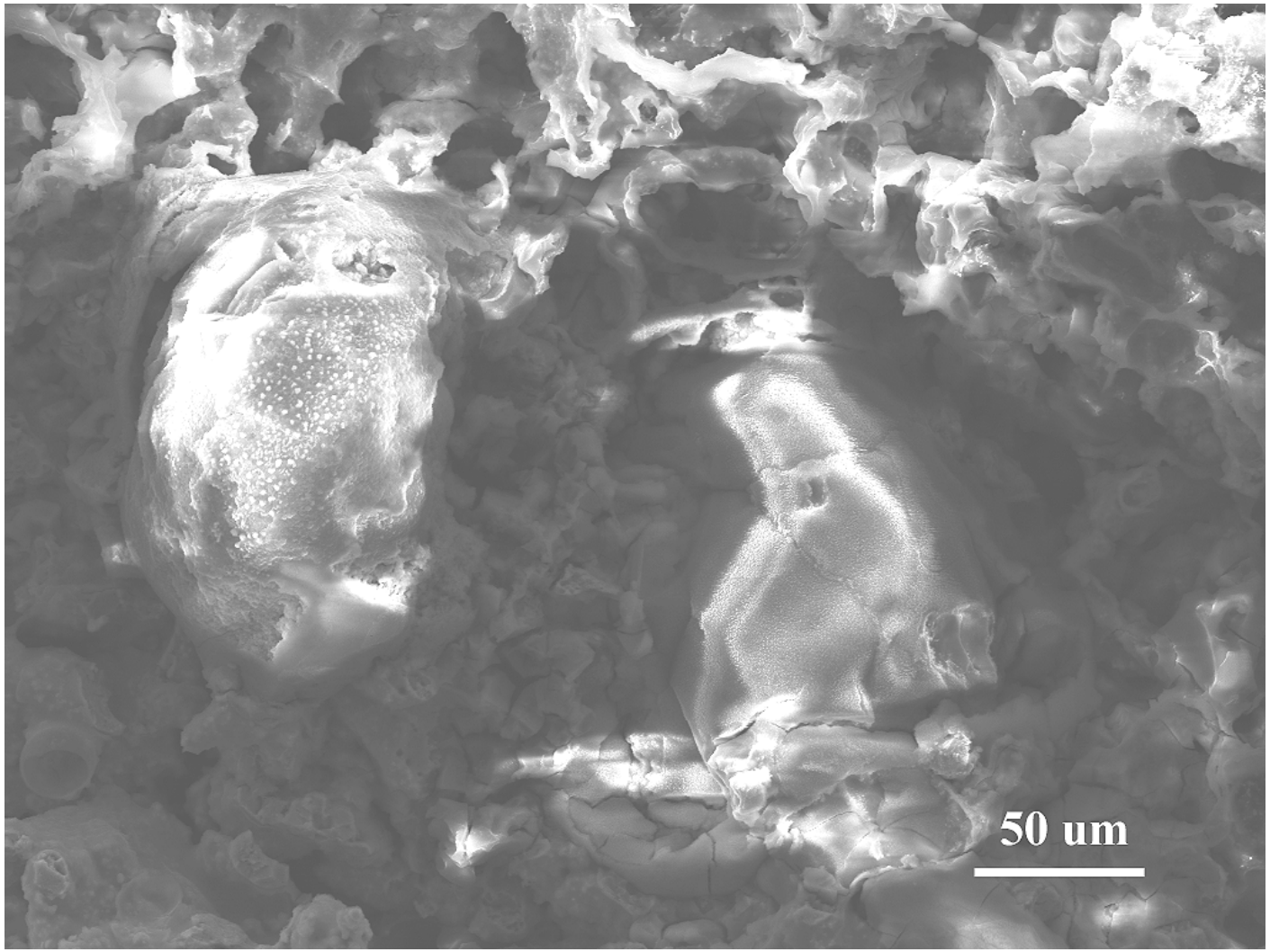

Figure 3.5-15 Area "B" of Location 2 - Fe_3Al Tensile Specimen Tn-Ax-16

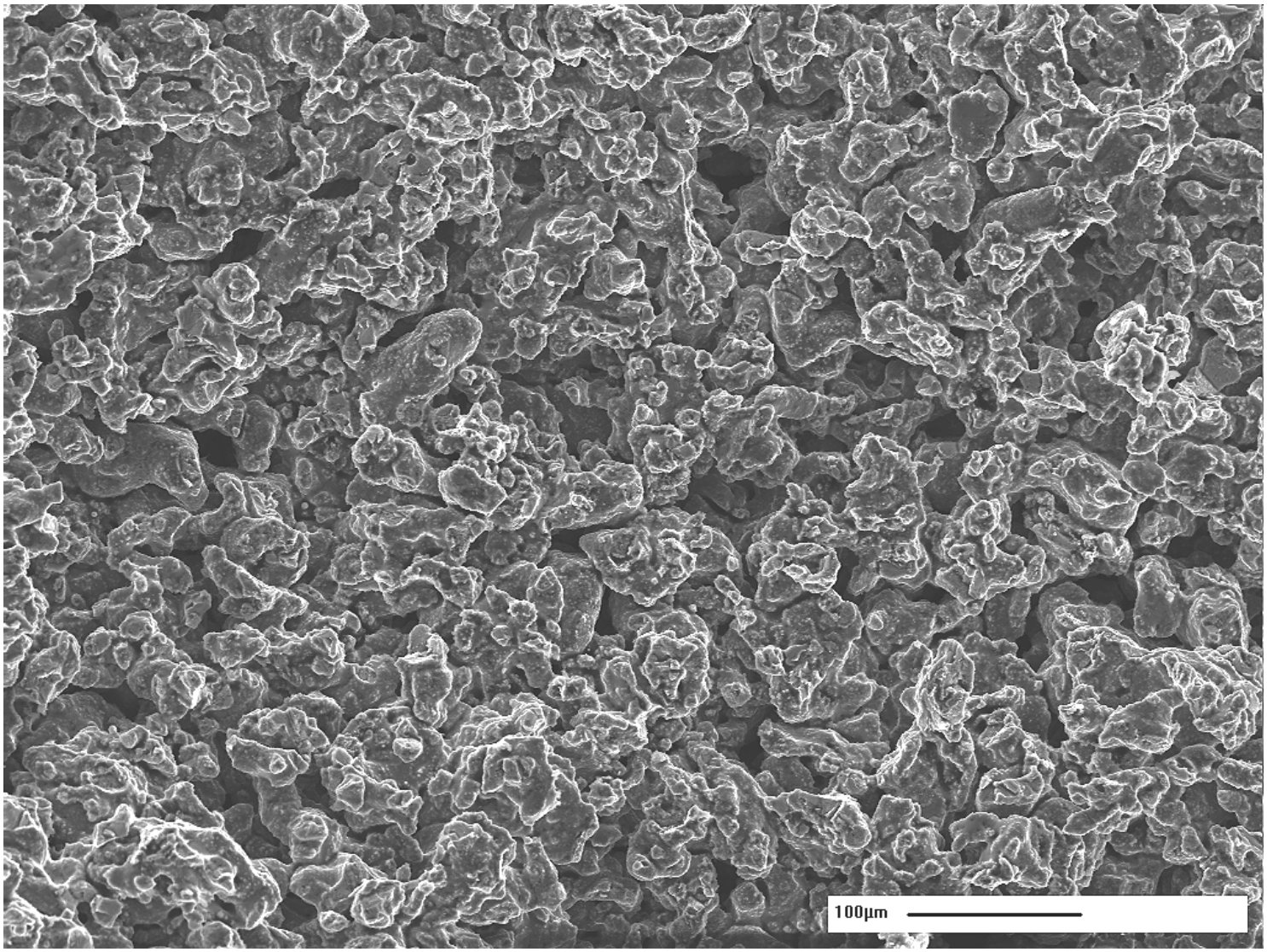

Figure 3.5-16 Fracture Surface of Fe_3Al Tensile Specimen Tn-Ax-22

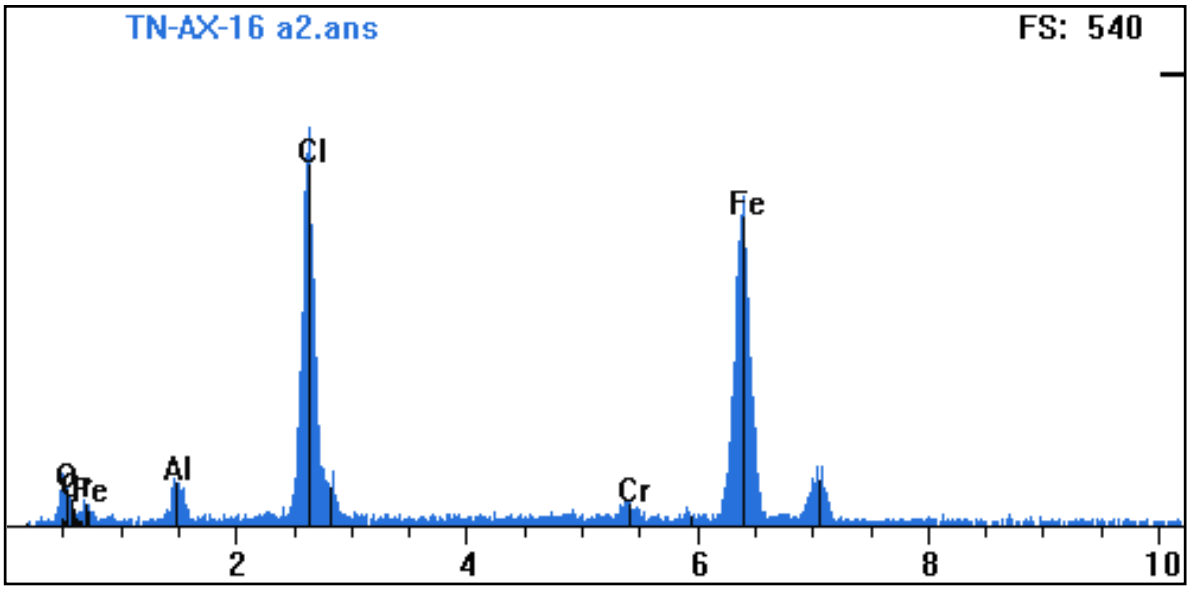

Figure 3.5-17 EDS Spectrum From Area "A" of Location 2 - Fe_3Al Tensile Specimen Tn-Ax-16

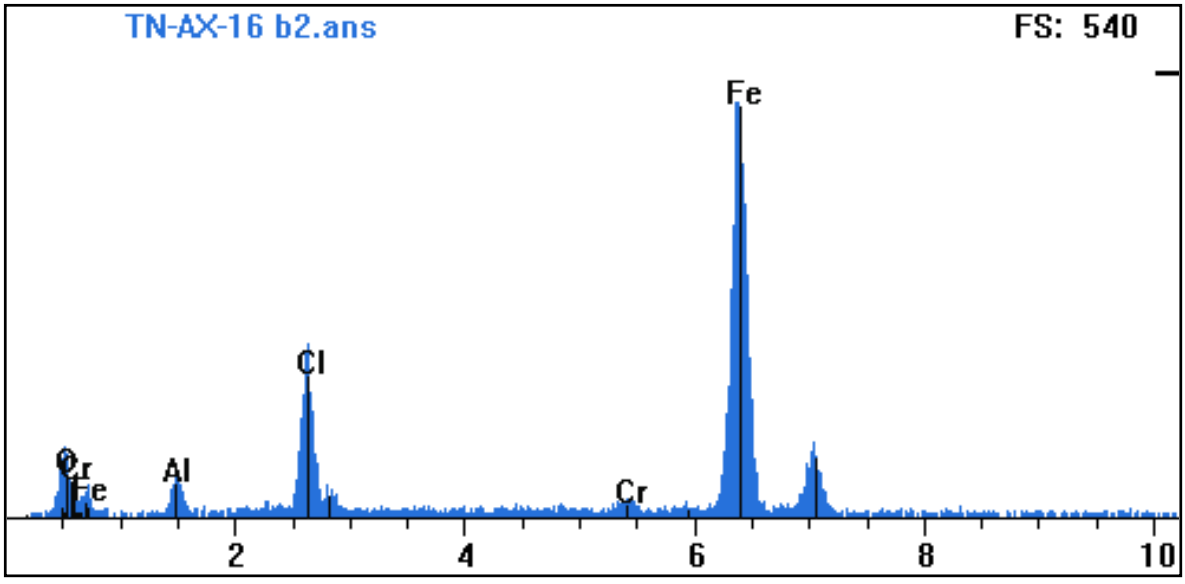

Figure 3.5-18 EDS Spectrum From Area "B" of Location 2 - Fe_3Al Tensile Specimen Tn-Ax-16

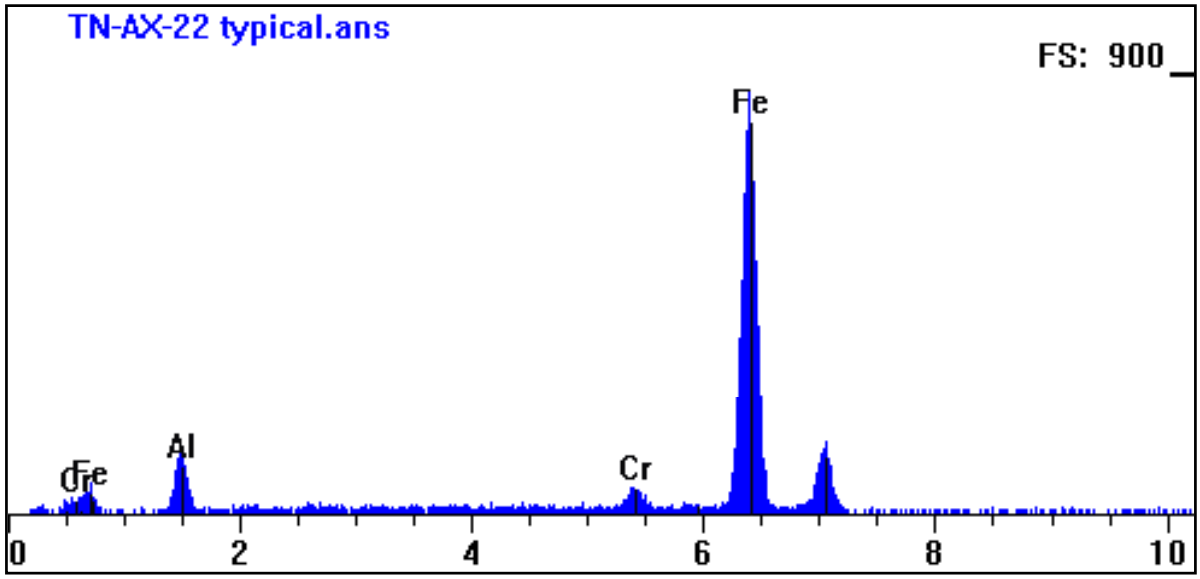

Figure 3.5-19 EDS Spectrum From Fe_3Al Tensile Specimen Tn-Ax-22

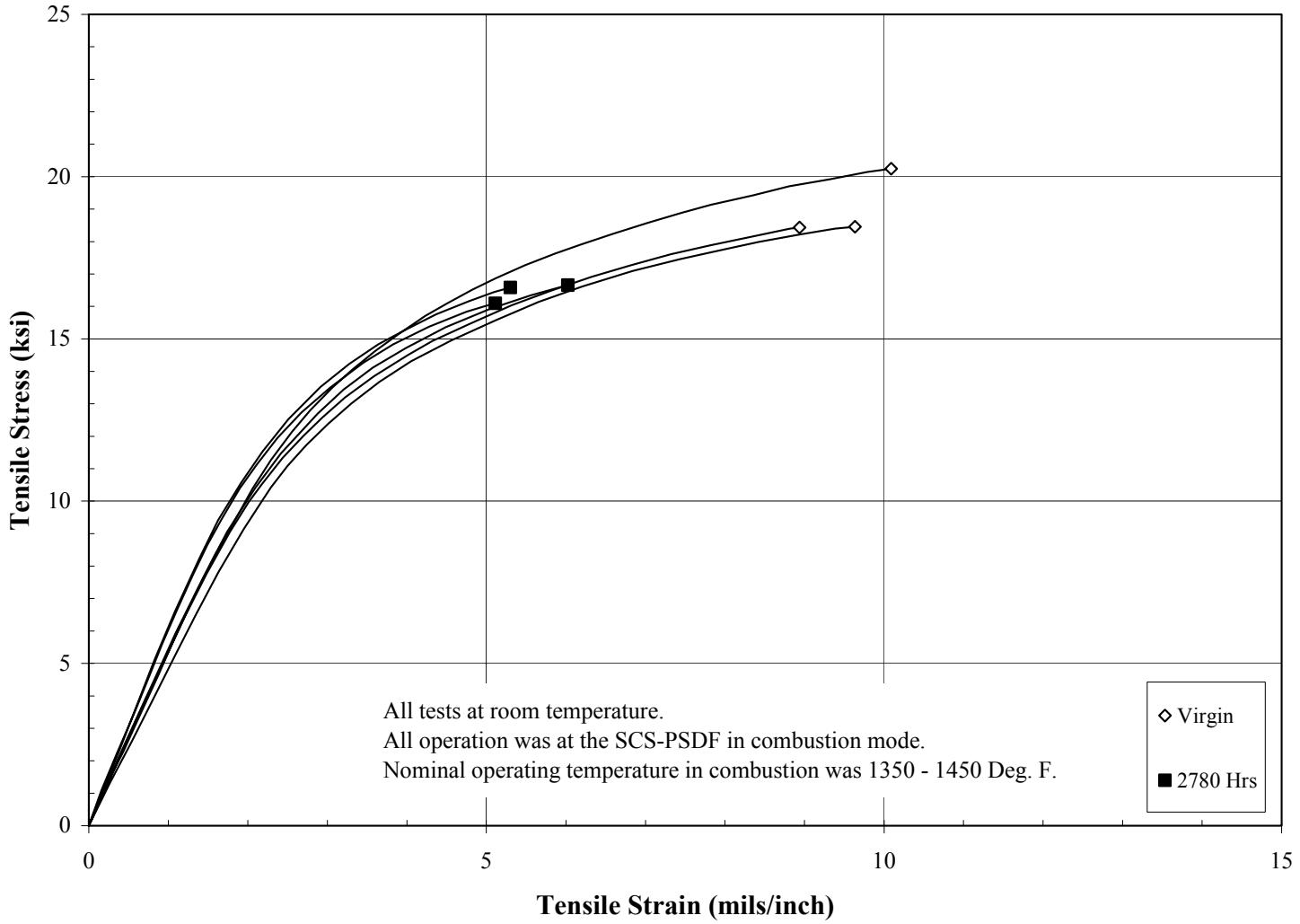

Figure 3.5-20 Axial Tensile Stress-Strain Responses at Room Temperature for Pall Fe_3Al After Combustion Operation

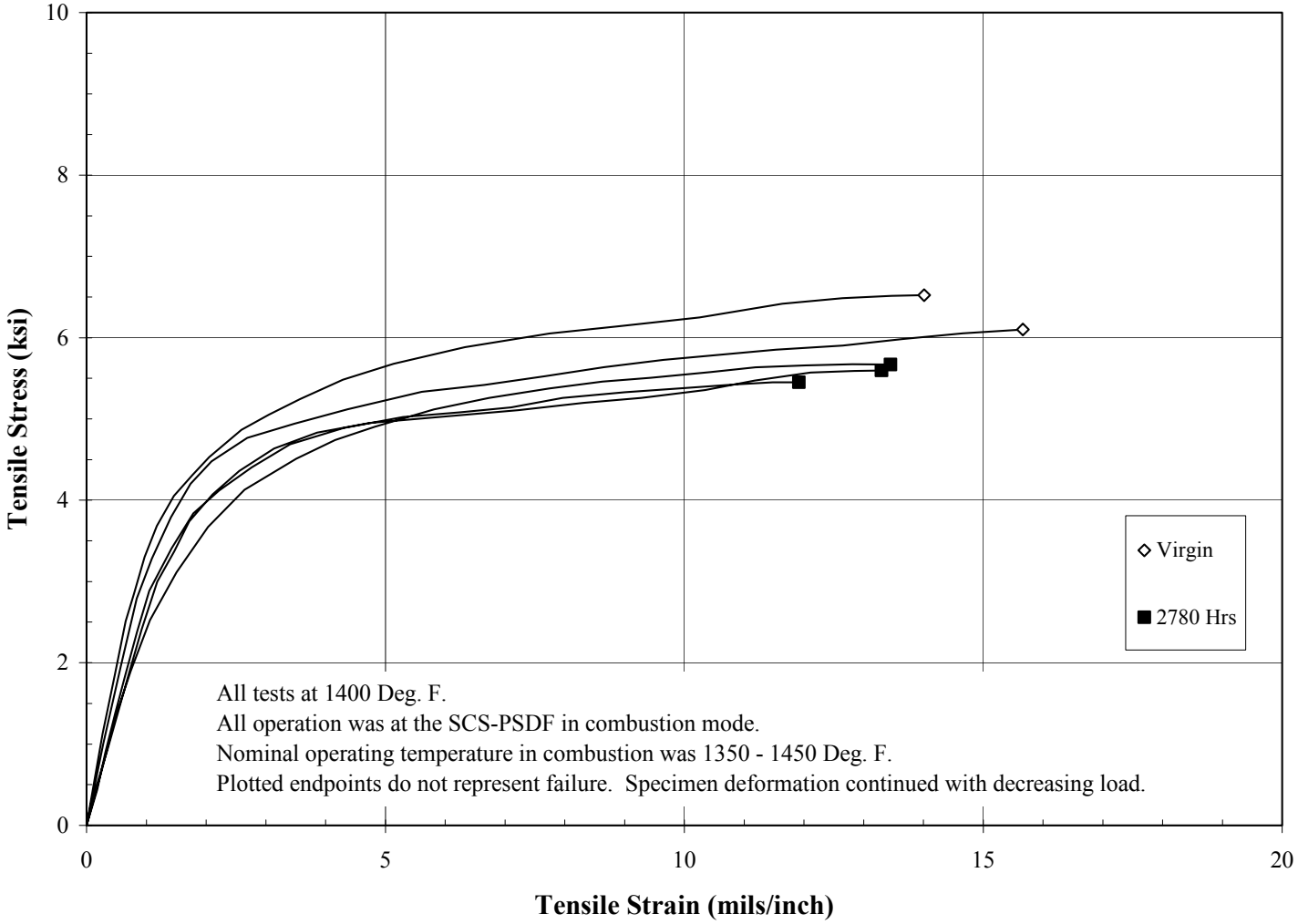

Figure 3.5-21 Axial Tensile Stress-Strain Responses at 1,400°F for Pall Fe_3Al After Combustion Operation

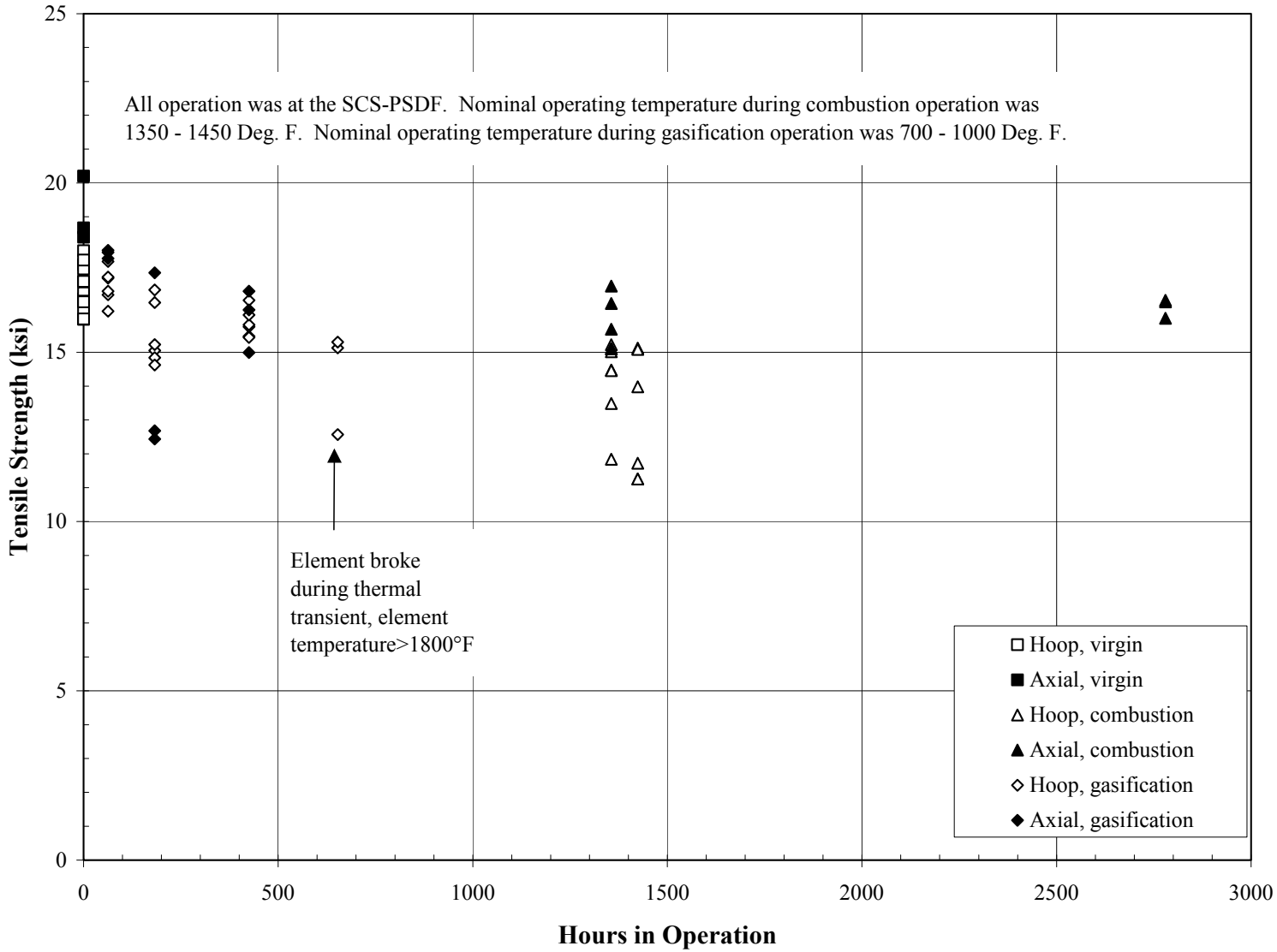

Figure 3.5-22 Room Temperature Tensile Strength of Pall Fe_3Al

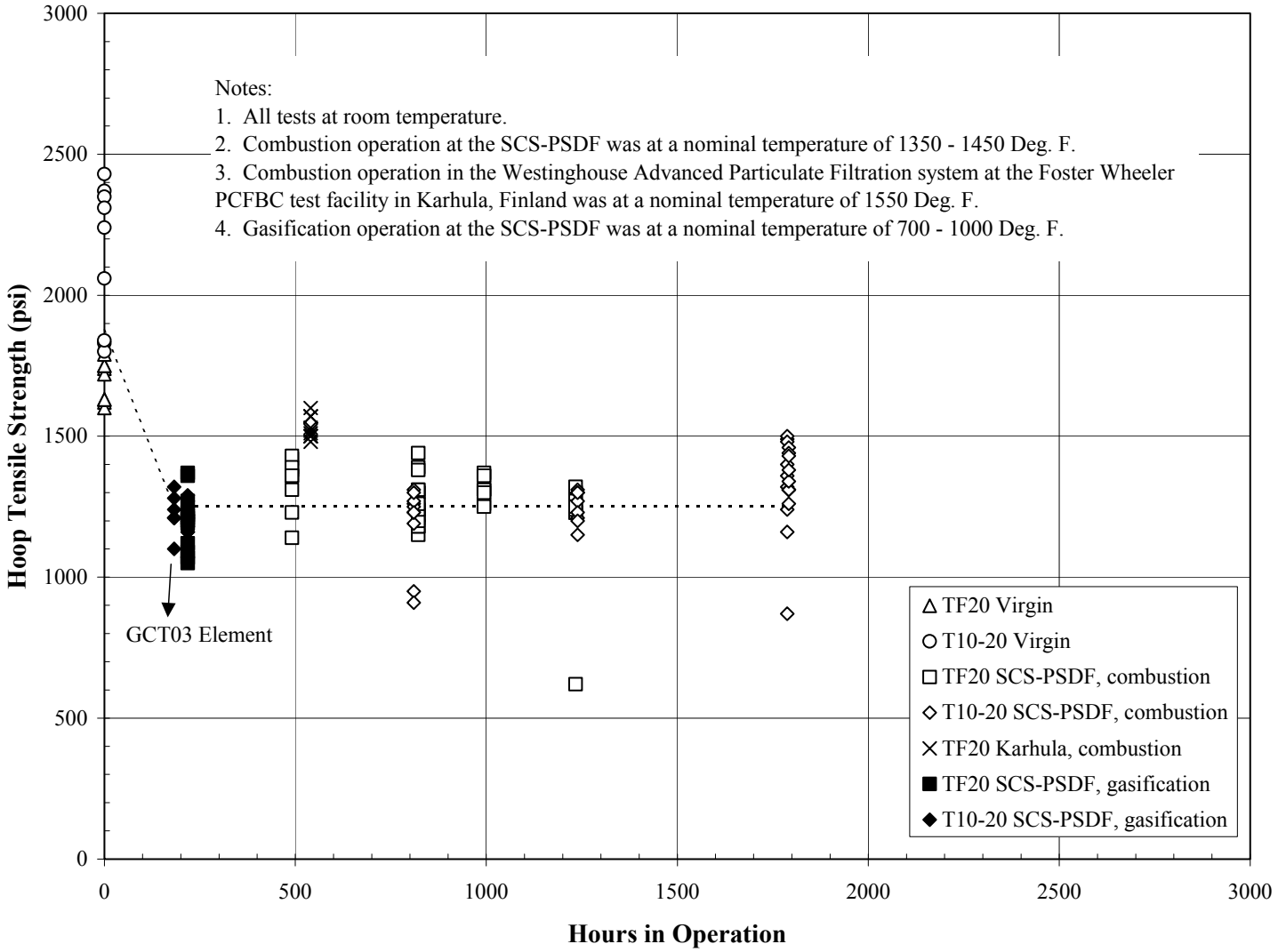

Figure 3.5-23 Room Temperature Hoop Tensile Strength of Schumacher TF20 and T10-20

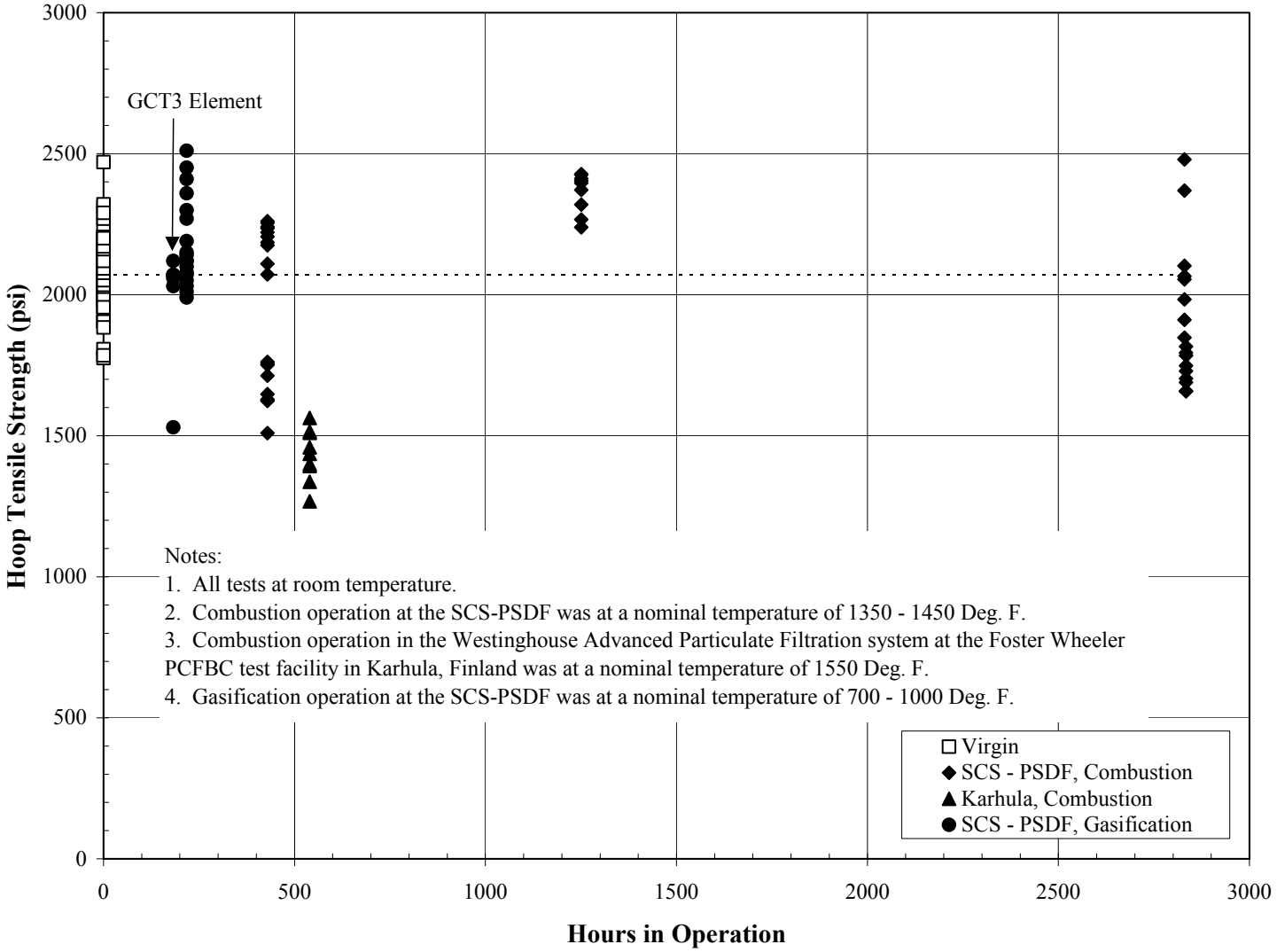

Figure 3.5-24 Room Temperature Hoop Tensile Strength of Pall 326

4.0 TRANSPORT REACTOR

4.1 TRANSPORT REACTOR TC06 RUN SUMMARY

Test run TC06 was started on July 4, 2001, with the startup of the atmospheric syngas burner fan and was completed on September 24, 2001, with an interruption in service between July 25 and August 19, due to a filter element failure in the PCD. During the outage, heat transfer fluid entered the disengager standpipe, making it necessary to remove all material from the reactor and the standpipe screw cooler. Over the course of the entire test run, the reactor temperature was varied between 1,725 and 1,825°F at pressures from 190 to 230 psig.

During the first portions of the run, the coal feeder experienced difficulty transferring coal from the lock hopper to the dispense vessel, a problem seen frequently in previous test runs. Whenever fine coal packed in the lock hopper, the dispense vessel would run out of coal, causing oxygen levels to build in the reactor and PCD. Later in the test run, operations began to feed material directly from the coal mill without allowing it to accumulate in the coal silo. This action prevented particle segregation and fine particle packing in the coal feeder lock hopper, allowing the coal feeder to run without interruption for over 278 hours.

The main air compressor also caused several reactor upsets. It surged while preheating the reactor with the start-up burner and during coal feed. Each time the compressor surged, the loss of air flow tripped all major reactor systems. To prevent more occurrences, a specialist tuned the compressor by adjusting parameters while the compressor passed air through the reactor loop. The compressor performance improved marginally.

The test run experienced a total of 1,025 hours on coal feed and 95 hours on coke breeze feed (used as a start-up fuel). Over the coarse of the test run, the reactor gasified 1,943 tons of Powder River Basin (PRB) coal. The sorbent used during the run was Ohio bucyrus limestone. The planned Transport Reactor operating conditions are shown in Table 4.1-1. The analyses for coal and limestone feed are summarized in Tables 4.1-2 and -3.

The primary objective of test run TC06 was as follows:

- Operational Stability – Characterize reactor loop and PCD operations for commercial performance with long-term tests by maintaining a near-constant coal-feed rate, air/coal ratio, riser velocity, solids-circulation rate, system pressure, and air distribution.

Secondary objectives included the continuation of the following reactor characterizations:

- Reactor Operations – Study the devolatilization and tar cracking effects from transient conditions during the transition from start-up burner to coke breeze to coal. Evaluate the effect of process operations on heat release, heat transfer, and accelerated fuel particle heatup rates. Study the effect of changes in reactor conditions on transient temperature profiles, pressure balance, and product gas

composition. Observe performance of new reactor temperature and coal-feed rate controllers.

- Effects of Reactor Conditions on Synthesis Gas Composition – Evaluate the effect of air distribution, steam/coal ratio, solids-circulation rate, and reactor temperature on CO/CO_2 ratio, synthesis gas lower heating value (LHV), carbon conversion, and cold and hot gas efficiencies.

- Recycle Gas Compressor Commissioning in Gasification Mode – Run the recycle gas compressor in bypass mode and evaluate the performance of the new moisture removal systems.

- Loop Seal Operations – Optimize loop seal operations and investigate increases to previously achieved maximum solids-circulation rate.

The activities that occurred during the outage preceding test run TC06 included 18 equipment revisions. Those revisions that most affected the process are listed below:

- Preparing the carbonizer coal feeder to serve as a coke breeze feeder for the Transport Reactor.

- Installing a second-level probe in the coal feeder dispense vessel to identify a loss of coal-feed situation.

- Programming a new automatic temperature controller for the Transport Reactor.

A summary of the events that occurred in TC06 is shown below.

Operations lit the atmospheric syngas burner on July 4, 2001, beginning test run TC06. On July 7, operations lit the start-up burner to preheat the reactor, while charging the reactor with sand. To bring the reactor from 1,200°F (the maximum temperature attainable by the start-up burner) to an optimum reactor temperature above the tar dew point, coke breeze was introduced as a startup fuel on July 10.

Coal feed began early on July 11, 2001, but was interrupted 2 hours later when the spent fines feeder plugged, causing material to back up into the PCD. Once maintenance cleared the line and the PCD had emptied, coal feed resumed at 09:30 on July 12 and was discontinued after less than 1 hour when the main air compressor surged, tripping all reactor systems. After experiencing difficulties with the start-up burner and the coal conveying line differential pressure, and another surge from the main air compressor, operations restored coal feed just after midnight on July 15.

The reactor ran very smoothly for 3 days at a pressure of 210 psig and a temperature between 1,750 and 1,770°F until coal packed in the feeder dispense vessel, preventing coal from entering the reactor. High oxygen levels caused a thermal event in the PCD, but the filter elements were not damaged. Coal feed resumed shortly thereafter, but reactor operations remained slightly

unstable for several hours. Once conditions stabilized, operations placed the reactor in automatic temperature control for the first time in any test run. The new controller and the reactor performed quite well, keeping the mixing zone temperature at 1,740°F except for a few coal feeder upsets in the morning of July 22, 2001.

Due to concerns about the main air compressor, a maintenance crew arrived on-site to tune the compressor on July 24, 2001. Operations stopped coal feed to prepare for the tuning procedure, which involved passing air through the reactor loop. Unfortunately, a gasification ash (g-ash) bridge that had formed on the PCD filter elements ignited as the air entered the filter vessel, causing some of the filter elements to break. Thus, operations had to shut down the entire system. During the outage, inspections revealed that heat transfer fluid had entered the reactor standpipe through a leak in the standpipe screw cooler. Maintenance had to remove all material from the reactor, repair the screw cooler, and repipe the heat transfer fluid before operations could resume.

Operations restarted the reactor burner on August 19, 2001. Coke breeze feed began on August 20, with coal feed following later that day. At the same time, a bubble formed in the standpipe that disturbed the circulation in the reactor. As fluidization flows to the reactor J-leg changed, the bubble disappeared and operations placed the reactor back into automatic temperature control.

In the next portion of the test run, the reactor ran at between 190 and 200 psig and around 1,700°F. The coal feeder generally performed poorly during this portion of the test run as fines continuously packed into the lock hopper. As a result, the coal feeder dispense vessel ran out of coal several times and coke breeze had to be used as a fuel until operations manually unpacked the lock vessel. Usually the events were short-lived, but on August 23 and on August 27, the dispense vessel ran completely out of coal, resulting in several offline hours during each occurrence.

Coal feed was again interrupted for 4 hours on August 27 when a torn spheri valve on one of the g-ash feeders caused material to accumulate in the PCD until maintenance could repair it. The reactor ran at 200 psig and around 1,715°F steadily from August 28 through September 2, when it began to experience more problems with the coal feeder. On September 12, after several more occasions of loss-of-coal feed caused by fine coal packing in the feeder lock hopper, operations began feeding ground coal continuously through the silos, not allowing coal to accumulate in the coal silos. The new feeding technique worked well and allowed the system to run very smoothly until the end of the run.

During the next portion of the test run, the reactor ran for 5 days at 200 psig and 1,700°F. Later, to test reactor stability at higher pressure, operations increased the pressure to 230 psig and 1,730°F. The test run ended on September 24, 2001, after accumulating 1,025 hours of coal feed and 1,214 hours of solids circulation.

Although several trips interrupted reactor operations, the reactor performed very well. Steady-state periods were long and reactor operations were stable, partially due to the new automatic

temperature controller. In addition, the new coal feeding technique virtually eliminated packing in the coal feeder, ensuring a steady-feed rate.

Coke breeze proved an invaluable source of fuel both during startup and whenever coal feed was interrupted. Since this material was used instead of coal to heat the reactor between 1,200 and 1,650°F, very little tar formed, and the gas analyzers were able to record the most reliable gasification data seen to date.

During TC06, the recycle gas compressor was run for the first time in gasification mode. All recycle gas flowed to the atmospheric syngas burner rather than the reactor loop. The moisture removal systems did not work as well as planned. The research team identified several improvements to attempt on the recycle gas loop.

After the test run was complete, process engineering and maintenance performed inspections on the reactor loop and the PCD. Except for some small egg-shaped deposits in the mixing zone and some soft agglomerations in the loop seal downcomer, the reactor interior appeared to be clean and the refractory in good condition. The sulfator refractory exhibited some shallow cracks that separated the refractory into small sections less than 12 inches in diameter as shown in Figure 4.1-1.

Also during the inspection, the maintenance crew found that the primary gas cooler had experienced a tube failure in several tubes and had to be repaired. Upon inspecting the lower standpipe, the crews found that improvements to the HTF system had prevented any fluid from entering the reactor.

The reactor temperatures ranged from 1,725 to 1,825 °F, while the reactor operating pressure varied from 190 to 230 psig. The coal-feed rate ranged from about 3,800 to over 6,100 lb/hr. Further description of these test periods is provided in Table 4.1-4.

The following test periods were selected as shown in Table 4.1-4:

TC06-I	Low operating pressure and temperature. Low coal-feed rate.
TC06-II	Low operating pressure. Low temperature. Moderate coal-feed rate.
TC06-III	Low pressure. Moderate temperature. Low coal-feed rate.
TC06-IV	Low pressure. Moderate temperature, coal-feed rate.
TC06-V	Low pressure. Moderately high temperature, feed rate.
TC06-VI	Low pressure. Moderately high temperature. High coal-feed rate.
TC06-VII	High pressure. Moderately high temperature. Low coal-feed rate.
TC06-VIII	High pressure, temperature. Low coal-feed rate.
TC06-IX	High pressure, temperature. Moderate coal-feed rate.
TC06-X	Moderate pressure. Moderately high temperature. High coal-feed rate.
TC06-XI	Moderate pressure, moderate temperature. High coal-feed rate.
TC06-XII	High pressure. High temperature. Moderate coal-feed rate.
TC06-XIII	High pressure. High temperature. High coal-feed rate.
TC06-XIV	High pressure and temperature. High coal-feed rate.

Table 4.1-1

TC06 Planned Operating Conditions for Transport Reactor

Start-up Bed Material	Sand, ~ 120 μm
Start-up Fuel	Coke Breeze
Fuel Type	Powder River Basin
Fuel Particle Size (mmd)	300 μm
Average Fuel-Feed Rate (pph)	5,000
Sorbent Type	Ohio Bucyrus Limestone
Sorbent Particle Size (mmd)	25 to 60 μm
Sorbent-Feed Rate	125 pph (Ca/S Molar Ratio of 2.0) for Sulfur Capture and Cracking Tar
Reactor Temperature (°F)	1,750 to 1,825
Reactor Pressure (psig)	240
Riser Gas Velocity (fps)	35 to 40 ft/s
Solids-Circulation Rate (pph)	100,000 to 400,000 (slip ratio = 2)
Primary Gas Cooler Bypass	0%
PCD Temperature (°F)	700 to 900
Total Gas-Flow Rate (pph)	18,000 to 26,000
Air/Coal Ratio	As Needed to Control Reactor Temperature
Primary Air Split ($1^{st}/2^{nd}$ levels)	80/20
Steam/Coal Ratio	0.0 to 0.4
Sulfator Operating Temperature (°F)	1,500 to 1,600
Planned Duration of Coal Feed	Nominally 1,000 hours

Table 4.1-2

Coal Analyses as Fed

	PRB
Moisture	20.93
Ash	5.23
Sulfur	0.26
C	57.02
H	3.74
N	0.66
O	12.16
Vol	37.39
Fix C	36.46
Heating Value(BTU/lb)	9,391

Table 4.1-3

Sorbent Analyses

	Bucyrus Limestone From Ohio
$CaCO_3$ (Wt %)	75.95
$MgCO_3$ (Wt %)	17.66
$CaSO_4$ (Wt %)	0.42
SiO_2	2.58
Inerts	3.39

Table 4.1-4

Operating Periods

	Subperiods	Duration Hours	MZ Temp Deg F	Rsr Temp Deg F	Pres psig	Coal Fd[1] Rate lb/hr	Air Flow lb/hr	Air/Coal	Air/C
TC06-I	TC06-18	9:00	1,690	1,664	190	3,715	12,391	3.34	5.82
TC06-II	TC06-19 TC06-20 TC06-21	25:00	1,707	1,684	190	4,084	13,269	3.25	5.67
TC06-III	TC06-47 TC06-48 TC06-49 TC06-50 TC06-51	84:45	1,755	1,697	200	3,382	12,304	3.60	6.29
TC06-IV	TC06-22 TC06-23 TC06-24 TC06-25 TC06-38 TC06-39 TC06-42 TC06-45	108:00	1,733	1,701	199	4,303	14,172	3.30	5.75
TC06-V	TC06-16 TC06-26 TC06-27 TC06-28	171:45	1,751	1,718	200	4,455	14,746	3.31	5.78

Table 4.1-4

Operating Periods (continued)

	Subperiods	Duration Hours	MZ Temp Deg F	Rsr Temp Deg F	Pres psig	Coal Fd[1] Rate lb/hr	Air Flow lb/hr	Air/Coal	Air/C
TC06-V (continued)	TC06-29 TC06-30 TC06-31 TC06-32 TC06-33 TC06-34 TC06-35 TC06-36 TC06-37 TC06-40 TC06-43 TC06-44 TC06-46	171:45	1,751	1,718	200	4,455	14,746	3.31	5.78
TC06-VI	TC06-17 TC06-41	9:00	1,763	1,733	198	4,635	15,630	3.37	5.88
TC06-VII	TC06-52 TC06-53	18:00	1,760	1,700	220	3,294	11,937	3.64	3.65
TC06-VIII	TC06-54	19:00	1,770	1,716	220	3,648	13,161	3.61	6.30
TC06-IX	TC06-55 TC06-56 TC06-57	28:00	1,772	1,723	220	4,135	14,118	3.45	6.02

Table 4.1-4

Operating Periods (continued)

	Subperiods	Duration Hours	MZ Temp Deg F	Rsr Temp Deg F	Pres psig	Coal Fd[1] Rate lb/hr	Air Flow lb/hr	Air/Coal	Air/C
TC06-X	TC06-5 TC06-6 TC06-7 TC06-8 TC06-9 TC06-10 TC06-11 TC06-12 TC06-13 TC06-14	86:45	1,754	1,739	211	4,907	16,784	3.43	5.99
TC06-XI	TC06-1 TC06-2 TC06-3 TC06-4	27:45	1,746	1,757	212	4,673	16,464	3.50	6.11
TC06-XII	TC06-58 TC06-59 TC06-60 TC06-61	45:30	1,771	1,725	230	4,411	14,546	3.33	5.81
TC06-XIII	TC06-62 TC06-64	31:00	1,775	1,729	230	4,984	16,111	3.23	5.64
TC06-XIV	TC06-63	19:00	1,788	1,745	230	5,027	16,392	3.26	5.69

[1] Coal-feed rate by carbon balance.

Figure 4.1-1 – View of Western Side of Sulfator Showing Cracks

4.2 GASIFIER OPERATIONAL ANALYSIS

The most important influence on the gasifier circulation rate is the height of the column of solids in the standpipe. A high standpipe level of fluidized solids will force solids at a rapid rate into the mixing zone, increasing the overall solids-circulation rate in the reactor loop. Figures 4.2-1, -2, and -3 show the effect of higher standpipe levels (LI339) on the pressure drop in the mixing zone and riser as an increasing mass of solids circulate through these areas, resulting in an increased holdup.

Increases in circulation rate tend to reduce the temperature extremes found in the gasifier. As the circulation rate increases, the difference in temperature between any two points should decrease. Figure 4.2-4 illustrates this effect by showing the difference in riser and mixing zone temperature as related to circulation rate, as measured by the riser differential pressure.

It has been expected that increases in the coal-feed rate would lead to an accumulation of solids in the bed. However, Figure 4.2-5, a plot of the change in LI339 over a short time and the coal-feed rate, shows that there is no appreciable change in accumulation rates as the coal-feed rate is changed. This is due to an appreciable increase in loading to PCD with an increase in coal-feed rate.

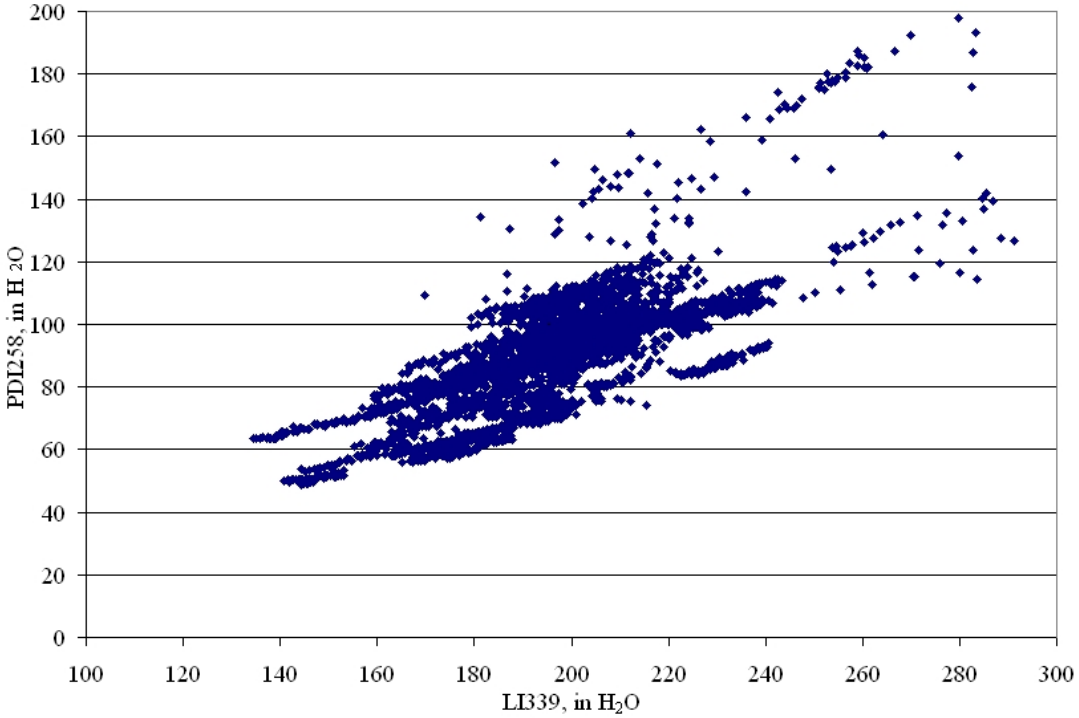

Figure 4.2-1 Effect of Standpipe Height on Riser DP

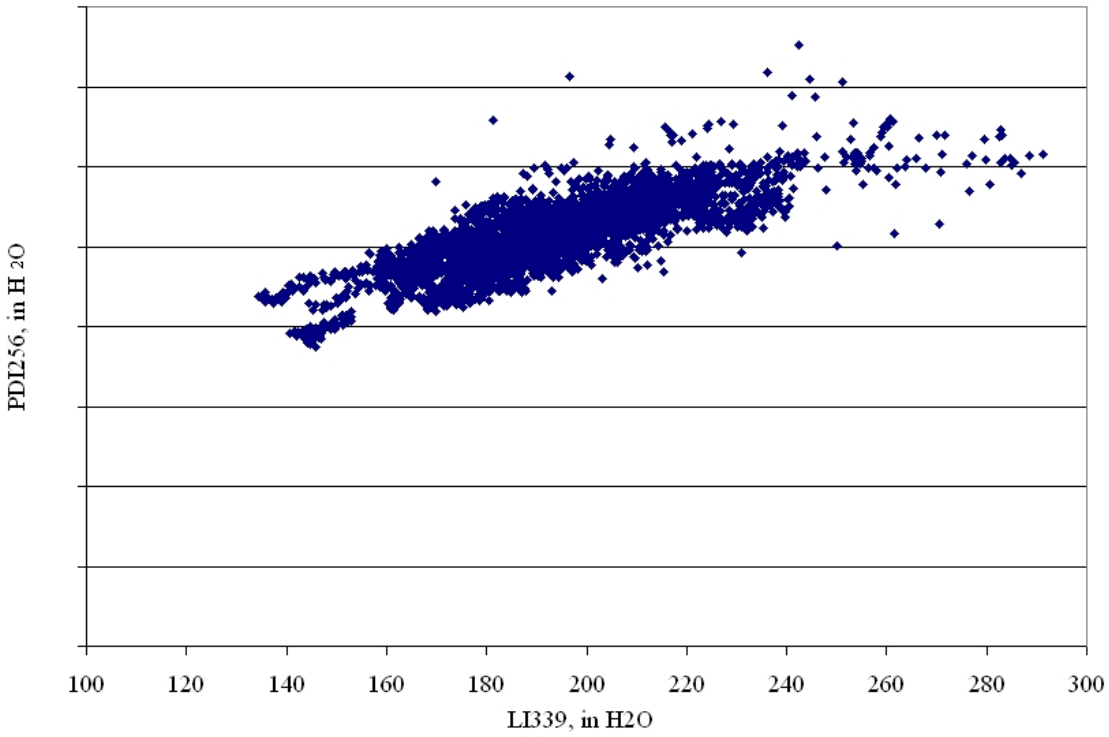

Figure 4.2-2 Effect of Standpipe Height on Mixing Zone DP

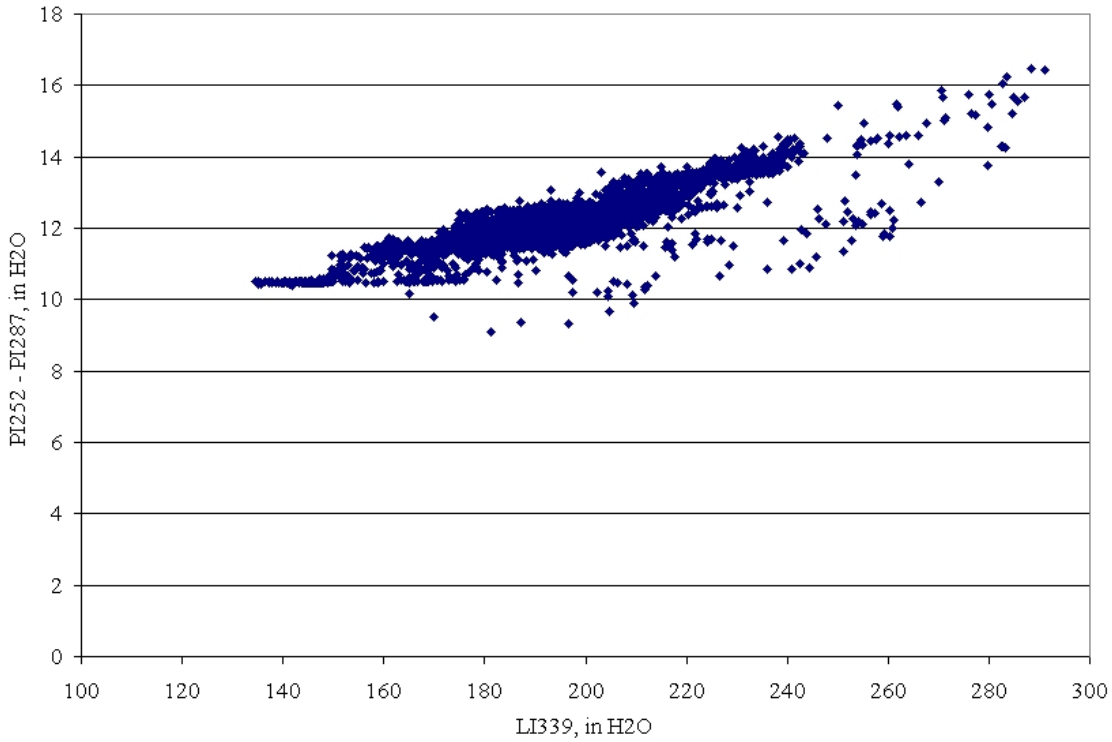

Figure 4.2-3 Effect of Standpipe Height on Combined Mixing Zone and Riser DP

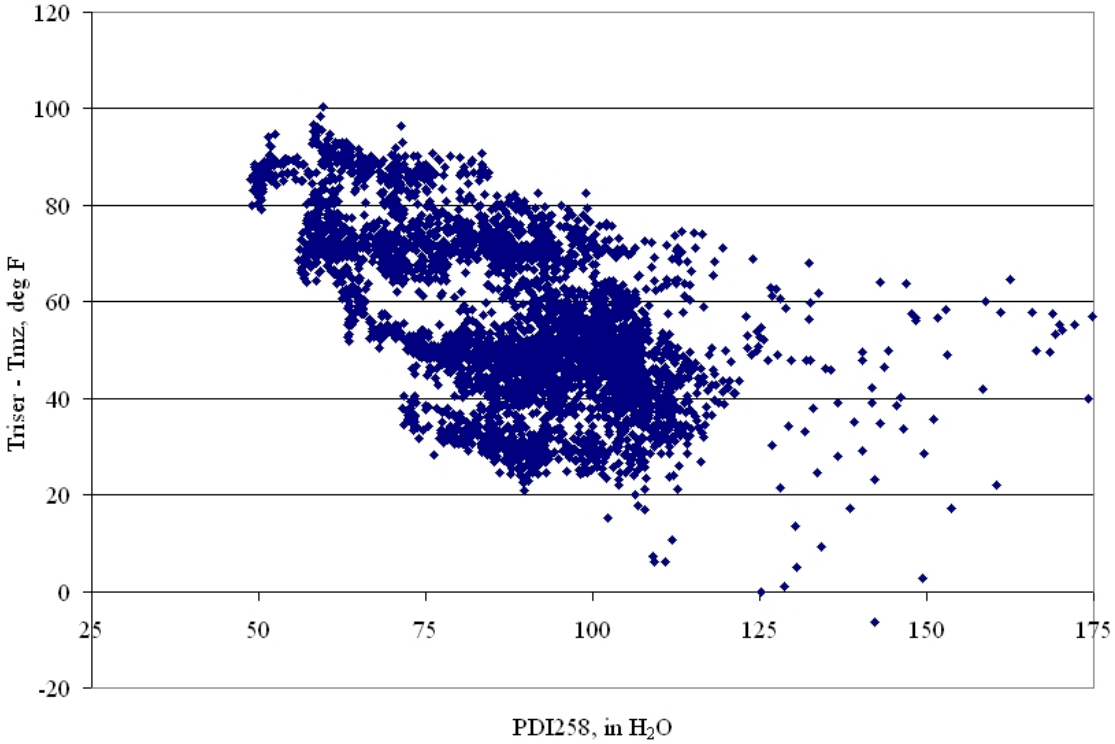

Figure 4.2-4 Effect of Circulation Rate on Temperature Difference From Mixing Zone to Riser

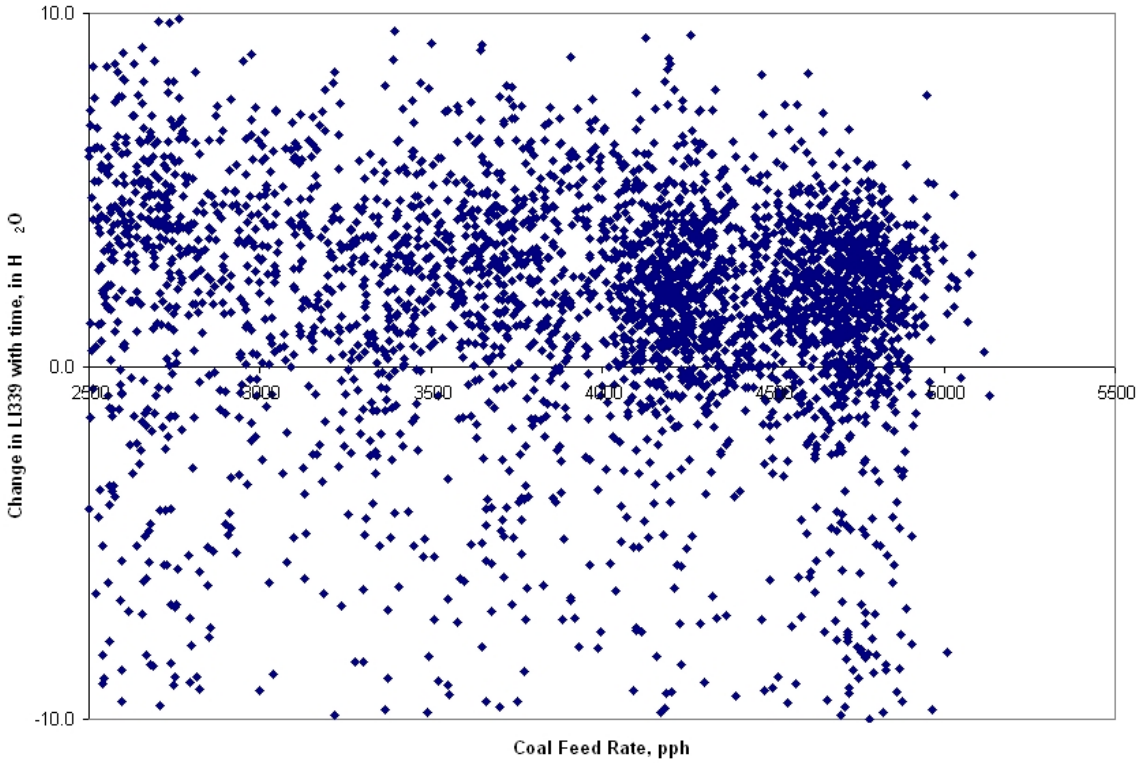

Figure 4.2-5 Effect of Coal-Feed Rate on Rate of Solids Accumulation in Standpipe

4.3 GAS ANALYSIS

During TC06, Transport Reactor and synthesis gas combustor outlet gas analyzers were continuously monitored and recorded by the plant information system (PI). Several in situ grab samples of synthesis gas moisture content were measured during the PCD outlet loading sampling. A train of gas impingers was used to measure NH_3 and HCN on two different days. This section will use gas analyzer data to show:

- Synthesis gas heating value.
- Synthesis gas molecular weight.
- Synthesis gas compositions, for CO, H_2, CO_2, H_2O, N_2, CH_4, $C_2H_6^+$, NH_3, HCN, and total reduced sulfur (H_2S, COS, and CS_2).
- Sulfur emissions.
- Equilibrium H_2S concentrations.

Run TC06 coal feed began on July 11, 2001, and ended on September 24, 2001. There was a 4-week outage (between July 24 and August 20) to replace broken filter elements. Test TC06 consisted of two periods. The first period was from July 14 to July 24, 2001. There were 14 steady periods of operation (TC06-1 to TC06-14). The steady periods of operation are shown in Table 4.3-1. The second period was from August 20 to September 24, 2001. There were 50 steady periods of operation (TC06-15 to TC06-64). The only coal used during TC06 was Powder River Basin (PRB) coal, which is a mixture of four different coals. The sorbent used was Ohio Bucyrus limestone.

The TC06 hourly averages for the mixing zone temperatures, PCD (particulate control device, FL0301) temperatures and reactor pressure control valve pressures are shown in Figure 4.3-1. The data for the operating periods are shown in Table 4.3-2.

For the first 265 hours of TC06, the mixing zone was at about 1,750°F. At 265 hours, the temperature was decreased to about 1,700°F. After 400 hours, the mixing zone temperature was increased to 1,750°F. The temperature was then between 1,730 and 1,775°F for the remainder of the run. The brief lower temperatures on Figure 4.3-1 were the periods during coal-feed trips. Usually the reactor could be maintained at pressure using the new coke breeze feeder and without depressurizing and using the start-up burner. There were no coal feeder trips from hour 763 to 986 because of improvements in the coal feeder operation strategy.

The Transport Reactor pressure was at 210 psig early in TC06 and then was decreased to 190 psig for about 150 hours. Most of TC06 was operated at 200 psig until 843 hours, when the pressure was increased to 220 psig, then 230 psig, and finally to 240 psig at the end of the run. The PCD inlet temperature slowly varied between 675 and 750°F.

TC06 hourly averages for the air rate and the nitrogen rate are shown in Figures 4.3-2. The air and nitrogen rates are listed for the operating periods in Table 4.3-2. The air rate was obtained from FI205. The air rate was between 16,000 to 17,500 lb/hr for the first 220 hours. After the 4-week break, the air rate increased from 14,000 to 16,000 lb/hr at hour 257. The air rate was decreased drastically to 12,500 lb/hr after a coal trip at hour 262. From hour 257 to hour 512,

the air rate slowly increased to about 14,750. At hour 760, the air rate was decreased to around 12,500 lb/hr until hour 863 to reflect a decrease in coal-flow rate. At hour 863, the air was increased until it reached 16,500 lb/hr at the end of TC06. The air rate followed the coal rate to maintain the reactor temperature constant.

The aeration-instrument nitrogen was obtained from FI609. It is estimated that about 1,000 lb/hr from FI609 does not enter the process but is used to seal valves, pressurized - depressurized feed, and ash lock hopper systems, and in the seals for the screw coolers. Values on Figure 4.3-2 and Table 4.3-2 assume that 1,000 lb/hr of nitrogen from FI609 does not enter the Transport Reactor. The nitrogen rate was between 5,500 and 7,750 lb/hr during the TC06. The nitrogen rate changed very gradually during the run.

The hourly synthesis gas (FI463_COMP) is plotted on Figure 4.3-3. The synthesis gas rate generally follows the coal and air rates, and periods of high and low air flow result in high and low synthesis gas rates. The synthesis gas rate was from 21,000 to 30,000 lb/hr.

The gas analyzer system analyzed synthesis gas for the following gases during TC06 using the associated analyzers:

CO	AI425, AI434B, AI453G, AI464C
CO_2	AI434C, AI464D
CH_4	AI464E
C_2^+	AI464F
H_2	AI464G
H_2O	AI7510
N_2	AI464B

The AI464B-G analyzers use a gas chromatograph and typically have about a 6-minute delay. The other three CO analyzers (AI425, AI434B, and AI464C) and CO_2 analyzer (AI434C) are IR based and give more real-time measurements. Since all analyzers (except for the H_2O analyzer) require that the gas sample be conditioned to remove water vapor, all these analyzers report gas compositions on a dry basis.

The locations of the synthesis gas analyzers are shown in Figure 4.3-4. All of the gas analyzers obtain gas samples from between the secondary gas cooler and the pressure letdown valve. The H_2O analyzer AI7510 obtains gas samples from between the pressure letdown valve and the syngas combustor. The GC analyzer AI464 normally samples between the PCD and the secondary gas cooler. This sample line plugged and the AI464 sample was taken between the secondary gas cooler and the pressure letdown valve during TC06.

The raw synthesis gas analyzer data was adjusted to produce the best estimate of the actual gas composition in three steps:

1. Choice of CO and CO_2 analyzer data to use.
2. Normalization of dry gas compositions (force to 100 percent total).
3. Conversion of dry compositions to wet compositions.

There is a measure of self-consistency when all or several of the four analyzers read the same value. There is also the choice of which analyzer to use when problems arise due to solids plugging the gas sampling lines. The TC06 hourly averages for the four CO analyzers are shown in Figure 4.3-5. For the first 64 hours of TC06, only AI434B was giving reasonable results. At hour 64, both AI434B and AI464C agreed with each other and remained in agreement with each other until the end of TC06. For the first 220 hours AI453G read zero and AI425 had wide variations. After a 4-week break at hour 220, all four CO analyzers agreed with each other until the end of TC06. The close agreement between the CO analyzers gives good confidence to the accuracy of the data. The low-CO measurements are either periods when the gas analyzers were being calibrated or are measurements during coal feeder trips. The CO compositions used in calculations were interpolated for times when the gas analyzers were being calibrated. The dry CO concentrations varied between 12 and 14 percent during TC06.

TC06 hourly averages data for the CO_2 analyzers are shown in Figure 4.3-6. Analyzer AI454D was not operating properly for the first 220 hours of TC06, while AI434C was giving reasonable results. After the 4-week break both analyzers agreed very well with each other. The low CO_2 measurements are either periods when the gas analyzers were being calibrated or are measurements made during coal feeder trips. The CO_2 compositions used in calculations were interpolated for times when the gas analyzers were being calibrated. The dry CO_2 concentrations varied between 8 and 9.5 percent during TC06. For the last 700 hours of TC06, the CO_2 concentration was very steady at 8 percent.

The TC06 hourly average gas analyzer data for H_2, CH_4, and C_2^+ are shown in Figure 4.3-7. For the first 60 hours of TC06 (TC06-1 to TC06-5), the hydrogen analyzer AI464G was not operating properly. Once the hydrogen analyzer was operating, it gave reasonable results until the end of the run. The hydrogen concentration varied between 6 and 8 percent, with most of the run at about 7.5-mole percent. Thermodynamic data (the water gas shift equilibrium constant) was used to estimate the hydrogen concentration for the first five operating periods from other gas analyzer data and the mixing zone temperature.

For the first 220 hours of TC06 (TC06-1 to -14), the methane analyzer AI464E was out of service. Once it was put in service, it gave reasonable results for the remainder of TC06. The methane concentration averaged 1.37 percent during the operating periods TC06-15 to -64, therefore that value was used for the first 14 operating periods.

The C_2^+ analyzer AI464F read 0.0 percent after 220 hours except when coke breeze was being fed to the Transport Reactor. During the first 220 hours, AI464F gave erratic readings, so for the first 220 hours of TC06 it was assumed that the C_2^+ was 0.0 percent.

The nitrogen analyzer AI464B was not giving reasonable results for TC06-3 to -5, so the nitrogen content was estimated by difference for these operating periods.

The hourly averages of the sum of the dry gas analyses are shown in Figure 4.3-8 for all the operating periods except the first five. The majority of the remaining 59 operating periods have the sum of dry gas compositions close to 99 percent indicating that the data is consistent. There is a concern on what is in the missing 1 percent of the gas or whether there is a consistent

1 percent error in the gas analyzers. There is no backup analyzer for the hydrogen, nitrogen, methane, or C_2^+ concentrations, so some of the error could be there. It is planned to have backup hydrogen, nitrogen, methane, and C_2^+ analyzers for the next gasification run. The first 14 operating periods have the sum of the dry compositions at 97 to 99 percent, which indicate that the gas composition data for those periods is not as good as the gas composition data for the operating periods TC06-15 to -64.

The AI7510 water analyzer data for the operating periods are shown in Figure 4.3-9 where they are compared with the in situ synthesis gas moisture measurement made during PCD outlet particulate sampling. The location of the water analyzer is between the pressure letdown valve and the synthesis gas combustor inlet. The location of the in situ H_2O measurement is between the PCD exit and the inlet of the secondary gas cooler. The locations of both sampling points are shown in Figure 4.3-4. The in situ measurement and gas analyzer data agreed well between hour 58 and 278, both before and after the 4-week break. From hour 296 to hour 586, AI7510 measured about 1 percent higher than the in situ analyses. Then from hour 608 to hour 760, the two H_2O measurements agreed with each other if one of the in situ measurements was excluded. From hour 787 to the end of TC06, half of the in situ measurements agreed with each and the other half the in situ data were again 1 to 2 percent below AI7510. These results are surprising since in the previous gasification runs AI7510 usually agreed well with the in situ data.

The steam feed rate is also shown in Figure 4.3-9. Both H_2O measurements were consistent with the increase and then decrease in stream rates in the first 100 hours of TC06. Both H_2O measurements increased from hour 500 to the hour 900, which would be consistent with a steam leak from HX0202. Between hour 900 and the end of TC06, the H_2O measurements slightly decreased due to increases in the air rate.

In previous gasification runs, the water-gas shift (WGS) reaction was used to interpolate H_2O measurements between in situ H_2O measurements and to check the consistency of the H_2O analyzer. The water-gas shift equilibrium constant should be a function of a Transport Reactor mixing zone or riser temperature. Plotted in Figure 4.3-9 are the H_2O concentrations calculated from the water-gas shift equilibrium constant based on the mixing zone temperature TI344 and using the measured H_2, CO, and CO_2 concentrations. The water-gas shift H_2O should give some guidance as to which H_2O measurement is more correct. There is no reactor temperature that correctly predicts the trends of either the in situ or the H_2O analyzer data. The in situ H_2O measurements analyzer readings will be used for further data analyses since oxygen and hydrogen balances agree better for the in situ measurements than the H_2O analyzer measurements. The H_2O compositions used in further calculations are based on interpolation between the in situ measurements.

The water-gas shift reaction and equilibrium constant:

$$CO + H_2O \leftrightarrow H_2 + CO_2 \quad (1)$$

$$Kp = \frac{(H_2)(CO_2)}{(H_2O)(CO)} \quad (2)$$

The water-gas shift equilibrium constant was used to estimate the hydrogen concentration using TI344 as the equilibrium temperature for operating periods TC06-1 to -5, since the equilibrium constant predicted the H_2O concentration very well for test periods TC06-6 (hour 74) to -18 (hour 270).

The best estimates of the wet gas compositions for the TC06 operating periods are shown in Table 4.3-3 and shown in Figure 4.3-10. Also shown in Table 4.3-3 are the synthesis gas molecular weights for each operating period. The CO concentration increased from 10 to 12 percent during the first 255 hours of TC06. After decreasing to 9 percent at hour 270, the CO concentration was constant at about 12 percent from hour 336 to hour 719. The CO concentration then dipped down to 11 percent from hour 711 to hour 859 during the period of low coal flow. As the coal rate was steadily increased from hour 829 to the end of the run, the CO concentration steadily increased up to 13.5 percent at the end of TC06.

The H_2 concentration was steady at about 7 percent during most of TC06. From hour 244 to hour 306, the H_2 concentration was about 6 percent. During the low coal flow from hour 760 to hour 859, the H_2 concentration also decreased to 6 percent. When the coal-feed rate was increased at hour 829, the H_2 concentration slowly increased to 7.5 percent at the end of TC06.

The CO_2 concentration was steady for the entire run at about 7.5 percent. The CH_4 concentration was steady at about 1.3 percent until the coal rate decreased at hour 760 when it decreased to 1.0 percent. When the coal rate increased at hour 829, the CH_4 increased to 1.5 percent.

The water-gas shift (WGS) equilibrium constant and the CO/CO_2 ratio, which were calculated from the gas data for each operating period, are listed in Table 4.3-3, and plotted in Figure 4.3-11. The water-gas shift equilibrium constant is not shown for the first five operating periods because there were no hydrogen data for those periods. For operating periods TC06-6 to -14, the water-gas shift was steady at between 0.60 and 0.65. From hour 244 to hour 400, the equilibrium constant was steady at between 0.7 and 0.8. From hour 400 to hour 873, the equilibrium constant decreased from 0.80 to 0.55. From hour 873 to the end of the run, the equilibrium constant was steady at between 0.5 and 0.6. The variation in equilibrium constant is surprising since the reactor temperature was held constant during TC06 and the equilibrium constant should only be a function of temperature. During the post-TC06 outage, it was discovered that the primary gas cooler (HX0202) was leaking steam into the synthesis gas. The extra H_2O in the synthesis gas would tend to lower the water-gas shift constant. It would appear that the steam leaks became significant at about hour 500, when the WGS constant started to decrease, and the H_2O content of the synthesis gas increased from about 7 to 9 percent (about 350 more lb/hr H_2O).

The CO/CO_2 ratio is varied from 1.1 to 1.6 during the first 308 hours of TC06. The CO/CO_2 ratio was then constant at about 1.6 from hour 308 to hour 719. During the lower coal-rate operation between hour 760 and hour 829, the CO/CO_2 ratio dropped to between 1.4 to 1.5. When the coal rate was increased between hour 829 to hour 926, the CO/CO_2 ratio increased to 1.8. For the last 60 hours of the run, the CO/CO_2 ratio was constant at 1.8.

The water-gas shift equilibrium, calculated from the mixing zone temperature TI344, is shown in Table 4.3-3 and plotted in Figure 4.3-12 against the measured water-gas shift equilibrium. The agreement was very good for the first 296 hours of TC06. Between hour 244 and hour 498, the measured equilibrium constant was consistently higher than the equilibrium constant calculated from the mixing zone temperature. From hour 505 to hour 586, the two equilibrium constants were the same. Between hour 608 and the end of TC06, the measured equilibrium constant was consistently lower than the equilibrium constant calculated from the mixing zone temperature. The mixing zone temperature equilibrium constant was unchanged during the run at 0.65, except between hour 254 and hour 419 when it increased to 0.7, and at the end of the run from hour 859 on when it was at 0.63. The low measured equilibrium constants produce a higher equilibrium temperature (around 1,900°F) than the maximum temperature in the reactor. The steam leakage from HX0202 that began around 500 hours was the probable cause of the decrease in measured water-gas shift constant.

The temperature at which the water gas-shift reaction data is at equilibrium is calculated from thermodynamic data and shown in Table 4.3-3 and varied from 1,639 to 1,978°F. This demonstrated that the water-gas shift reaction essentially "freezes" at the reactor temperatures and does not further react at the lower temperatures in the primary gas cooler or the PCD. This is surprising since gas-gas reactions like the water-gas shift reaction should be fast reactions. In order to have the water-gas shift reaction to proceed at lower temperatures than the Transport Reactor, a catalyst is required.

The lower heating value (LHV) for each gas composition was calculated and is shown in Table 4.3-3 and plotted in Figure 4.3-13. The LHV value was calculated using the formula:

$$\mathrm{LHV(Btu/SCF)} = \left\{ \begin{matrix} 275\times(\mathrm{H_2\%}) + 322\times(\mathrm{CO\%}) + \\ 913\times(\mathrm{CH_4\%}) + 1641\times(\mathrm{C_2H_6^+\%}) \end{matrix} \right\} / 100 \qquad (3)$$

The raw LHV was from 57 to 77 Btu/SCF. The LHV were generally constant, about 65 to 70 Btu/SCF for the first 719 hours. As the coal rate decreased, the LHV decreased down to about 60 Btu/SCF. At the end of TC06, when the coal rate was increased, the LHV increased up to 76 Btu/SCF.

The PSDF Transport Reactor adds more N_2 per lb synthesis gas than a commercial reactor because of the additional PSDF sampling purges, additional PSDF instrument purges, and the need to aerate the lower portion of the reactor. Instrument purges would be proportionally smaller in a commercial design due to the scale factor (number of instruments stay the same size as plant size increases). Any additional N_2 added to the riser requires additional fuel to bring the additional N_2 up to operating temperatures. This additional fuel then requires additional air, which then adds additional N_2 to the reactor and further dilutes the synthesis gas. The aeration gas will be supplied by recycle gas in a commercial-sized reactor. The PSDF Transport Reactor heat loss per lb of coal fed is much greater that the heat loss from a commercial-sized reactor. To correct for the lower heat loss per lb of coal fed, the additional coal required to compensate

for the heat loss is subtracted from the coal-feed rate. To estimate the commercial synthesis LHV, the following components are deleted from the raw synthesis gas:

- All aeration nitrogen ("nonair" nitrogen).
- Air nitrogen that is required for burning additional coal that is used for heating aeration nitrogen to the reactor process temperature.
- Carbon dioxide from burning the additional coal required for heating aeration nitrogen.
- Water vapor from burning the additional coal required for heating aeration nitrogen.
- Air nitrogen required for burning additional coal that is required to compensate for the reactor heat loss of 1.5×10^6 Btu/hr.
- Carbon dioxide from burning the additional coal required for the reactor heat loss.
- Water vapor from burning the additional coal required for the reactor heat loss.

The sum of all these corrections is the adiabatic nitrogen-corrections LHV. The aeration nitrogen was determined by subtracting the air nitrogen from the synthesis gas nitrogen. Note that these corrections change the water-gas shift equilibrium constant, the CO/CO_2 ratio, and the air-to-coal ratio. These calculations are an oversimplification of the gasification process. A more sophisticated model is required to correctly predict the effect of decreasing aeration nitrogen and reactor heat loss. The adiabatic N_2 corrected LHV for each operating period are shown in Table 4.3-4 and plotted in Figure 4.3-13. All the N_2 corrected LHV were between 104 and 124 Btu/SCF and follow the trends of the raw gas LHV.

The synthesis gas compositions and synthesis gas-flow rate can be checked by an oxygen balance around the synthesis gas combustor (SGC) since the synthesis gas combustor exit O_2 is measured by AIT8775. The synthesis gas combustor oxygen balance was calculated for each operating period by using the following thermal oxidizer process tags:

- Primary air flow, FI8773.
- Secondary air flow, FIC8772.
- Quench air flow, FI8771.
- Propane flow, FI8753.
- Oxygen concentration, AIT8775.

During TC06, it was discovered that temperature- and pressure-compensated flow rates for FIC8772 and FI8771 were calculated by the DCS but were not being stored in PI. At 14:00 September 4, 2001, the temperature and pressure compensated flow rates for FIC8772 and FI8771 were added to PI and could be used in synthesis gas combustor calculations. A correlation factor was developed from post-September 4 data to estimate the compensated pre-September 4 FIC8772 and FI8771 values and these values were used for pre-September 4 data analysis.

The measured and mass balance calculated O_2 values are shown in Figure 4.3-14 and Table 4.3-5. The measured- and calculated-O_2 concentrations agreed well with each other for nearly all the operating periods. Both were around 6-percent O_2 for most of the run. The agreement is good for up to the first nine operating periods (hour 124). The agreement is poor for the next five periods until the 4-week break in operations with the calculated oxygen about

1 percent less than the measured oxygen. The agreement is then excellent from the 4-week break until hour 760, even when the oxygen content increased from 6 to 8 percent. From hour 711 to hour 850, the calculated oxygen was from 0.5 to 1.0 percent below the measured oxygen. After hour 873 until the end of TC06, the agreement was excellent between the measured and calculated oxygen. The operating periods when the calculated oxygen was lower than the measured oxygen were typically when one of the air flow meters to the synthesis gas combustor was reading low. The agreement between measured and calculated oxygen concentration was about the same whether the analyzer H_2O or the in situ H_2O measurement was used.

The synthesis gas LHV can be estimated by doing an energy balance around the synthesis gas combustor. The synthesis gas combustor energy balance is done by estimating the synthesis gas combustor heat loss to make the synthesis gas LHV calculated by the synthesis gas combustor energy balance agree with LHV calculated from the synthesis gas analyzer data. In GCT2, the synthesis gas combustor heat loss was usually between 1.5 and 4.0 x 10^6 Btu/hr to obtain agreement. In GCT3, the best fit was 1.0 x 10^6 Btu/hr. The best fit for the GCT4 data was 2.25 x 10^6 Btu/hr. The best fit of the TC06 data was also 2.25 x 10^6 Btu/hr. A comparison between the measured LHV and the synthesis gas combustor energy balance LHV using a synthesis gas combustor heat loss of 2.25 x 10^6 Btu/hr is shown in Figure 4.3-15. The SGC combustor energy balance LHV was close to the analyzer measured value for the first 220 hours. From hour 234 to hour 336, the gas analysis LHV was less than the synthesis gas combustor LHV. After hour 336, the two LHV had excellent agreement with each other.

Since the Transport Reactor H_2S analyzer was not working during TC06, the H_2S concentration and sulfur emissions from the Transport Reactor were not directly measured. The synthesis gas combustor SO_2 analyzer (AI534A) measures the total sulfur emissions from the Transport Reactor. The total sulfur emissions consists of H_2S, COS, and CS_2. The main sulfur species in coal gasification are considered to be H_2S and carbon oxysulfide (COS). There should also be only a minor amount of carbon disulfide (CS_2). Waltz Mills KRW gasifier data indicates that the majority of the gaseous sulfur is present as H_2S, with the balance COS. KRW typically measured concentrations of 100 to 200 ppm COS for 0.6 to 1.0 percent sulfur fuels. The sulfur emissions for the operating periods of TC06 are plotted in Figure 4.3-16 and listed in Table 4.3-5. Since the synthesis gas combustor exit-gas-flow rate is about twice that of the synthesis gas rate, the synthesis gas total reduced sulfur concentration is about twice that of the measured synthesis gas combustor SO_2 concentration.

The sulfur emissions were from 155 to 230 ppm for the beginning of TC06 up to hour 255. At hour 270, the sulfur emissions dropped to between 100 and 150 ppm until hour 587 when the sulfur emissions increased to above 150 ppm. After hour 648 the sulfur emissions dropped below 150 ppm and were between 100 to 150 ppm to the end of the run.

The equilibrium H_2S concentration in coal gasification using limestone is governed by three reversible reactions:

$$CaCO_3 \leftrightarrow CaO + CO_2 \tag{4}$$

$$H_2S + CaO \leftrightarrow CaS + H_2O \tag{5}$$

$$H_2S + CaCO_3 \leftrightarrow CaS + H_2O + CO_2 \quad (6)$$

Reaction (4) is the limestone calcination reaction. At thermodynamic equilibrium, the CO_2 partial pressure should be a function of only the system temperature as long as there are both $CaCO_3$ and CaO present according to the equilibrium constant:

$$K_1 = P^O_{CO_2} \quad (7)$$

where P^O_{CO2} is the partial pressure of CO_2. A plot of the partial pressure of CO_2 and temperature is shown in Figure 4.3-15 of the GCT1 report. At thermodynamic equilibrium, $CaCO_3$ and CaO only coexist on the equilibrium curve, while above the curve only $CaCO_3$ exists, and below the curve only CaO exists. Typically, there are both $CaCO_3$ and CaO present in the PCD solids. This is because of kinetic limitations and the quick cooling down of the solids in the fuel gas from the reactor temperatures to PCD temperatures. This quick cooling down tends to "freeze" reactions at higher equilibrium temperatures than would be indicated by the actual system exit temperature.

The H_2S equilibrium is governed by reactions (5) and (6), with the associated equilibrium constants:

$$K_2 = \frac{P^O_{H_2O}}{P^O_{H_2S}} \quad (8)$$

$$K_3 = \frac{P^O_{H_2O} P^O_{CO_2}}{P^O_{H_2S}} \quad (9)$$

Equations (8) and (9) state that the equilibrium H_2S concentrations in the $CaCO_3$-CaO-CaS system is a function of the system temperature and the CO_2 and H_2O partial pressures. As the CO_2 and H_2O partial pressures increase, so would H_2S partial pressures. The equilibrium constants are all functions of temperature and can be determined using thermodynamic data with Aspen simulations. A more detailed description of the H_2S equilibrium calculations is provided (starting on page 4.3-7) in the GCT1 final report.

The minimum thermodynamic H_2S concentrations for each operating period were calculated from the measured partial pressures of CO_2 and H_2O and are shown in Table 4.3-5. The measured total reduced sulfur and minimum H_2S concentrations are compared in Figure 4.3-16. The measured total reduced sulfur emissions had a lot of scatter as compared to the measured sulfur emissions. For the first 700 hours of TC06, the measured emissions seemed to follow the equilibrium concentrations, either above or below them in a random pattern. After 700 hours, the equilibrium H_2S concentrations were consistently below the measured sulfur emissions, usually by about 50 ppm. These observations are consistent with observations from operation at Beijing Research Institute of Coal Chemistry in the early 1990's (Guohai Liu, personal communications). This is surprising since the total reduced sulfur consists of not only H_2S, but also COS and CS_2 and should be higher than the equilibrium H_2S. The choice of the in situ H_2O

measurement increases the equilibrium H_2S since the in situ H_2O measurements were generally higher than the H_2O analyzer measurements.

The temperature at which the equilibrium H_2S concentration is determined is about 1,650°F, indicating that all the H_2S removal takes place in the Transport Reactor and not in the primary gas cooler or the PCD. Therefore, limestone addition after the reactor will not produce any additional H_2S removal. Thermodynamics also predicts that increasing the reactor temperature should increase H_2S emissions, while lowering the reactor temperature will decrease H_2S emissions.

Ammonia and HCN concentration data were taken by extracting synthesis gas and collecting NH_3 and HCN in liquid solutions. The solutions were then analyzed for NH_3 and HCN. The data was taken on July 17, 2001, (hour 67 to 71, TC06-6) and July 24 (hour 224 to 227, right after the end of TC06-14). The results are shown in Table 4.3-6. The ammonia was from 1,296 to 1,910 ppm and the HCN was from 42 to 72 ppm. The NH_3 and HCN concentrations increased during the July 17 sampling periods, while the NH_3 and HCN concentrations were constant during the July 24 sampling.

Table 4.3-1 Operating Periods

Operating Period	Start Time	End Time	Duration Hours	Operating Average Time	Period Relative Hours
TC06-1	7/15/01 17:45	7/16/01 02:30	8:45	7/15/01 22:07	21
TC06-2	7/16/01 04:30	7/16/01 08:30	4:00	7/16/01 6:30	29
TC06-3	7/16/01 08:30	7/16/01 12:30	4:00	7/16/01 10:30	34
TC06-4	7/16/01 12:30	7/16/01 23:30	11:00	7/16/01 18:00	41
TC06-5	7/17/01 03:30	7/17/01 11:30	8:00	7/17/01 7:30	55
TC06-6	7/17/01 21:00	7/18/01 09:00	12:00	7/18/01 3:00	74
TC06-7	7/18/01 09:00	7/18/01 17:00	8:00	7/18/01 13:00	84
TC06-8	7/18/01 17:00	7/18/01 22:15	5:15	7/18/01 19:37	91
TC06-9	7/19/01 21:45	7/20/01 13:00	15:15	7/20/01 5:22	124
TC06-10	7/21/01 00:15	7/21/01 05:15	5:00	7/21/01 2:45	146
TC06-11	7/21/01 05:30	7/21/01 14:30	9:00	7/21/01 10:00	153
TC06-12	7/22/01 16:45	7/23/01 03:45	11:00	7/22/01 22:15	189
TC06-13	7/23/01 03:45	7/23/01 12:45	9:00	7/23/01 8:15	199
TC06-14	7/24/01 05:00	7/24/01 09:15	4:15	7/24/01 7:07	222
TC06-15	8/20/01 20:30	8/21/01 00:30	4:00	8/20/01 22:30	234
TC06-16	8/21/01 00:30	8/21/01 17:15	16:45	8/21/01 8:52	244
TC06-17	8/21/01 17:15	8/21/01 22:15	5:00	8/21/01 19:45	255
TC06-18	8/22/01 23:15	8/23/01 08:15	9:00	8/23/01 3:45	270
TC06-19	8/23/01 10:45	8/23/01 16:45	6:00	8/23/01 13:45	280
TC06-20	8/24/01 17:30	8/24/01 21:30	4:00	8/24/01 19:30	297
TC06-21	8/25/01 00:00	8/25/01 15:00	15:00	8/25/01 7:30	309
TC06-22	8/26/01 00:00	8/26/01 21:00	21:00	8/26/01 10:30	336
TC06-23	8/26/01 23:30	8/27/01 11:30	12:00	8/27/01 5:30	354
TC06-24	8/28/01 01:30	8/28/01 08:30	7:00	8/28/01 5:00	374
TC06-25	8/28/01 11:00	8/29/01 07:00	20:00	8/28/01 21:00	390
TC06-26	8/29/01 07:00	8/30/01 22:00	39:00	8/30/01 2:30	420
TC06-27	8/31/01 00:00	8/31/01 16:00	16:00	8/31/01 8:00	449
TC06-28	9/1/01 02:00	9/1/01 07:00	5:00	9/1/01 4:30	470
TC06-29	9/1/01 09:00	9/1/01 15:00	6:00	9/1/01 12:00	477
TC06-30	9/1/01 15:00	9/2/01 03:00	12:00	9/1/01 21:00	486
TC06-31	9/2/01 03:00	9/2/01 07:00	4:00	9/2/01 5:00	494
TC06-32	9/2/01 07:00	9/2/01 11:00	4:00	9/2/01 9:00	498

Table 4.3-1 Operating Periods (continued)

Operating Period	Start Time	End Time	Duration Hours	Operating Period Average Time	Operating Period Relative Hours
TC06-33	9/2/01 13:45	9/2/01 18:45	5:00	9/2/01 16:15	505
TC06-34	9/3/01 02:00	9/3/01 12:00	10:00	9/3/01 7:00	520
TC06-35	9/3/01 18:00	9/4/01 01:00	7:00	9/3/01 21:30	534
TC06-36	9/4/01 09:00	9/4/01 14:00	5:00	9/4/01 11:30	548
TC06-37	9/4/01 16:00	9/4/01 21:00	5:00	9/4/01 18:30	555
TC06-38	9/4/01 23:00	9/5/01 18:00	19:00	9/5/01 8:30	569
TC06-39	9/5/01 18:00	9/6/01 09:00	15:00	9/6/01 1:30	586
TC06-40	9/6/01 19:15	9/7/01 03:15	8:00	9/6/01 23:15	608
TC06-41	9/8/01 07:45	9/8/01 11:45	4:00	9/8/01 9:45	643
TC06-42	9/8/01 11:45	9/8/01 18:45	7:00	9/8/01 15:15	648
TC06-43	9/9/01 08:45	9/9/01 16:45	8:00	9/9/01 12:45	670
TC06-44	9/10/01 06:15	9/10/01 21:15	15:00	9/10/01 13:45	695
TC06-45	9/11/01 02:15	9/11/01 09:15	7:00	9/11/01 5:45	711
TC06-46	9/11/01 11:15	9/11/01 17:15	6:00	9/11/01 14:15	719
TC06-47	9/13/01 04:15	9/13/01 09:30	5:15	9/13/01 6:52	760
TC06-48	9/13/01 09:30	9/15/01 10:30	49:00	9/14/01 10:00	787
TC06-49	9/15/01 12:00	9/15/01 22:00	10:00	9/15/01 17:00	818
TC06-50	9/15/01 22:00	9/16/01 10:30	12:30	9/16/01 4:15	829
TC06-51	9/16/01 11:00	9/16/01 19:00	8:00	9/16/01 15:00	840
TC06-52	9/16/01 19:15	9/17/01 07:15	12:00	9/17/01 1:15	850
TC06-53	9/17/01 07:15	9/17/01 13:15	6:00	9/17/01 10:15	859
TC06-54	9/17/01 14:00	9/18/01 9:00	19:00	9/17/01 23:30	873
TC06-55	9/18/01 13:00	9/19/01 9:00	20:00	9/18/01 23:00	896
TC06-56	9/19/01 09:00	9/19/01 13:00	4:00	9/19/01 11:00	908
TC06-57	9/19/01 13:45	9/19/01 17:45	4:00	9/19/01 15:45	913
TC06-58	9/19/01 19:15	9/20/01 15:15	20:00	9/20/01 5:15	926
TC06-59	9/20/01 16:15	9/21/01 00:15	8:00	9/20/01 20:15	941
TC06-60	9/21/01 00:30	9/21/01 06:30	6:00	9/21/01 3:30	949
TC06-61	9/21/01 09:30	9/21/01 21:00	11:30	9/21/01 15:15	960
TC06-62	9/21/01 21:00	9/22/01 13:00	16:00	9/22/01 5:00	974
TC06-63	9/22/01 19:00	9/23/01 14:00	19:00	9/23/01 4:30	998
TC06-64	9/23/01 15:00	9/24/01 06:00	15:00	9/23/01 22:30	1,016

Table 4.3-2 Operating Conditions

Operating Periods	Average Relative Hours	Mixing Zone Temperature TI344 °F	Pressure PI287 psig	PCD Inlet Temperature TI458 °F	Air Rate lb/hr	Synthesis Gas Rate lb/hr	Nitrogen Rate[1] lb/hr
TC06-1	21	1,756	212	752	16,201	28,356	6,697
TC06-2	29	1,733	212	743	15,773	27,784	6,684
TC06-3	34	1,737	212	754	16,627	29,080	6,117
TC06-4	41	1,746	212	752	16,865	29,532	6,308
TC06-5	55	1,748	212	752	16,721	29,426	6,313
TC06-6	74	1,750	212	749	16,868	29,686	6,494
TC06-7	84	1,748	212	748	16,726	29,321	6,598
TC06-8	91	1,759	212	753	17,252	30,154	6,740
TC06-9	124	1,755	210	752	16,690	29,207	6,777
TC06-10	146	1,757	210	756	17,259	30,206	6,961
TC06-11	153	1,756	210	755	17,163	30,009	6,950
TC06-12	189	1,756	210	752	16,233	28,487	6,730
TC06-13	199	1,759	210	755	16,799	29,276	6,613
TC06-14	222	1,766	210	759	16,575	28,916	6,753
TC06-15	234	1,717	196	737	14,830	26,589	7,254
TC06-16	244	1,739	196	757	15,226	26,858	6,750
TC06-17	255	1,751	196	757	15,775	27,328	6,774
TC06-18	270	1,690	190	732	12,391	23,618	7,776
TC06-19	280	1,702	190	735	13,318	24,328	7,046
TC06-20	297	1,701	200	709	13,213	23,760	6,623
TC06-21	309	1,711	190	713	13,265	23,969	6,749
TC06-22	336	1,720	196	710	13,625	24,226	6,474
TC06-23	354	1,721	196	712	14,080	24,772	6,546
TC06-24	374	1,723	200	716	13,880	24,490	6,441
TC06-25	390	1,726	200	718	14,093	24,694	6,502
TC06-26	420	1,748	200	726	14,461	24,986	6,497
TC06-27	449	1,745	200	725	14,464	25,051	6,426
TC06-28	470	1,748	200	728	14,573	25,354	6,573
TC06-29	477	1,742	200	723	14,286	25,032	6,465
TC06-30	486	1,744	200	727	14,613	25,384	6,402
TC06-31	494	1,747	200	728	14,525	25,308	6,512
TC06-32	498	1,752	200	727	14,080	25,240	6,620

1. Feed Nitrogen was determined by subtracting 1,000 lb/hr from FI609 reading to account for nitrogen losses.

Table 4.3-2 Operating Conditions (continued)

Operating Periods	Average Relative Hours	Mixing Zone Temperature TI344 °F	Pressure PI287 psig	PCD Inlet Temperature TI458 °F	Air Rate lb/hr	Synthesis Gas Rate lb/hr	Nitrogen Rate[1] lb/hr
TC06-33	505	1,750	200	730	14,914	25,660	6,386
TC06-34	520	1,751	200	730	14,969	25,936	6,623
TC06-35	534	1,753	200	728	14,767	25,553	6,626
TC06-36	548	1,756	200	732	14,999	26,668	6,491
TC06-37	555	1,756	200	729	14,957	25,692	6,332
TC06-38	569	1,740	200	723	14,456	25,212	6,447
TC06-39	586	1,745	200	723	14,416	25,127	6,451
TC06-40	608	1,756	200	727	14,578	25,439	6,333
TC06-41	643	1,778	200	729	15,449	26,691	6,413
TC06-42	648	1,756	200	712	14,520	25,486	6,341
TC06-43	670	1,770	200	721	15,228	26,374	6,402
TC06-44	695	1,770	200	721	15,231	26,429	6,389
TC06-45	711	1,752	200	708	14,353	25,608	6,786
TC06-46	719	1,760	200	711	14,923	25,959	6,261
TC06-47	760	1,753	200	675	12,176	22,001	6,200
TC06-48	787	1,755	200	679	12,450	22,284	6,028
TC06-49	818	1,755	200	674	12,213	22,018	6,106
TC06-50	829	1,755	200	673	12,032	21,843	6,167
TC06-51	840	1,755	200	672	12,027	21,741	6,297
TC06-52	850	1,756	220	670	11,841	21,331	6,297
TC06-53	859	1,768	220	679	12,129	21,456	6,115
TC06-54	873	1,770	220	692	13,161	23,013	6,047
TC06-55	896	1,772	220	700	14,009	24,166	5,866
TC06-56	908	1,770	220	705	14,309	24,370	5,938
TC06-57	913	1,772	220	705	14,471	24,906	5,933
TC06-58	926	1,770	230	698	14,087	24,021	5,577
TC06-59	941	1,772	230	704	14,419	24,578	5,571
TC06-60	949	1,774	230	711	15,055	25,582	5,715
TC06-61	960	1,772	230	713	15,167	25,913	5,902
TC06-62	974	1,773	230	727	16,099	27,491	6,129
TC06-63	998	1,788	230	733	16,392	27,579	6,043
TC06-64	1016	1,776	230	725	16,124	27,376	6,019

Note: Feed Nitrogen was determined by subtracting 1,000 pounds per hour from FI609 reading to account for nitrogen losses

Table 4.3-3 Gas Compositions, Molecular Weight, and Heating Value

Operating Period	Average Relative Hour	H_2O Mole %	CO Mole %	H_2[1] Mole %	CO_2 Mole %	CH_4[2] Mole %	$C_2H_6^{+2}$ Mole %	N_2[3] Mole %	Total Mole %	Measured WGS K_p	WGS Eqm. Temp. ^{O}F	Calculated WGS K_p @ TI344	Syngas MW lb./Mole	Syngas CO/CO_2 Ratio	Syngas LHV Btu/SCF
TC06-1	21	10.9	10.4	10.2	7.1	1.2	0.0	60.2	100.0			0.64	25.2	1.5	73
TC06-2	29	10.9	10.0	10.1	7.1	1.2	0.0	60.7	100.0			0.66	25.3	1.4	71
TC06-3	34	10.9	9.4	9.5	7.2	1.2	0.0	61.8	100.0			0.66	25.4	1.3	68
TC06-4	41	10.7	10.0	9.8	7.2	1.2	0.0	61.1	100.0			0.65	25.4	1.4	70
TC06-5	55	10.4	9.7	9.1	7.2	1.2	0.0	62.4	100.0			0.65	25.6	1.3	67
TC06-6	74	9.8	10.3	7.1	8.3	1.2	0.0	63.2	100.0	0.58	1,829	0.65	26.4	1.2	64
TC06-7	84	9.5	10.2	7.1	8.4	1.3	0.0	63.5	100.0	0.62	1,782	0.65	26.4	1.2	64
TC06-8	91	9.2	10.8	7.2	8.2	1.3	0.0	63.4	100.0	0.60	1,809	0.64	26.4	1.3	66
TC06-9	124	7.8	10.5	7.1	7.9	1.3	0.0	65.4	100.0	0.69	1,707	0.64	26.5	1.3	65
TC06-10	146	7.5	11.1	7.1	8.0	1.3	0.0	65.0	100.0	0.68	1,714	0.64	26.5	1.4	67
TC06-11	153	7.4	11.3	7.1	7.9	1.3	0.0	65.0	100.0	0.66	1,736	0.64	26.5	1.4	68
TC06-12	189	7.2	11.6	6.7	7.5	1.3	0.0	65.7	100.0	0.61	1,799	0.64	26.6	1.6	68
TC06-13	199	7.1	11.6	7.0	7.8	1.3	0.0	65.3	100.0	0.66	1,742	0.64	26.6	1.5	68
TC06-14	222	7.9	11.4	6.9	7.6	1.3	0.0	65.0	100.0	0.58	1,831	0.63	26.5	1.5	67
TC06-15	234	6.7	11.0	5.2	8.7	1.7	0.0	66.6	100.0	0.61	1,789	0.68	27.1	1.3	66
TC06-16	244	6.7	11.2	6.2	9.2	1.5	0.0	65.2	100.0	0.76	1,649	0.66	27.0	1.2	67
TC06-17	255	6.7	12.0	7.4	8.1	1.4	0.0	64.4	100.0	0.75	1,653	0.65	26.5	1.5	72
TC06-18	270	6.7	9.0	5.7	8.1	1.3	0.0	69.1	100.0	0.77	1,639	0.71	27.0	1.1	57
TC06-19	280	6.7	10.4	6.3	8.2	1.5	0.0	67.0	100.0	0.75	1,654	0.70	26.8	1.3	64
TC06-20	297	6.5	10.7	6.2	8.1	1.5	0.0	67.0	100.0	0.72	1,678	0.70	26.8	1.3	66
TC06-21	309	6.4	10.6	6.1	7.9	1.4	0.0	67.6	100.0	0.72	1,677	0.69	26.9	1.3	64
TC06-22	336	6.1	11.9	6.5	7.4	1.5	0.0	66.6	100.0	0.68	1,722	0.68	26.7	1.6	70
TC06-23	354	5.9	12.1	6.6	7.5	1.5	0.0	66.4	100.0	0.70	1,699	0.68	26.7	1.6	71
TC06-24	374	5.8	11.8	6.7	7.7	1.4	0.0	66.5	100.0	0.75	1,652	0.67	26.8	1.5	70
TC06-25	390	5.8	12.0	6.9	7.8	1.5	0.0	66.0	100.0	0.77	1,638	0.67	26.7	1.5	71
TC06-26	420	5.8	12.2	6.9	7.7	1.3	0.0	66.1	100.0	0.75	1,653	0.65	26.7	1.6	70
TC06-27	449	6.2	11.9	6.9	7.7	1.4	0.0	65.8	100.0	0.72	1,675	0.65	26.6	1.5	70
TC06-28	470	6.3	11.7	6.9	7.7	1.2	0.0	66.1	100.0	0.71	1,687	0.65	26.7	1.5	68
TC06-29	477	6.4	11.6	6.9	7.8	1.4	0.0	65.8	100.0	0.74	1,665	0.66	26.6	1.5	69
TC06-30	486	6.4	12.0	7.0	7.7	1.4	0.0	65.5	100.0	0.71	1,687	0.65	26.6	1.5	70
TC06-31	494	6.4	11.7	6.9	7.7	1.3	0.0	66.0	100.0	0.71	1,686	0.65	26.7	1.5	68
TC06-32	498	6.4	11.2	6.7	7.8	1.1	0.0	66.9	100.0	0.73	1,670	0.65	26.7	1.4	64

Notes:

1. TC06-1 to TC06-5: H_2 determined from water-gas shift reaction and thermodynmaic equilibrium data.
2. TC06-1 to TC06-14: CH_4 and C_2^+determined from the average of TC06-15 to TC06-64 data.
3. TC06-3 to TC06-5: N_2 data determined by difference.

Table 4.3-3 Gas Compositions, Molecular Weight, and Heating Value (continued)

Operating Period	Average Relative Hour	H_2O Mole %	CO Mole %	H_2 Mole %	CO_2 Mole %	CH_4 Mole %	$C_2H_6^+$ Mole %	N_2 Mole %	Total Mole %	Measured WGS K_p	WGS Eqm. Temp. ^OF	Calculated WGS K_p @ TI344	Syngas MW lb./Mole	Syngas CO/CO_2 Ratio	Syngas LHV Btu/SCF
TC06-33	505	6.4	12.3	7.1	7.7	1.3	0.0	65.2	100.0	0.69	1,709	0.65	26.6	1.6	71
TC06-34	520	6.4	12.0	6.9	7.6	1.3	0.0	65.8	100.0	0.67	1,727	0.65	26.6	1.6	69
TC06-35	534	6.5	12.1	6.8	7.4	1.2	0.0	66.0	100.0	0.64	1,764	0.65	26.6	1.6	69
TC06-36	548	6.5	12.3	6.9	7.4	1.2	0.0	65.8	100.0	0.64	1,763	0.64	26.6	1.7	69
TC06-37	555	6.6	12.5	7.2	7.5	1.3	0.0	64.9	100.0	0.65	1,752	0.64	26.5	1.7	72
TC06-38	569	6.9	12.0	7.0	7.7	1.3	0.0	65.1	100.0	0.65	1,747	0.66	26.5	1.6	70
TC06-39	586	7.0	12.0	7.0	7.6	1.3	0.0	65.2	100.0	0.63	1,772	0.65	26.5	1.6	70
TC06-40	608	7.4	12.0	6.9	7.5	1.2	0.0	65.0	100.0	0.59	1,824	0.64	26.5	1.6	69
TC06-41	643	8.1	12.3	7.1	7.5	1.2	0.0	63.7	100.0	0.54	1,887	0.62	26.4	1.6	70
TC06-42	648	8.0	11.9	7.0	7.6	1.3	0.0	64.1	100.0	0.56	1,855	0.64	26.4	1.6	70
TC06-43	670	7.7	12.2	7.1	7.6	1.2	0.0	64.1	100.0	0.58	1,837	0.63	26.4	1.6	70
TC06-44	695	7.5	12.1	7.0	7.6	1.3	0.0	64.6	100.0	0.58	1,828	0.63	26.5	1.6	70
TC06-45	711	8.1	11.1	6.6	7.6	1.2	0.0	65.4	100.0	0.55	1,871	0.65	26.5	1.5	65
TC06-46	719	8.2	12.0	7.1	7.6	1.3	0.0	63.7	100.0	0.54	1,882	0.64	26.4	1.6	70
TC06-47	760	8.5	10.6	6.2	7.5	1.0	0.0	66.2	100.0	0.51	1,926	0.65	26.6	1.4	61
TC06-48	787	7.8	11.2	6.4	7.5	1.1	0.0	66.1	100.0	0.55	1,877	0.64	26.6	1.5	63
TC06-49	818	7.8	11.1	6.3	7.4	1.0	0.0	66.3	100.0	0.54	1,886	0.64	26.7	1.5	63
TC06-50	829	8.0	10.6	6.1	7.5	0.9	0.0	66.9	100.0	0.54	1,888	0.64	26.7	1.4	59
TC06-51	840	8.2	10.9	6.4	7.4	1.0	0.0	66.1	100.0	0.53	1,894	0.64	26.6	1.5	62
TC06-52	850	8.3	11.0	6.2	7.4	1.0	0.0	66.1	100.0	0.50	1,941	0.64	26.6	1.5	62
TC06-53	859	8.5	11.0	6.2	7.3	0.9	0.0	66.1	100.0	0.48	1,978	0.63	26.6	1.5	61
TC06-54	873	8.4	11.6	6.5	7.4	1.0	0.0	65.0	100.0	0.49	1,962	0.63	26.5	1.6	64
TC06-55	896	7.8	12.3	6.9	7.4	1.2	0.0	64.4	100.0	0.52	1,910	0.63	26.5	1.7	69
TC06-56	908	7.3	12.6	7.0	7.4	1.2	0.0	64.5	100.0	0.56	1,856	0.63	26.5	1.7	71
TC06-57	913	7.3	12.6	6.9	7.4	1.2	0.0	64.7	100.0	0.56	1,861	0.63	26.5	1.7	70
TC06-58	926	7.3	13.0	7.0	7.3	1.3	0.0	64.1	100.0	0.54	1,882	0.63	26.5	1.8	73
TC06-59	941	7.5	13.2	7.1	7.3	1.3	0.0	63.6	100.0	0.53	1,906	0.63	26.4	1.8	74
TC06-60	949	7.6	13.1	7.1	7.3	1.4	0.0	63.5	100.0	0.52	1,915	0.63	26.4	1.8	75
TC06-61	960	7.7	13.1	7.1	7.4	1.4	0.0	63.4	100.0	0.52	1,915	0.63	26.4	1.8	74
TC06-62	974	7.5	13.1	7.2	7.5	1.4	0.0	63.3	100.0	0.55	1,876	0.63	26.4	1.7	75
TC06-63	998	7.3	13.5	7.3	7.4	1.4	0.0	63.1	100.0	0.55	1,879	0.62	26.4	1.8	76
TC06-64	1016	7.2	13.3	7.5	7.5	1.5	0.0	63.0	100.0	0.58	1,825	0.63	26.3	1.8	77

1. TC06-1 to TC06-5: H_2 determined from water-gas shift reaction and thermodynmaic equilibrium data.
2. TC06-1 to TC06-14: CH_4 and C_2^+determined from the average of TC06-15 to TC06-64 data.
3. TC06-3 to TC06-5: N_2 data determined by difference.

Table 4.3-4 Corrected[2] Gas Compositions, Molecular Weight, and Heating Value

Operating Period	Average Relative Hour	H_2O Mole %	CO Mole %	H_2 Mole %	CO_2 Mole %	CH_4 Mole %	$C_2H_6^+$ Mole %	N_2 Mole %	Total Mole %	Syngas MW lb./Mole	Syngas LHV Btu/SCF
TC06-1	21	14.9	16.4	16.0	7.7	1.9	0.0	43.1	100.0	23.3	114
TC06-2	29	15.1	16.0	16.2	7.8	1.9	0.0	43.0	100.0	23.3	114
TC06-3	34	15.2	15.2	15.3	8.0	2.0	0.0	44.2	100.0	23.5	109
TC06-4	41	14.8	15.9	15.5	8.0	1.9	0.0	43.8	100.0	23.5	112
TC06-5	55	14.6	15.9	14.9	8.1	2.0	0.0	44.5	100.0	23.7	110
TC06-6	74	13.6	16.8	11.5	9.9	2.0	0.0	46.2	100.0	25.0	104
TC06-7	84	13.2	16.5	11.6	10.0	2.1	0.0	46.6	100.0	25.0	104
TC06-8	91	12.5	17.4	11.7	9.6	2.0	0.0	46.7	100.0	25.0	107
TC06-9	124	10.6	17.8	12.1	9.4	2.2	0.0	48.0	100.0	25.0	110
TC06-10	146	10.0	18.6	11.9	9.5	2.2	0.0	47.8	100.0	25.1	113
TC06-11	153	9.9	19.0	11.9	9.3	2.2	0.0	47.7	100.0	25.1	114
TC06-12	189	9.6	19.8	11.5	8.7	2.2	0.0	48.1	100.0	25.1	116
TC06-13	199	9.4	19.4	11.7	9.1	2.2	0.0	48.2	100.0	25.2	115
TC06-14	222	10.7	19.0	11.5	8.8	2.2	0.0	47.9	100.0	25.1	113
TC06-15	234	8.9	19.2	9.1	10.9	3.0	0.0	48.7	100.0	26.1	115
TC06-16	244	8.7	18.7	10.3	11.5	2.5	0.0	48.3	100.0	26.0	112
TC06-17	255	8.6	19.7	12.2	9.5	2.3	0.0	47.7	100.0	25.2	118
TC06-18	270	9.8	18.3	11.6	10.7	2.7	0.0	47.0	100.0	25.4	115
TC06-19	280	9.1	19.0	11.6	10.2	2.7	0.0	47.3	100.0	25.3	118
TC06-20	297	8.7	19.4	11.3	9.9	2.8	0.0	48.0	100.0	25.4	119
TC06-21	309	8.6	19.5	11.3	9.8	2.6	0.0	48.2	100.0	25.4	118
TC06-22	336	7.9	21.1	11.6	8.7	2.7	0.0	48.1	100.0	25.2	124
TC06-23	354	7.5	21.3	11.6	8.7	2.6	0.0	48.4	100.0	25.3	124
TC06-24	374	7.4	20.8	11.7	9.2	2.5	0.0	48.4	100.0	25.4	122
TC06-25	390	7.3	20.8	11.9	9.2	2.6	0.0	48.3	100.0	25.3	123
TC06-26	420	7.3	20.8	11.8	8.9	2.2	0.0	49.0	100.0	25.3	120
TC06-27	449	7.9	20.3	11.8	9.0	2.3	0.0	48.6	100.0	25.3	119
TC06-28	470	8.1	20.1	11.8	9.1	2.1	0.0	48.8	100.0	25.3	117
TC06-29	477	8.2	20.1	11.9	9.3	2.4	0.0	48.1	100.0	25.2	120
TC06-30	486	8.1	20.3	11.9	9.0	2.3	0.0	48.3	100.0	25.2	119
TC06-31	494	8.2	20.1	11.9	9.1	2.2	0.0	48.5	100.0	25.3	118
TC06-32	498	8.5	20.2	12.1	9.4	1.9	0.0	47.9	100.0	25.3	116

Notes:
1. See Table 4.3-3 for assumptions on gas compositions.
2. Correction is to assume that only air nitrogen is in the synthesis gas and that the reactor is adiabatic.

Table 4.3-4 Corrected[2] Gas Compositions, Molecular Weight, and Heating Value (continued)

Operating Period	Average Relative Hour	H_2O Mole %	CO Mole %	H_2 Mole %	CO_2 Mole %	CH_4 Mole %	$C_2H_6^+$ Mole %	N_2 Mole %	Total Mole %	Syngas MW lb./Mole	Syngas LHV Btu/SCF
TC06-33	505	8.1	20.5	11.8	8.8	2.2	0.0	48.5	100.0	25.2	119
TC06-34	520	8.3	20.4	11.6	8.8	2.2	0.0	48.7	100.0	25.3	117
TC06-35	534	8.4	20.7	11.5	8.4	2.1	0.0	48.8	100.0	25.2	118
TC06-36	548	8.6	21.4	12.0	8.6	2.0	0.0	47.5	100.0	25.1	120
TC06-37	555	8.5	20.7	11.9	8.5	2.1	0.0	48.3	100.0	25.1	119
TC06-38	569	9.1	20.1	11.9	8.9	2.3	0.0	47.8	100.0	25.1	118
TC06-39	586	9.2	20.3	11.8	8.7	2.2	0.0	47.9	100.0	25.1	117
TC06-40	608	9.9	20.2	11.7	8.5	2.0	0.0	47.6	100.0	25.1	116
TC06-41	643	10.8	19.9	11.6	8.5	2.0	0.0	47.3	100.0	25.0	114
TC06-42	648	10.9	19.7	11.7	8.7	2.2	0.0	46.7	100.0	25.0	116
TC06-43	670	10.2	20.0	11.7	8.7	2.0	0.0	47.4	100.0	25.1	115
TC06-44	695	10.0	20.0	11.6	8.7	2.1	0.0	47.6	100.0	25.1	115
TC06-45	711	11.3	19.4	11.4	8.8	2.1	0.0	47.0	100.0	25.0	113
TC06-46	719	11.1	19.7	11.5	8.7	2.2	0.0	46.9	100.0	25.0	115
TC06-47	760	12.3	19.4	11.3	8.7	1.8	0.0	46.5	100.0	25.0	110
TC06-48	787	10.9	20.2	11.4	8.6	1.9	0.0	46.9	100.0	25.1	114
TC06-49	818	11.1	20.2	11.4	8.6	1.9	0.0	46.7	100.0	25.1	114
TC06-50	829	11.6	19.7	11.3	8.9	1.7	0.0	46.9	100.0	25.1	110
TC06-51	840	11.7	19.8	11.6	8.6	1.9	0.0	46.4	100.0	25.0	113
TC06-52	850	12.0	19.9	11.2	8.6	1.9	0.0	46.5	100.0	25.0	112
TC06-53	859	12.1	19.7	11.0	8.3	1.6	0.0	47.3	100.0	25.1	108
TC06-54	873	11.7	19.9	11.2	8.3	1.7	0.0	47.2	100.0	25.0	110
TC06-55	896	10.4	20.5	11.4	8.2	1.9	0.0	47.6	100.0	25.1	115
TC06-56	908	9.5	20.7	11.4	8.3	1.9	0.0	48.3	100.0	25.2	115
TC06-57	913	9.6	20.8	11.5	8.3	2.0	0.0	48.0	100.0	25.1	116
TC06-58	926	9.5	21.1	11.4	8.1	2.1	0.0	47.8	100.0	25.1	119
TC06-59	941	9.6	21.2	11.4	8.0	2.1	0.0	47.6	100.0	25.1	119
TC06-60	949	9.8	20.9	11.3	8.1	2.2	0.0	47.7	100.0	25.1	119
TC06-61	960	9.9	20.9	11.3	8.1	2.2	0.0	47.5	100.0	25.1	119
TC06-62	974	9.7	20.7	11.4	8.3	2.3	0.0	47.5	100.0	25.1	119
TC06-63	998	9.3	21.0	11.4	8.1	2.1	0.0	48.0	100.0	25.1	118
TC06-64	1016	9.1	20.9	11.7	8.3	2.4	0.0	47.6	100.0	25.1	121

Notes:

1. See Table 4.3-3 for assumptions on gas compositions.
2. Correction is to assume that only air nitrogen is in the synthesis gas and that the reactor is adiabatic.

Table 4.3-5 Synthesis Gas Combustor Calculations

Operating Period	Average Relative Hour	AIT8775 SGC Exit O_2 M %	Calculated SGC Exit O_2 M %	Gas Analyzer LHV Btu/SCF	Energy Balance LHV[1] Btu/SCF	Combustor SO_2 AI534A ppm	Syngas Total Reduced Sulfur[2] ppm	Thermo. Equlibrium H_2S ppm
TC06-1	21	6.0	5.4	73	68	74	155	223
TC06-2	29	6.0	5.2	71	66	85	175	223
TC06-3	34	6.0	5.9	68	68	107	228	224
TC06-4	41	6.1	5.6	70	67	94	198	221
TC06-5	55	6.0	5.5	67	65	98	205	214
TC06-6	74	6.0	6.1	64	67	87	184	214
TC06-7	84	6.1	6.1	64	68	76	163	208
TC06-8	91	6.2	6.4	66	69	73	160	198
TC06-9	124	6.1	6.3	65	67	85	186	166
TC06-10	146	6.1	5.6	67	65	91	189	160
TC06-11	153	6.1	5.8	68	67	90	191	158
TC06-12	189	6.4	5.7	68	65	85	179	149
TC06-13	199	6.1	5.6	68	66	86	179	150
TC06-14	222	6.1	5.5	67	65	80	165	165
TC06-15	234	7.5	7.7	66	72	68	165	143
TC06-16	244	6.6	6.6	67	70	86	193	147
TC06-17	255	5.8	5.7	72	72	99	212	140
TC06-18	270	7.6	7.7	57	63	48	112	138
TC06-19	280	7.8	7.9	64	69	41	101	138
TC06-20	297	7.7	7.9	66	71	40	99	136
TC06-21	309	7.4	7.5	64	69	65	154	130
TC06-22	336	6.8	6.9	70	73	63	147	123
TC06-23	354	6.1	6.3	71	73	66	146	119
TC06-24	374	5.6	5.5	70	71	48	101	120
TC06-25	390	7.3	7.4	71	73	56	136	120
TC06-26	420	6.0	5.9	70	70	43	93	120
TC06-27	449	6.1	5.9	70	70	59	126	129
TC06-28	470	6.1	5.7	68	67	52	109	131
TC06-29	477	6.1	5.9	69	70	63	136	132
TC06-30	486	6.1	6.0	70	71	59	128	132
TC06-31	494	6.0	5.6	68	68	68	142	132
TC06-32	498	5.8	5.3	64	62	67	134	133

Notes:

1. Energy LHV calcualted assuming the sythesis gas combustor heat loss was 2.25 x 10^6 Btu/hr.
2. Synthesis gas total reduced sulfur (TRS) estimated from Synthesis gas combustor SO_2 analyzer data.

Table 4.3-5 Synthesis Gas Combustor Calculations (continued)

Operating Period	Average Relative Hour	AIT8775 SGC Exit O_2 M %	Calculated SGC Exit O_2 M %	Gas Analyzer LHV Btu/SCF	Energy Balance LHV[1] Btu/SCF	Combustor SO_2 AI534A ppm	Syngas Total Reduced Sulfur[2] ppm	Thermo. Equlibrium H_2S ppm
TC06-33	505	6.3	6.2	71	72	48	105	132
TC06-34	520	6.1	5.8	69	69	58	124	132
TC06-35	534	6.1	5.9	69	69	49	105	132
TC06-36	548	6.1	5.7	69	67	55	116	132
TC06-37	555	6.3	6.4	72	72	47	106	136
TC06-38	569	6.1	6.1	70	70	67	146	143
TC06-39	586	6.0	6.0	70	69	75	161	144
TC06-40	608	6.0	6.0	69	69	75	161	151
TC06-41	643	6.2	6.2	70	70	89	196	166
TC06-42	648	6.1	6.1	70	70	80	176	165
TC06-43	670	6.1	6.1	70	70	64	140	159
TC06-44	695	6.1	6.1	70	69	70	153	155
TC06-45	711	6.1	5.6	65	65	69	141	166
TC06-46	719	6.2	6.1	70	71	56	122	170
TC06-47	760	6.1	5.9	61	62	62	127	172
TC06-48	787	6.1	5.5	63	63	65	133	158
TC06-49	818	6.1	5.4	63	62	65	131	159
TC06-50	829	6.0	5.1	59	58	56	109	163
TC06-51	840	6.1	5.5	62	60	73	148	166
TC06-52	850	6.1	5.2	62	60	54	108	175
TC06-53	859	6.6	6.1	61	60	57	118	177
TC06-54	873	6.5	6.2	64	64	65	138	177
TC06-55	896	6.5	6.4	69	70	58	128	164
TC06-56	908	6.5	6.3	71	71	63	139	154
TC06-57	913	6.3	6.1	70	69	65	142	153
TC06-58	926	6.6	6.5	73	73	60	136	155
TC06-59	941	6.6	6.3	74	74	54	122	158
TC06-60	949	6.3	6.0	75	74	41	92	161
TC06-61	960	6.2	5.9	74	74	58	127	163
TC06-62	974	6.0	5.7	75	74	56	121	162
TC06-63	998	6.4	6.2	76	75	57	128	157
TC06-64	1016	6.1	5.9	77	77	54	120	154

Notes:

1. Energy LHV calcualted assuming the sythesis gas combustor heat loss was 2.25 x 10^6 Btu/hr.
2. Synthesis gas total reduced sulfur (TRS) estimated from Synthesis gas combustor SO_2 analyzer data.

Table 4.3-6 Ammonia & Hydrogen Cyanide Data

Operating Period	Relative Hour	Date	Time Start	Time End	NH_3 ppm	HCN ppm
	67	7/17/01	19:52	20:01	1,296	
	68	7/17/01	20:49	20:55		42.1
TC06-6	69	7/17/01	21:55	22:01	1,476	
TC06-6	70	7/17/01	22:30	22:36		51.4
TC06-6	71	7/17/01	23:33	23:41	1,770	
TC06-6	71	7/18/01	00:06	00:10		72.1
(1)	224	7/24/01	09:03	09:11	1,845	
(1)	225	7/24/01	09:34	09:39	1,910	
(1)	225	7/24/01	09:57	10:02	1,823	
(1)	225	7/24/01	10:20	10:24	1,770	
(1)	226	7/24/01	10:45	10:48		72.0
(1)	226	7/24/01	11:07	11:11		69.0
(1)	226	7/24/01	11:28	11:33		72.0
(1)	227	7/24/01	11:46	11:49		70.1

Note:1. Data obtained just after the end of Operating Period TC06-14.

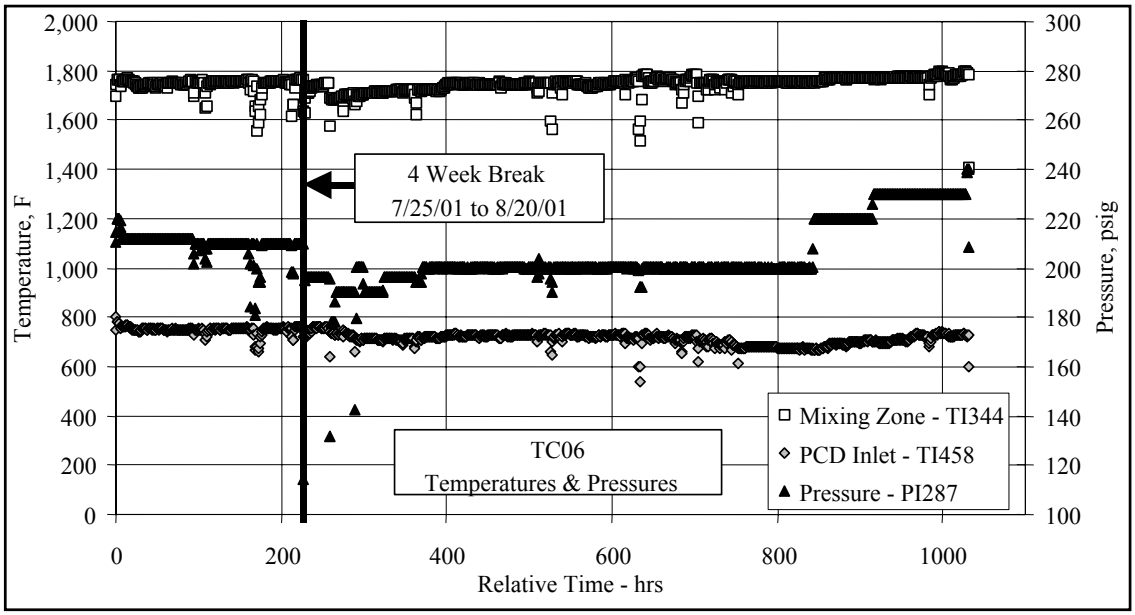

Figure 4.3-1 Temperatures & Pressures

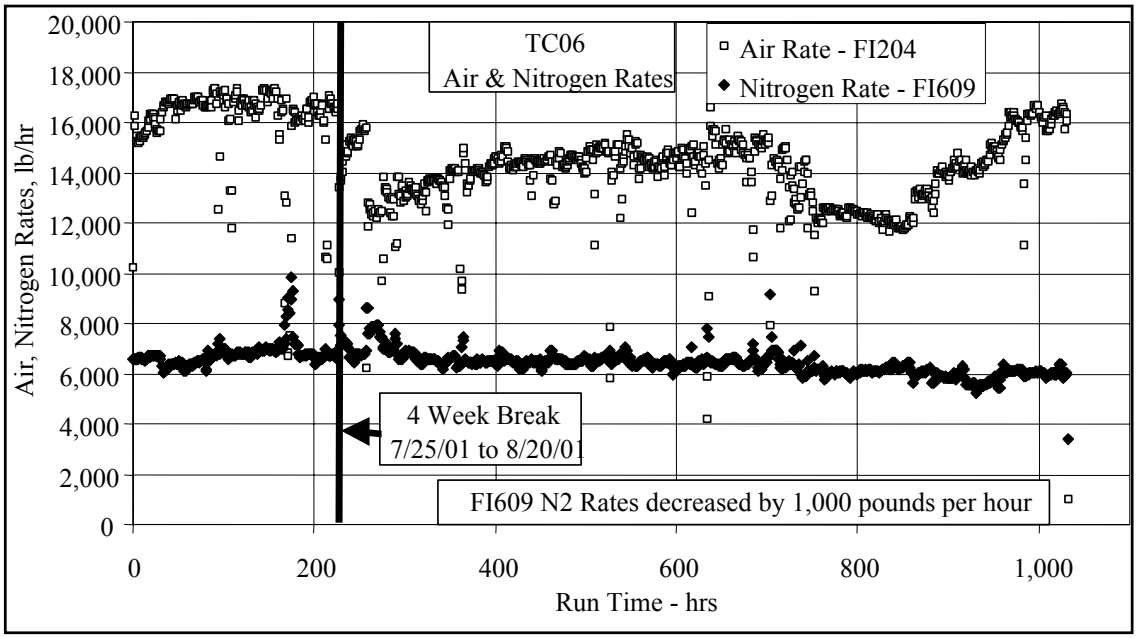

Figure 4.3-2 Air & Nitrogen Rates

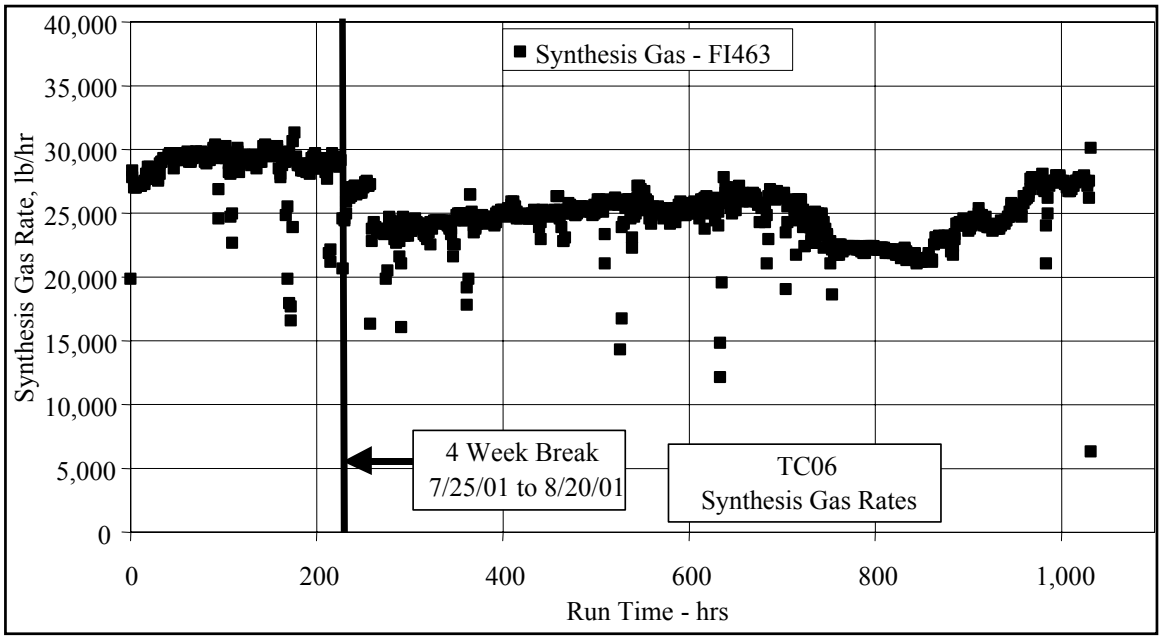

Figure 4.3-3 Synthesis Gas Rates

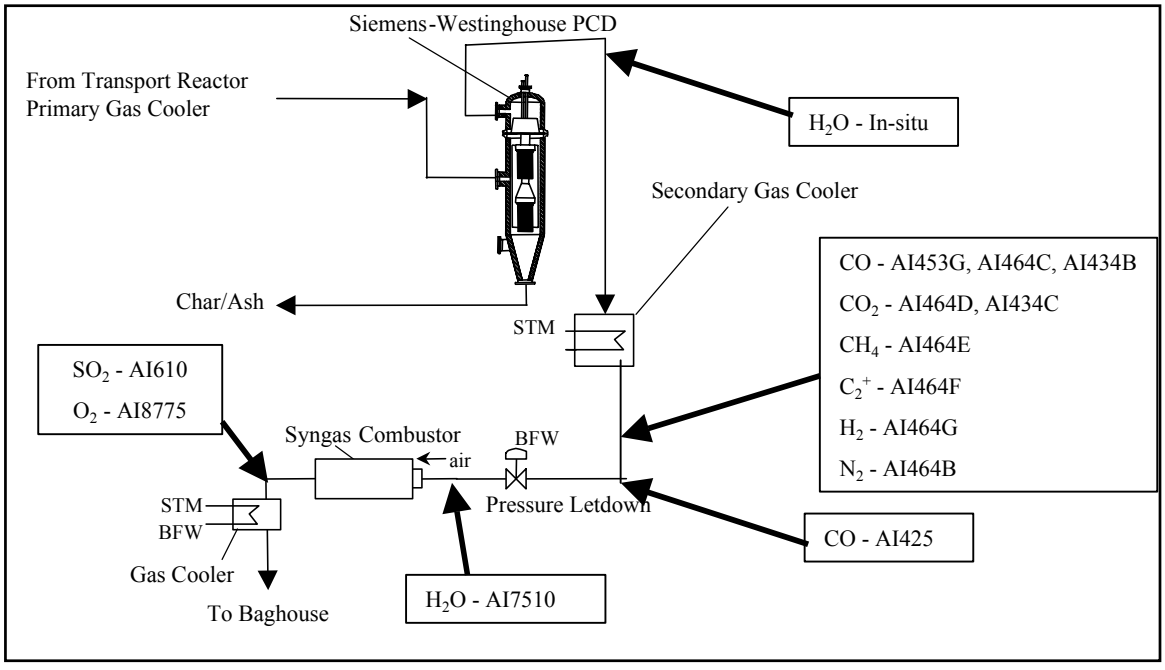

Figure 4.3-4 Gas Sampling Locations

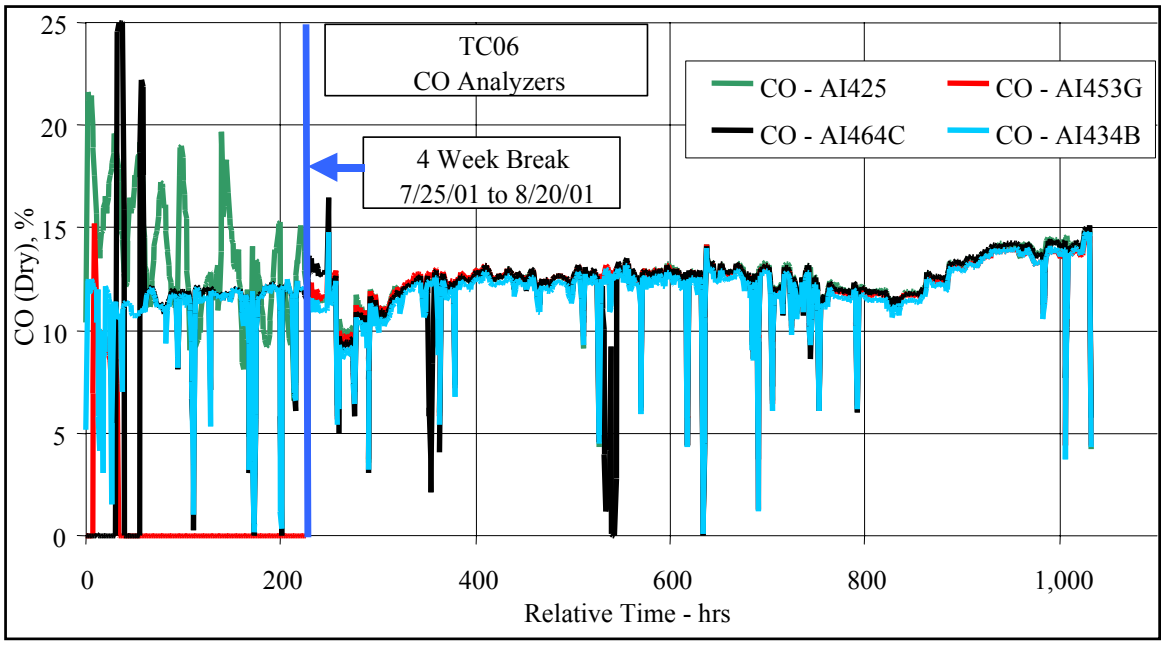

Figure 4.3-5 CO Analyzer Data

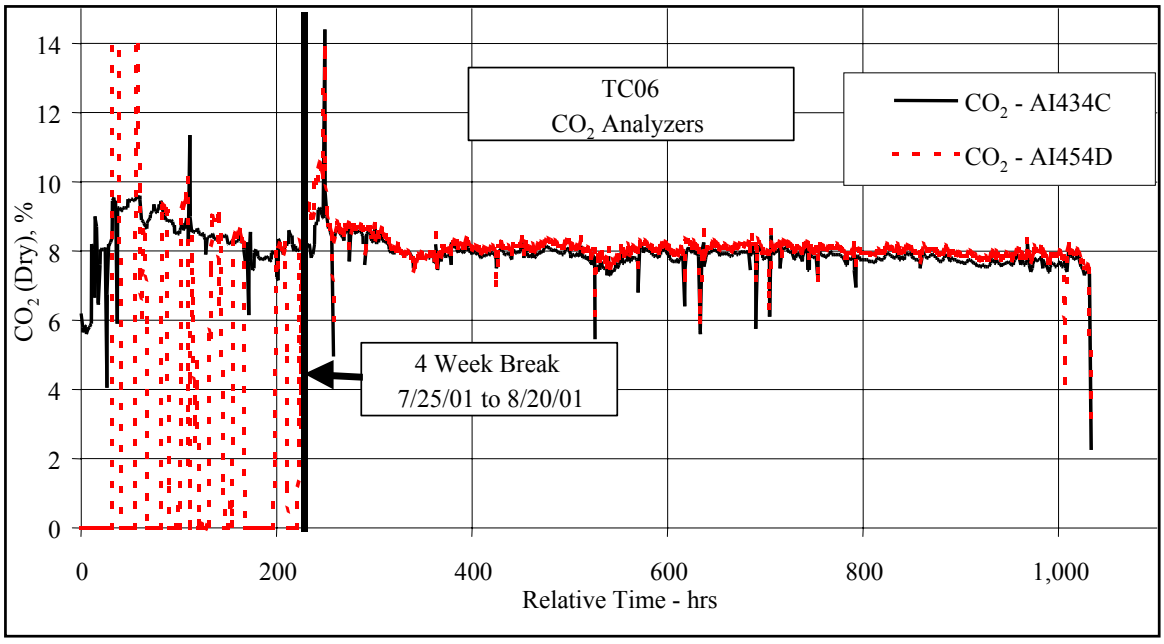

Figure 4.3-6 CO_2 Analyzer Data

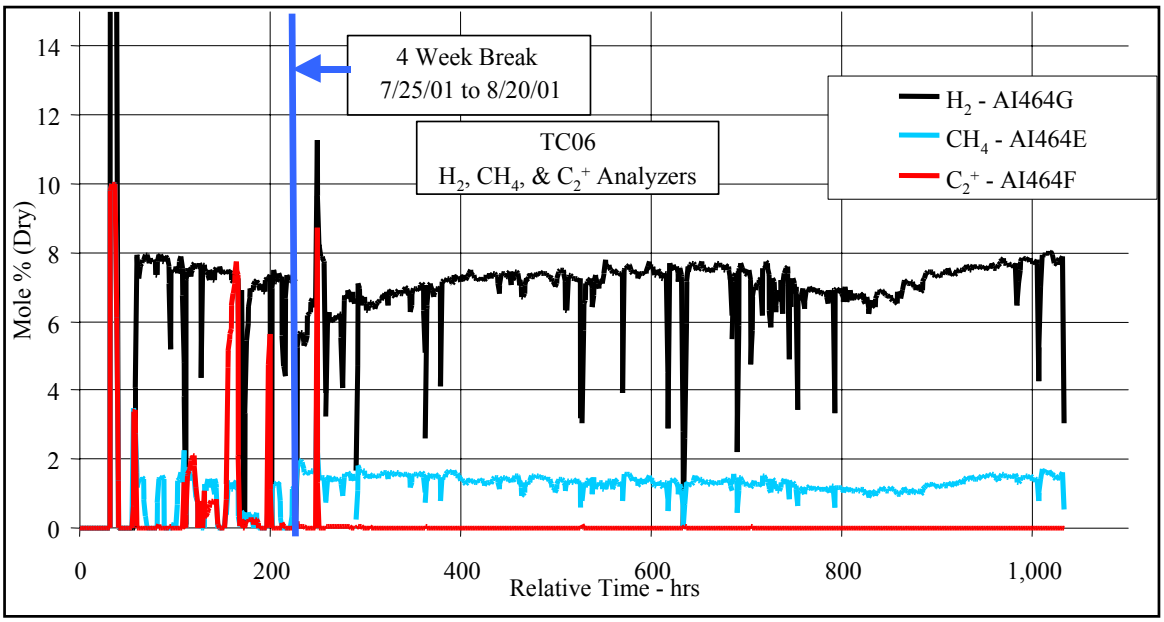

Figure 4.3-7 Analyzer H_2, CH_4, C_2^+ Data

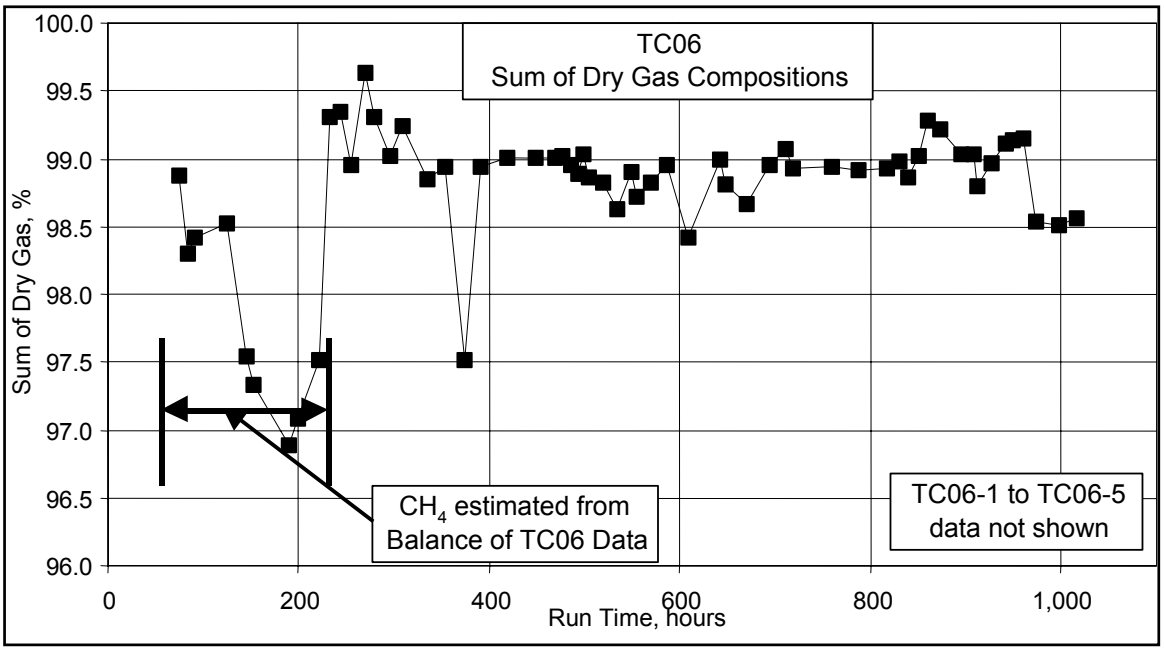

Figure 4.3-8 Sum of Dry Gas Compositions

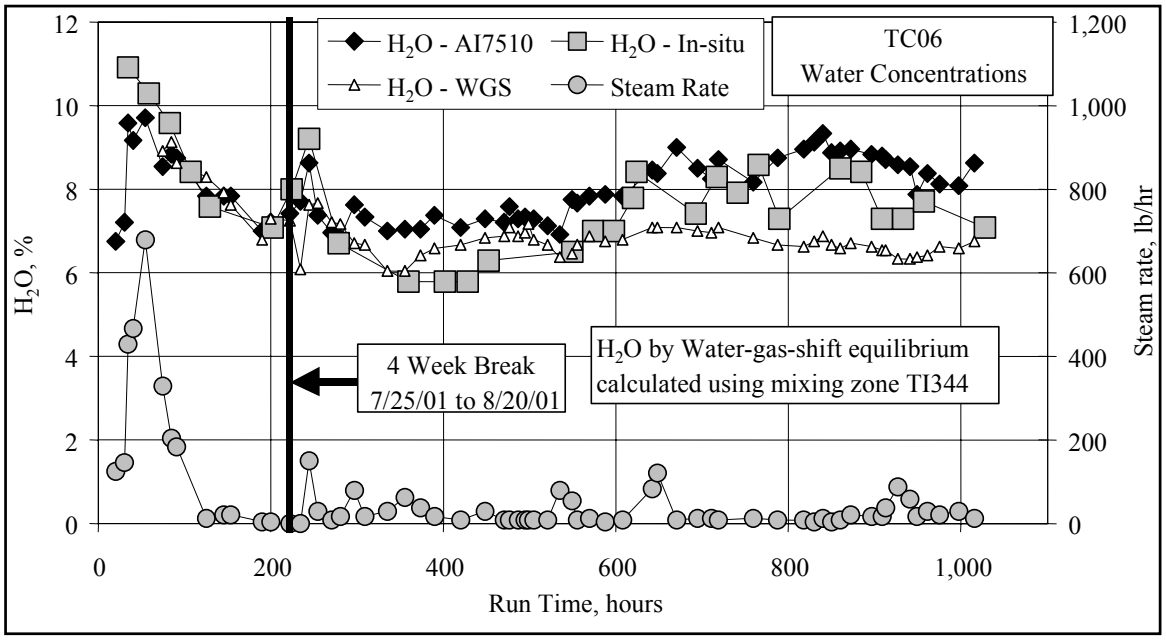

Figure 4.3-9 H_2O Data

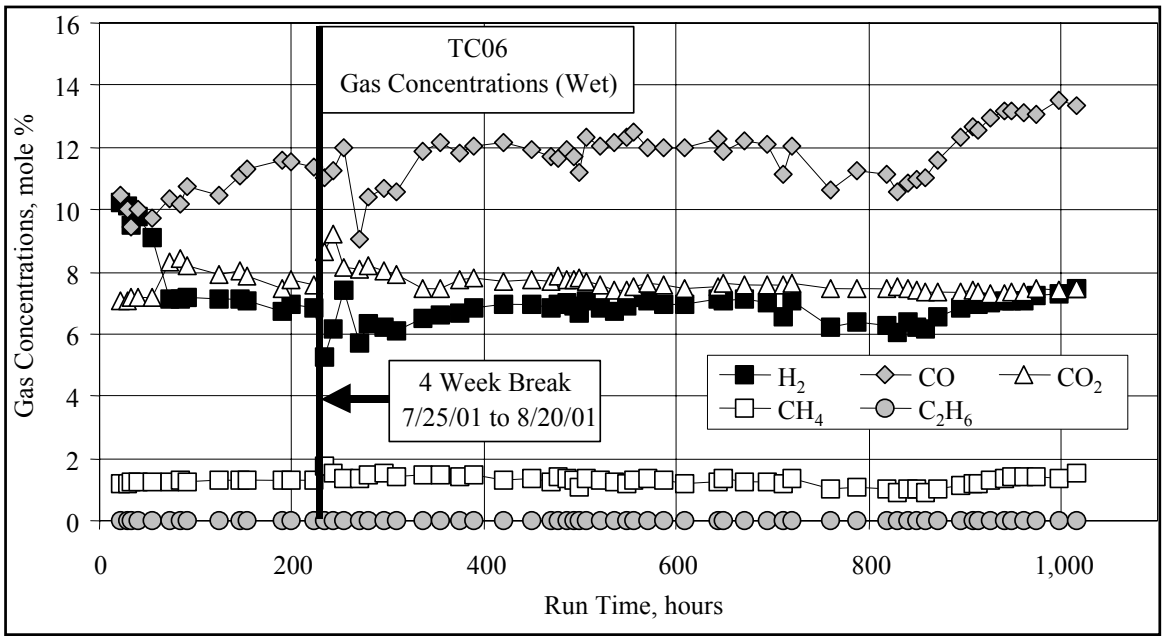

Figure 4.3-10 Wet Synthesis Gas Compositions

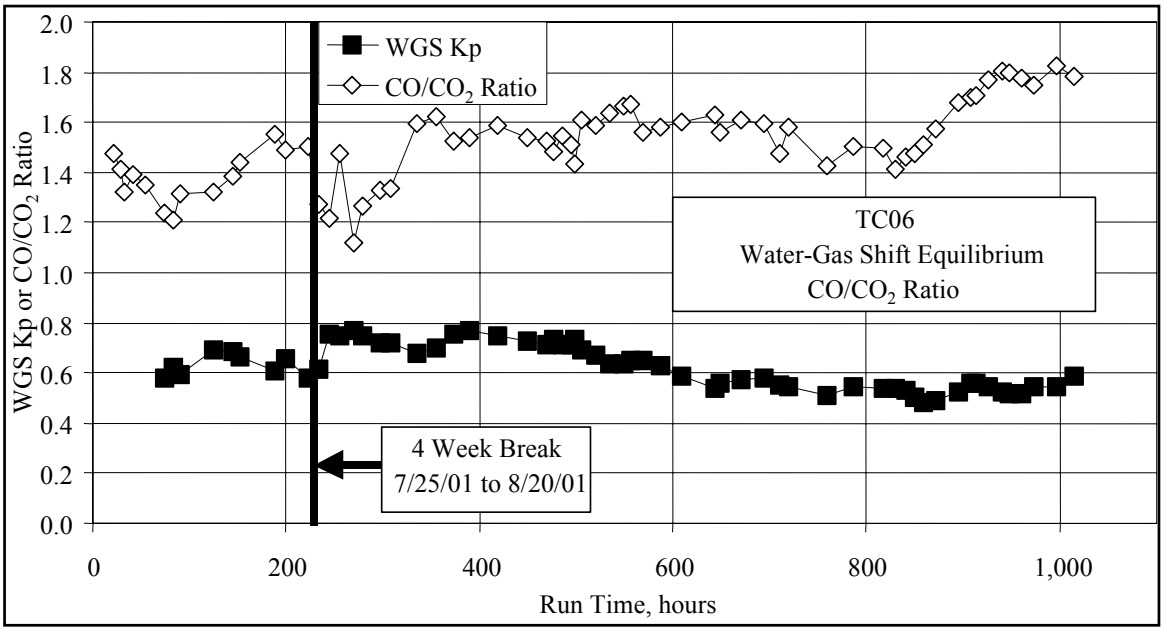

Figure 4.3-11 Water-Gas Shift Equilibrium and CO/CO_2 Ratio

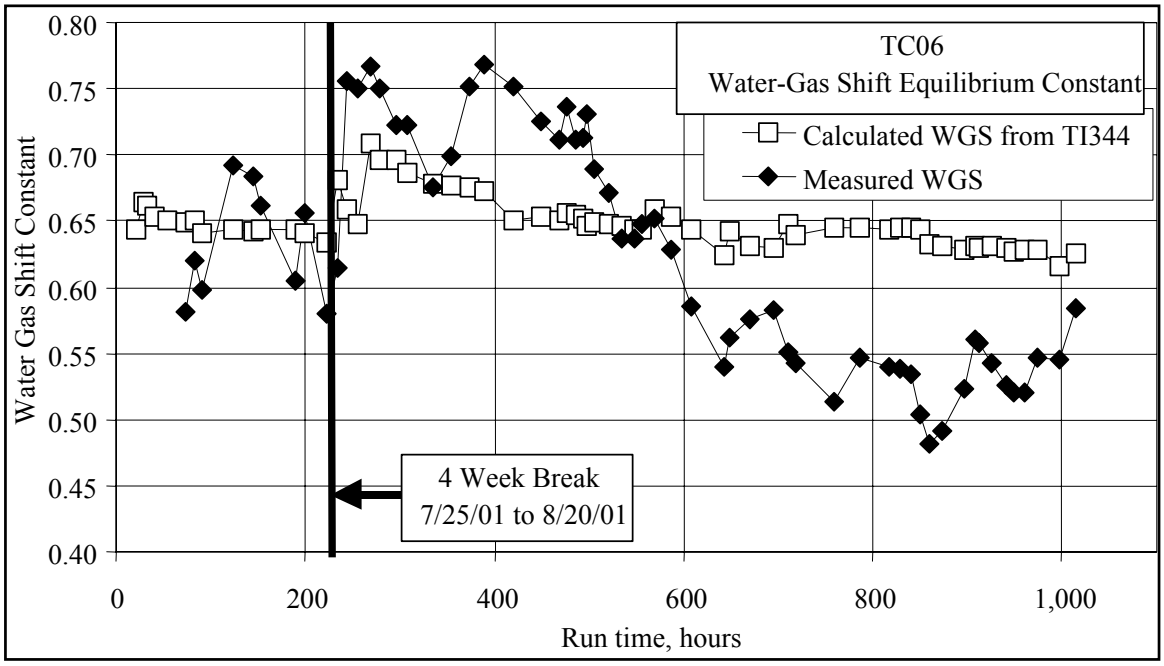

Figure 4.3-12 Water-Gas Shift Equilibrium

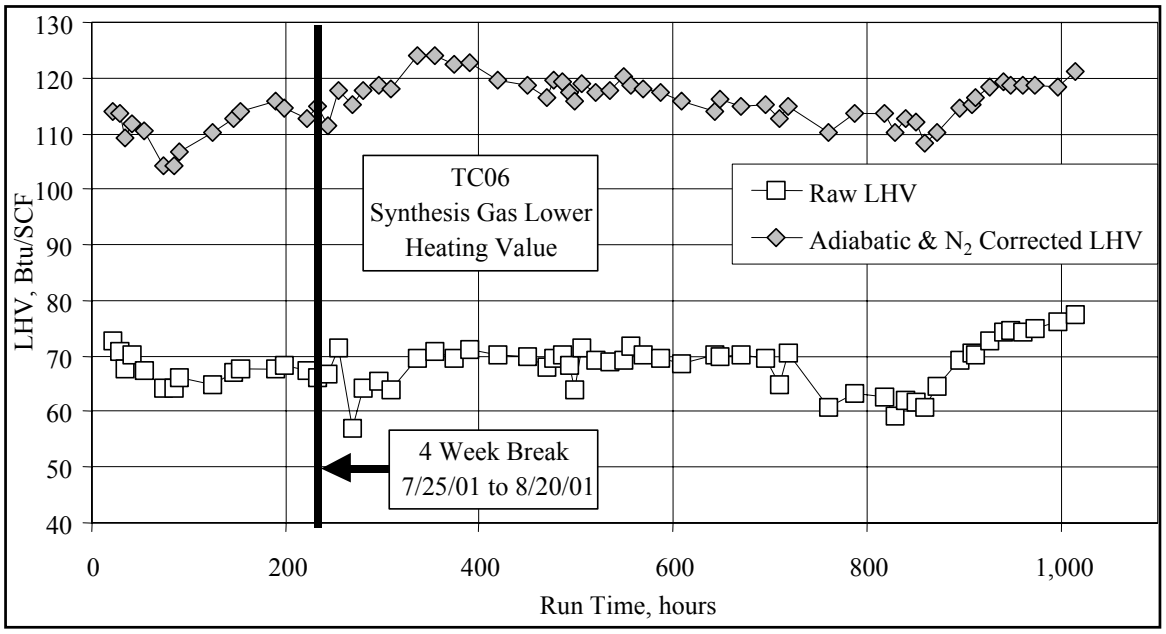

Figure 4.3-13 Synthesis Gas Lower Heating Values

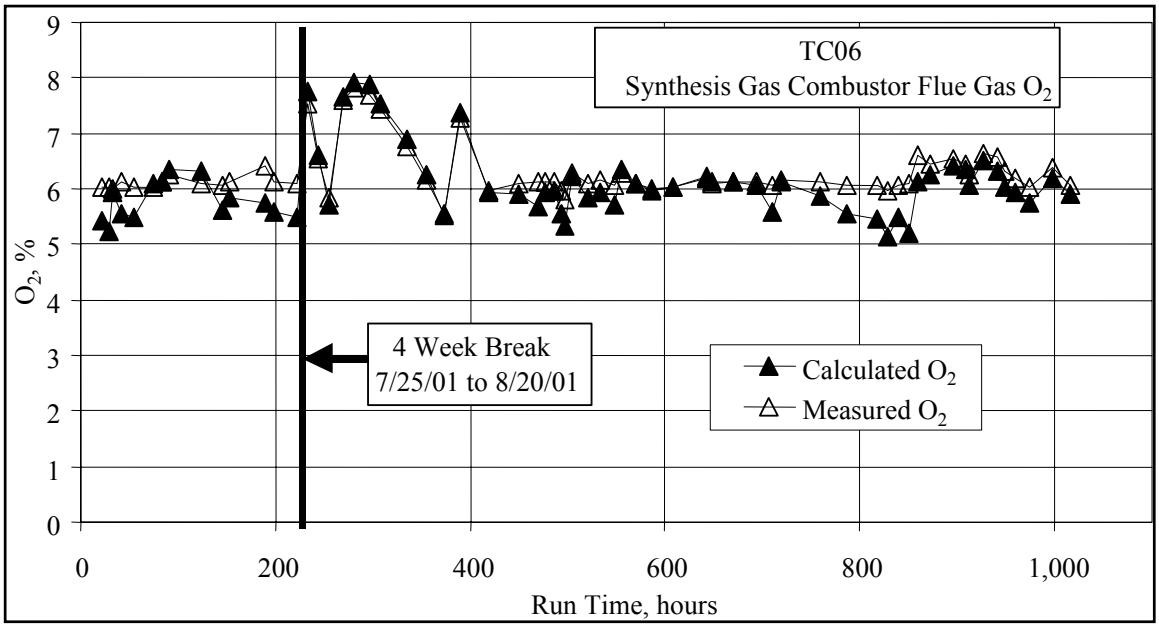

Figure 4.3-14 Synthesis Gas Combustor Outlet Oxygen

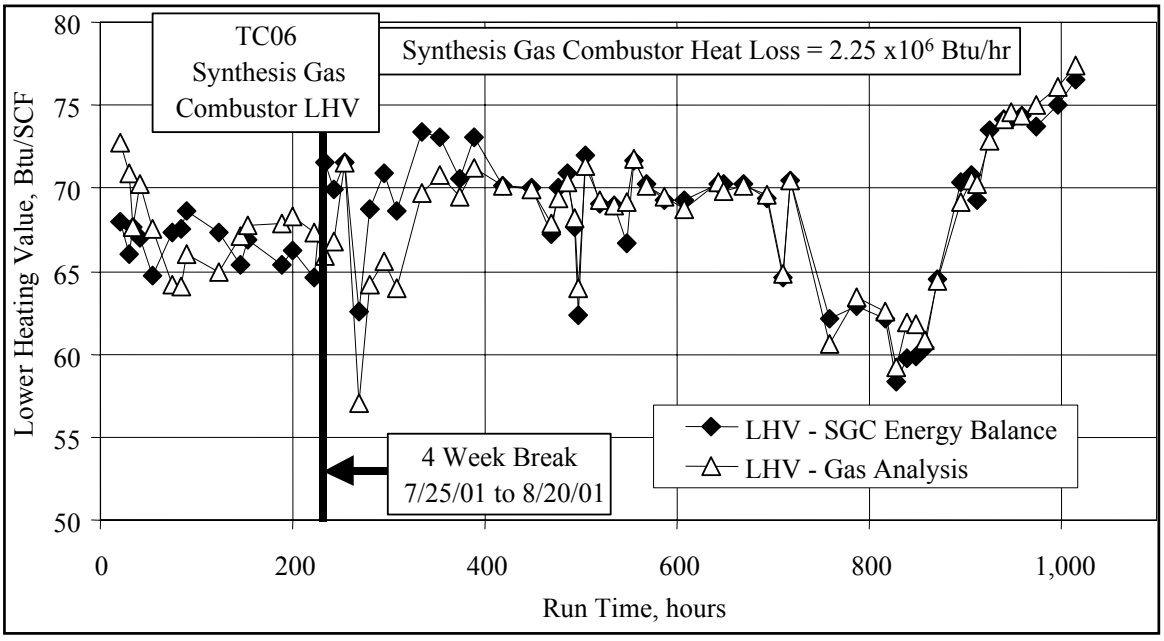

Figure 4.3-15 Synthesis Gas Combustor LHV

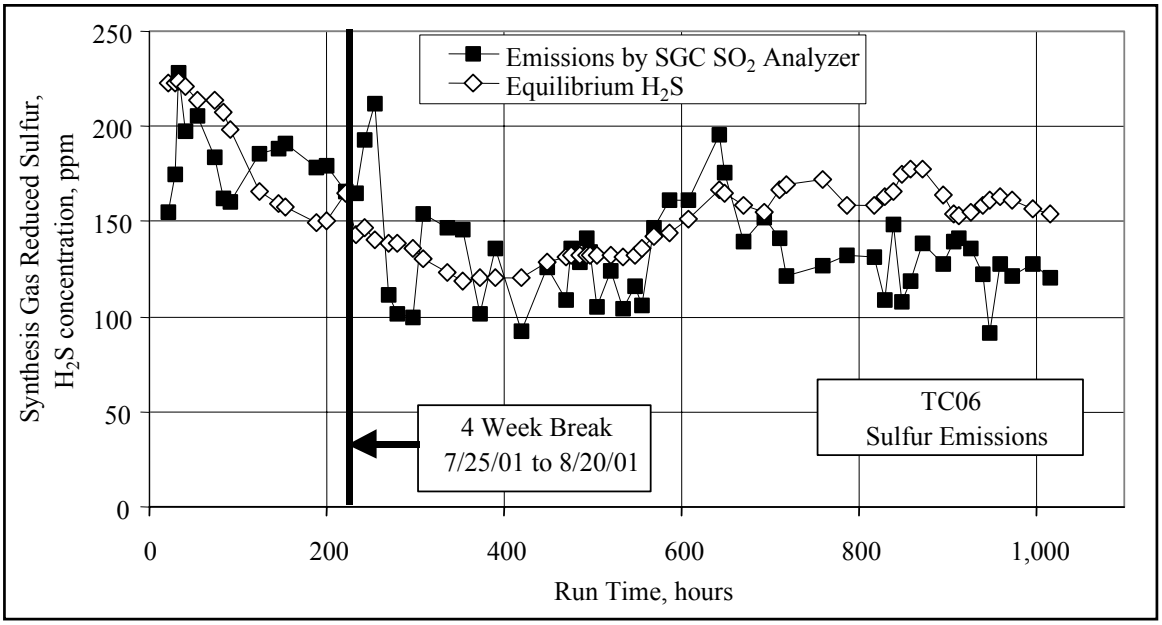

Figure 4.3-16 Sulfur Emissions

4.4 SOLIDS ANALYSES

During TC06, solid samples were collected from the fuel feed system (FD0210), the sorbent feed system (FD0220), the Transport Reactor standpipe, the standpipe spent solids transport system (FD0510), and the PCD fine solids transport system (FD0520). In situ solids samples were also collected from the PCD inlet. The sample locations are shown in Figure 4.4-1.

These solids were analyzed for chemical composition and particle size. This section will use the chemical analysis and particle size data to show:

- Chemical composition changes.
- Particle size and bulk density changes.

Table 4.4-1 shows the average coal composition for the samples analyzed during TC06. The first samples taken after both startups were excluded from the averages in Table 4.4-1 because the coal moisture level was low, probably due to air drying between testing. The coal carbon and moisture contents as sampled from FD0210 are shown in Figure 4.4-2. The average coal carbon was 57-weight percent and the average moisture was 21-weight percent.

Figure 4.4-3 shows the fuel sulfur and ash as sampled from the fuel feed system during TC06. The average values are provided in Table 4.4-1. The Powder River Basin (PRB) average coal sulfur was 0.26 percent and varied from 0.36 percent to 0.23 percent. The initial point and the first point after the 4-week shutdown are high due to the dryness of the stored coal. The coal ash was 5.2 percent and was very constant during TC06, with only a few points drifting up to 7 percent at around 740 hours.

The coal higher heating value (HHV) and lower heating value (LHV) are shown in Figure 4.4-4 and the TC06 average values are provided in Table 4.4-1. The LHV was determined from HHV by reducing the heating value to account for the coal moisture and hydrogen. The low moisture in the coal during the first several samples after the initial startup and the startup after the 4-week break caused the LHV and HHV to be higher than during the rest of the TC06. The HHV slightly increased during TC06 from 9,100 to 9,600 Btu/lb, and the LHV increased during TC06 from 8,500 to 9,000 Btu/lb.

Average values for TC06 coal moisture, carbon, hydrogen, nitrogen, sulfur, ash, oxygen, volatiles, fixed-carbon, higher heating value, lower heating value, CaO, SiO_2, Al_2O_3, Fe_2O_3, and MgO are provided in Table 4.4-1.

FD0220 was used during TC06 to feed Ohio Bucyrus limestone into the Transport Reactor. The average composition of the samples taken during TC06 are shown in Table 4.4-2 (two samples are excluded from the averages, as the samples contained a mixture of sand and limestone). The $CaCO_3$ and $MgCO_3$ contents are shown in the plot in Figure 4.4-5. The $CaCO_3$ average concentration was 76 percent, and the $MgCO_3$ average concentration was 17.7 percent. Both were constant during TC06.

The chemical compositions of the solid compounds produced by the Transport Reactor were determined using the solids chemical analysis and the following assumptions:

1. All carbon dioxide measured came from $CaCO_3$, hence moles CO_2 = moles $CaCO_3$.
2. All sulfide sulfur measured came from CaS.
3. All calcium not taken by CaS and $CaCO_3$ came from CaO.
4. All magnesium came from MgO.
5. Total carbon is measured, which is the sum of organic and inorganic (CO_2) carbon. The organic carbon is the total carbon minus the inorganic carbon (CO_2).
6. Inerts are the sum of the P_2O_5, K_2O, Na_2O, and TiO_2 concentrations.

It will be assumed that all iron in both the standpipe and PCD solids is in the form of Fe_2O_3 and not in the reduced forms of Fe_3O_4 or FeO. Thermodynamically, the mild-reducing conditions in the Transport Reactor should reduce all Fe_2O_3 to FeO. It is more likely that the iron in the standpipe and PCD solids is a mixture of Fe_2O_3 and Fe_3O_4. KBR data indicates that Fe_2O_3 is reduced to Fe_3O_4 at the temperatures and reducing conditions currently used in the Transport Reactor.

It will also be assumed that no FeS is formed in the Transport Reactor and that all the sulfur in the standpipe and PCD fines solids is as CaS. It is thermodynamically possible that some FeS is formed, but most of the captured sulfur should be in the form of CaS due to the larger amount of calcium than iron in the system.

Solids were sampled from the standpipe on a regular basis during TC06 except when the standpipe sampler was plugged between August 30 and September 5, 2001. Only one standpipe sample was taken during this period. Table 4.4-3 shows the results from the standpipe analyses. The standpipe solids are the solids that recirculate through the mixing zone, riser, and standpipe and change slowly with time, since a small amount of solids are taken out of the standpipe via FD0510 and ash gradually replaces sand. FD0510 was operated during TC06 to control the standpipe level. The flow rates for FD0510 and FD0520 solids are provided in Section 4.5.

On startup, the standpipe solids mainly contained SiO_2, with 80.4 percent at the start of TC06 and 81.7-percent SiO_2 after the 4-week break. This is because the starting bed material at both times was sand with 96.7-percent SiO_2 and 1.45-percent Al_2O_3. The standpipe did not contain sand at zero hours (July 15, 2001 01:00) and the restart (August 20, 2001, 16:00) since there were several periods of coal and coke breeze operation prior to the starting of the clock for the test. As the run progressed, the start-up sand was slowly replaced by CaO, Al_2O_3, Fe_2O_3, and other inerts until about 700 hours when the steady-state reactor solids composition was reached. This is shown in Figure 4.4-6. It took about 480 hours after the 4-week break to reach the steady-state solids composition. The SiO_2 content slowly decreases until about 700 hours. After 700 hours, the SiO_2 content was constant. Both the Al_2O_3 and the CaO increased to replace the SiO_2.

The standpipe solids data in Table 4.4-3 show that none of the volatile elements (sulfur and carbon) are present in very high concentrations after the unit is in operation for a few days. The organic carbon quickly decreases after startup to less than 0.5 percent. The high start-up carbon is probably due to the coke breeze used on startup. The heating value of the standpipe solids sampled was measured and was either 0.0 or <100 Btu/lb for all samples.

The standpipe $CaCO_3$ was at very low levels, less than 0.4 percent, indicating that there was very little inorganic carbon in the reactor. Since there was a much higher level of CaO than $CaCO_3$, all calcium that circulated in the standpipe was completely calcined. Since the standpipe calcium could come from either sorbent or fuel calcium, it is unknown whether the standpipe solids calcium was from sorbent or fuel calcium. Whatever the source, it was completely calcined. Long-term operation on a lower calcium fuel will be required to determine whether the standpipe accumulates fuel or sorbent calcium.

The sulfur level in the solids was very low, less than 0.5 percent as CaS for all of the samples. This indicates that all of the sulfur removed from the synthesis gas is removed via the PCD solids and is not accumulating in the reactor or leaving with the reactor solids. The MgO, Fe_2O_3, and other inerts contents are not included in the plot in Figure 4.4-9, but they follow the same trends as the CaO and Al_2O_3, that is, they are accumulating in the reactor as the sand is replaced by feed solids.

Figure 4.4-7 shows the organic carbon (total carbon minus CO2 carbon$_2$) for the PCD solids sampled from FD0520. The organic carbon content for every PCD fines sample analyzed is also shown in Table 4.4-4. Since FD0520 ran continuously during TC06, solid samples were taken often, with a goal of one sample every 4 hours. About half of the TC06 PCD solids that were sampled were analyzed. Solids recovered in situ during the PCD inlet particulate sampling were analyzed. The in situ carbon contents were compared with the FD0520 solids in Figure 4.4-7. The in situ organic carbon analyses shown in Figure 4.4-7 are only the ones in which both the total carbon and the CO_2 were measured. The in situ solids organic carbon analyses compared well with the FD0520 solids except for the two in situ analyses at hours 692 and 739, when the in situ samples were taken close to a period of coke breeze addition. Periods of low organic carbon content from hours 800 to 900 indicate excellent carbon conversion.

The organic carbon started the run at 46 percent, and decreased to between 25 and 32 percent (with two outliers) for the first 220 hours. After the 4-week break, the organic carbon increased to 40 percent until hour 330, and then gradually decreased to 10 percent at hour 860 as the coal rate was decreased. As the coal rate was increased at hour 900, the organic carbon increased from 10 to 42 percent by the end of TC06.

Figure 4.4-8 and Table 4.4-4 show the amounts of SiO_2 and CaO in the PCD solids as sampled from FD0520. Also, included in the plot on Figure 4.4-8, are the in situ solids concentrations for SiO_2 and CaO. The in situ samples showed good agreement with the FD0520 samples for the first 600 hours of TC06. For the last 400 hours of TC06 the in situ SiO_2 and CaO analyses were consistently lower than the FD0520 analyses. The SiO_2 concentration was between 16 and 28 percent for the first 300 hours of operation if the second analysis is ignored. The general trend of the SiO_2 concentration from hour 300 to 900 was a gradual rise in SiO_2 concentration from 15 to 27 percent. The increase in coal rate for the last 100 hours of TC06 then decreased

the SiO_2 concentration to 17 percent. The source of SiO_2 in the PCD fines could be from start-up sand, coal ash, or limestone.

The trends in the TC06 fine ash CaO concentrations were similar to the SiO_2 concentrations. The CaO concentration was between 10 and 25 percent for the first 300 hours of operation. The general trend of the CaO concentration from hour 300 to 900 was a gradual rise from 18 to 30 percent. The increase in coal rate for the last 100 hours of TC06 then decreased the CaO concentration to 20 percent. The source of CaO in the PCD fines could be from the coal ash or limestone.

Figure 4.4-9 and Table 4.4-4 show the amounts of $CaCO_3$ and CaS in the PCD solids as sampled from FD0520. Also, shown in Figure 4.4-9, are the in situ solids concentrations for $CaCO_3$ and CaS. The in situ samples $CaCO_3$ concentration was consistently about 0.5 to 2.0 percent higher than the $CaCO_3$ concentration from the samples collected at FD0520. The lower $CaCO_3$ concentration is a result of a lower measured CO_2 in the FD0520 solids. This may be due to the FD0520 samples being slightly degassed in the PCD or FD0520 by aeration or backpulse nitrogen. The in situ CaS and FD0520 CaS sample analyses agreed with each other during TC06.

For the first 220 hours, the $CaCO_3$ concentration was constant at between 6 and 9 percent if one sample is ignored. The $CaCO_3$ concentration then slowly decreased between 280 hours and 800 hours from 10 to 5 percent. The PCD fines calcination is defined as:

$$\%\ \text{Calcination} = \frac{\text{M}\%\ \text{CaO}}{\text{M}\%\ \text{CaO} + \text{M}\%\ \text{CaCO}_3} \qquad (1)$$

The PCD fines calcination is shown in the plot in Figure 4.4-10. The PCD fines calcination increased between hours 240 and 800 from about 80 to 90 percent. From hours 860 to 977, the PCD fines calcination decreased down to 82 percent. The data does not indicate 80-percent limestone calcination since the calcium in the PCD fines comes from both the PRB ash and the limestone fed as sorbent. The percent limestone calcination is compared with the CO_2 partial pressure in Section 4.5.

The PCD fines CaS concentrations shown in Figure 4.4-9 varied from 3.5 percent to nearly 0.0 percent with no real pattern. This indicates a large variation of sulfur removal during TC06. The calcium sulfation is defined as:

$$\%\text{Sulfation} = \frac{\text{M}\%\text{CaS}}{\text{M}\%\text{CaO} + \text{M}\%\text{CaCO}_3 + \text{M}\%\text{CaS}} \qquad (2)$$

The PCD fines sulfation was below 15 percent for all of TC06 and usually below 10 percent indicating poor calcium utilization. Again, the calcium in the PCD fines came from both the sorbent and the PRB ash.

Table 4.4-4 provides the PCD fines compositions for the samples collected in FD0520. The consistency is excellent in that the totals add up to between 96.0 and 104.3 percent. Additional components in Table 4.4-4, other than those shown in the plot in Figures 4.4-7, -8, and -9, are

MgO, Fe_2O_3, and Al_2O_3. The MgO concentration was between 5 and 8 percent during TC06. The Fe_2O_3 concentration was between 2.6 and 4.4 percent. The Al_2O_3 concentration was between 6 and 11 percent. Also given on Table 4.4-4 are the HHV, LHV, and volatiles for the PCD gasification ash (fines). As expected, the trend of heating values follows the carbon content of the PCD fines.

Nine FD0510 solid samples were taken during TC06, but they were not analyzed because the standpipe samples should give a more accurate view of the circulating solids composition.

FD0510 samples were taken while the reactor was being drained of solids on September 24 and 25, 2001, after TC06 testing was complete. Table 4.4-5 provides analyses of six samples collected from FD0510 while the reactor was being drained of solids. The main component was SiO_2 at 32 to 47 percent. The solids sampled first, shown in Table 4.4-5, are solids from the bottom of the reactor. The six samples do not indicate that any of the components were being segregated at the top or bottom of the reactor.

The Sauter mean diameter (SMD) and mass mean diameter (D_{50}) particle size of the coal feed to the Transport Reactor in TC06 are shown in the plot on Figure 4.4-11. The coal SMD particle size varied a lot during the first 100 hours of operation between 160 and 350 μm. After hour 110, the coal became finer and was between 125 and 175 μm SMD. The period from hour 150 to hour 300 was a period of numerous coal trips which coincided with the coal SMD diameter being less than 175 μm. At hour 260, the SMD increased to about 200 μm and was steady at 200 μm, until hour 401, when it decreased to about 175 μm. The particle size was then constant between 150 and 210 μm until hour 580. At hour 600, the SMD decreased to 100 microns, with one sample as low as 90 μm. The period from hour 600 to hour 750 was a period of numerous coal trips which also coincided with fine coal fed to the reactor. The particle size then increased to 225 μm at hour 800. The SMD particle size was then steady between 175 and 250 μm from hour 800 until the end of TC06. This was a period of only one coal trip.

The D_{50} was 50 to 100 μm larger than the SMD during TC06.

A measure of the amount of fines in the coal would be the percent of the smallest size fraction present. High fines content could result in increased number of coal feeder outages due to coal feeder plugging caused by the packing of coal fines. To show the level of fines in the coal feed, the percent of ground coal less than 45 μm is plotted in Figure 4.4-12. The fines percent was 3 to 14 percent during the first 100 hours of testing. The coal fines then increased to between 20 and 30 percent from hours 150 to 200. This was a period of numerous coal trips. After the 4-week break, the coal fines decreased down to between 5 and 10 percent from hours 278 to 361. The fines were at 20 to 25 percent around hour 440. From hours 500 to 650, the fines were at 5 to 15 percent. The coal fines spiked up again at hour 645 and increased up to 44 percent at hour 750. During this period of high coal fines, there were numerous coal trips. The fines percent then decreased down to below 15 percent at hour 790. The coal fines remained below 15 percent for the remainder of TC06. This final period of low coal fines was during a period of only one coal feeder trip.

The SMD and D_{50} of the solids sampled from the sorbent feeder FD0220 are shown in the plot in Figure 4.4-13. The SMD was usually between 10 to 20 μm for the first 260 hours of TC06. Between hours 361 and 500, the sorbent particle size averaged about 10 μm. From hours 500 to 750, the particle size was between 7 and 15 μm SMD with one sample above 20 μm. Around hour 800, the SMD increased to 20 μm for three samples. After hour 810, the particle size was between 4 and 12 μm. The D_{50} was consistently higher than the SMD. The high spikes of SMD result in high spikes of 50 and 60 μm D_{50}.

The TC06 standpipe solids particulate sizes are shown in Figure 4.4-14. The particle size of the solids increased as the start-up sand was replaced by CaO and Al_2O_3. The SMD of the reactor solids increased from 150 to 175 μm during the first 220 hours of operation. After the reactor solids were replaced by fresh sand during the 4-week break, the reactor solids SMD fell to 140 μm. From hours 200 to 700 the reactor solid SMD increased from 140 to 180 μm. After the reactor solids concentration stopped changing at hour 700, the SMD was between 160 and 180 μm. The D_{50} was consistently about 20 μm less than the SMD.

Figure 4.4-15 shows the plot of the SMD and D_{50} for the PCD solids sampled from FD0520. The PCD fines SMD was fairly constant for the first 500 hours of TC06 at about 10 μm. From hours 500 to 800, the SMD slowly increased from 10 to 13 microns. When the coal rate was increased, the SMD then slowly decreased back down to about 11 μm. The D_{50} showed the same trend as the SMD, starting the run at 15 μm, then increasing to 20 μm, and then falling back down to 15 μm.

Figure 4.4-16 shows a plot of all the solids SMD particle size. The Transport Reactor is fed 300 μm coal and 10 μm limestone and produces 150 μm reactor solids and 10 μm PCD fines. The coal, reactor solids, and PCD fines particle sizes were essentially constant during TC06, while the limestone particle size was slowly decreasing.

The TC06 standpipe bulk densities are shown in Figure 4.4-17. The bulk density of the solids decrease slightly as the start-up sand is replaced by CaO and Al_2O_3. The standpipe solids bulk density decreased from 90 to 85 lb/ft^3 during the first 220 hours of operation. After the reactor solids were replaced by fresh sand during the 4-week break, the reactor solids bulk density returned to about 90 lb/ft^3. From hours 220 to 700, the bulk density decreased from 90 lb/ft^3 per cubic foot to between 80 and 85 lb/ft^3. The bulk density then remained at between 80 and 85 lb/ft^3 until the end of TC06 and after the reactor solids had reached the steady-state composition at hour 700.

Figure 4.4-17 is a plot of the bulk density for the PCD solids sampled from FD0520. For the first 200 hours, the bulk density of the PCD fines was about 20 lb/ft^3. After the 4-week break the PCD fines bulk solids were constant at between 20 and 30 lb/ft^3 from hours 220 to 724. During the period of low coal-feed rate, the bulk density increased to nearly 30 lb/ft^3. When the coal-feed rate was increased, the bulk density decreased to 25 lb/ft^3.

Table 4.4-1 Coal Analyses

	Value	Standard Deviation
Moisture, Wt%	20.93	1.08
Carbon, Wt%	57.02	1.04
Hydrogen[1], Wt%	3.74	0.12
Nitrogen, Wt%	0.66	0.05
Sulfur, Wt%	0.26	0.02
Ash, Wt%	5.23	0.45
Volatiles, Wt%	37.39	8.83
Fixed Carbon, Wt%	36.46	9.44
Higher Heating Value, Btu/lb	9,391	129
Lower Heating Value, Btu/lb	8,828	133
CaO, Wt %	1.27	0.13
SiO_2, Wt %	1.66	0.24
Al_2O_3, Wt %	0.88	0.10
MgO, Wt %	0.28	0.02
Fe_2O_3, Wt %	0.33	0.06
Ca/S, mole/mole	2.83	0.29
Fe/S, mole/mole	0.51	0.07

1. All analyses are as sampled at FD0210.
2. Hydrogen in coal is reported separately from hydrogen in moisture.
3. Samples AB08556 and AB08558 excluded.

Table 4.4-2 Limestone Analysis

Compound	Weight %	Standard Deviation
$CaCO_3$	75.95	1.29
$MgCO_3$	17.66	0.76
$CaSO_4$	0.42	0.33
SiO_2	2.58	0.32
Al_2O_3	0.93	0.27
Other Inerts[2]	0.65	0.39
H_2O	0.15	0.04
Total	98.34	

1. All analyses are as sampled at FD0220.
2. Other inerts consist of Fe_2O_3, P_2O_5, Na_2O, K_2O, and TiO_2.

Table 4.4-3 Standpipe Analysis

Sample Number	Sample Date & Time	Sample Run Time Hours	SiO_2 Wt. %	Al_2O_3 Wt. %	Fe_2O_3 Wt. %	Other Inerts[1] Wt. %	$CaCO_3$ Wt. %	CaS Wt. %	CaO Wt. %	MgO Wt. %	Organic Carbon Wt. %	Total Wt. %
AB08565	7/15/01 8:00	7	80.4	3.2	1.0	1.3	0.0	0.2	3.1	0.6	2.9	92.7
AB08566	7/15/01 12:00	11	86.9	4.2	1.4	1.1	0.1	0.2	3.9	0.7	1.6	100.2
AB08567	7/15/01 20:30	20	85.5	4.4	1.5	1.2	0.2	0.3	4.7	0.8	2.0	100.6
AB08568	7/16/01 4:00	27	84.9	6.0	1.5	1.3	0.2	0.2	4.5	0.8	0.5	100.0
AB08577	7/16/01 12:00	35	81.6	5.4	1.7	1.6	0.3	0.1	7.3	1.2	0.6	99.8
AB08578	7/16/01 20:00	43	82.8	5.1	2.0	1.4	0.2	0.0	7.3	1.2	0.4	100.3
AB08613	7/17/01 12:00	59	76.5	7.4	1.6	1.8	0.1	0.0	10.2	1.6	0.2	99.3
AB08615	7/18/01 4:00	75	66.7	7.5	2.1	2.1	0.2	0.0	17.6	2.6	0.1	99.0
AB08639a	7/18/01 12:00	83	67.2	7.2	2.7	2.1	0.1	0.2	17.2	2.6	0.4	99.6
AB08639	7/18/01 12:00	83	67.7	7.3	2.7	2.3	0.0	0.0	17.0	2.6	0.2	99.7
AB08640	7/18/01 20:00	91	70.0	6.8	2.8	2.0	0.2	0.3	15.7	2.4	0.2	100.4
AB08641	7/19/01 4:00	99	74.3	7.8	2.5	2.2	0.0	0.0	11.6	1.7	0.3	100.2
AB08667	7/19/01 20:00	115	70.1	8.1	2.3	2.3	0.0	0.0	14.4	2.1	0.1	99.5
AB08683	7/20/01 12:00	131	68.0	8.2	2.7	2.4	0.0	0.0	16.4	2.2	0.4	100.2
AB08684	7/21/01 12:45	156	65.8	9.2	2.8	2.4	0.0	0.0	16.7	2.2	0.1	99.2
AB08685	7/22/01 12:00	179	59.8	9.4	3.3	2.5	0.1	0.0	21.3	2.8	0.4	99.6
AB08686	7/22/01 20:00	187	62.8	8.8	3.9	1.9	0.0	0.0	20.1	2.5	0.2	100.2
AB08687	7/23/01 4:00	195	60.5	9.0	4.1	2.0	0.0	0.0	21.8	2.7	0.2	100.3
AB08725	7/23/01 12:01	203	64.0	10.1	4.2	2.5	0.0	0.0	17.7	2.3	0.3	101.2
AB08827	8/21/01 8:00	243	81.7	4.7	3.9	1.7	0.2	0.1	8.5	1.3	1.0	103.0
AB08834	8/21/01 20:00	255	81.2	4.2	1.4	1.6	0.3	0.0	9.6	1.4	0.2	99.8
AB08847	8/23/01 0:00	266	79.6	5.2	1.4	1.5	0.2	0.0	9.2	1.3	1.3	99.7
AB08859	8/23/01 12:00	278	73.7	6.5	1.7	1.8	0.3	0.1	12.6	1.9	8.9	107.4
AB08861	8/23/01 20:00	286	76.6	6.1	2.0	1.9	0.3	0.1	9.5	1.4	1.5	99.4
AB08874	8/25/01 20:00	321	73.1	7.4	1.5	2.3	0.3	0.1	9.9	1.5	0.5	96.5
AB08878	8/26/01 20:00	345	72.6	6.9	1.8	2.1	0.3	0.0	13.7	2.0	0.3	99.7
AB08944	8/27/01 8:00	357	70.0	8.6	2.1	2.5	0.3	0.4	13.1	1.9	0.4	99.3
AB08958	8/28/01 16:00	385	68.8	9.5	2.1	2.6	0.3	0.1	14.3	2.0	0.6	100.3
AB08979	8/29/01 20:00	413	64.1	9.0	2.3	2.5	0.3	0.3	18.7	2.4	0.1	99.8
AB09006	8/30/01 20:00	437	60.4	9.9	2.5	2.8	0.2	0.2	20.7	2.6	0.8	100.1
AB09108	9/5/01 20:00	581	48.9	11.3	2.9	3.1	0.3	0.0	29.1	3.5	0.4	99.5
AB09191	9/11/01 4:00	709	42.1	14.6	3.8	3.0	0.2	0.3	31.3	4.5	0.0	99.8
AB09206	9/11/01 16:00	721	39.2	13.3	4.6	2.6	0.3	0.1	34.1	5.0	1.2	100.5
AB09242	9/13/01 4:00	757	39.0	13.3	4.6	2.7	0.3	0.5	33.9	4.9	0.9	100.1
AB09247	9/13/01 20:00	773	33.4	12.0	4.4	2.9	0.5	0.3	41.5	5.3	0.5	100.7
AB09274	9/14/01 8:00	785	36.2	16.0	4.1	3.1	0.3	0.2	36.0	4.7	0.1	100.7
AB09277	9/15/01 8:00	809	36.2	12.1	3.8	3.1	0.4	0.3	39.8	4.7	0.1	100.5
AB09283	9/16/01 8:00	833	33.3	12.4	3.6	3.1	0.4	0.2	41.6	5.3	0.1	100.0
AB09321	9/17/01 12:00	861	30.5	13.5	3.6	3.2	0.4	0.4	42.5	5.7	0.0	99.7
AB09345	9/18/01 16:00	889	32.4	13.3	3.8	3.3	0.3	0.2	41.6	5.1	0.3	100.4
AB09353	9/19/01 16:00	913	33.4	14.2	3.7	3.6	0.3	0.2	39.5	5.3	0.1	100.3
AB09376	9/20/01 20:00	941	32.4	14.4	3.8	3.4	0.3	0.2	39.9	5.5	0.1	100.1
AB09425	9/21/01 20:00	965	34.4	14.7	3.9	3.7	0.2	0.3	37.1	5.2	0.2	99.7
AB09427	9/22/01 20:00	989	38.2	15.5	4.0	4.0	0.3	0.2	32.8	4.8	1.3	101.1
AB09433	9/23/01 20:00	1013	36.5	15.4	3.8	3.7	0.3	0.1	34.4	4.8	0.3	99.3
AB09453	9/24/01 12:00	1029	36.3	15.2	3.9	3.7	0.3	0.1	35.7	4.9	0.4	100.3

1. Other inserts consist of P_2O_5, Na_2O, K_2O, and TiO_2.

Table 4.4-4 PCD Fines From FD0520

Sample Number	Sample Date & Time	Sample Run Time Hours	SiO_2 Wt. %	Al_2O_3 Wt. %	Fe_2O_3 Wt. %	Other Inerts[1] Wt. %	$CaCO_3$ Wt. %	CaS Wt. %	CaO Wt. %	MgO Wt. %	Organic C ($C\text{-}CO_2$) Wt. %	Total Wt. %	HHV Btu/lb.	LHV Btu/lb.
AB08559	7/15/01 8:00	7	19.1	6.5	3.3	1.7	7.8	3.4	10.5	3.6	46.3	102.2	6,888	6,815
AB08560	7/16/01 0:01	23	35.9	6.8	2.6	1.8	4.4	2.2	7.9	2.5	40.1	104.3	5,490	5,433
AB08561	7/16/01 8:00	31	28.0	8.0	2.9	2.2	7.2	2.8	13.9	4.3	30.7	100.0	4,797	4,749
AB08580	7/16/01 16:00	39	22.9	9.5	3.7	2.6	7.3	1.9	23.1	5.6	25.4	101.8	3,855	3,806
AB08582	7/17/01 8:00	55	21.3	9.7	3.6	2.5	7.7	0.6	24.5	5.6	26.4	101.8	3,605	3,554
AB08618	7/18/01 8:00	79	19.1	8.5	3.0	2.0	8.0	1.0	22.6	5.5	30.1	99.9	4,425	4,369
AB08669	7/19/01 8:00	103	16.5	8.4	3.4	2.1	8.9	1.0	25.1	6.0	28.5	100.0	4,313	4,261
AB08671	7/20/01 8:00	127	17.3	8.3	3.5	2.1	8.6	1.1	23.6	5.7	32.0	102.3	4,442	4,384
AB08706	7/21/01 10:00	153	23.1	8.8	3.4	2.1	7.6	1.1	23.8	5.6	25.0	100.4	3,782	3,735
AB08708	7/22/01 8:00	175	16.6	7.4	3.1	1.9	6.6	2.8	10.0	3.2	49.9	101.3	7,408	7,341
AB08709	7/22/01 16:00	183	19.1	9.8	4.0	2.1	5.8	2.7	11.9	3.3	43.4	102.1	6,359	6,290
AB08710	7/23/01 8:00	199	19.7	9.3	4.0	2.4	8.1	1.5	23.4	5.6	26.6	100.5	4,041	3,996
AB08729	7/24/01 8:00	223	21.3	9.4	4.4	2.3	6.8	1.3	20.4	5.1	30.1	101.0	4,353	4,296
AB08816	8/21/01 8:00	243	23.7	8.9	3.2	2.3	7.2	0.7	20.0	5.3	27.9	99.3	4,164	4,105
AB08835	8/21/01 19:00	254	23.8	7.5	2.8	2.4	6.5	0.5	21.1	4.9	32.8	102.4	4,437	4,387
AB08862	8/23/01 16:00	282	14.4	6.2	2.5	2.0	10.0	1.1	20.0	5.1	39.1	100.3	5,899	5,837
AB08886	8/25/01 16:00	317	13.6	6.2	2.2	1.7	9.4	1.8	18.7	5.3	40.2	99.0	6,109	6,049
AB08889	8/26/01 16:00	341	14.6	5.8	2.0	1.7	8.4	1.7	19.7	5.0	40.1	99.0	5,856	5,798
AB08890	8/27/01 0:00	349	16.5	6.8	2.2	1.6	8.3	1.7	18.1	5.1	40.6	101.0	6,032	5,965
AB08891	8/27/01 8:00	357	17.3	6.3	2.2	1.8	8.4	1.5	21.3	5.2	32.0	96.0	4,855	4,805
AB08959	8/28/01 16:00	385	16.2	6.7	2.7	2.1	8.8	2.1	19.2	5.1	38.2	101.1	5,201	5,145
AB08961	8/29/01 8:00	401	20.8	8.5	2.9	2.1	7.8	2.2	18.1	5.2	34.1	101.8	5,128	5,072
AB08977	8/30/01 0:00	417	19.5	7.8	3.1	2.4	8.4	1.0	23.8	5.8	26.9	98.7	4,159	4,118
AB08999	8/30/01 8:00	425	23.0	8.5	3.1	2.3	7.8	0.7	21.8	5.3	26.3	98.7	4,029	3,983
AB09000	8/31/01 0:00	441	17.2	7.5	2.9	2.4	7.7	1.8	20.2	5.4	34.1	99.1	5,212	5,161
AB09038	9/1/01 0:01	465	20.9	8.1	3.1	2.6	6.8	0.7	23.5	5.5	28.8	99.9	4,086	4,038
AB09040	9/1/01 16:00	481	18.0	7.6	3.2	2.4	8.1	1.1	22.1	5.6	32.6	100.7	4,983	4,933
AB09042	9/2/01 16:00	505	20.3	8.1	3.2	2.5	7.4	0.9	24.1	5.6	26.6	98.8	4,077	4,032
AB09051	9/3/01 12:00	525	24.1	9.0	3.1	2.3	7.3	0.8	21.6	5.3	28.0	101.5	4,068	4,021
AB09045	9/4/01 0:00	537	22.0	8.6	3.0	2.3	7.4	1.6	19.1	5.0	28.8	97.9	4,602	4,554
AB09082	9/4/01 16:00	553	22.0	8.4	3.0	2.2	6.6	0.7	19.7	5.0	30.2	97.8	4,642	4,583
AB09084	9/5/01 8:00	569	17.7	8.0	3.1	2.5	7.2	0.9	19.8	5.1	34.7	99.0	5,099	5,049
AB09110	9/6/01 8:00	593	18.2	7.6	3.1	2.4	6.8	1.9	18.5	4.9	32.8	96.2	4,759	4,705
AB09130	9/7/01 0:00	609	22.9	9.3	3.4	2.4	6.5	1.7	19.8	5.3	26.9	98.3	4,163	4,119
AB09161	9/7/01 16:00	625	26.5	10.1	3.7	2.8	4.9	0.6	25.6	5.4	20.1	99.8	3,032	3,001
AB09164	9/9/01 8:00	665	21.5	8.8	3.5	2.6	6.2	1.4	21.9	5.2	27.4	98.6	4,053	4,011
AB09166	9/10/01 0:00	681	20.5	9.1	3.6	2.8	7.1	2.1	22.3	5.8	25.8	99.2	3,867	3,828
AB09194	9/10/01 16:00	697	25.7	10.0	3.4	2.4	6.3	0.6	21.9	5.0	24.2	99.4	3,672	3,620
AB09195	9/11/01 8:00	713	21.9	8.9	3.1	2.2	7.4	1.1	19.4	4.9	30.0	98.9	4,602	4,547
AB09248	9/14/01 0:00	777	21.7	9.7	3.7	2.8	6.4	0.8	28.8	7.0	19.2	100.2	2,996	2,966
AB09249	9/14/01 8:00	785	22.7	9.5	3.5	2.7	5.9	0.9	26.0	6.3	20.2	97.8	3,082	3,050
AB09266	9/15/01 8:00	809	21.6	8.9	3.4	2.7	6.2	1.1	27.6	6.4	20.3	98.1	3,009	2,976
AB09269	9/16/01 8:00	833	21.5	9.0	3.6	2.7	7.0	0.7	31.1	8.1	15.1	98.9	2,392	2,366
AB09270	9/16/01 16:00	841	24.9	10.3	4.0	3.1	5.4	0.9	26.5	6.5	19.7	101.2	2,815	2,785
AB09273a	9/17/01 10:30	860	27.0	11.4	4.1	2.8	5.3	0.5	30.3	6.8	10.6	98.6	1,628	1,606
AB09314	9/18/01 0:00	873	26.9	11.3	4.0	2.8	5.6	0.7	28.9	6.5	13.0	99.7	2,064	2,037
AB09341	9/18/01 16:00	889	24.6	10.5	3.7	2.9	6.3	0.3	27.5	6.4	16.9	99.1	2,651	2,619
AB09359	9/19/01 16:00	913	24.0	11.0	3.3	2.8	6.3	0.9	23.5	6.0	21.1	98.9	3,132	3,094
AB09372	9/20/01 8:00	929	24.3	10.5	2.8	2.5	6.7	2.0	18.1	5.0	26.9	98.9	4,232	4,189
AB09373	9/20/01 16:00	937	22.4	9.6	2.9	2.8	6.7	2.0	20.8	5.4	29.1	101.7	4,214	4,167
AB09415	9/21/01 16:30	962	16.4	7.9	2.8	2.4	7.6	1.2	19.8	5.1	37.2	100.3	5,260	5,202
AB09417	9/22/01 8:00	977	18.7	8.4	2.8	2.4	6.5	1.6	16.8	4.4	41.8	103.5	5,669	5,601
AB09421	9/23/01 16:00	1009	17.8	8.2	2.9	2.4	6.6	1.7	18.8	4.7	40.3	103.3	5,511	5,451
AB09451	9/24/01 12:00	1029	18.6	8.5	3.0	2.4	7.8	2.1	20.9	5.6	33.2	102.1	4,968	4,916

Note: Other inerts consist of P_2O_5, Na_2O, K_2O, & TiO_2

Table 4.4-5 Reactor Samples From FD0510

p

Sample Number	Sample Date & Time	SIO_2 Wt. %	Al_2O_3 Wt. %	Other Inerts[1] Wt. %	$CaCO_3$ Wt. %	CaS Wt. %	CaO Wt. %	MgO Wt. %	Organic C Wt. %	Total Wt. %
AB09454	9/24/01 16:15	42.8	12.3	6.9	0.5	0.2	30.4	4.3	0.2	97.7
AB09456	9/24/01 18:00	32.6	14.7	7.8	0.2	0.3	37.0	5.5	0.3	98.4
AB09458	9/24/01 20:00	33.8	14.8	7.7	0.2	0.2	37.7	5.4	0.3	100.0
AB09461	9/24/01 23:00	33.4	14.5	7.7	0.2	0.1	38.7	5.5	0.2	100.2
AB09463	9/25/01 1:00	37.9	15.0	7.8	0.3	0.1	34.2	4.8	0.3	100.3
AB09465	9/25/01 3:00	47.0	16.0	7.8	0.3	0.1	25.1	3.5	0.3	100.1

Notes:

1. Other inerts consist of Fe_2O_3, P_2O_5, Na_2O, K_2O, & TiO_2
2. 9/24 & 9/25 samples were taken at the end of TC06 while the reactor was being drained.

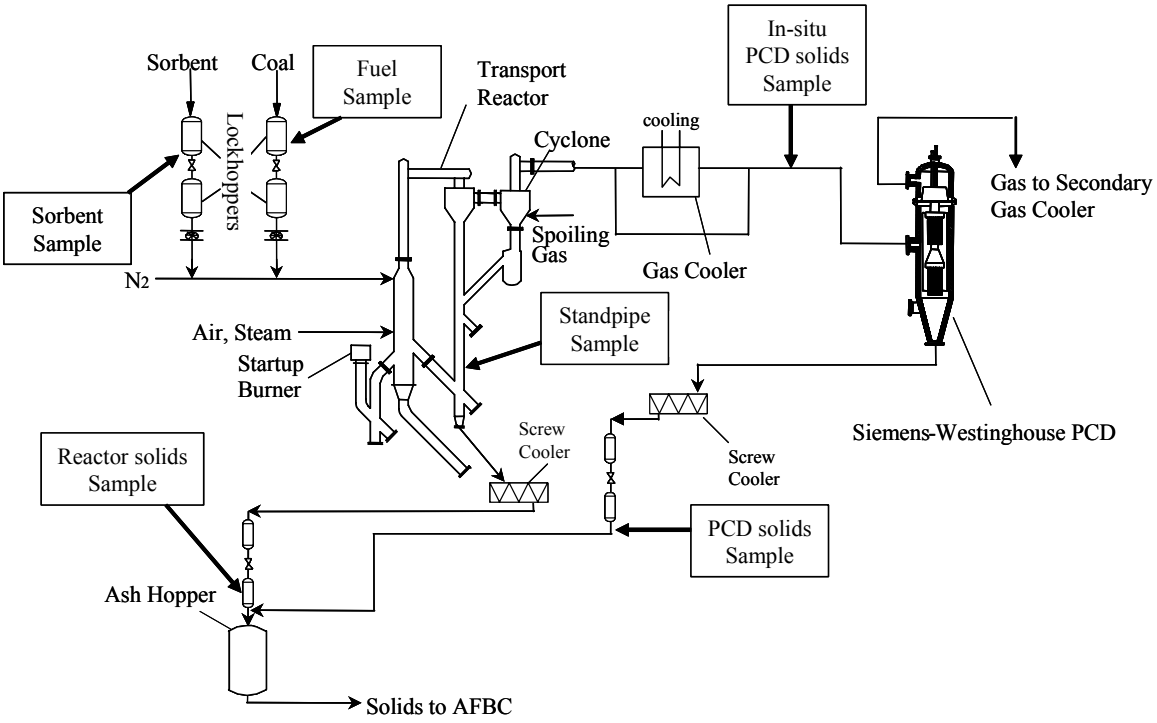

Figure 4.4-1 Solid Sample Locations

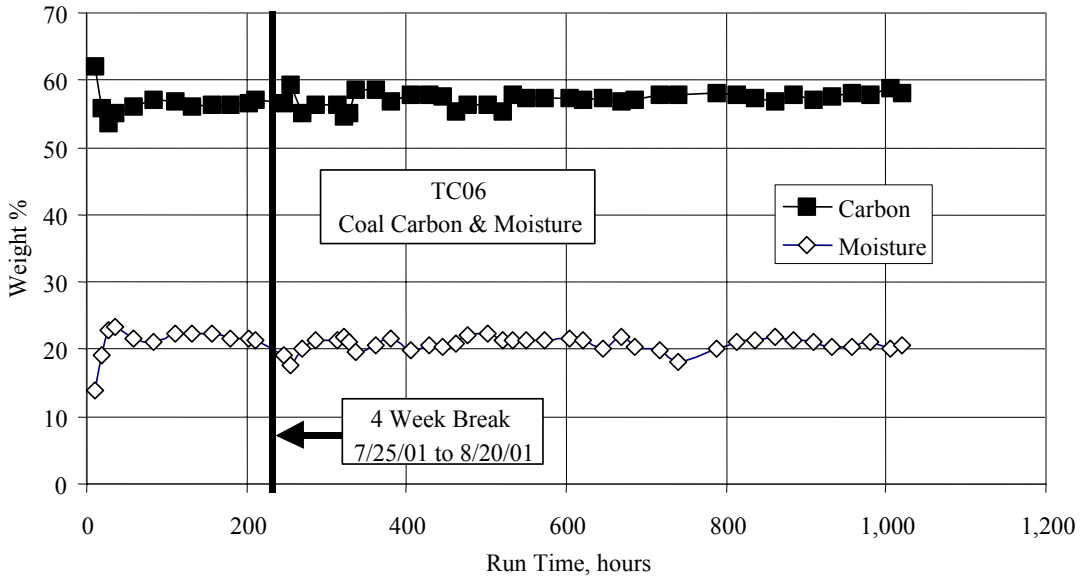

Figure 4.4-2 Coal Carbon and Moisture

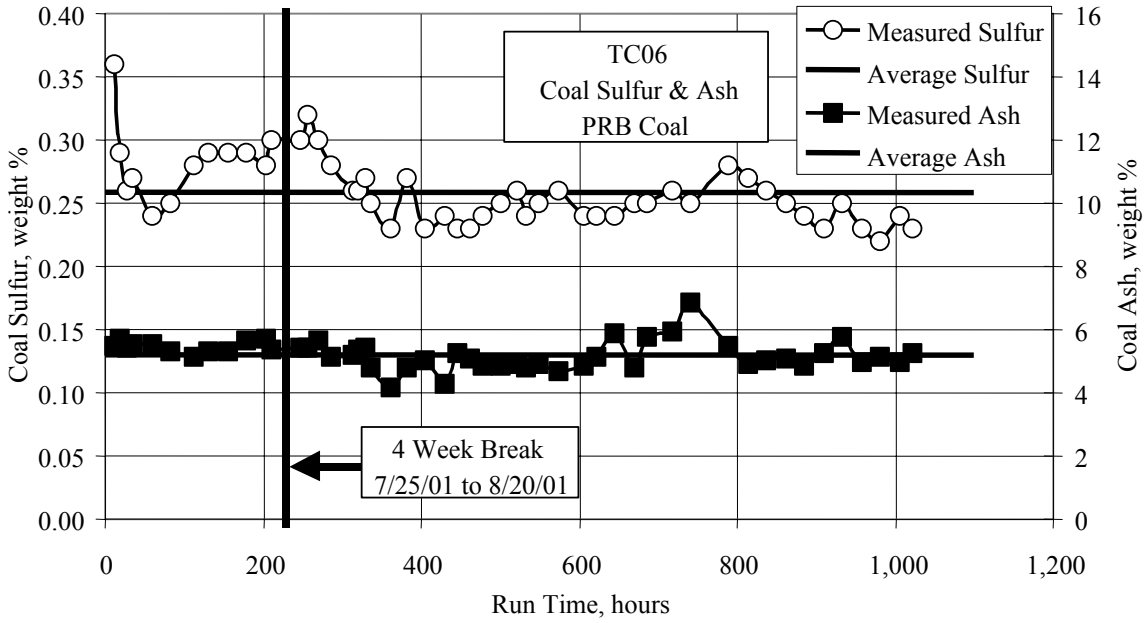

Figure 4.4-3 Coal Sulfur and Ash

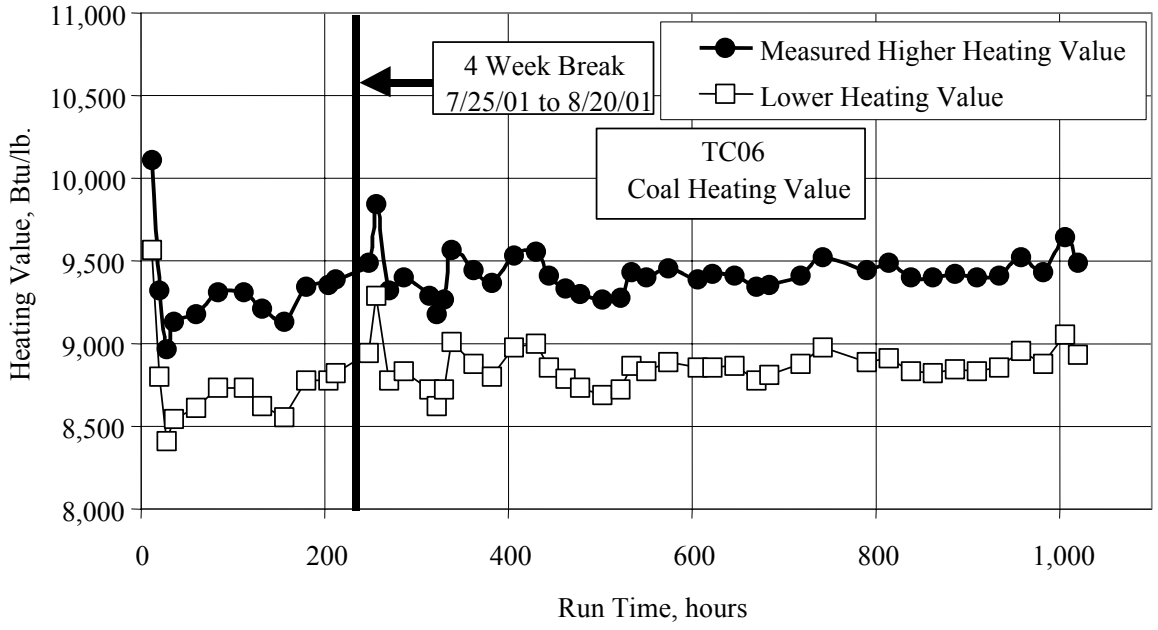

Figure 4.4-4 Coal Heating Value

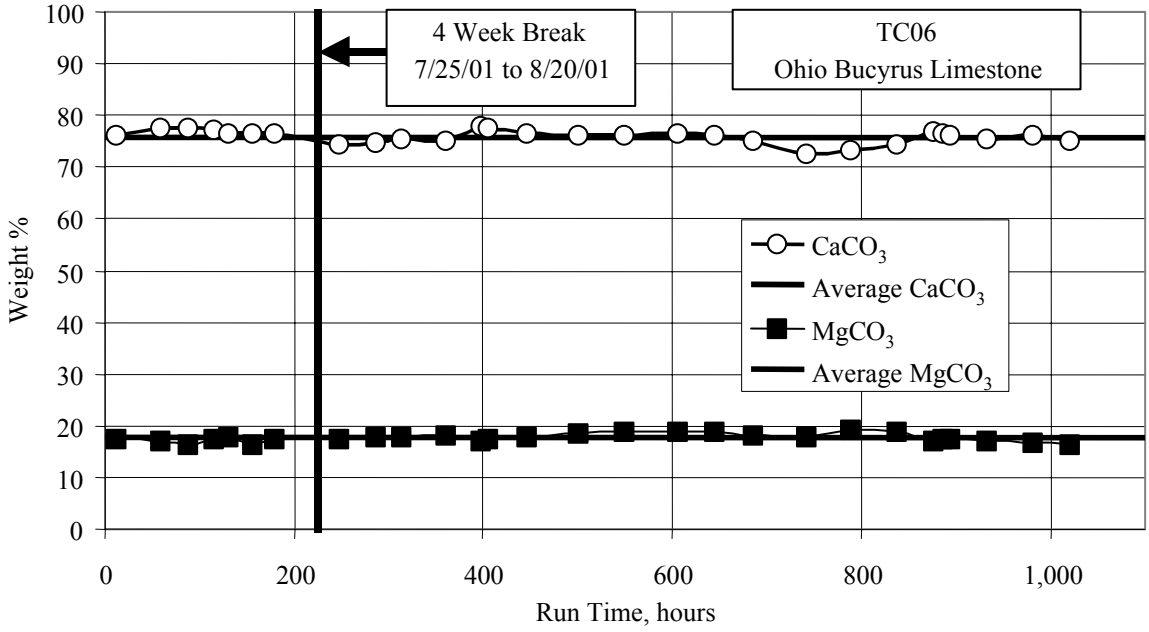

Figure 4.4-5 Limestone $CaCO_3$ and $MgCO_3$

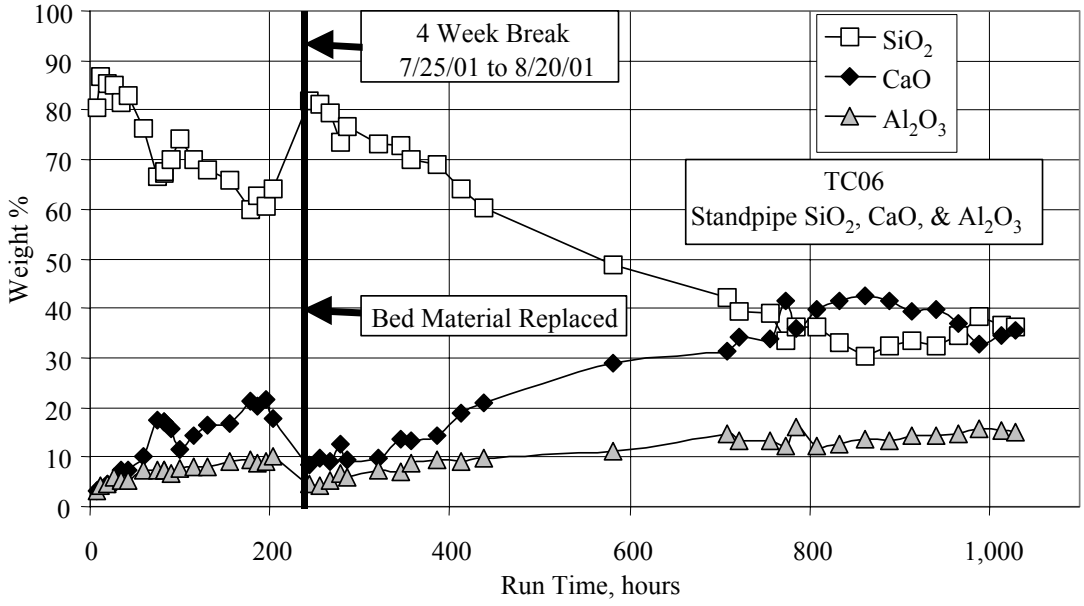

Figure 4.4-6 Standpipe SiO_2, CaO, and Al_2O_3

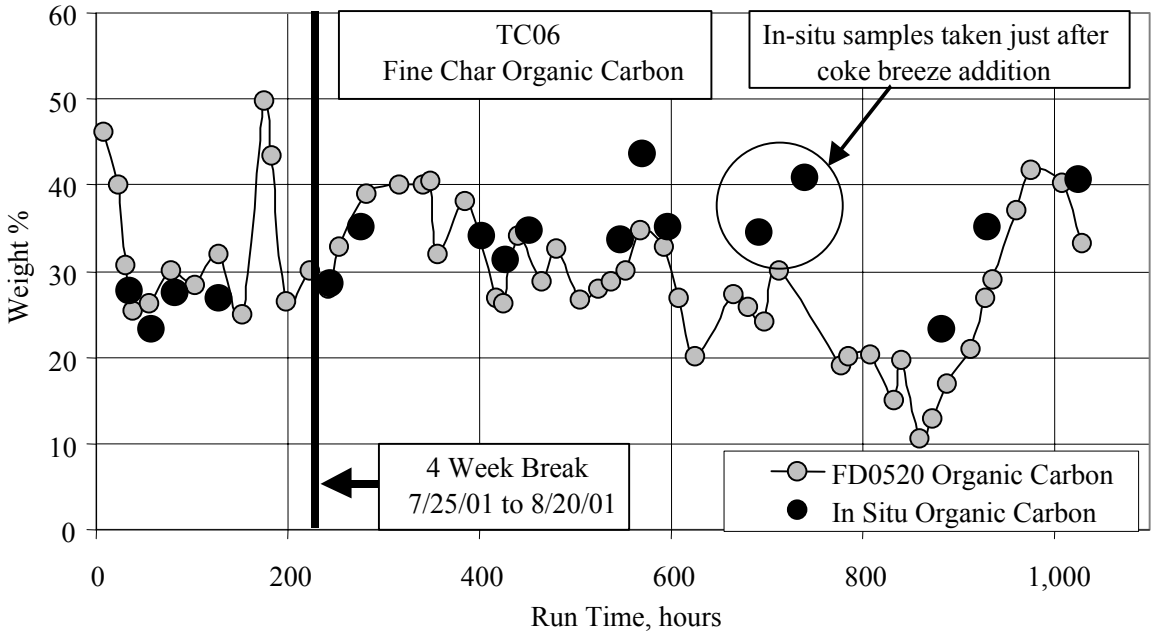

Figure 4.4-7 PCD Fines Organic Carbon

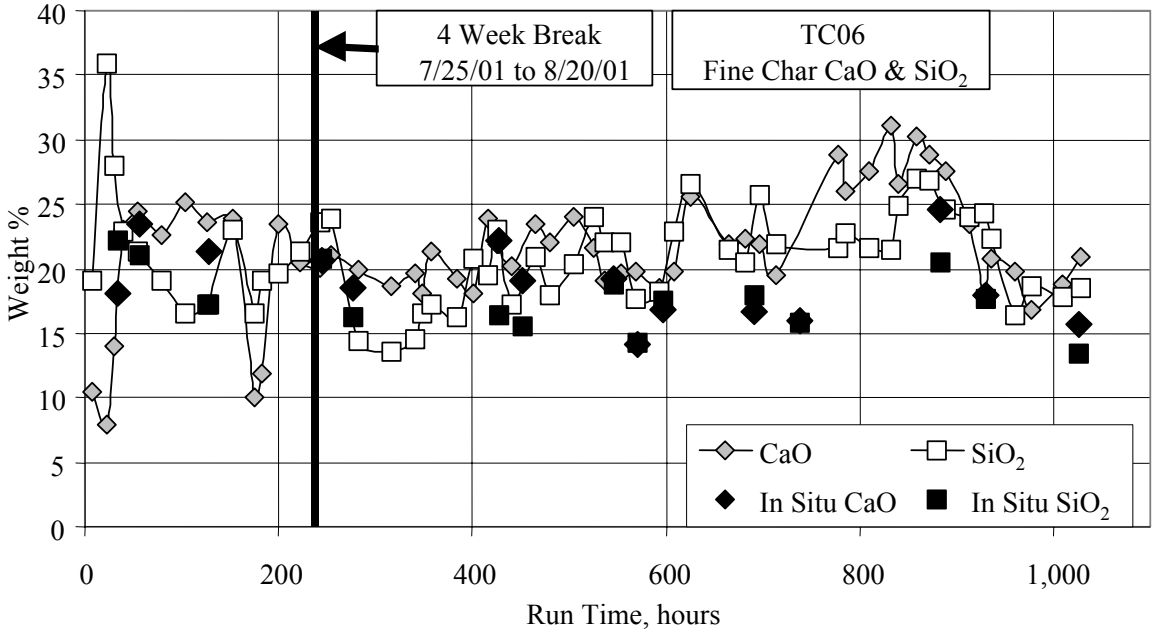

Figure 4.4-8 PCD Fines SiO_2, and CaO

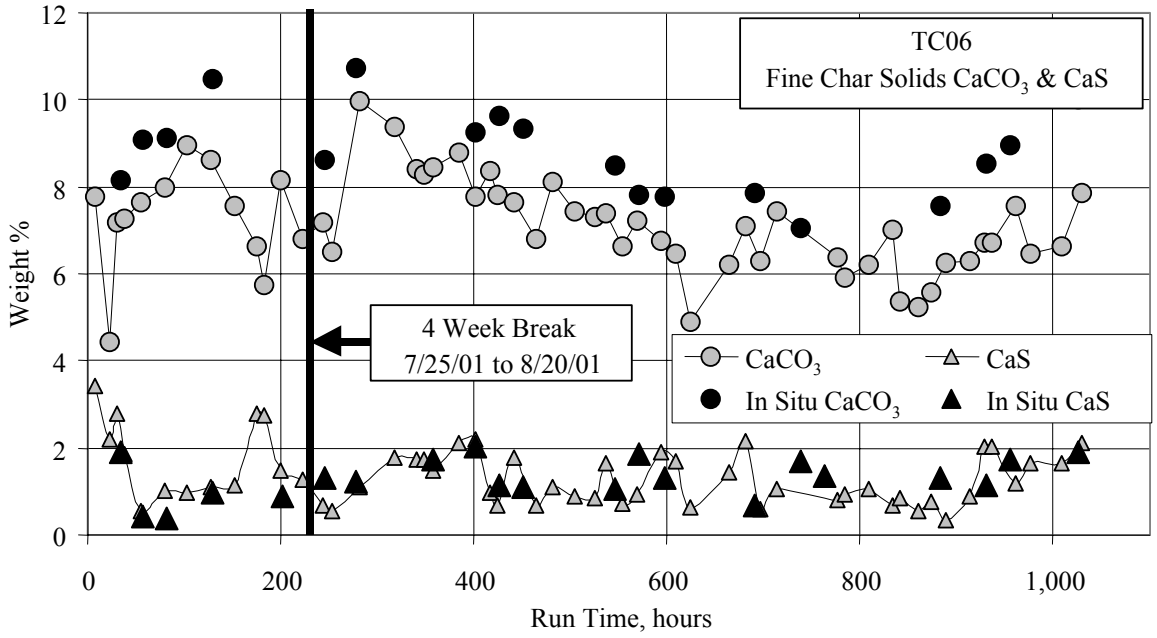

Figure 4.4-9 PCD Fines $CaCO_3$ and CaS

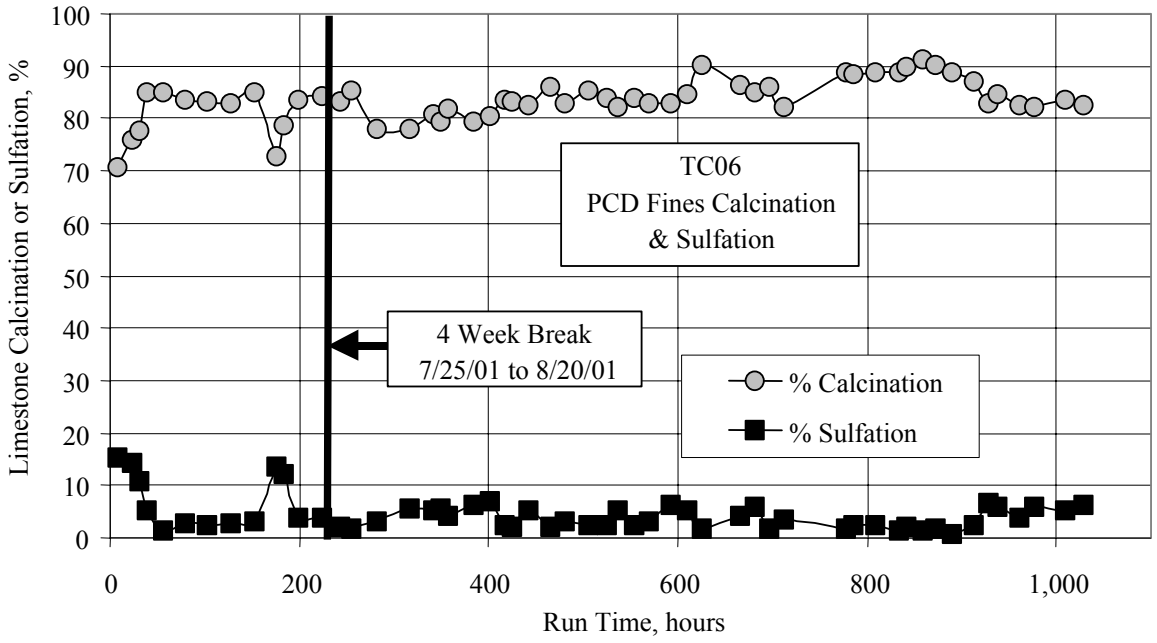

Figure 4.4-10 PCD Fines Calcination and Sulfation

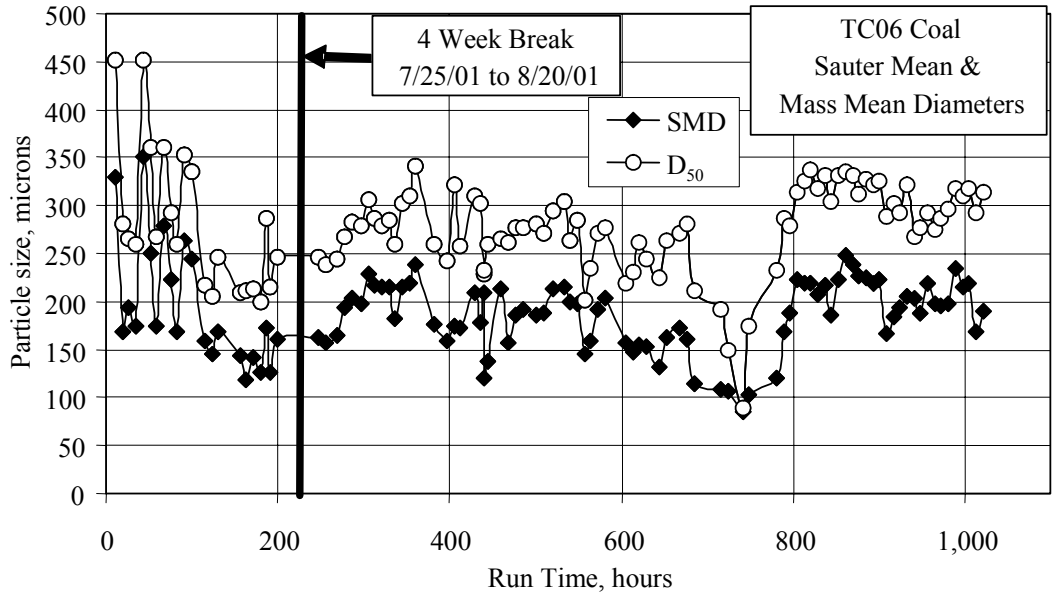

Figure 4.4-11 Coal Particle Size

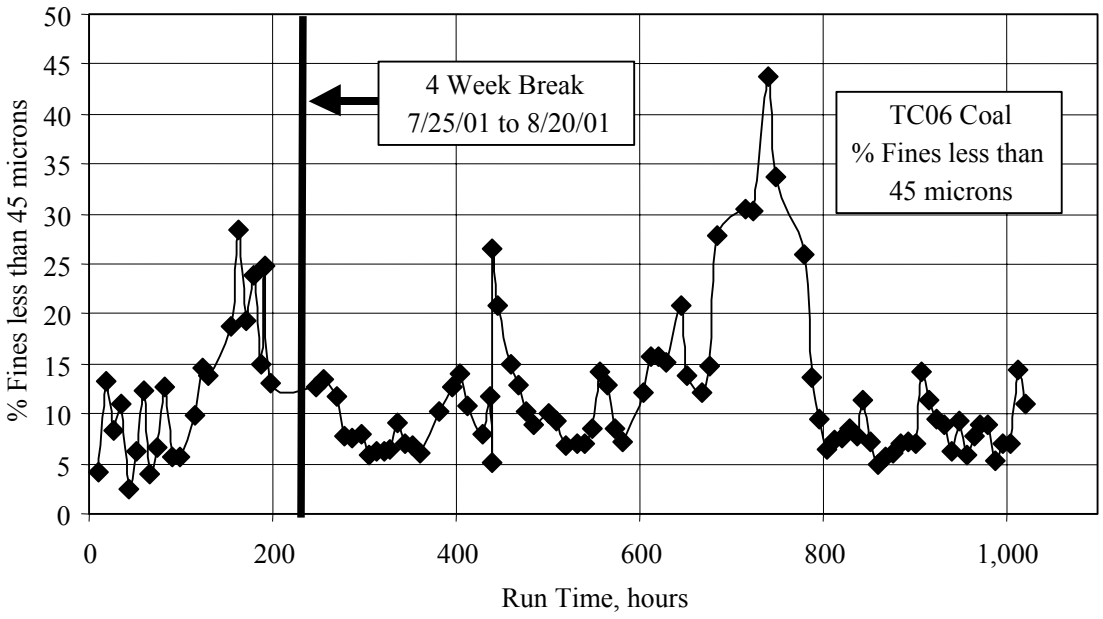

Figure 4.4-12 Percent Coal Fines

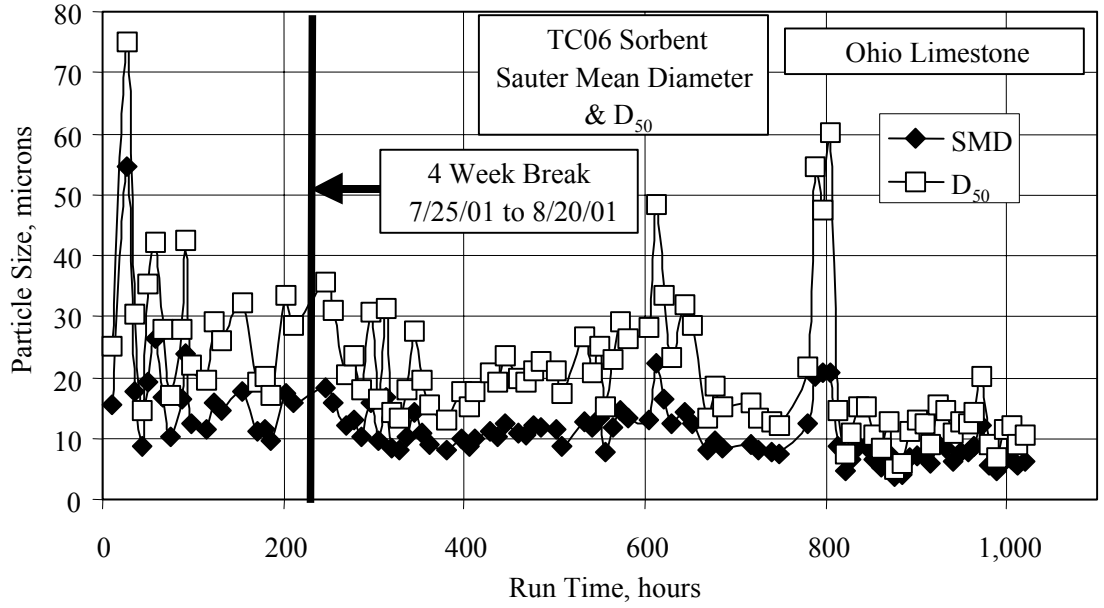

Figure 4.4-13 Sorbent Particle Size

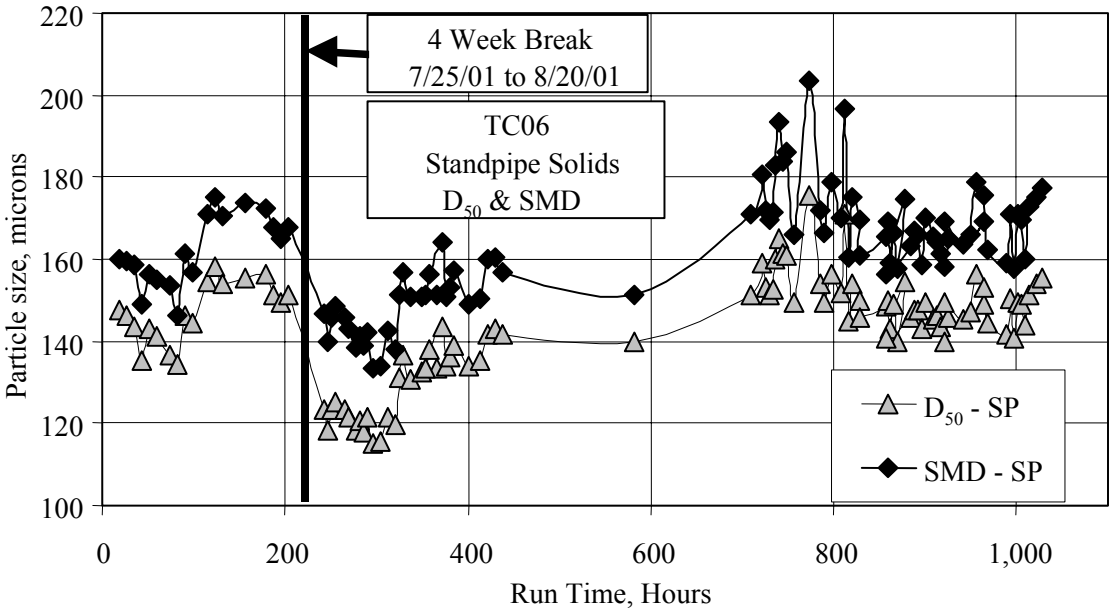

Figure 4.4-14 Standpipe Solids Particle Size

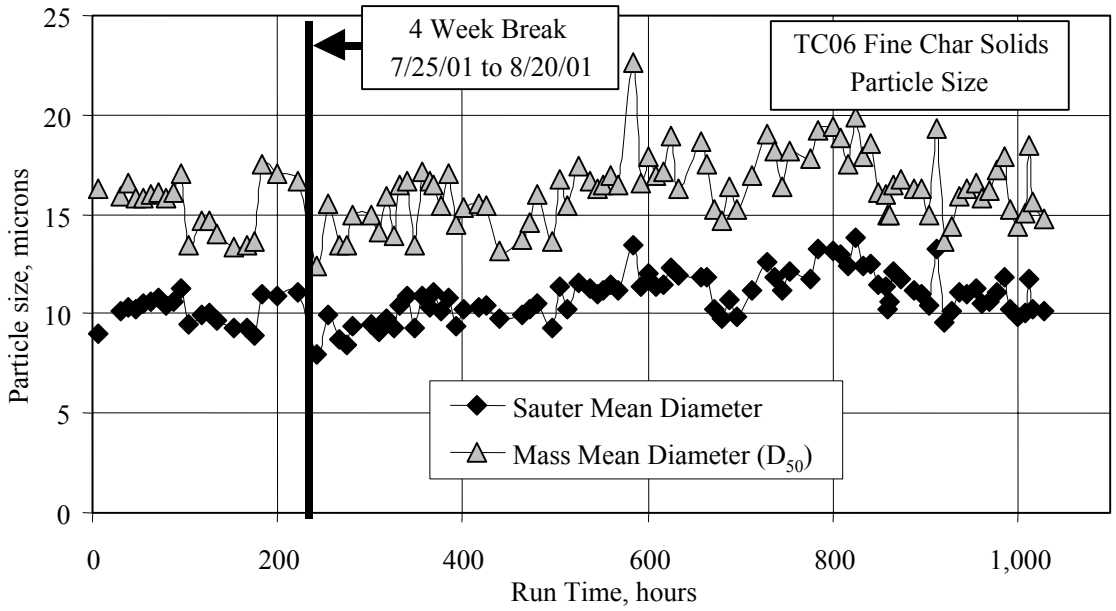

Figure 4.4-15 PCD Fines Particle Size

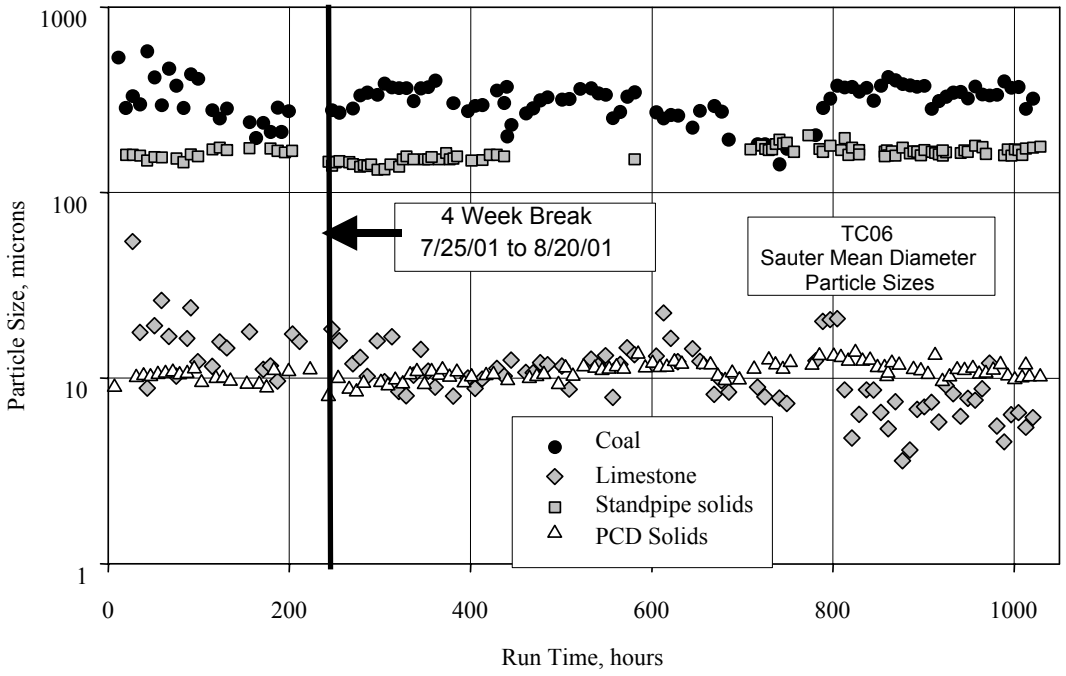

Figure 4.4-16 Particle-Size Distribution

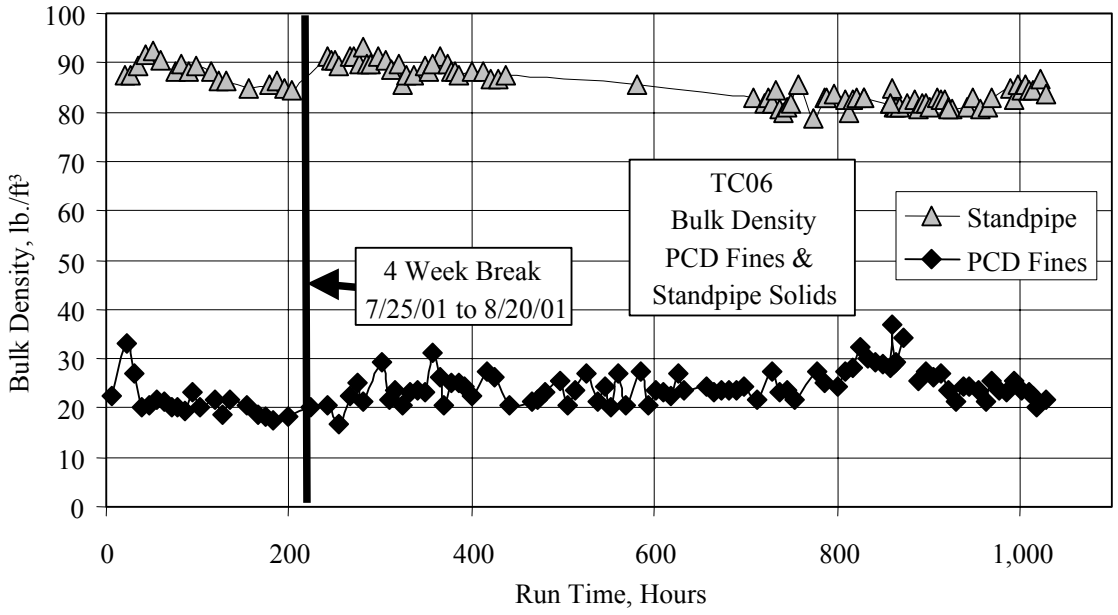

Figure 4.4-17 Standpipe and PCD Fines Solids Bulk Density

4.5 MASS AND ENERGY BALANCES

Using the gas analyses, solids analyses, and process flows entering and leaving the Transport Reactor, the following were determined:

- Coal rate.
- Overall mass balance.
- Nitrogen balance.
- Carbon conversion.
- Sulfur balance.
- Sulfur removal.
- Hydrogen balance.
- Oxygen balance.
- Calcium balance.
- Sulfur capture dependence on calcium-to-sulfur ratio.
- Silicon dioxide balance.
- Energy balance.
- Gasification efficiencies.

The process flows into the KBR Transport Reactor process are:

- Coal flow through FD0210.
- Sorbent flow through FD0220.
- Air flow measured by FI205.
- Nitrogen flow measured by FI609.
- Steam flow measured by FI204.

The process flows from the KBR Transport Reactor process are:

- Synthesis gas-flow rate from the PCD measured by FI465.
- PCD solids flow through FD0520.
- Reactor solids flow through FD0510.

The coal flow through FD0210 is usually determined by a correlation between feeder speed and coal dumps from the FD0210 surge bin between fills. In both GCT3 and GCT4 this method resulted in both carbon and energy balance being 10 to 20 percent high. It appeared that the coal rates determined from the FD0210 weigh cell data were consistently higher than actual. For TC06, the Transport Reactor carbon balance will be used to determine the coal rate. This is similar to the method used to determine the coal rate in combustion when the coal rate was determined by the flue gas rate, flue gas CO_2, and the fuel carbon.

The sorbent flow through FD0220 was determined from a correlation between feeder speed and sorbent dumps from the FD0220 storage bin between fills. This sorbent fill, feeder speed data, and correlation are shown in Figure 4.5-1. The correlation for the sorbent feeder is:

$$\text{Sorbent rate (lb/hr)} = 48.15(\text{rpm}) + 44.005 \quad (1)$$

The operating period limestone rates are shown in Table 4.5-1.

The hourly average air- and nitrogen-flow rates are shown in Figure 4.3-2 and the hourly synthesis gas rates are shown in Figure 4.3-3. Table 4.5-2 provides the air, nitrogen, and synthesis gas operating period flow rates. The synthesis gas rate was checked for all the operating periods using an oxygen balance around the synthesis gas combustor and found to be in excellent agreement with the synthesis gas combustor data for most of the operating periods.

It is estimated that about 1,000 lb/hr nitrogen from FI609 does not enter the process but is used to seal valves, pressurize/depressurize feed and ash lock hopper systems, and in the seals for the screw coolers. Values shown in Table 4.5-2 and Figure 4.3-2 assume that 1,000 lb/hr of nitrogen from FI609 does not enter the Transport Reactor. A small amount of nitrogen (~200 lb/hr) is added via FI6080 to the Transport Reactor through the coke breeze feed line to keep the line clear between periods of coke breeze feed. This is included in the feed nitrogen.

The steam rate to the reactor was determined from either FIC289, which measures the steam flow to the reactor J-leg, or FI204, which measures the total steam flow to the reactor. FI204 was used for TC06-1 through TC06-17 and FIC289 was used for TC06-18 to TC06-64. The choice was based on which instrument was reading above zero during the operating period. The hourly average steam rate is shown in Figure 4.3-9. Not much steam was fed to the reactor after hour 100.

The solids flow from the PCD can be determined from two different methods by using:

1. In situ particulate sampling data upstream of the PCD.

2. FD0530 weigh cell data.

The best measurement of the solids flow to the PCD is the in situ PCD inlet particulate determination. Using the synthesis gas-flow rate, the solids flow to the PCD can be determined since the PCD captures all of the solids.

The FD0530 weigh cell data can be used to determine the PCD solids flow only if both the FD0530 feeder and the FD0510 feeder (standpipe solids) are off, because FD0520 and FD0510 both feed into FD0530 and FD0530 feeds the sulfator (atmospheric fluidized-bed combustor, AFBC). This method assumes that the PCD solids level in the PCD and FD0502 screw cooler are constant, that is the PCD solids level is neither increasing nor decreasing. The results for the first two methods are compared in Figure 4.5-2. Rates for use in the operating period mass and energy balance were interpolated between the in situ measurements and weigh cell measurements. The interpolated rates used for the operating periods in mass and energy calculations are shown in Table 4.5-2.

The FD0530 weigh cell measurements had a large scatter. Occasionally there seemed to be a daily cycle to the variations in FD0520 flow. With the exception of four of the in situ samples, the in situ samples agreed with the weigh cell readings. For the first 700 hours of operation, the PCD fines rate was about 300 to 450 lb/hr. When the coal rate was decreased at about 700 hours, the PCD fines rate decreased to about 200 lb/hr. As the coal rate was increased at the end of TC06, the PCD fines rate slowly returned to 425 lb/hr.

Solids were regularly withdrawn from the reactor to control the standpipe level during TC06, so the combined rates of FD0520 and FD0510 could be determined using FD0530 weigh cell data. The FD0510 rate can be estimated by the difference between the sum of the combined rates and an interpolated FD0520 rate. The FD0510 rate was then correlated to the FD0206 feeder speed. The correlation is shown on Figure 4.5-3 and is:

$$\text{FD0510 rate (lb/hr)} = 74.639(\text{rpm}) + 77.77 \qquad (2)$$

The FD0510 rate shows a lot of scatter and correlates poorly to the FD0206 feeder speed. The FD0510 rate varied between 50 and 350 lb/hr. The large variation is due to the scatter in the FD0520 rates and the use of interpolated FD0520 rates.

The FD0510 rates for the steady operating periods are shown in Table 4.5-2. Since FD0510 was usually not operated for an entire operating period, the values shown in Table 4.5-2 and used in the mass balances have been prorated down from the FD0510 rates determined, as if FD0510 had been operating continuously. The approximate time that it takes for the Transport Reactor circulating solids to reach a constant value (steady-state value) can be determined from the average FD510 rate and the initial reactor volume of solids. Key assumptions in this calculation are that the Transport Reactor circulating solids stay in the reactor and most of the PCD fines that go through FD0520 are "once through solids." The reactor then can be modeled as a constant-volume, well-mixed reactor. The starting solids in the Transport Reactor are about 6,000 lb of sand. The average FD0510 withdrawal rate was about 85 lb/hr. The Transport Reactor residence time constant is then about 71 hours. Three residence times (283 hours) result in 95-percent reactor turnover, which would have been achieved at hour 431. Four residence times (284 hours) result in 98-percent reactor turnover, which would have been reached at 504 hours. Using Figure 4.4-6, it is clear that the reactor had not reached steady compositions until at least after hour 600. Possible explanations for this imbalance are that the reactor solids rate was lower than 85 lb/hr or that more sand had been added to the reactor than 6,000 lb.

In GCT3 and GCT4, both the carbon balance and energy balance were off by 10 to 20 percent, and it was speculated that this was due to FD0210 weigh cell data reading about 15 percent too high. Using coal rates determined by FD0210 weigh cell data again produced a TC06 carbon balance that had 10 to 20 percent more carbon entering the Transport Reactor than exiting the Transport Reactor. The other large carbon flows (synthesis gas carbon flow and PCD solids carbon flow) are independently checked, so it is likely that the weigh cell coal rate is in error. The coal rate was then determined by a carbon balance using the coal carbon, PCD carbon, synthesis gas carbon, standpipe carbon, synthesis gas rate, PCD solids rate, the reactor solids rates, and the reactor carbon accumulation. The results of this calculation are shown in

Table 4.5-1, where the Transport Reactor carbon flows are listed for each operating period. The carbon balance coal-flow rate is about 80 percent of the FD0210 weigh cell coal-flow rate.

The carbon balance coal-flow rate and the air-to-coal ratio for the operating periods are shown in the plot in Figure 4.5-4. The carbon balance coal-flow rates for the operating periods are provided in Table 4.5-2. The coal rate increased from 4,600 to 5,000 lb/hr from the start of the run to hour 74 and was constant at about 5,000 lb/hr until the 4-week break. From hour 280 to hour 695 the coal rate was gradually increased from 4,000 to 4,500 lb/hr. The coal rate was decreased to about 3,300 lb/hr at hour 760. The coal rate was then increased from 3,300 to 5,000 lb/hr from hour 873 and hour 974. For the last two operating periods the coal rate was steady at about 5,000 lb/hr. The air-to-coal ratio was at about 3.5 for the first 55 hours of TC06 and from hour 55 to hour 760, the air-to-coal ratio was at 3.3 to 3.4. When the coal rate was decreased, the air-to-coal ratio increased to 3.6, and when the coal rate increased, the air-to-coal ratio returned to about 3.3. The air rate was controlled either manually or automatically to maintain a desired reactor temperature. Since the desired set point temperature did not change much during TC06, the air-to-coal ratio was constant during TC06.

The synthesis gas LHV compared to the coal rate is shown in the plot in Figure 4.5-5. The LHV increased with the coal rate. The nonair nitrogen rate was constant during TC06 and as the coal rate increases, the relative amount of nonair nitrogen to air nitrogen decreases, thus reducing the nitrogen in the synthesis gas. This of course increases the LHV.

Carbon conversion is defined as the percent fuel carbon that is gasified to CO, CO_2, CH_4, C_2H_6, and higher hydrocarbons. The carbon conversion is the measure of how much carbon is rejected by the gasifier with the PCD and reactor solids. This rejected carbon is typically burned in a less efficient combustor and results in a less efficient use of the fuel. The carbon conversion against the coal rate is shown in the plot in Figure 4.5-5. The carbon conversions for each operating period are provided in Table 4.5-1. The carbon conversion was between 95 and 99 percent and was a weak function of coal-feed rate. As the coal rate increased the carbon conversion slightly decreased.

Material balances are useful in checking the accuracy and consistency of the data obtained as well as determining periods of operation where the data is suitable for model development or commercial plant design. Material balances for each operating period are provided in Figure 4.5-6 showing the relative difference (relative error) of Transport Reactor feeds in minus products out divided by the feeds ({In-Out}/In) and the absolute difference (absolute error) of the feeds and the products (In-Out). The overall material balance was excellent, with most of the run within ±3.0 percent for the relative difference (±1500 lb/hr for the absolute difference). The first 220 hours had the worst material balance. The material balance improved from -6 to -4 percent in the periods before the 4-week break. The periods from the 4-week break to hour 670 show the best material balance with relative errors from 0.0 to -3.0 percent (0 to -1200 lb/hr). The two outliers are at hours 498 and 548 (TC06-32 and TC06-36). These two operating periods were during the operation of the recycle gas compressor. The recycle gas compressor was operated during only one other operating period, TC06-57 (hour 913), and had no effect on the mass balance. There was a slight negative bias for the remainder of the run, averaging about -2 percent relative error (-1000 lb/hr). If 500 lb/hr of steam were leaking into

the reactor from hour 220 to the end of the run, the mass balance would bracket the 0-percent mass balance line.

The gas composition data in Section 4.3 have no effect on the overall mass balance. The solids compositions affect the mass balance through the coal rate determined by carbon balance. The main contributors to the material balance are the synthesis gas rate (21,000 to 30,000 lb/hr), air rate (11,000 to 17,000 lb/hr), nitrogen rate (5,500 to 7,300 lb/hr), and coal rate (3,500 to 5,100 lb/hr).

The relative split between the flow rates of solids collected by the PCD and removed from the standpipe through FD0510 are shown in the plot in Figure 4.5-7 and listed on Table 4.5-2. The split follows the same trends as the flow rates. About 80 percent of the solids are removed by the PCD at higher coal rates of 4,000 to 5,000 lb/hr and 70 percent of the solids are removed by the PCD at coal rates of 3,400 lb/hr. It would appear that lower coal rates generate slightly more coarse material than higher coal rates.

Test period nitrogen balances are shown in the plot in Figure 4.5-8 and listed in Table 4.5-3. Typical nitrogen flows for TC06-61 are shown in Table 4.5-4. The first two operating periods (TC06-1 and TC06-2) had excellent nitrogen balances. The next three operating periods (TC06-3 to TC06-5) had the worse nitrogen balance at -5-percent agreement (-500 lb/hr nitrogen). For these three periods the nitrogen analyzer was out of service and the synthesis gas nitrogen was estimated by difference. For the rest of the first 220 hours of operation the nitrogen balance was -2 to -3 percent (-200 to -300 lb/hr nitrogen). For the remainder of TC06 the nitrogen balances were between 0 and +2 percent (0 to +200 lb), except for a few operating periods. The two low points were at hours 498 and 548, when the recycle gas compressor was in operation. The high periods of up to 4-percent error were during the increase in coal rates. For most of TC06 the nitrogen balance was centered +2 percent (+200 lb/hr nitrogen). The nitrogen balance would have been perfect for most of the run if the amount of lost nitrogen was reduced by 1,100 lb/hr rather than 1,000 lb/hr. The nitrogen flows as shown in Table 4.5-4 are dominated by the air, nitrogen, and synthesis gas flow. None of the solids contributes significantly to the nitrogen balance. The use of the in situ H_2O data rather than the analyzer H_2O data improved the nitrogen balance.

Sulfur balances for all the TC06 operating periods are provided in Figure 4.5-9 and Table 4.5-5. The synthesis gas sulfur compounds were not directly measured, but estimated from syngas combustor SO_2 analyzer data and synthesis gas combustor flue gas flow. The sulfur balances are not good. For TC06, the sulfur balance was biased high by 20 to 60 percent (2 to 8 lb/hr). From hour 700 to the rest of TC06, the sulfur balance was consistently off by 5 lb/hr even through the swings in coal-feed rate. The consistent error of 5 lb/hr could indicate a consistent error in the SGC SO_2 measurements or the measurement of the coal sulfur. An increase of 40 percent in the SGC SO_2 measurements would close the sulfur balance. The sulfur mass balance is difficult to close due to the low sulfur content of the PRB coal and PCD fines.

With such large errors in the sulfur balances, it is difficult to determine the correct sulfur removal. There are three different methods to determine the sulfur removals:

1. From synthesis gas sulfur emissions (using the synthesis gas combustor flue gas rate and synthesis gas combustor flue gas SO_2 measurement) and the feed-sulfur rate (using the feed-coal rate and coal sulfur content). (Gas method.)

2. From PCD solids analysis (using PCD solids-flow rate and PCD solids sulfur content) and the feed-sulfur rate. (Solids method.)

3. From the gas analysis data and the PCD solids data. (Products method.)

The three sulfur removals are shown in the plot in Figure 4.5-10 and in Table 4.5-5. The sulfur in the fuel is an inaccurate measurement due to the multiplication of a very small number (coal sulfur) by a very large number (coal-feed rate). The low coal sulfur contents (0.25- to 0.35-weight-percent sulfur) increase the error in feed sulfur. The gaseous sulfur measurement is also the product of a small number (SGC SO_2) and a large number (SCG flue gas rate). However, the consistent error in the sulfur balance of 4 lb/hr is disturbing since it implies that the SGS SO_2 measurement is 40 percent lower than the actual measurement. This is because it is more accurate to measure gas-flow rates and compositions and these flows and compositions are measured continuously. The PCD fines sulfur rate may have inaccuracies in the very low sulfur in the PCD solids. There is no accumulation of sulfur-containing solids in the reactor during TC06 because the standpipe and FD0510 reactor samples contained very small amounts of sulfur. The gas method sulfur removal was between 30 and 75 percent for most of TC06, with most of the removals between 50 and 70 percent. The sulfur removals by the products and solids methods varied widely during TC06, from between 0 and 55 percent.

The synthesis gas combustor SO_2 concentration was used for the sulfur emissions shown in Table 4.5-5. The sulfur emissions based on the gas analyses are from 0.14 to 0.39 lb SO_2 per MBtu coal fed.

Operating periods hydrogen balances are provided in Figure 4.5-11 and Table 4.5-3 with typical values shown in Table 4.5-4. The coal and synthesis gas streams dominate the hydrogen balance, especially since very little steam was fed to the Transport Reactor during TC06. The best hydrogen balances were from hours 297 to 548 when the hydrogen balance was 0 to -5 percent (0 to -20 lb hydrogen per hour). For the first 200 hours, the hydrogen balance was low by -10 to -40 percent. From hours 550 to 840, the hydrogen balance decreased down to -25 percent then increased to -10 percent at the end of the run. This is probably due to the primary gas cooler (HX0202) steam leak, which leaked steam into the Transport Reactor during TC06. This steam leak got progressively worse during TC06. The coal rate increase seemed to improve the hydrogen balance. Using the in situ synthesis gas moisture measurements rather than the analyzer moisture measurements makes the hydrogen balance better for most of the operating periods. If about 360 lb/hr of steam (40 lb/hr hydrogen) were leaking into the reactor through HX0202 for the last 400 hours of TC06, the hydrogen balance would be nearly perfect.

Operating period oxygen balances are shown in Figure 4.5-12 and Table 4.5-3, with typical values provided in Table 4.5-4. The TC06 operating periods oxygen balance had a consistent low bias. The oxygen balance was usually low, from -3 to -13 percent (-200 to -600 lb/hr oxygen). This may be a result of the HX0202 steam leak. The oxygen balance was consistently off by about -500 lb/hr oxygen (equivalent to 560 lb/hr steam) from hour 640 to the end of the

test. The oxygen balance would have been excellent if 560 lb/hr of steam was leaking into the reactor. Note the large oxygen contribution of the feed coal since PRB has a high oxygen content (moisture plus elemental oxygen). From hours 297 to 569, the oxygen balance was off by -250 lb/hr of oxygen (that is equivalent to 280 lb/hr steam). Using the in situ synthesis gas moisture measurements rather than the analyzer moisture measurements made the oxygen balance better for most of the operating periods.

Operating period calcium balances are provided in Figure 4.5-13 and Table 4.5-3, with typical values shown in Table 4.5-4. The PRB operation is characterized by low sorbent-feed rates because of low sulfur in the PRB coal. About half of the inlet calcium comes from fuel and half from sorbent. The calcium balances were mixed during TC06, with a calcium balance varying from a positive to negative bias. This is probably due to the low calcium flows in the system, the inaccuracies of the sorbent and coal feeder flows, and since the calcium flow is the result of multiplying a small number (calcium in the coal) by a large number (coal-flow rate). TC06 started with a positive calcium bias and then fell to a negative bias from hours 41 to 84 with a minimum of -20 percent at hour 55. The calcium balance was then positive from hours 91 to 336 with a maximum of +35 percent. There was then a long period of negative calcium balances from hours 354 to 896, with a minimum of -47 percent. From hours 913 to 960, the calcium balances were excellent with between +5 and -5 percent agreement. This was the period of increasing coal rate and was after the reactor reached a constant composition.

The PCD fines calcium is typically not totally calcined, as shown in Figure 4.4-10 where the calcium calcination was 70 to 90 percent. The level of sorbent limestone calcination can be calculated by a mass balance since the sorbent limestone and the coal calcium-feed rates are known. The sorbent limestone calcination calculation uses the assumption that the calcium in the coal ash has not recarbonated. Figure 4.5-14 shows the estimate of the limestone calcination for TC06 assuming that the calcium from the coal ash in the PCD solids is neglected. The limestone sorbent calcination varied from 55 to 90 percent and is usually less than the total calcium calcination. The poor calcium balance is probably responsible for the wide variations in the limestone calcination. Also shown in the plot in Figure 4.5-14 is the $CaCO_3$ calcination temperature calculated from the CO_2 partial pressure in the synthesis gas. Figure 4.3-15 of the GCT1 final report shows a plot of the CO_2 partial pressure for the $CaCO_3$-CaO-CO_2 system. The calcination temperature varied between 1,640 and 1,660°F, slightly below the mixing zone temperature of 1,700 to 1,800°F. If the $CaCO_3$ is at equilibrium at the mixing zone temperatures, it should all calcine to CaO and CO_2. As the CaO cools, thermodynamic equilibrium predicts that the CaO should recarbonate to $CaCO_3$ at the PCD temperatures of 700 to 750°F.

It can not be determined from the data whether the limestone calcined and then recarbonated as thermodynamics would predict or whether the limestone only partially calcined. It is probably the former since compound decomposition reactions (like limestone calcination) are fast and go quickly to completion. The recarbonation reaction is also fast, but is limited by the mass transfer of the CO_2 into the PCD fines particle. It is likely that the mass transfer prevents the solids sampled from FD0520 to be completely carbonated.

Figure 4.5-15 is a plot of TC06 sulfur emissions (expressed as lb SO_2 emitted per MBtu coal fed) and products method sulfur removal as a function of calcium to sulfur ratio (Ca/S), based on the coal and sorbent fed to the Transport Reactor. It would appear that the sulfur emissions are independent of the feed Ca/S when the feed Ca/S ratio is above 2.25. The sulfur emissions are based on the synthesis gas combustor SO_2 analyzer and are shown in Table 4.5-5. When the feed Ca/S ratios are below 2.25, the sulfur emissions are higher and the SO_2 removal is lower. Above a Ca/S ratio of 2.25, the sulfur removal and sulfur emissions are constant. Due to the poor sulfur and calcium balances, the actual trend might not be evident due to the errors in the data.

Figure 4.5-16 is a plot of TC06 sulfur emissions (expressed as lb SO_2 emitted per MBtu coal fed) and sulfur removal by products as a function of calcium to sulfur ratio (Ca/S) measured in the PCD solids samples from FD0520. The measured PCD solids Ca/S ratio is much higher than the feed Ca/S because the PRB coal has high calcium content. There does not appear to be any trend in PCD solids Ca/S with sulfur emissions. The results seen in Figure 4.5-16 demonstrate that when the PCD solids contain very little sulfur (high Ca/S), the SO_2 removals are low and the SO_2 emissions are high, which is reasonable by sulfur balance. The calcium sulfation is the reciprocal of the Ca/S ratio based on the PCD fines solids.

Operating periods SiO_2 balances are shown in Figure 4.5-17, with typical values shown in Table 4.5-4. Table 4.5-3 provides the results of the SiO_2 balances for all of the operating periods. The SiO_2 balance mainly reflects the coal, reactor draw-off rate, and PCD solids rate, since the limestone sorbent typically had only 2.5 percent SiO_2. The SiO_2 balance is similar to the calcium balance since both are dominated by the coal and PCD solids rates and compositions. The SiO_2 balances were generally very poor, with the SiO_2 balances less than -50 percent for the most of the first 600 hours of operation. The SiO_2 balance was always biased negative (that is, there were more SiO_2 leaving the reactor than entering). The SiO_2 balance seemed to improve as startup sand was purged from the reactor. The poor SiO_2 balance might be due to the reactor accumulation/depletion term, which is difficult to estimate. The best SiO_2 balances were between hours 926 and 960, the same periods as when the CaO balance was the best and the reactor was at the steady-state solids composition.

The gas-flow rates were self-consistent as shown by the good overall mass balance, which is dominated by the gas-flow rate measurements and was -3 to + 0.0 percent for the last 800 hours of TC06. The nitrogen balance was also excellent at (0.0 to +2.0 percent) for the last 800 hours. The sulfur balance was poor with a high bias at +50 percent (+5-lb sulfur per hour). The hydrogen and oxygen balances were of by about -10 percent, which could be explained by a steam leak from HX0202 into the transport rector. The calcium balance was not good (- 50 to +30 percent), usually with a negative bias. The SiO_2 balance had a high negative bias from -200 to 0 percent. Both the calcium and SiO_2 balances seemed to improve as the reactor reached the steady-state solids composition (possibly due to the difficulty in estimating reactor solids accumulation).

The Transport Reactor energy balance for TC06 is shown in Figure 4.5-18, with standard conditions chosen to be 1.0 atmosphere pressure and 80°F temperature. Table 4.5-6 breaks down the individual components of the energy balance for each operating period. The "energy in" consists of the coal, air, and steam fed to the Transport Reactor. The nitrogen and sorbent

fed to the reactor were considered to be at the standard conditions (80°F) and hence have zero enthalpy. The "energy out" consisted of the synthesis gas and PCD solids. The lower heating value of the coal and PCD solids was used in order to be consistent with the lower heating value of the synthesis gas. While the reactor solids sampled from FD0510 flow had no latent heat, there was a small amount of sensible heat in the FD0510 solids. The energy of the synthesis gas was determined at the Transport Reactor cyclone exit. The sensible enthalpy of the synthesis gas was determined by overall gas heat capacity from the synthesis gas compositions and the individual gas heat capacities. The synthesis gas and PCD solids energy consists of both latent and sensible heat. The heat loss in the reactor was estimated to be 1.5 x 10^6 Btu/hr, which was measured during a previous Transport Reactor combustion test.

For most of the test runs, the TC06 energy balance was biased low by -0 to -5 percent (-0 to -2.0 MBtu/hr). This is a much better energy balance than previous runs when the coal-flow rates were based on the FD0210 weigh cell data. An increase in coal-flow rates by 4 percent would put most of the operating periods in energy balance. The carbon balance would then be off by 4 percent. The first five operating periods had very low balances of -10 to -20 percent, then after 73 hours, were from -3 to -5 percent out of balance. The first two operating periods after the restart (TC06-15 and TC06-16) had high energy balances of +5 percent. The final 500 hours of TC06 had very stable energy balances at around -4 percent (-1.5 MBtu/hr). This energy imbalance of -1.5 MBtu per hour would be eliminated if the Transport Reactor were assumed to be adiabatic. Any steam that was leaked into the process from HX0202 would also improve the energy balance (and the oxygen and hydrogen balances). The equivalent amount of steam required to account for 1.5 MBtu/hr is 1,250 lb/hr of steam, which seems excessive. The best estimate would be that about 560 lb/hr steam leaked into the reactor unmeasured (from the oxygen balance) and the Transport Reactor heat loss was about 0.8 MBtu/hr rather than 1.5 MBtu/hr. The addition of the loop seal increased the solids circulation rate, which should increase the average standpipe temperature. The higher standpipe temperature should have increased the heat loss of the standpipe.

Gasification efficiency is defined as the percent of the coal energy that is converted to potentially useful synthesis gas energy. Two types of gasification efficiencies are used: cold gas efficiency and hot gas efficiency. The cold gas efficiency is the amount of coal energy that is available to a gas turbine as latent heat of the synthesis gas.

Similar to sulfur removal, the cold gas efficiency can be calculated at least three different ways, since the energy balance is off by up to about 4 percent, and each result could be different. If there were a perfect energy balance, all three calculations would produce the same result. Three calculation methods for cold gasification consistent with the three methods of sulfur removal were performed.

1. Based on the coal feed heat (coal latent heat) and the latent heat of the synthesis gas, this method assumes that the coal feed heat and the synthesis gas latent heat are correct. (Gas method.)

2. Based on the feed heat (coal latent heat) and the latent heat of the synthesis gas determined by a Transport Reactor energy balance, not the gas method, this method assumes that the synthesis gas latent heat is incorrect. (Solids method.)

3. Based on the coal feed heat determined by Transport Reactor energy balance and the synthesis gas sensible heat, this assumes that the coal feed is error. (Products method.)

The cold gas gasification efficiencies for the three calculation methods are shown in the plot in Figure 4.5-19. For all of the operating periods, the products method is between the solids and gas methods. The gas method is higher than the solids for each operating period when the energy balance has a negative error, which is all but two of the operating periods. Since the energy balance is good, all three methods are usually within 5 percent of each other. Only the products method is listed on Table 4.5-6 because the products method is probably the most accurate since it does not use the coal rate determined by carbon balance. The products analysis cold gas gasification efficiencies were between 58 to 65 percent.

The hot gasification efficiency is the amount of coal energy that is available to a gas turbine plus a heat recovery steam generator. The hot gas efficiency counts both the latent and sensible heat of the synthesis gas. Similar to the cold gasification efficiency and the sulfur removal, the hot gas efficiency can be calculated at least three different ways. Since the energy balance is off by up to -4 percent, each efficiency will be different. The three calculation methods for hot gasification are identical with the three methods of cold gasification efficiency calculation except for the inclusion of the synthesis gas sensible heat into the hot gasification efficiency.

The hot gasification efficiency assumes that the sensible heat of the synthesis gas can be recovered in a heat recovery steam generator, so the hot gasification efficiency is always higher than the cold gasification efficiency. The three gasification calculation methods are shown in the plot in Figure 4.5-20 and the products method given in Table 4.5-6.

For all of the operating periods, the products method is essentially equal to the solids method. This is because the amount of inlet coal heat is about the same as the total synthesis gas heat, and it makes little difference whether the synthesis gas heat or the coal heat is corrected. The gas method is higher than the solids and products methods except for when the energy balance has a negative error (only two of the operating periods). Since the energy balance is good, all three methods are usually within 5 percent of each other. The products method hot gasification efficiencies were from 91 to 96 percent. These high efficiencies are a result of the low PCD fines carbon content and low PCD fines rates. As with the cold gasification efficiencies, the hot gasification efficiency by-products should be more accurate than the hot gasification efficiencies by the gas and solids. It is possible to obtain higher than 100-percent gasification efficiencies because they are based on the feed coal heat, not the total feed heat. Greater than 100-percent gasification efficiencies imply that the sum of the steam and air input heat is greater than the heat loss and PCD solids heat, which is unlikely except at very high carbon conversions. The first five gas methods are over 110 percent, and are clearly in error.

Two main sources of losses in efficiency are the reactor heat loss and the latent heat of the PCD solids. The reactor heat loss of 1.5×10^6 Btu/hr is about 4 percent of the feed coal energy, while the total energy of the PCD solids was about 4.5 percent of the feed coal energy. The heat loss percentage will decrease as the reactor size is increased. While the Transport Reactor does not recover the latent heat of the PCD solids, this latent heat could be recovered in a combustor.

The heat of the PCD solids can be decreased by decreasing both the PCD solids carbon content (heating value) and the PCD solids rate.

Gasification efficiencies can be calculated from the adiabatic nitrogen-corrected gas heating values that are shown in Section 4.3. The adiabatic nitrogen-corrected cold gasification efficiencies shown in the plot in Figure 4.5-21 and the products method-corrected cold gasification efficiencies are listed in Table 4.5-6 for all of the operating periods. Only the cold gasification efficiencies based on the products are provided in Table 4.5-6 because they are the most representative of the actual gasification efficiencies. The products method adiabatic nitrogen-corrected cold gasification efficiencies were from 72 to 76 percent for TC06. The adiabatic nitrogen-correction increases the cold gasification efficiencies by about 8 percent for most of the operating periods. The adiabatic nitrogen correction does not increase the hot gasification efficiency because the deleted nitrogen lowers the synthesis gas sensible heat and increases the synthesis gas latent heat. Both changes effectively cancel each other out.

Table 4.5-1

Carbon Rates

Operating Period	Average Relative Hours	Carbon In (Feed)			Carbon Out (Products)					Carbon Conversion %
		Coal[1] lb/hr	Sorbent lb/hr	Total lb/hr	Syngas lb/hr	Standpipe[2] lb/hr	PCD Solids lb/hr	Accumulation lb/hr	Total lb/hr	
TC06-1	21	2,651	24	2,676	2,524	1.3	150	0.92	2,676	95.2
TC06-2	29	2,513	12	2,526	2,411	0.5	114	0.01	2,526	95.9
TC06-3	34	2,536	12	2,549	2,447	0.5	101	0.42	2,549	96.5
TC06-4	41	2,651	12	2,663	2,569	0.5	94	-0.01	2,663	96.9
TC06-5	55	2,594	12	2,605	2,502	0.2	103	0.03	2,605	96.5
TC06-6	74	2,798	17	2,816	2,689	0.2	126	-0.02	2,816	96.1
TC06-7	84	2,764	17	2,782	2,649	0.2	132	0.05	2,782	95.8
TC06-8	91	2,880	23	2,903	2,773	0.3	130	-0.03	2,903	96.3
TC06-9	124	2,715	23	2,738	2,604	0.3	134	-0.02	2,738	95.9
TC06-10	146	2,874	23	2,897	2,786	0.2	111	-0.02	2,897	96.9
TC06-11	153	2,866	23	2,889	2,781	0.1	108	0.02	2,889	97.0
TC06-12	189	2,721	24	2,745	2,619	0.2	126	0.07	2,745	96.2
TC06-13	199	2,817	25	2,842	2,727	0.2	114	0.03	2,842	96.8
TC06-14	222	2,751	25	2,775	2,653	0.4	122	-0.08	2,775	96.5
TC06-15	234	2,620	16	2,637	2,522	0.8	114	0.11	2,637	96.3
TC06-16	244	2,717	19	2,736	2,617	0.6	118	0.07	2,736	96.3
TC06-17	255	2,766	22	2,788	2,658	0.2	130	0.00	2,788	96.1
TC06-18	270	2,062	19	2,081	1,941	3.1	136	0.74	2,081	94.1
TC06-19	280	2,305	19	2,325	2,178	5.8	141	-0.38	2,325	94.5
TC06-20	297	2,292	19	2,311	2,156	1.0	154	0.30	2,311	94.1
TC06-21	309	2,279	19	2,298	2,135	0.7	162	0.04	2,298	93.7
TC06-22	336	2,421	19	2,440	2,263	0.3	177	0.04	2,440	93.5
TC06-23	354	2,495	19	2,514	2,349	0.3	165	0.03	2,514	94.1
TC06-24	374	2,459	15	2,474	2,307	0.5	166	0.13	2,474	93.8
TC06-25	390	2,517	15	2,532	2,365	0.6	166	-0.08	2,532	94.0
TC06-26	420	2,488	15	2,504	2,376	0.4	127	-0.01	2,504	95.5
TC06-27	449	2,472	17	2,490	2,373	0.8	116	-0.08	2,490	96.0
TC06-28	470	2,457	15	2,472	2,358	0.6	113	0.35	2,472	96.0
TC06-29	477	2,465	15	2,480	2,356	0.6	124	0.07	2,480	95.6
TC06-30	486	2,527	15	2,542	2,413	0.5	129	0.10	2,542	95.5
TC06-31	494	2,468	15	2,484	2,358	0.5	125	0.10	2,484	95.5
TC06-32	498	2,377	15	2,392	2,269	0.5	123	0.16	2,392	95.4

Notes:

1. Coal carbon determined by carbon balance.
2. Standpipe carbon flow intermittent. Rate shown is average FD0510 rate during operating period.

Table 4.5-1

Carbon Rates (continued)

Operating Period	Average Relative Hours	Carbon In (Feed)			Carbon Out (Products)					Carbon Conversion
		Coal[1] lb/hr	Sorbent lb/hr	Total lb/hr	Syngas lb/hr	Standpipe[2] lb/hr	PCD Solids lb/hr	Accumulation lb/hr	Total lb/hr	%
TC06-33	505	2,574	15	2,589	2,469	0.5	120	-0.02	2,589	95.9
TC06-34	520	2,544	15	2,559	2,439	0.4	119	0.05	2,559	95.9
TC06-35	534	2,495	15	2,510	2,392	0.4	117	0.06	2,510	95.9
TC06-36	548	2,627	15	2,642	2,509	0.4	133	-0.20	2,642	95.5
TC06-37	555	2,594	15	2,609	2,475	0.4	135	-0.22	2,609	95.4
TC06-38	569	2,517	15	2,532	2,389	0.4	143	-0.06	2,532	94.9
TC06-39	586	2,498	15	2,514	2,371	0.4	143	0.01	2,514	94.9
TC06-40	608	2,476	15	2,491	2,380	0.3	111	-0.04	2,491	96.1
TC06-41	643	2,621	15	2,636	2,552	0.2	84	0.00	2,636	97.4
TC06-42	648	2,486	12	2,498	2,411	0.2	87	0.05	2,498	97.0
TC06-43	670	2,597	15	2,613	2,517	0.1	96	0.00	2,613	96.9
TC06-44	695	2,601	15	2,616	2,506	0.1	110	0.00	2,616	96.3
TC06-45	711	2,406	15	2,422	2,303	0.2	119	0.00	2,422	95.7
TC06-46	719	2,578	14	2,592	2,480	0.9	112	0.28	2,592	96.2
TC06-47	760	1,944	15	1,959	1,896	0.8	62	-0.07	1,959	97.5
TC06-48	787	2,021	15	2,036	1,984	0.3	51	0.01	2,036	98.2
TC06-49	818	1,971	15	1,986	1,942	0.2	43	0.02	1,986	98.6
TC06-50	829	1,889	15	1,904	1,867	0.1	37	-0.01	1,904	98.8
TC06-51	840	1,931	8	1,939	1,898	0.1	41	-0.01	1,939	98.3
TC06-52	850	1,884	15	1,899	1,867	0.1	32	0.00	1,899	99.1
TC06-53	859	1,874	15	1,889	1,866	0.1	23	0.02	1,889	99.6
TC06-54	873	2,094	15	2,109	2,081	0.2	28	-0.02	2,109	99.4
TC06-55	896	2,312	15	2,327	2,286	0.3	41	0.03	2,327	98.9
TC06-56	908	2,375	15	2,390	2,343	0.2	47	-0.05	2,390	98.7
TC06-57	913	2,415	15	2,430	2,380	0.1	50	0.03	2,430	98.5
TC06-58	926	2,403	15	2,418	2,350	0.2	68	-0.01	2,418	97.8
TC06-59	941	2,510	15	2,525	2,438	0.2	87	-0.02	2,525	97.1
TC06-60	949	2,625	15	2,640	2,542	0.2	97	0.02	2,640	96.9
TC06-61	960	2,675	15	2,690	2,574	0.2	116	0.02	2,690	96.2
TC06-62	974	2,870	15	2,885	2,746	0.6	138	-0.02	2,885	95.7
TC06-63	998	2,938	15	2,953	2,795	0.9	157	0.01	2,953	95.1
TC06-64	1,016	2,930	15	2,945	2,785	0.3	160	0.04	2,945	95.1

Notes:

1. Coal carbon determined by carbon balance.
2. Standpipe carbon flow intermittent. Rate shown is average rate during operating period.

Table 4.5-2

Feed Rates, Product Rates, and Mass Balance

		Feeds (In)						Products (Out)							
Operating Period	Average Relative Hours	Coal[4] lb/hr	Sorbent FD0220 lb/hr	Air FI205 lb/hr	Nitrogen FI609[1] lb/hr	Steam FI204[2] lb/hr	Total lb/hr	Syngas FI465 lb/hr	PCD Solids FD0520 lb/hr	SP Solids FD0510[3] lb/hr	Reactor Accumulation lb/hr	Total lb/hr	In - Out lb/hr	(In- Out)/In %	PCD Solids/ Total Solids Out %
TC06-1	21	4,759	195	16,201	6,697	125	27,976	28,356	363	80	56	28,855	-879	-3.1	82
TC06-2	29	4,542	100	15,773	6,684	146	27,245	27,784	344	86	1	28,216	-971	-3.6	80
TC06-3	34	4,600	100	16,627	6,117	431	27,875	29,080	338	80	69	29,567	-1,691	-6.1	81
TC06-4	41	4,789	98	16,865	6,308	466	28,527	29,532	350	98	-3	29,977	-1,450	-5.1	78
TC06-5	55	4,633	98	16,721	6,313	681	28,446	29,426	377	88	10	29,900	-1,454	-5.1	81
TC06-6	74	4,926	150	16,868	6,494	329	28,767	29,686	417	99	-11	30,191	-1,424	-5.0	81
TC06-7	84	4,837	152	16,726	6,598	203	28,515	29,321	430	80	20	29,851	-1,336	-4.7	84
TC06-8	91	5,047	198	17,252	6,740	182	29,420	30,154	427	104	-13	30,672	-1,253	-4.3	80
TC06-9	124	4,826	198	16,690	6,777	12	28,504	29,207	414	98	-9	29,711	-1,207	-4.2	81
TC06-10	146	5,106	198	17,259	6,961	22	29,546	30,206	398	98	-9	30,692	-1,146	-3.9	80
TC06-11	153	5,082	198	17,163	6,950	19	29,412	30,009	395	81	14	30,499	-1,088	-3.7	83
TC06-12	189	4,816	206	16,233	6,730	4	27,989	28,487	332	88	32	28,939	-951	-3.4	79
TC06-13	199	4,976	210	16,799	6,613	6	28,605	29,276	396	90	11	29,774	-1,169	-4.1	81
TC06-14	222	4,824	210	16,575	6,753	1	28,363	28,916	396	113	-23	29,403	-1,040	-3.7	78
TC06-15	234	4,635	142	14,830	7,254	0	26,862	26,589	395	80	12	27,075	-213	-0.8	83
TC06-16	244	4,781	164	15,226	6,750	149	27,070	26,858	394	79	8	27,340	-270	-1.0	83
TC06-17	255	4,699	193	15,775	6,774	28	27,470	27,328	385	79	2	27,793	-323	-1.2	83
TC06-18	270	3,715	164	12,391	7,776	6	24,053	23,618	364	79	19	24,080	-27	-0.1	82
TC06-19	280	4,129	164	13,318	7,046	18	24,675	24,328	356	79	-5	24,758	-83	-0.3	82
TC06-20	297	4,071	164	13,213	6,623	80	24,151	23,760	378	80	24	24,242	-91	-0.4	83
TC06-21	309	4,053	164	13,265	6,749	16	24,247	23,969	394	80	5	24,448	-201	-0.8	83
TC06-22	336	4,226	164	13,625	6,474	29	24,518	24,226	429	80	9	24,744	-226	-0.9	84
TC06-23	354	4,261	164	14,080	6,546	61	25,112	24,772	453	80	8	25,313	-201	-0.8	85
TC06-24	374	4,277	129	13,880	6,441	37	24,764	24,490	451	80	23	25,043	-279	-1.1	85
TC06-25	390	4,395	130	14,093	6,502	15	25,134	24,694	441	110	-15	25,231	-97	-0.4	80
TC06-26	420	4,307	131	14,461	6,497	8	25,404	24,986	418	102	-3	25,503	-99	-0.4	80
TC06-27	449	4,333	148	14,464	6,426	27	25,399	25,051	348	104	-10	25,493	-94	-0.4	77
TC06-28	470	4,388	131	14,573	6,573	9	25,674	25,354	369	80	50	25,852	-178	-0.7	82
TC06-29	477	4,372	130	14,286	6,465	9	25,262	25,032	381	80	11	25,504	-243	-1.0	83
TC06-30	486	4,477	131	14,613	6,402	9	25,631	25,384	398	80	14	25,877	-245	-1.0	83
TC06-31	494	4,374	131	14,525	6,512	10	25,552	25,308	413	80	15	25,816	-264	-1.0	84
TC06-32	498	4,213	129	14,080	6,620	10	25,052	25,240	420	80	26	25,765	-713	-2.8	84

Notes:

1. Nitrogen feed rate reduced by 1,000 pounds per hour to account for losses in feed systems and seals.
2. Steam rate taken from FI204 for TC06-1 to TC06-17 and from FIC289 for TC06-18 to TC06-64.
3. FD0510 was not always operated during an entire test period. FD0510 flow rates shown have been prorated to account for the actual time of FD0510 operation.
4. Coal Rate by carbon balance.

Table 4.5-2

Feed Rates, Product Rates, and Mass Balance (continued)

		Feeds (In)						Products (Out)								
Operating Period	Average Relative Hours	Coal[4] lb/hr	Sorbent FD0220 lb/hr	Air FI205 lb/hr	Nitrogen FI609[1] lb/hr	Steam FIC298[2] lb/hr	Total lb/hr	Syngas FI465 lb/hr	PCD Solids FD0520 lb/hr	SP Solids FD0510[3] lb/hr	Reactor Accumulation lb/hr	Total lb/hr	In - Out lb/hr	(In- Out)/In %	PCD Solids/ Total Solids Out %
TC06-33	505	4,579	129	14,914	6,386	10	26,018	25,660	432	80	-3	26,168	-150	-0.6	84
TC06-34	520	4,575	130	14,969	6,623	8	26,305	25,936	417	79	9	26,440	-135	-0.5	84
TC06-35	534	4,319	129	14,767	6,626	79	25,920	25,553	398	79	11	26,041	-121	-0.5	83
TC06-36	548	4,588	129	14,999	6,491	56	26,263	26,668	435	79	-41	27,141	-878	-3.3	85
TC06-37	555	4,529	131	14,957	6,332	8	25,957	25,692	425	79	-46	26,150	-193	-0.7	84
TC06-38	569	4,389	129	14,456	6,447	12	25,433	25,212	411	83	-13	25,693	-260	-1.0	83
TC06-39	586	4,359	131	14,416	6,451	6	25,364	25,127	417	99	4	25,647	-283	-1.1	81
TC06-40	608	4,329	131	14,578	6,333	9	25,379	25,439	399	103	-11	25,929	-550	-2.2	80
TC06-41	643	4,572	129	15,449	6,413	82	26,645	26,691	350	80	-1	27,120	-475	-1.8	81
TC06-42	648	4,338	103	14,520	6,341	123	25,425	25,486	349	79	23	25,937	-512	-2.0	81
TC06-43	670	4,561	131	15,228	6,402	10	26,332	26,374	345	81	1	26,801	-468	-1.8	81
TC06-44	695	4,538	131	15,231	6,389	12	26,301	26,429	430	85	-1	26,944	-643	-2.4	83
TC06-45	711	4,176	130	14,353	6,786	12	25,457	25,608	395	82	-1	26,084	-627	-2.5	83
TC06-46	719	4,464	122	14,923	6,261	10	25,780	25,959	375	80	26	26,439	-659	-2.6	82
TC06-47	760	3,358	129	12,176	6,200	11	21,875	22,001	271	100	-8	22,365	-490	-2.2	73
TC06-48	787	3,483	129	12,450	6,028	8	22,098	22,284	245	98	4	22,632	-533	-2.4	71
TC06-49	818	3,410	129	12,213	6,106	9	21,867	22,018	225	103	14	22,360	-493	-2.3	69
TC06-50	829	3,286	129	12,032	6,167	5	21,618	21,843	218	103	-7	22,157	-539	-2.5	68
TC06-51	840	3,373	67	12,027	6,297	11	21,776	21,741	211	97	-8	22,041	-265	-1.2	68
TC06-52	850	3,299	129	11,841	6,297	6	21,573	21,331	204	107	1	21,643	-70	-0.3	66
TC06-53	859	3,289	129	12,129	6,115	7	21,669	21,456	200	91	26	21,772	-103	-0.5	69
TC06-54	873	3,648	129	13,161	6,047	20	23,005	23,013	205	109	-13	23,314	-308	-1.3	65
TC06-55	896	4,020	130	14,009	5,866	15	24,040	24,166	217	91	11	24,486	-446	-1.9	70
TC06-56	908	4,159	130	14,309	5,938	18	24,555	24,370	224	115	-25	24,685	-130	-0.5	66
TC06-57	913	4,226	131	14,471	5,933	37	24,797	24,906	231	80	19	25,237	-440	-1.8	74
TC06-58	926	4,180	130	14,087	5,577	87	24,061	24,021	253	109	-6	24,377	-316	-1.3	70
TC06-59	941	4,339	130	14,419	5,571	59	24,518	24,578	276	100	-9	24,945	-427	-1.7	73
TC06-60	949	4,525	129	15,055	5,715	16	25,440	25,582	286	79	8	25,956	-515	-2.0	78
TC06-61	960	4,601	130	15,167	5,902	28	25,828	25,913	307	88	7	26,315	-487	-1.9	78
TC06-62	974	4,954	128	16,099	6,129	22	27,332	27,491	332	89	-2	27,910	-578	-2.1	79
TC06-63	998	5,027	130	16,392	6,043	29	27,621	27,579	377	94	1	28,051	-430	-1.6	80
TC06-64	1016	5,014	131	16,124	6,019	13	27,301	27,376	411	88	11	27,887	-585	-2.1	82

Notes:

1. Nitrogen feed rate reduced by 1,000 pounds per hour to account for losses in feed systems and seals.
2. Steam rate taken from FI204 for TC06-1 to TC06-17 and from FIC289 for TC06-18 to TC06-64.
3. FD0510 was not always operated during an entire test period. FD0510 flow rates shown have been prorated to account for the actual time of FD0510 operation.
4. Coal Rate by carbon balance.

Table 4.5-3

Nitrogen, Hydrogen, Oxygen, and Silicon Mass Balances

Operating Period	Average Relative Hours	Nitrogen[1]		Hydrogen		Oxygen		Calcium		SiO_2	
		(In- Out) / In	In - Out	(In- Out) / In	In - Out	(In- Out) / In	In - Out	(In- Out) / In	In - Out	(In- Out) / In	In - Out
		%	lb/hr	%	lb/hr	%	lb/hr	%	lb/hr	%	lb/hr
TC06-1	21	1.1	218	-62.1	-203	-16.0	-886	61.6	63	-169.7	-149
TC06-2	29	0.5	98	-63.5	-201	-16.1	-859	30.7	22	-124.9	-97
TC06-3	34	-4.8	-908	-48.7	-172	-9.7	-566	12.9	9	-159.2	-130
TC06-4	41	-3.4	-661	-45.6	-168	-10.2	-608	-3.6	-3	-88.0	-74
TC06-5	55	-4.9	-938	-32.5	-124	-5.2	-317	-19.0	-14	-99.1	-78
TC06-6	74	-2.4	-471	-21.8	-79	-13.0	-770	-5.3	-5	-72.4	-59
TC06-7	84	-1.7	-326	-25.8	-88	-14.0	-806	-11.6	-10	-86.1	-68
TC06-8	91	-1.7	-336	-23.2	-82	-12.8	-763	4.8	5	-66.3	-56
TC06-9	124	-3.0	-594	-21.1	-67	-8.7	-489	5.6	6	-62.9	-51
TC06-10	146	-2.6	-520	-16.1	-54	-9.2	-535	11.8	12	-53.8	-51
TC06-11	153	-2.3	-467	-15.7	-53	-8.8	-511	13.3	14	-56.0	-55
TC06-12	189	-2.7	-516	-12.4	-39	-6.6	-359	34.4	36	-40.8	-40
TC06-13	199	-3.2	-624	-12.7	-42	-7.5	-424	13.3	14	-35.1	-37
TC06-14	222	-2.0	-386	-19.6	-62	-9.2	-513	21.8	23	-58.4	-52
TC06-15	234	2.7	512	-0.2	-1	-10.0	-506	11.3	10	-102.8	-85
TC06-16	244	2.3	427	3.8	12	-9.5	-508	18.7	17	-89.2	-78
TC06-17	255	2.4	453	-11.7	-37	-8.9	-475	25.5	26	-64.6	-61
TC06-18	270	2.3	391	-8.7	-21	-7.9	-331	10.0	8	-104.9	-73
TC06-19	280	1.7	289	-6.5	-18	-7.5	-343	15.4	13	-53.7	-38
TC06-20	297	1.1	177	-1.9	-5	-4.5	-204	10.0	9	-100.2	-66
TC06-21	309	0.4	75	-2.8	-8	-4.9	-221	9.3	8	-78.8	-52
TC06-22	336	0.2	29	-1.3	-4	-3.3	-154	1.7	2	-84.6	-58
TC06-23	354	0.5	82	-0.5	-1	-2.9	-138	-5.7	-5	-144.3	-82
TC06-24	374	0.1	14	0.7	2	-3.7	-177	-23.0	-18	-135.2	-84
TC06-25	390	1.1	196	-0.5	-1	-4.3	-205	-14.5	-11	-107.1	-74
TC06-26	420	1.3	232	-1.9	-5	-4.0	-196	-19.8	-15	-130.6	-84
TC06-27	449	1.0	177	-4.2	-12	-4.5	-220	3.7	3	-60.5	-45
TC06-28	470	0.7	115	-3.4	-10	-4.8	-237	-19.4	-15	-106.5	-77
TC06-29	477	0.5	85	-5.6	-16	-5.8	-281	-14.9	-12	-80.6	-55
TC06-30	486	0.4	71	-4.9	-15	-5.4	-269	-19.4	-15	-82.5	-57
TC06-31	494	0.4	63	-4.8	-14	-5.3	-257	-26.6	-21	-95.4	-65
TC06-32	498	-1.6	-282	-3.8	-11	-7.0	-330	-35.4	-27	-116.1	-76
TC06-33	505	1.0	170	-4.2	-13	-5.3	-266	-28.2	-23	-81.8	-59

Notes:

1. Nitrogen feed rate reduced by 1,000 pounds per hour to account for losses in feed systems and seals.

Table 4.5-3

Nitrogen, Hydrogen, Oxygen, and Silicon Mass Balances (continued)

Operating Period	Average Relative Hours	Nitrogen[1]		Hydrogen		Oxygen		Calcium		SiO_2	
		(In- Out) / In	In - Out	(In- Out) / In	In - Out	(In- Out) / In	In - Out	(In- Out) / In	In - Out	(In- Out) / In	In - Out
		%	lb/hr	%	lb/hr	%	lb/hr	%	lb/hr	%	lb/hr
TC06-34	520	0.7	119	-3.1	-9	-4.6	-233	-20.0	-16	-91.9	-69
TC06-35	534	1.1	189	-3.4	-10	-3.7	-186	-13.1	-10	-109.6	-71
TC06-36	548	-2.7	-490	-3.2	-10	-6.4	-328	-2.7	-2	-65.3	-46
TC06-37	555	0.9	166	-7.0	-21	-6.0	-301	0.9	1	-58.2	-39
TC06-38	569	1.1	197	-9.9	-29	-7.5	-367	-9.5	-7	-71.9	-46
TC06-39	586	1.2	209	-9.7	-28	-7.6	-372	-18.0	-14	-94.1	-61
TC06-40	608	0.8	145	-13.2	-38	-8.9	-434	-15.2	-12	-100.9	-67
TC06-41	643	1.6	292	-16.1	-50	-10.3	-542	-8.3	-7	-30.2	-28
TC06-42	648	1.5	258	-15.1	-45	-10.1	-504	-29.6	-21	-48.4	-42
TC06-43	670	1.3	237	-15.3	-46	-10.4	-532	-4.9	-4	-50.4	-37
TC06-44	695	0.9	160	-14.0	-42	-9.7	-494	-23.5	-19	-53.5	-49
TC06-45	711	1.1	191	-19.7	-54	-11.7	-563	-14.8	-11	-40.5	-35
TC06-46	719	1.5	265	-20.7	-61	-12.6	-630	-21.3	-16	-30.2	-29
TC06-47	760	1.7	266	-24.1	-54	-12.9	-518	-20.3	-14	-21.1	-16
TC06-48	787	0.9	141	-18.2	-42	-11.1	-458	-18.8	-13	-34.2	-23
TC06-49	818	1.2	182	-18.3	-41	-11.4	-459	-26.2	-18	-66.3	-36
TC06-50	829	0.8	129	-19.7	-43	-11.9	-469	-20.9	-14	-51.1	-27
TC06-51	840	2.9	445	-21.3	-48	-12.8	-508	-45.9	-23	-52.3	-28
TC06-52	850	4.0	619	-21.9	-48	-12.5	-491	-15.7	-11	-62.6	-33
TC06-53	859	3.6	558	-21.7	-48	-11.5	-457	-21.9	-15	-67.3	-36
TC06-54	873	2.3	375	-21.4	-52	-11.7	-511	-7.3	-5	-47.5	-27
TC06-55	896	1.0	168	-16.7	-45	-10.0	-466	-2.3	-2	-29.1	-20
TC06-56	908	2.0	344	-11.1	-31	-7.8	-372	6.6	5	-10.2	-8
TC06-57	913	0.3	59	-10.8	-31	-7.7	-376	4.2	3	-10.6	-9
TC06-58	926	0.7	113	-8.2	-23	-6.5	-311	3.2	2	-8.3	-7
TC06-59	941	0.5	82	-10.2	-30	-7.9	-388	1.4	1	-2.0	-2
TC06-60	949	0.4	61	-13.4	-40	-8.9	-451	3.4	3	-1.6	-1
TC06-61	960	0.7	122	-13.2	-40	-9.4	-483	0.3	0	-8.5	-7
TC06-62	974	0.1	27	-12.5	-41	-9.4	-514	9.2	8	-3.8	-3
TC06-63	998	0.9	162	-9.7	-32	-8.2	-457	-0.7	-1	-19.8	-17
TC06-64	1016	0.3	47	-12.1	-40	-8.8	-481	-15.4	-13	-26.4	-23

Notes:
1. Nitrogen feed rate reduced by 1,000 pounds per hour to account for losses in feed systems and seals.

Table 4.5-4

Typical Component Mass Balances

	Nitrogen[1]	Hydrogen	Oxygen	Calcium	SiO_2
Operating Period	TC06-61	TC06-61	TC06-61	TC06-61	TC06-61
Date	9/21/01	9/21/01	9/21/01	9/21/01	9/21/01
Time Start	09:30	09:30	09:30	09:30	09:30
Time End	21:00	21:00	21:00	21:00	21:00
Fuel	PRB	PRB	PRB	PRB	PRB
Sorbent	OH LS	OH LS	OH LS	OH LS	OH LS
Mixing Zone Temperature, °F	1,450	1,450	1,450	1,450	1,450
Pressure, psig	230	230	230	230	230
In, pounds/hr					
Fuel	29	281	1,406	41	75
Sorbent			60	39	3
Air	11,420	22	3,642		
Nitrogen	6,095				
Steam		3	25		
Total	17,545	305	5,133	81	78
Out, pounds/hr					
Synthesis Gas	17,422	344	5,573		
PCD Solids	1	1	37	54	52
Reactor			6	24	30
Accumulation			1	2	3
Total	17,423	346	5,616	80	84
(In-Out)/In, %	0.7%	-13.2%	-9.4%	0.3%	-8.5%
(In-Out), pounds per hour	122	-40	-483	0	-7

1. Feed nitrogen decreased by 1,000 pounds per hour.

Table 4.5-5

Sulfur Balances

Operating Period	Average Relative Hours	Feeds (In)	Products (Out)					In - Out	(In- Out)/In	Sulfur Removal			Sulfur
		Coal	Syngas	PCD Solids	Reactor	Accumulation	Total			Gas	Products	Solids	Emissions
		lb/hr	lb/hr	lb/hr	lb/hr	lb/hr	lb/hr	lb/hr	%	%	%	%	lb SO_2/MBtu
TC06-1	21	13.5	5.6	3.9	0.1	0.1	9.6	3.9	28.8	59	41	29	0.25
TC06-2	29	12.0	6.2	4.1	0.1	0.0	10.3	1.6	13.5	48	40	34	0.29
TC06-3	34	12.3	8.3	3.8	0.0	0.0	12.2	0.2	1.4	32	31	30	0.39
TC06-4	41	12.6	7.4	2.7	0.0	0.0	10.0	2.5	20.2	42	27	21	0.33
TC06-5	55	11.4	7.6	1.1	0.0	0.0	8.7	2.7	23.7	34	13	10	0.35
TC06-6	74	12.1	6.6	1.7	0.0	0.0	8.3	3.8	31.2	45	20	14	0.29
TC06-7	84	12.2	5.8	1.9	0.1	0.0	7.8	4.4	36.2	52	25	16	0.25
TC06-8	91	13.1	5.9	1.9	0.1	0.0	7.8	5.2	39.9	55	24	14	0.25
TC06-9	124	13.8	6.6	2.0	0.0	0.0	8.5	5.3	38.3	53	23	14	0.29
TC06-10	146	14.8	6.9	2.0	0.0	0.0	8.9	5.9	40.1	54	23	13	0.29
TC06-11	153	14.7	6.9	2.1	0.0	0.0	9.1	5.7	38.5	53	24	15	0.29
TC06-12	189	13.8	6.1	3.3	0.0	0.0	9.5	4.3	31.2	55	35	24	0.27
TC06-13	199	14.0	6.3	2.8	0.0	0.0	9.1	4.9	35.2	55	30	20	0.27
TC06-14	222	14.5	5.8	2.3	0.0	0.0	8.0	6.4	44.4	60	28	16	0.26
TC06-15	234	13.9	5.2	1.2	0.0	0.0	6.4	7.5	53.7	63	19	9	0.24
TC06-16	244	14.4	6.1	1.2	0.0	0.0	7.3	7.1	49.4	58	16	8	0.27
TC06-17	255	14.9	7.0	1.0	0.0	0.0	8.0	6.9	46.5	53	12	7	0.32
TC06-18	270	11.1	3.1	1.4	0.0	0.0	4.6	6.6	59.1	72	31	13	0.18
TC06-19	280	11.9	2.9	1.7	0.0	0.0	4.7	7.2	60.8	75	37	14	0.15
TC06-20	297	11.1	2.8	2.3	0.0	0.0	5.2	5.9	53.3	75	45	21	0.15
TC06-21	309	10.7	4.4	2.8	0.0	0.0	7.2	3.4	32.3	59	39	26	0.23
TC06-22	336	10.8	4.3	3.3	0.0	0.0	7.6	3.2	30.0	61	44	30	0.21
TC06-23	354	10.0	4.3	3.2	0.1	0.0	7.6	2.4	23.8	57	42	32	0.22
TC06-24	374	11.0	3.0	3.7	0.1	0.0	6.8	4.2	38.1	73	56	34	0.15
TC06-25	390	11.2	4.0	4.1	0.1	0.0	8.2	3.0	26.7	64	51	37	0.20
TC06-26	420	10.1	2.8	2.4	0.1	0.0	5.3	4.9	47.9	73	46	24	0.14
TC06-27	449	10.0	3.8	2.2	0.1	0.0	6.0	4.0	39.7	62	36	22	0.19
TC06-28	470	10.3	3.3	1.3	0.0	0.0	4.7	5.6	54.4	68	29	13	0.16
TC06-29	477	10.5	4.1	1.7	0.0	0.0	5.8	4.7	44.7	61	29	16	0.20
TC06-30	486	10.9	3.9	1.9	0.0	0.0	5.8	5.0	46.4	64	32	17	0.19
TC06-31	494	10.7	4.3	1.8	0.0	0.0	6.1	4.6	42.7	60	29	17	0.21
TC06-32	498	10.4	4.0	1.8	0.0	0.0	5.8	4.5	43.7	61	30	17	0.20

Notes:

1. Synthesis gas sulfur emissions determined from synthesis gas combustor SO_2 analyzer.

Table 4.5-5

Sulfur Balances (continued)

Operating Period	Average Relative Hours	Feeds (In)	Products (Out)					In - Out	(In- Out)/In	Sulfur Removal			Sulfur Emissions
		Coal lb/hr	Syngas lb/hr	PCD Solids lb/hr	Reactor lb/hr	Accumulation lb/hr	Total lb/hr	lb/hr	%	Gas %	Products %	Solids %	lb SO_2/MBtu
TC06-33	505	11.5	3.3	1.7	0.0	0.0	5.0	6.6	56.9	72	34	15	0.15
TC06-34	520	11.8	3.9	1.6	0.0	0.0	5.4	6.4	53.9	67	29	13	0.18
TC06-35	534	10.4	3.2	2.6	0.0	0.0	5.8	4.6	44.0	69	45	25	0.16
TC06-36	548	11.5	3.7	1.9	0.0	0.0	5.6	5.8	50.8	67	34	17	0.17
TC06-37	555	11.5	3.3	1.4	0.0	0.0	4.7	6.8	59.0	71	30	12	0.15
TC06-38	569	11.4	4.5	1.9	0.0	0.0	6.3	5.1	44.7	61	29	16	0.22
TC06-39	586	11.0	4.9	3.0	0.0	0.0	7.9	3.1	27.9	56	38	28	0.24
TC06-40	608	10.4	5.0	3.0	0.0	0.0	7.9	2.4	23.5	52	37	29	0.24
TC06-41	643	11.0	6.3	1.5	0.0	0.0	7.9	3.1	27.9	42	19	14	0.30
TC06-42	648	10.5	5.4	1.7	0.1	0.0	7.2	3.3	31.2	48	24	16	0.27
TC06-43	670	11.4	4.5	2.5	0.1	0.0	7.0	4.4	38.2	61	36	22	0.21
TC06-44	695	11.5	4.9	1.7	0.1	0.0	6.7	4.8	41.6	58	26	15	0.23
TC06-45	711	10.8	4.4	1.8	0.1	0.0	6.2	4.6	42.2	60	29	17	0.22
TC06-46	719	11.6	3.8	1.7	0.1	0.0	5.7	5.9	51.1	67	31	15	0.18
TC06-47	760	8.8	3.4	1.0	0.2	0.0	4.6	4.2	47.8	62	24	12	0.21
TC06-48	787	9.6	3.6	1.0	0.1	0.0	4.7	4.9	51.0	63	22	11	0.22
TC06-49	818	9.1	3.5	0.9	0.1	0.0	4.5	4.6	50.4	62	21	10	0.22
TC06-50	829	8.6	2.9	0.7	0.1	0.0	3.7	5.0	57.5	67	20	8	0.18
TC06-51	840	8.7	3.9	0.8	0.1	0.0	4.7	4.0	45.6	56	16	9	0.24
TC06-52	850	8.4	2.8	0.6	0.1	0.0	3.5	4.9	57.9	67	19	7	0.18
TC06-53	859	8.2	3.1	0.5	0.1	0.0	3.7	4.5	54.7	63	14	6	0.20
TC06-54	873	8.9	3.8	0.6	0.1	0.0	4.6	4.3	48.6	57	14	7	0.22
TC06-55	896	9.5	3.7	0.5	0.1	0.0	4.3	5.1	54.1	61	12	5	0.20
TC06-56	908	9.6	4.1	0.8	0.1	0.0	5.0	4.6	48.2	57	16	8	0.21
TC06-57	913	9.8	4.3	0.9	0.1	0.0	5.3	4.6	46.4	57	18	9	0.21
TC06-58	926	10.2	4.0	2.0	0.1	0.0	6.0	4.2	41.0	61	33	19	0.20
TC06-59	941	10.5	3.6	2.3	0.1	0.0	6.0	4.5	43.0	66	39	22	0.18
TC06-60	949	10.7	2.8	2.1	0.1	0.0	5.0	5.7	53.4	74	42	19	0.13
TC06-61	960	10.5	4.0	1.7	0.1	0.0	5.8	4.7	44.4	62	30	17	0.19
TC06-62	974	11.0	4.0	2.2	0.1	0.0	6.4	4.7	42.3	63	36	20	0.17
TC06-63	998	11.7	4.3	2.8	0.1	0.0	7.1	4.6	39.4	64	39	24	0.18
TC06-64	1016	11.8	4.0	3.3	0.0	0.0	7.3	4.5	37.8	66	45	28	0.17

Notes:
1. Synthesis gas sulfur emissions determined from synthesis gas combustor SO_2 analyzer.

Table 4.5-6

Energy Balances

Operating Period	Average Relative Hours	Feeds (In)				Products (Out)					In - Out	(In- Out)/In	Efficiency		
		Coal	Air	Steam	Total	Syngas	PCD Solids	Reactor Solids	Heat Loss	Total			Raw[2]		Corrected[2,4]
		10^6 Btu/hr	10^6 Btu/hr	10^6 Btu/hr	10^6 Btu/hr	10^6 Btu/hr	10^6 Btu/hr	10^6 Btu/hr	10^6 Btu/hr	10^6 Btu/hr	10^6 Btu/hr	%	Cold %	Hot %	Cold %
TC06-1	21	41.3	1.0	0.0	42.4	45.3	2.2	0.04	1.5	49.1	-6.7	-15.7	64.6	94.4	73.7
TC06-2	29	38.4	1.0	0.1	39.4	43.6	1.8	0.04	1.5	47.0	-7.6	-19.2	64.4	94.9	74.1
TC06-3	34	39.2	1.0	0.6	40.8	44.2	1.7	0.04	1.5	47.4	-6.6	-16.2	64.2	96.5	74.4
TC06-4	41	41.0	1.1	0.6	42.7	46.1	1.5	0.05	1.5	49.2	-6.5	-15.2	65.3	97.1	75.3
TC06-5	55	39.8	1.0	0.9	41.8	44.3	1.5	0.04	1.5	47.4	-5.7	-13.5	64.8	97.5	75.6
TC06-6	74	42.8	1.1	0.4	44.3	42.1	2.0	0.05	1.5	45.6	-1.4	-3.1	62.2	95.5	72.6
TC06-7	84	42.2	1.1	0.3	43.6	41.6	2.1	0.04	1.5	45.2	-1.7	-3.9	61.5	94.8	71.8
TC06-8	91	44.1	1.1	0.2	45.4	43.6	2.1	0.05	1.5	47.2	-1.8	-3.9	62.4	95.1	72.6
TC06-9	124	41.8	1.1	0.0	42.9	41.5	2.0	0.05	1.5	45.1	-2.2	-5.1	61.8	94.4	72.7
TC06-10	146	43.8	1.1	0.0	44.9	43.8	1.8	0.05	1.5	47.1	-2.2	-4.8	63.0	95.3	73.8
TC06-11	153	43.5	1.1	0.0	44.6	43.8	1.8	0.04	1.5	47.1	-2.5	-5.6	63.3	95.2	74.1
TC06-12	189	42.3	1.0	0.0	43.3	41.4	2.0	0.04	1.5	44.9	-1.6	-3.7	62.9	94.3	73.9
TC06-13	199	43.7	1.1	0.0	44.7	42.9	1.9	0.04	1.5	46.3	-1.5	-3.5	63.2	94.8	73.9
TC06-14	222	42.6	1.0	0.0	43.6	42.1	1.9	0.06	1.5	45.6	-2.0	-4.6	62.6	94.6	73.3
TC06-15	234	41.5	1.0	0.0	42.4	36.8	1.8	0.04	1.5	40.2	2.2	5.3	62.5	93.9	73.8
TC06-16	244	42.7	1.0	0.2	43.9	38.1	1.8	0.04	1.5	41.4	2.4	5.6	62.6	94.4	73.2
TC06-17	255	41.8	1.0	0.0	42.8	41.3	1.9	0.04	1.5	44.7	-1.9	-4.4	64.0	94.5	74.2
TC06-18	270	32.6	0.8	0.0	33.4	29.6	2.1	0.04	1.5	33.2	0.2	0.5	58.4	91.3	72.3
TC06-19	280	36.2	0.8	0.0	37.1	33.5	2.2	0.04	1.5	37.2	-0.1	-0.4	60.8	92.1	72.7
TC06-20	297	35.8	0.8	0.1	36.7	32.9	2.4	0.04	1.5	36.9	-0.2	-0.4	61.3	91.5	72.8
TC06-21	309	35.4	0.8	0.0	36.3	32.7	2.6	0.04	1.5	36.8	-0.5	-1.4	60.2	91.0	72.0
TC06-22	336	37.6	0.9	0.0	38.5	35.3	2.7	0.04	1.5	39.5	-1.1	-2.8	62.1	91.3	73.0
TC06-23	354	38.0	0.9	0.1	39.0	36.6	2.6	0.04	1.5	40.7	-1.7	-4.5	62.7	92.0	73.4
TC06-24	374	37.8	0.8	0.0	38.6	35.7	2.5	0.04	1.5	39.7	-1.0	-2.7	62.2	91.9	73.1
TC06-25	390	38.9	0.9	0.0	39.9	36.6	2.5	0.05	1.5	40.7	-0.8	-2.0	62.8	92.2	73.4
TC06-26	420	38.7	0.9	0.0	39.6	36.9	2.1	0.05	1.5	40.6	-0.9	-2.4	62.9	93.2	73.6
TC06-27	449	38.3	0.9	0.0	39.3	36.9	1.8	0.05	1.5	40.3	-1.0	-2.6	63.4	93.8	74.2
TC06-28	470	38.4	0.9	0.0	39.4	36.7	1.8	0.04	1.5	40.0	-0.6	-1.5	62.7	93.9	73.9
TC06-29	477	38.2	0.9	0.0	39.1	36.6	2.0	0.04	1.5	40.2	-1.0	-2.6	63.1	93.4	74.0
TC06-30	486	39.0	0.9	0.0	40.0	37.6	2.1	0.04	1.5	41.2	-1.2	-3.0	63.2	93.4	73.8
TC06-31	494	38.1	0.9	0.0	39.0	36.7	2.0	0.04	1.5	40.3	-1.2	-3.2	62.5	93.3	73.5
TC06-32	498	36.7	0.9	0.0	37.6	35.0	2.0	0.04	1.5	38.6	-1.0	-2.6	60.9	93.0	72.9

Notes:

1. Nitrogen and sorbent assumed to enter the system at ambient temperature and therefore have zero enthalpy.
2. Using coal inlet heat determined from energy balance.
3. Reference conditions are 80°F and 14.7 psia.
4. Correction is to assume that only air nitrogen is in the synthesis gas and that the reactor is adiabatic.

Table 4.5-6

Energy Balances (continued)

Operating Period	Average Relative Hours	Feeds (In)				Products (Out)					In - Out	(In- Out)/In	Efficiency		
		Coal	Air	Steam	Total	Syngas	PCD Solids	Reactor Solids	Heat Loss	Total			Raw[2]		Corrected[2,4]
													Cold	Hot	Cold
		10^6 Btu/hr	10^6 Btu/hr	10^6 Btu/hr	10^6 Btu/hr	10^6 Btu/hr	10^6 Btu/hr	10^6 Btu/hr	10^6 Btu/hr	10^6 Btu/hr	10^6 Btu/hr	%	%	%	%
TC06-33	505	39.8	1.0	0.0	40.8	38.5	2.0	0.04	1.5	42.0	-1.2	-3.1	63.6	93.8	74.0
TC06-34	520	39.9	0.9	0.0	40.9	38.1	1.9	0.04	1.5	41.5	-0.6	-1.5	63.1	93.9	73.9
TC06-35	534	38.3	0.9	0.0	39.2	37.4	2.0	0.04	1.5	40.9	-1.7	-4.4	62.8	93.6	73.7
TC06-36	548	40.5	1.0	0.0	41.5	39.4	2.2	0.04	1.5	43.1	-1.6	-3.9	62.4	93.4	73.4
TC06-37	555	40.1	1.0	0.0	41.1	38.9	2.2	0.04	1.5	42.6	-1.5	-3.7	63.4	93.4	73.5
TC06-38	569	39.0	0.9	0.0	40.0	37.5	2.2	0.04	1.5	41.3	-1.3	-3.3	62.7	92.9	73.1
TC06-39	586	38.7	0.9	0.0	39.6	37.1	2.2	0.05	1.5	40.8	-1.2	-3.1	62.6	92.9	73.1
TC06-40	608	38.3	0.9	0.0	39.3	37.4	1.8	0.05	1.5	40.8	-1.5	-3.9	62.8	93.9	73.5
TC06-41	643	40.5	1.0	0.1	41.6	40.2	1.4	0.04	1.5	43.1	-1.5	-3.6	64.3	95.6	74.6
TC06-42	648	38.4	0.9	0.0	39.4	37.9	1.4	0.04	1.5	40.8	-1.5	-3.7	64.1	95.0	74.7
TC06-43	670	40.1	1.0	0.0	41.1	39.5	1.5	0.04	1.5	42.6	-1.5	-3.7	63.8	95.0	74.2
TC06-44	695	40.1	1.0	0.0	41.0	39.3	1.8	0.04	1.5	42.6	-1.6	-3.9	63.2	94.3	73.6
TC06-45	711	37.0	0.9	0.0	37.9	36.1	1.9	0.04	1.5	39.6	-1.7	-4.4	61.4	93.3	72.7
TC06-46	719	39.7	1.0	0.0	40.6	39.0	1.8	0.04	1.5	42.4	-1.8	-4.3	63.5	94.2	73.6
TC06-47	760	30.0	0.7	0.0	30.8	29.6	1.1	0.05	1.5	32.2	-1.4	-4.5	60.6	94.1	73.6
TC06-48	787	31.0	0.8	0.0	31.8	30.8	0.9	0.05	1.5	33.2	-1.5	-4.6	62.0	95.0	74.8
TC06-49	818	30.3	0.7	0.0	31.1	30.1	0.7	0.05	1.5	32.4	-1.4	-4.4	61.9	95.2	75.1
TC06-50	829	29.1	0.7	0.0	29.8	28.8	0.6	0.05	1.5	31.0	-1.2	-4.1	60.7	95.1	74.6
TC06-51	840	29.8	0.7	0.0	30.5	29.6	0.7	0.05	1.5	31.9	-1.4	-4.4	61.7	95.2	75.0
TC06-52	850	29.1	0.7	0.0	29.8	29.0	0.5	0.05	1.5	31.1	-1.3	-4.2	61.8	95.5	75.2
TC06-53	859	29.0	0.7	0.0	29.7	29.1	0.4	0.04	1.5	31.0	-1.3	-4.4	61.4	95.9	74.6
TC06-54	873	32.2	0.8	0.0	33.1	32.5	0.5	0.05	1.5	34.5	-1.5	-4.5	63.0	96.3	75.1
TC06-55	896	35.5	0.9	0.0	36.5	35.8	0.7	0.04	1.5	38.0	-1.6	-4.4	64.5	96.4	75.7
TC06-56	908	36.8	0.9	0.0	37.7	36.7	0.8	0.06	1.5	39.0	-1.4	-3.6	64.6	96.3	75.3
TC06-57	913	37.4	0.9	0.0	38.3	37.3	0.8	0.04	1.5	39.7	-1.3	-3.5	64.8	96.4	75.8
TC06-58	926	37.0	0.9	0.1	38.0	36.9	1.1	0.05	1.5	39.6	-1.6	-4.2	65.0	95.6	75.4
TC06-59	941	38.6	0.9	0.1	39.5	38.3	1.3	0.05	1.5	41.2	-1.6	-4.1	65.2	95.2	75.1
TC06-60	949	40.3	0.9	0.0	41.3	40.0	1.5	0.04	1.5	43.0	-1.7	-4.2	65.1	95.0	74.8
TC06-61	960	41.1	0.9	0.0	42.1	40.5	1.7	0.04	1.5	43.7	-1.7	-4.0	64.7	94.6	74.3
TC06-62	974	44.1	1.0	0.0	45.1	43.2	2.0	0.04	1.5	46.8	-1.6	-3.6	64.8	94.5	74.1
TC06-63	998	45.3	1.0	0.0	46.3	43.9	2.3	0.05	1.5	47.7	-1.4	-3.1	64.7	94.1	73.6
TC06-64	1,016	45.1	1.0	0.0	46.1	44.0	2.4	0.04	1.5	47.9	-1.8	-3.8	65.1	93.8	73.9

Notes:

1. Nitrogen and sorbent assumed to enter the system at ambient temperature and therefore have zero enthalpy.
2. Using coal inlet heat determined from energy balance.
3. Reference conditions are 80°F and 14.7 psia.
4. Correction is to assume that only air nitrogen is in the synthesis gas and that the reactor is adiabatic.

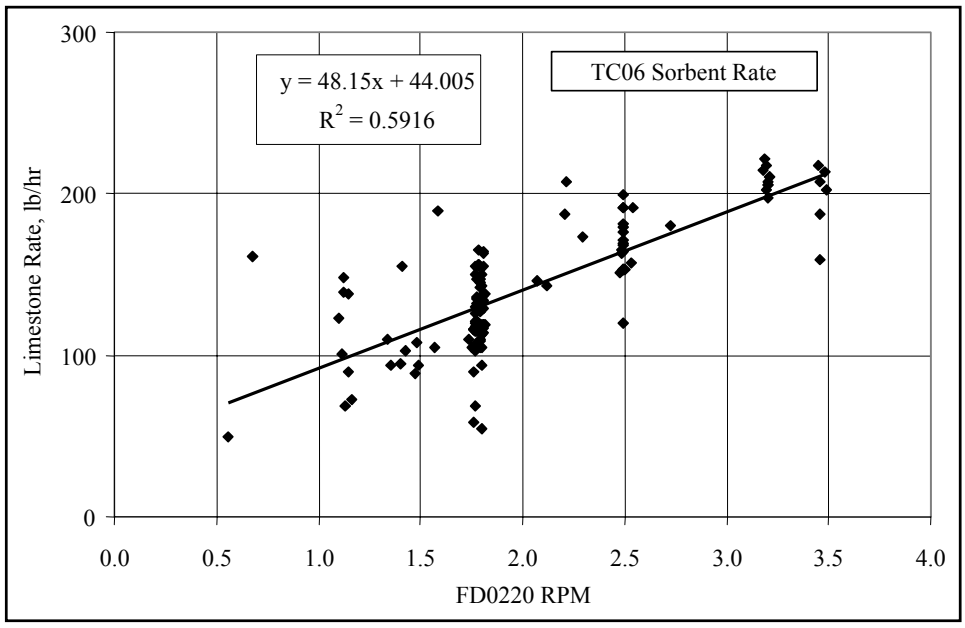

Figure 4.5-1 Sorbent Feeder Correlation

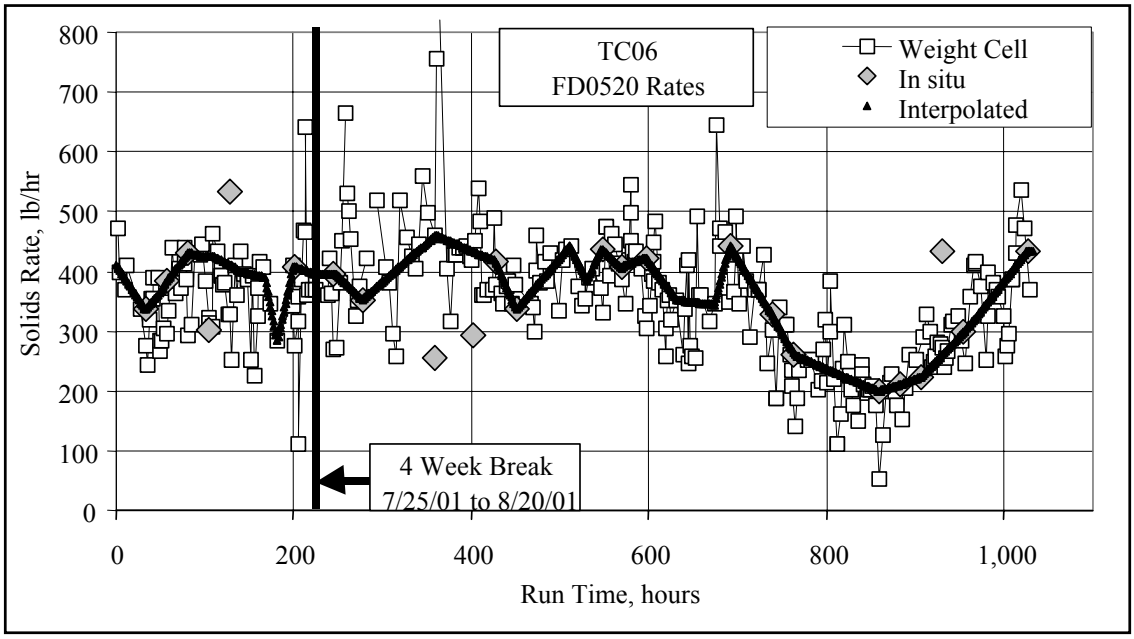

Figure 4.5-2 PCD Fines Rate

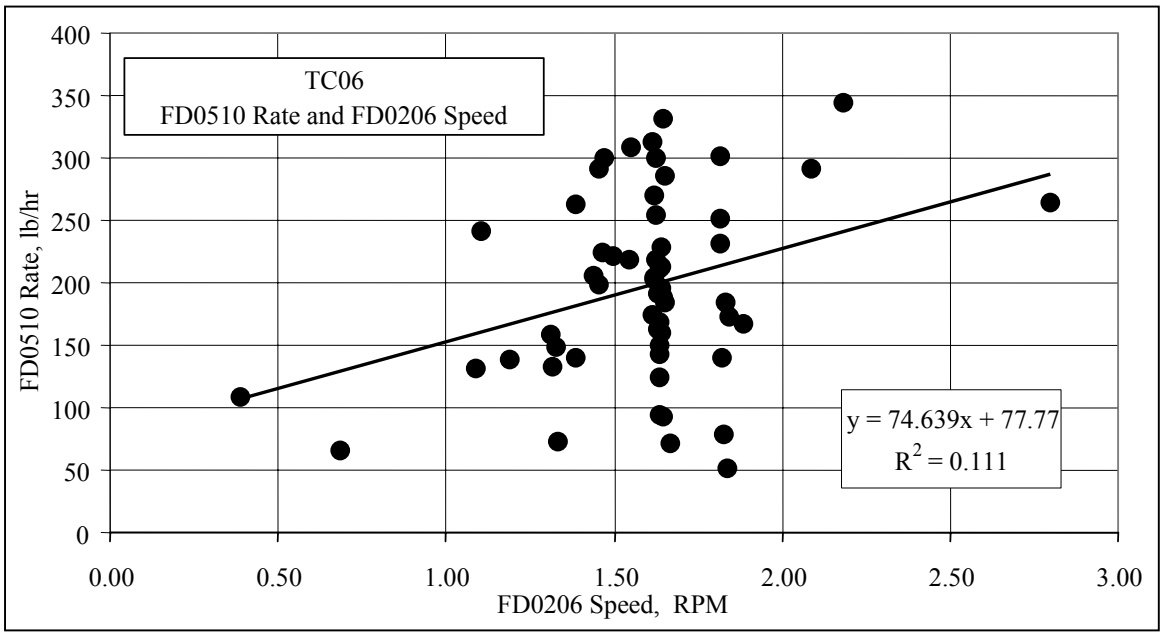

Figure 4.5-3 FD0510 Rate Correlation

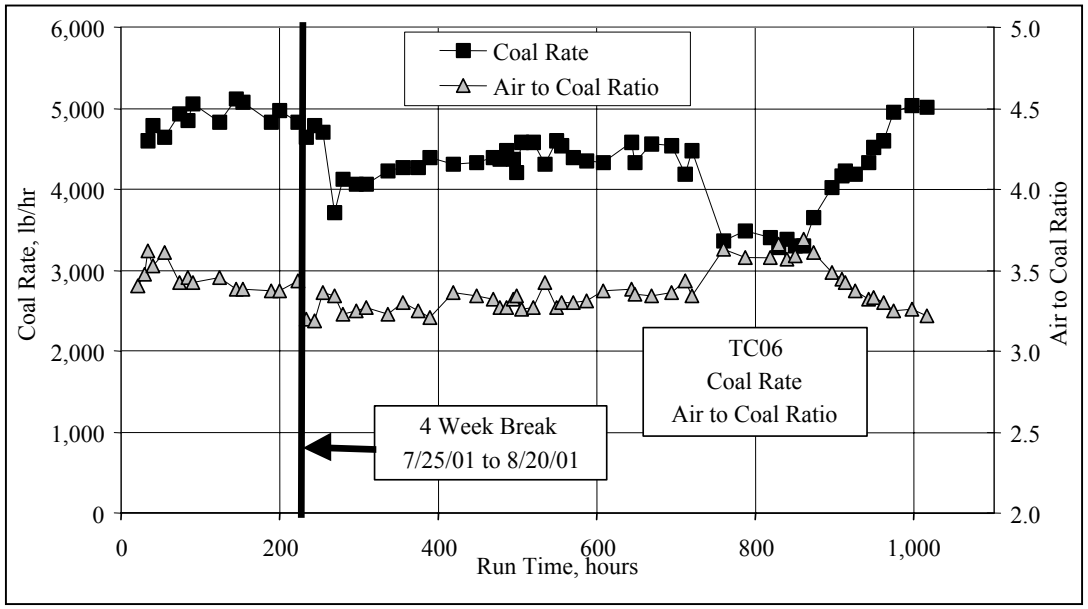

Figure 4.5-4 Coal and Air-to-Coal Ratio

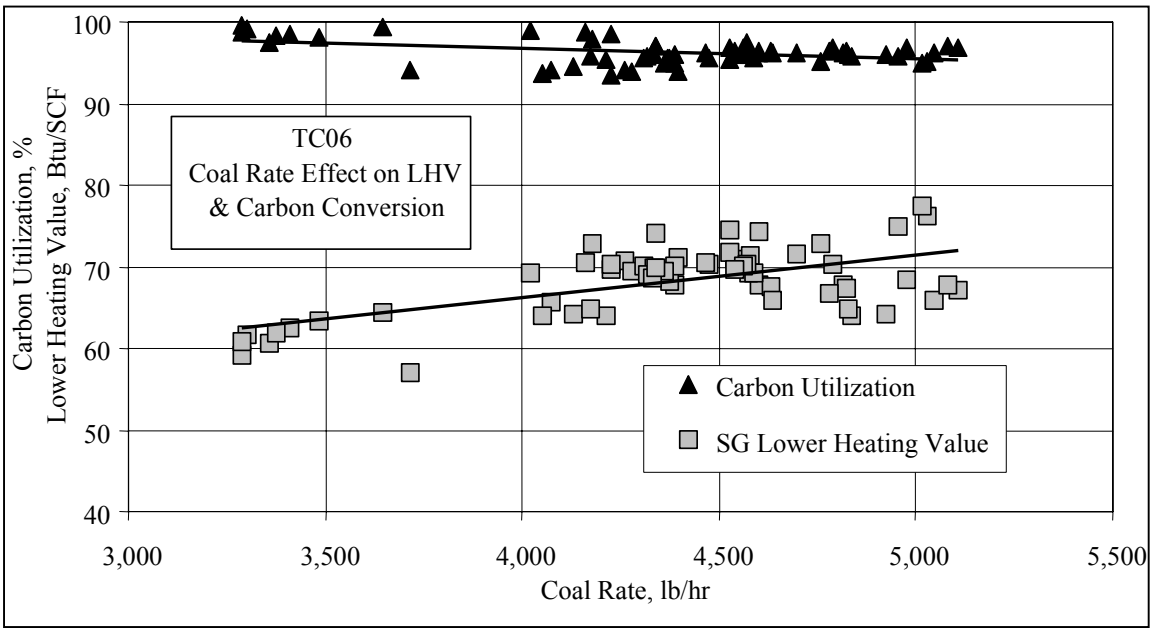

Figure 4.5-5 Effect of Coal Rate on LHV and Carbon Conversion

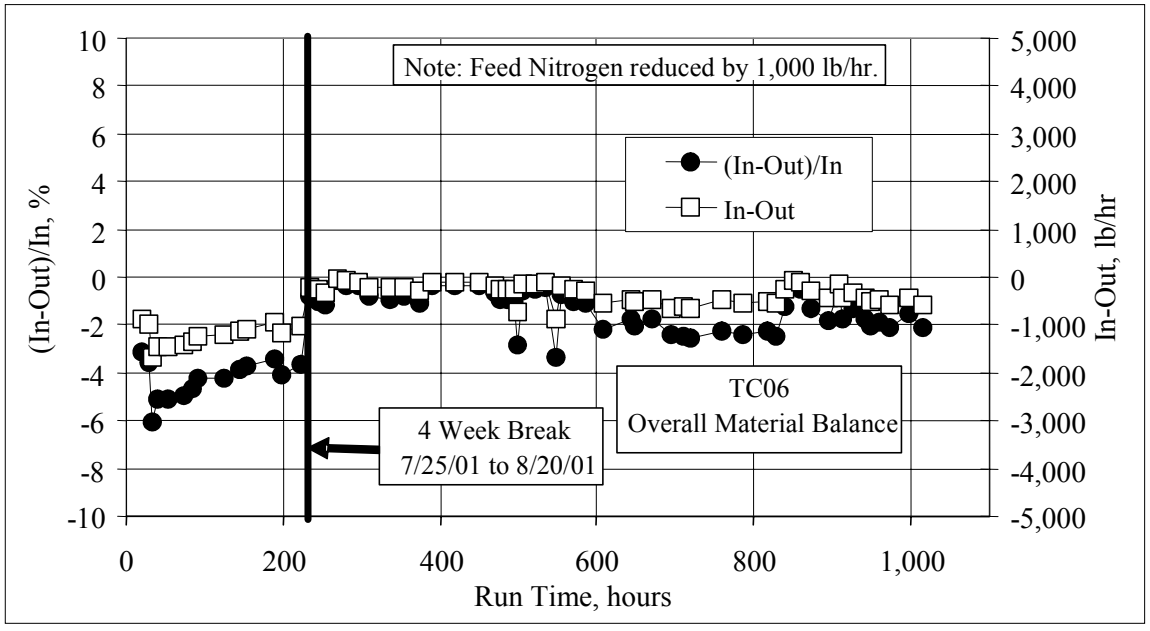

Figure 4.5-6 Overall Material Balance

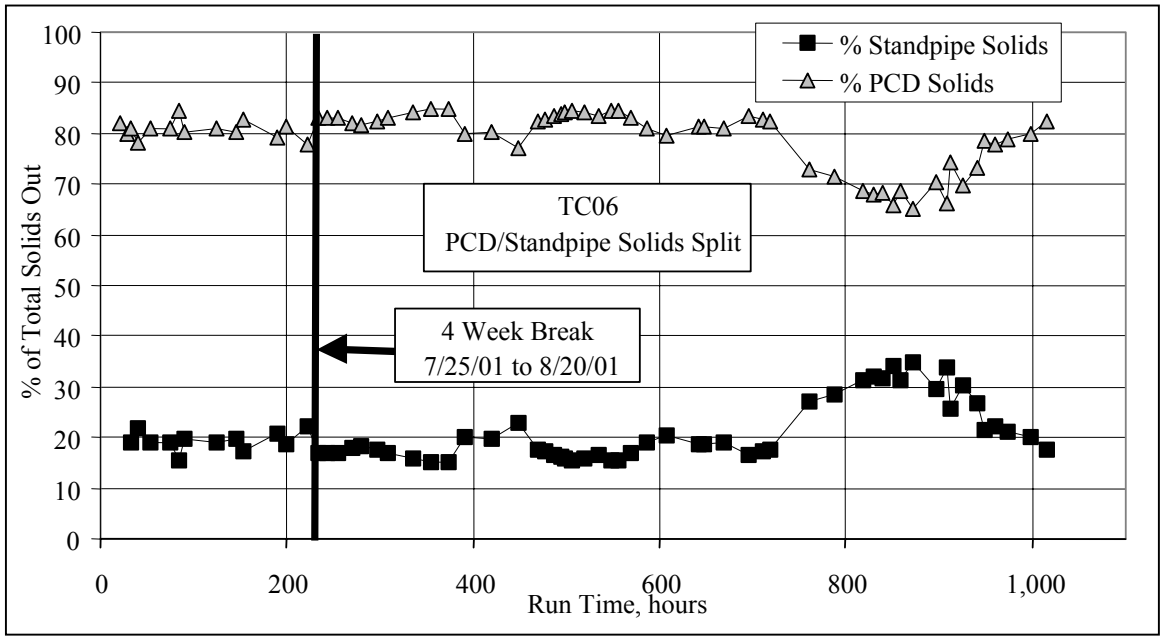

Figure 4.5-7 Reactor Products Flow Split

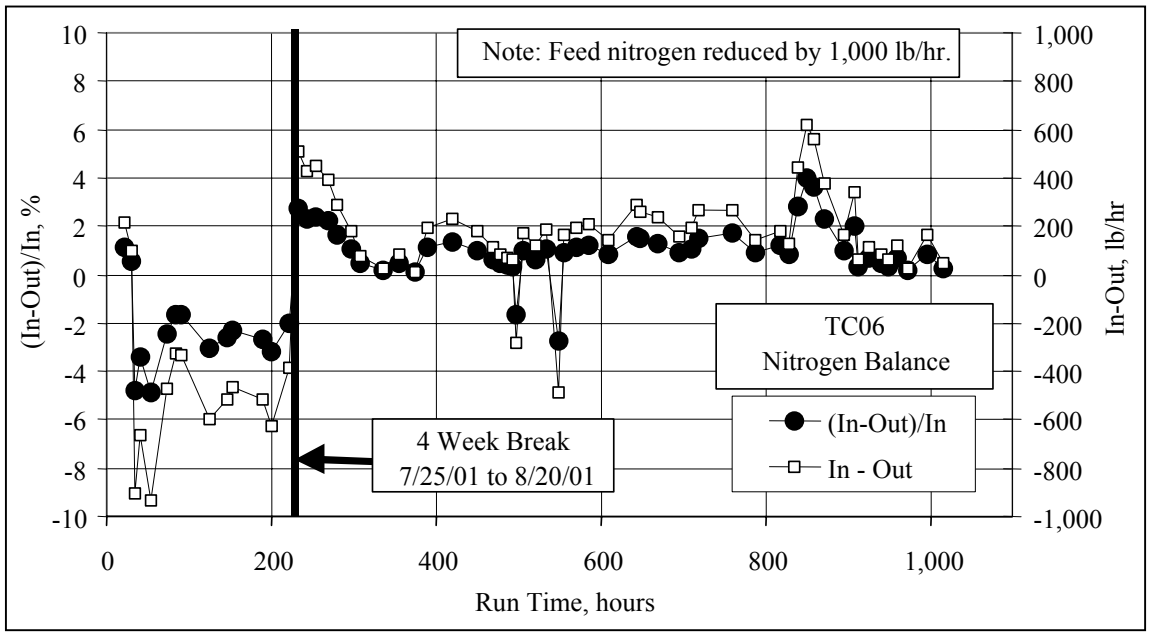

Figure 4.5-8 Nitrogen Balance

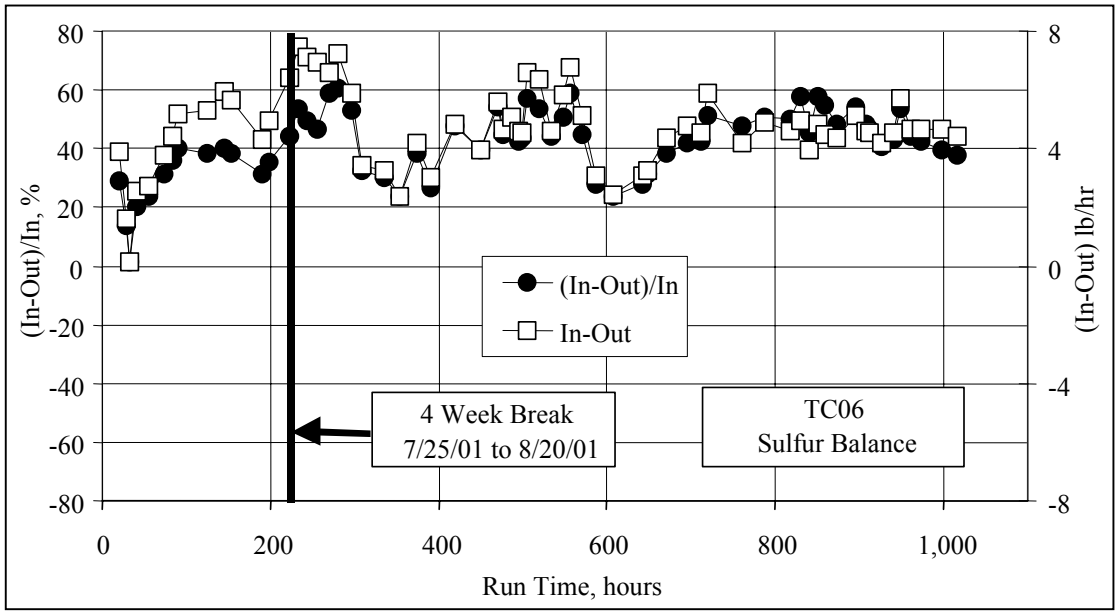

Figure 4.5-9 Sulfur Balance

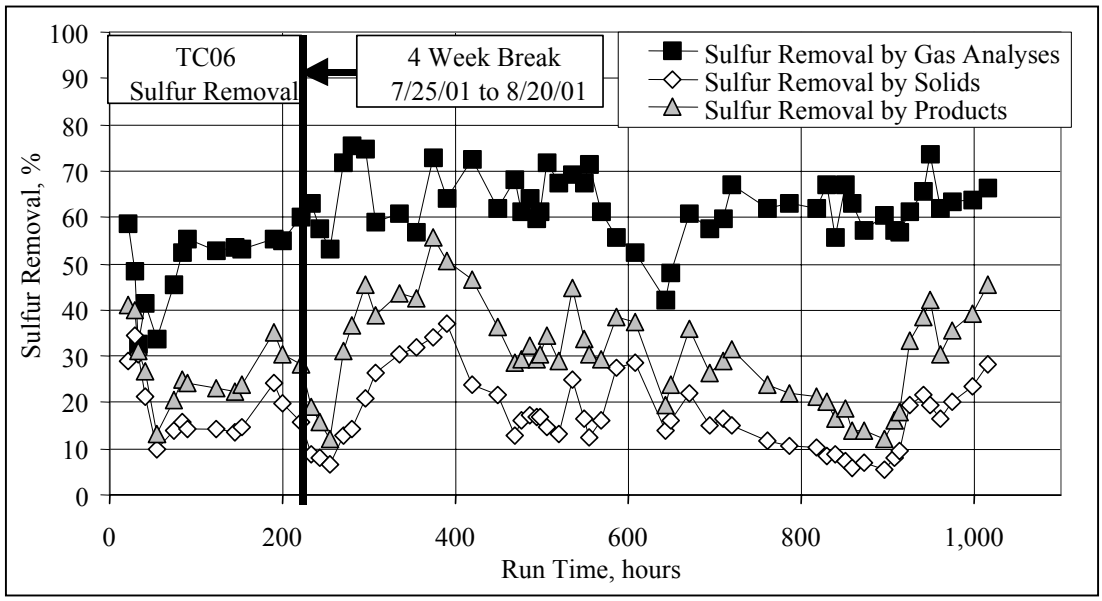

Figure 4.5-10 Sulfur Removal

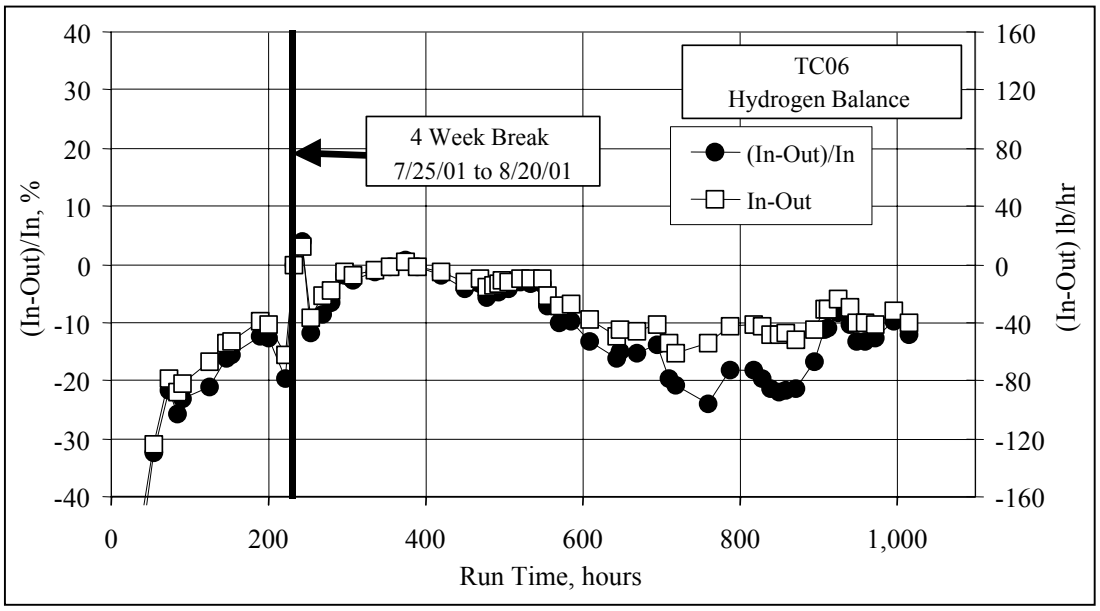

Figure 4.5-11 Hydrogen Balance

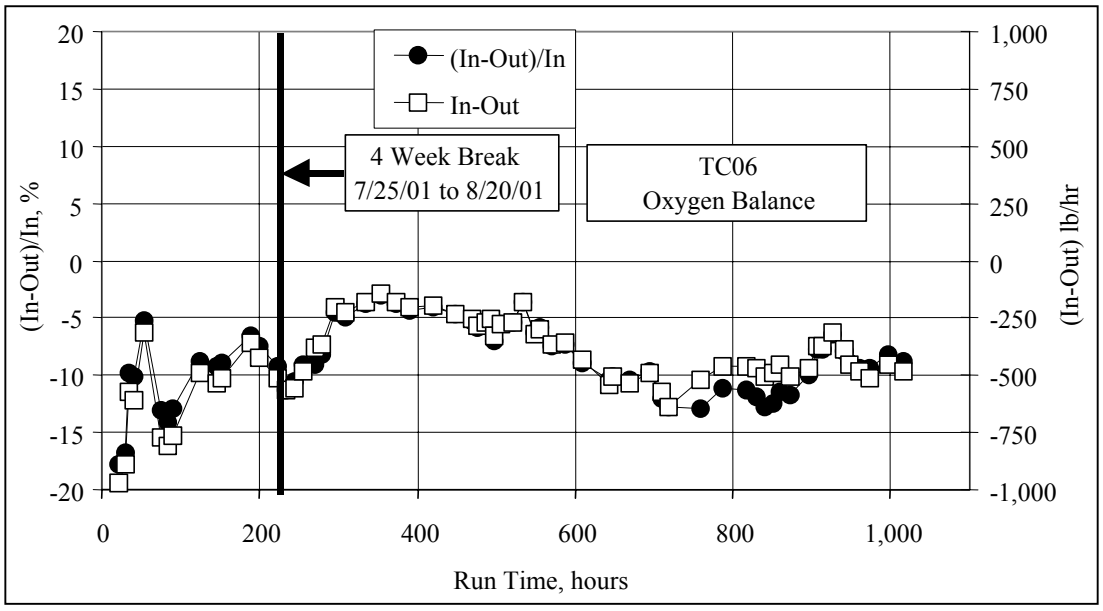

Figure 4.5-12 Oxygen Balance

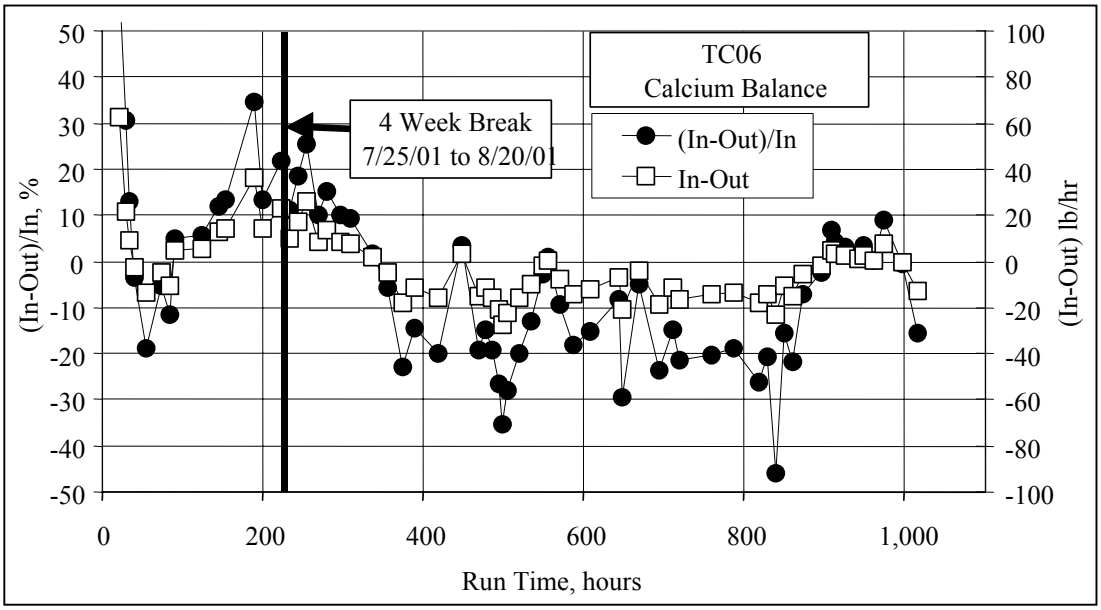

Figure 4.5-13 Calcium Balance

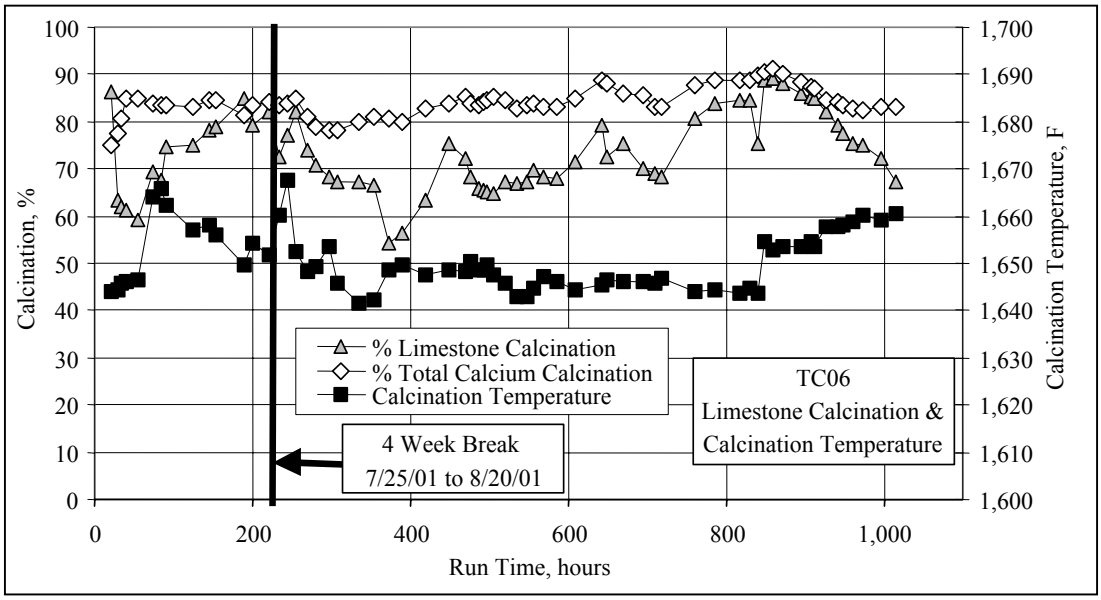

Figure 4.5-14 Calcination and Calcination Temperature

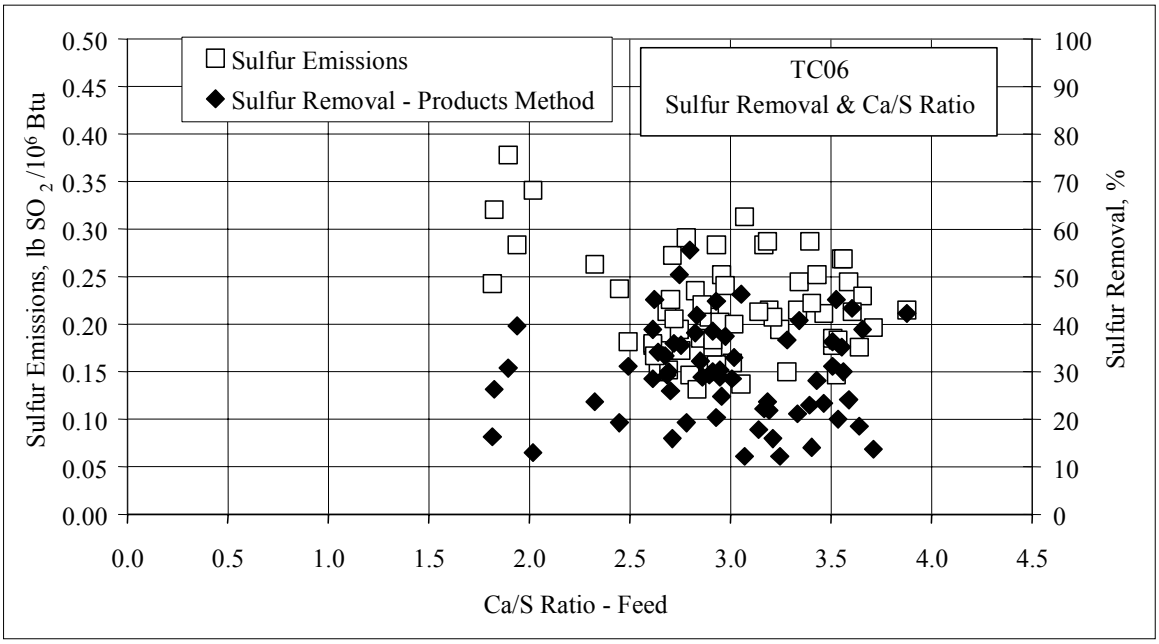

Figure 4.5-15 Sulfur Emissions and Feed Ca/S Ratio

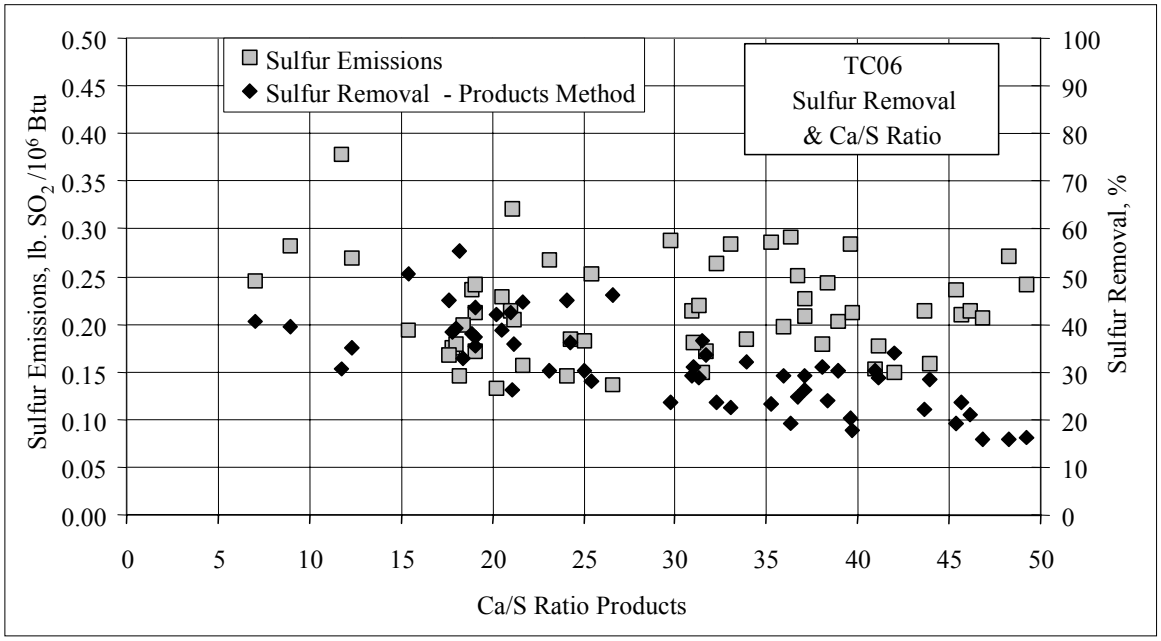

Figure 4.5-16 Sulfur Emissions and PCD Solids Ca/S Ratio

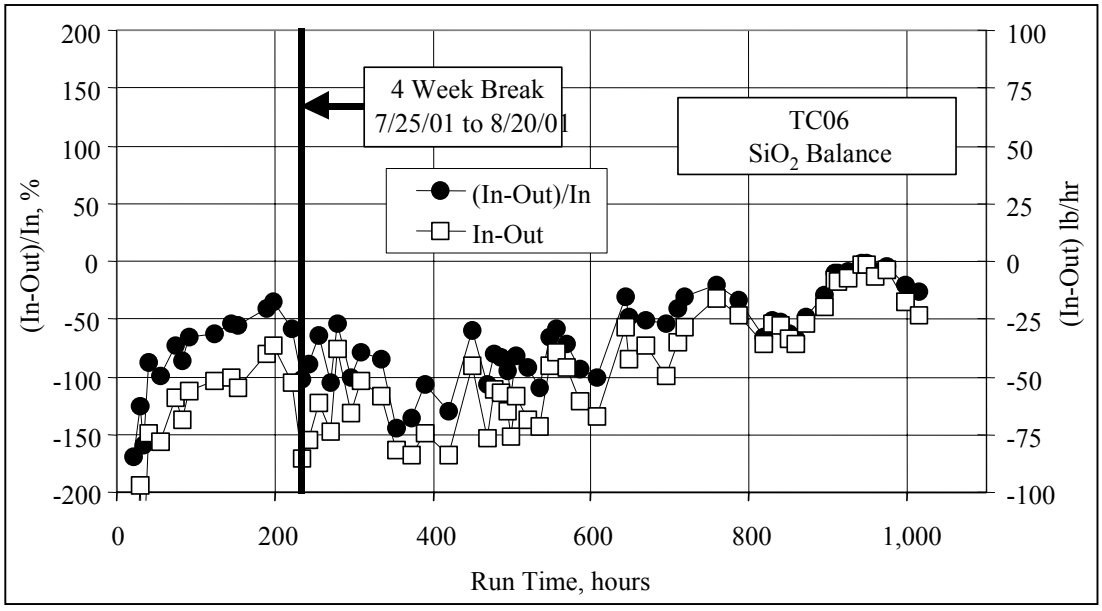

Figure 4.5-17 SiO_2 Balance

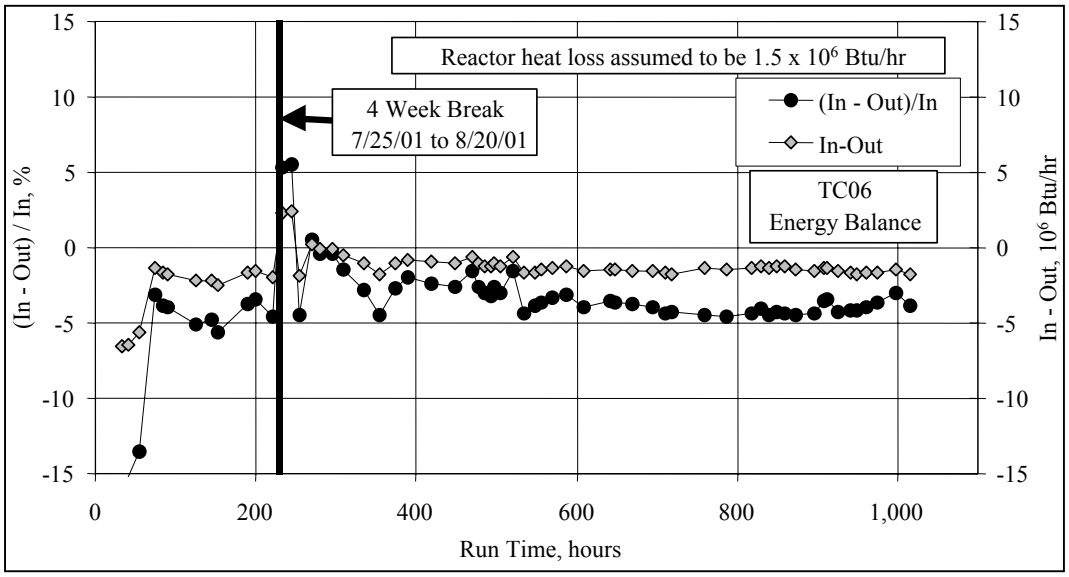

Figure 4.5-18 Energy Balance

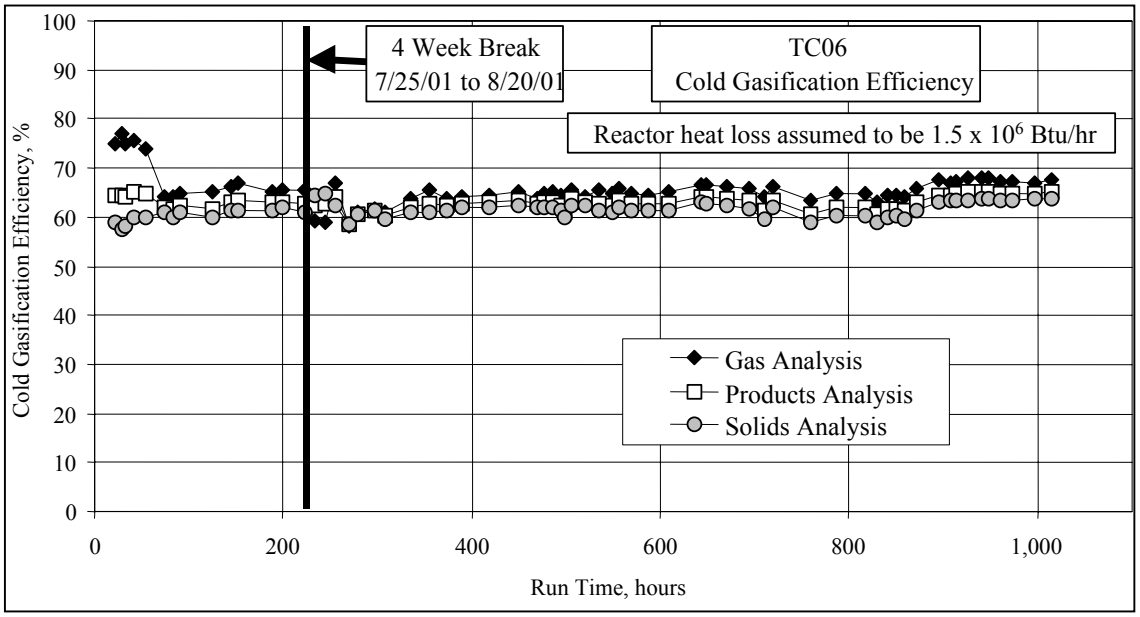

Figure 4.5-19 Cold Gasification Efficiency

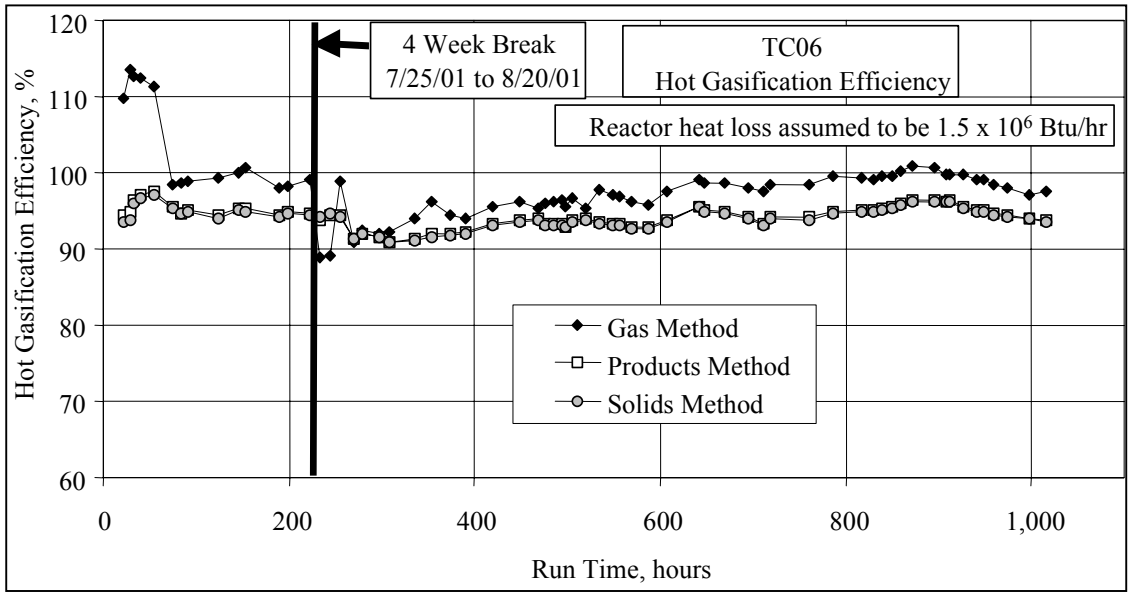

Figure 4.5-20 Hot Gasification Efficiency

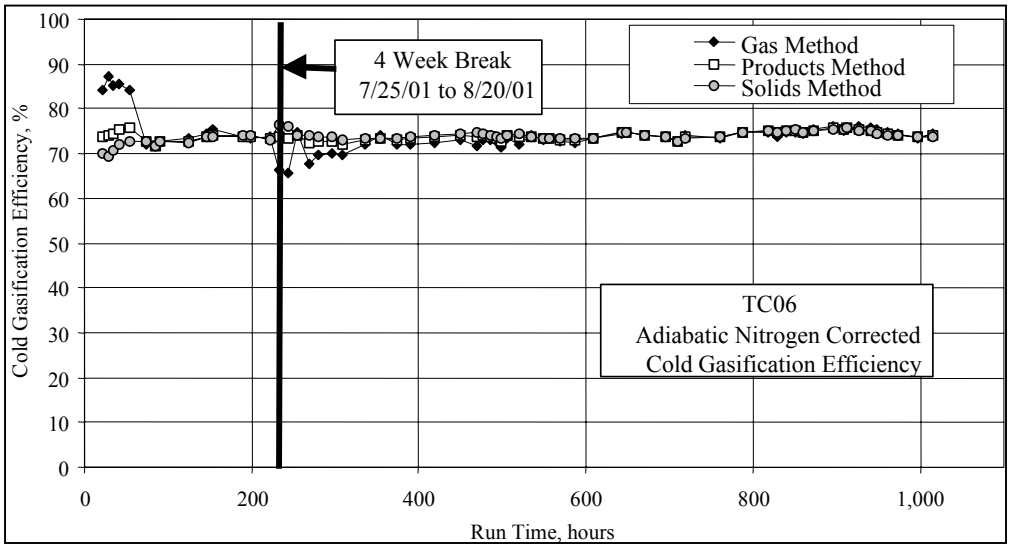

Figure 4.5-21 Nitrogen-Corrected Cold Gasification Efficiency

4.6 SULFATOR OPERATIONS

During TC06, the sulfator (atmospheric fluidized-bed combustor, AFBC) was operated for almost 1,500 hours and fired gasification ash (g-ash) from the gasifier for a total of 524 hours. The average bed temperature during fuel feed was about 1,370ºF with about 12 percent of the time spent above 1,500ºF compared to a design operating temperature of 1,600 to 1,650ºF. The lower temperature operations were sufficient to achieve high carbon conversion and to sulfate calcium sulfide to calcium sulfate. Figure 4.6-1 shows the percentage of carbon found in the g-ash fed to the sulfator and in the ash exiting the sulfator. The carbon content in the feed material to sulfator ranged from 10 to 50 percent. A large percentage of feed to the sulfator was fine ash, sorbent-derived materials and g-ash collected by PCD. The carbon content of the fine ash from the sulfator was below 1 percent. Figure 4.6-2 shows the percentage sulfides found in the g-ash fed to the sulfator and in the ash exiting the sulfator. The sulfides in PCD fines ranged from 0.2 to 1.5 percent, while the sulfide content of fine ash from sulfator was nearly zero during most of the test run, indicating high conversion of sulfide to sulfate in the sulfator.

At startup, the sulfator is filled with sand as a start-up bed material. As the run progresses, some of the same are elutriated out of the bed while some of the ash material from the g-ash collects in the bed. Most of the g-ash fed to the sulfator is fine and it is carried over to the baghouse with little accumulation in the sulfator. Figure 4.6-3 shows the average particle size of the g-ash feed, the ash carried over to the baghouse, and the solids collected from the sulfator overflow. Notice that the feed has a very small particle size and that the average particle size of the bed declines as ash accumulates, which is due to attrition and elutriation of the sand.

During previous runs the bed has become less well mixed as the test run progressed. Early in the run all bed thermocouples will read within about 100ºF of one another, but after a few hundred hours of operation the range can be greater than 1,000ºF. This has been attributed to refractory that has spalled from the walls blocking some of the nozzles on the air distribution grid. Before TC06, the refractory walls of the sulfator were sprayed with sodium silicate to harden the refractory. As can be seen in Figure 4.6-4, the temperature profile remained within a narrow range throughout TC06. In addition, an inspection carried out after the run indicated that the refractory was mostly intact.

To help with startup, a modification was made to the sulfator steam system prior to TC06. The steam flow control valve is unable to adequately control steam flow at the lower flows that is needed for startup. This results in much higher than needed steam flow to the cooling coils and reduced bed temperature. To counter this, a small bypass has been added around the main control valve with a smaller controller to be used for start-up conditions. For TC06, this arrangement provided about 40ºF higher bed temperature from the start-up heater. Additional gains in bed temperature from the heater are expected to be achieved in future test runs as the new configuration can further reduce steam flow.

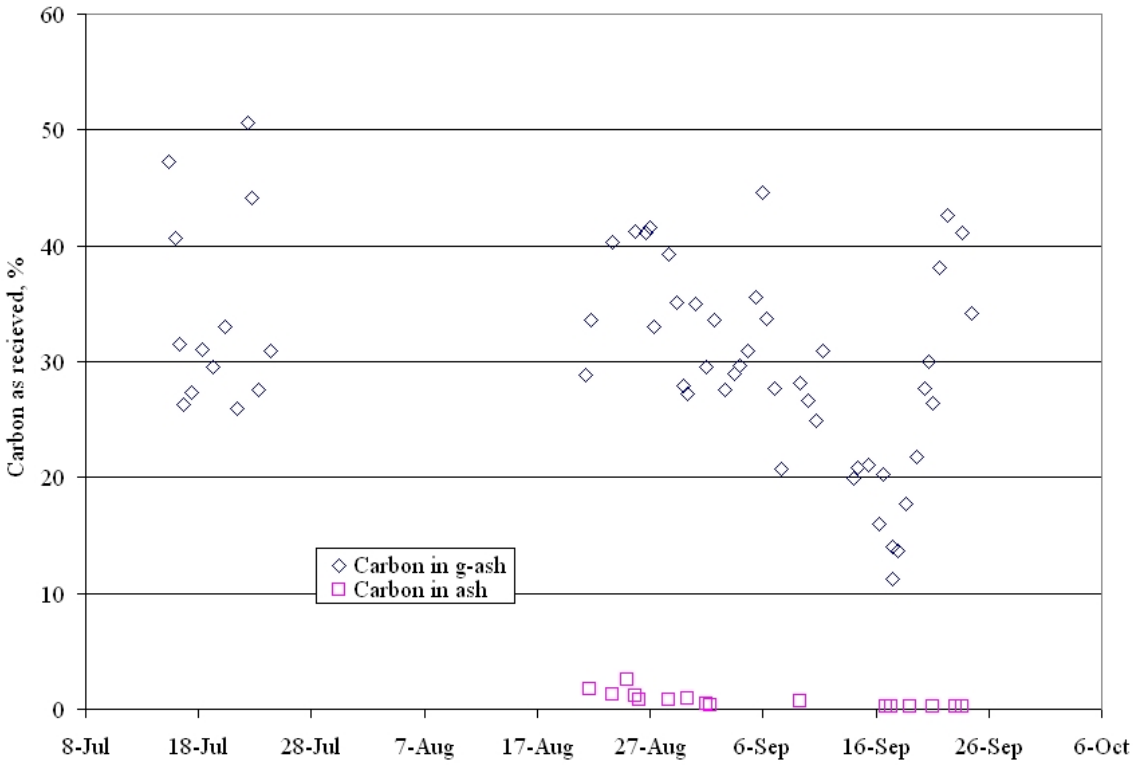

Figure 4.6-1 Carbon in G-ash (Feed) and Ash

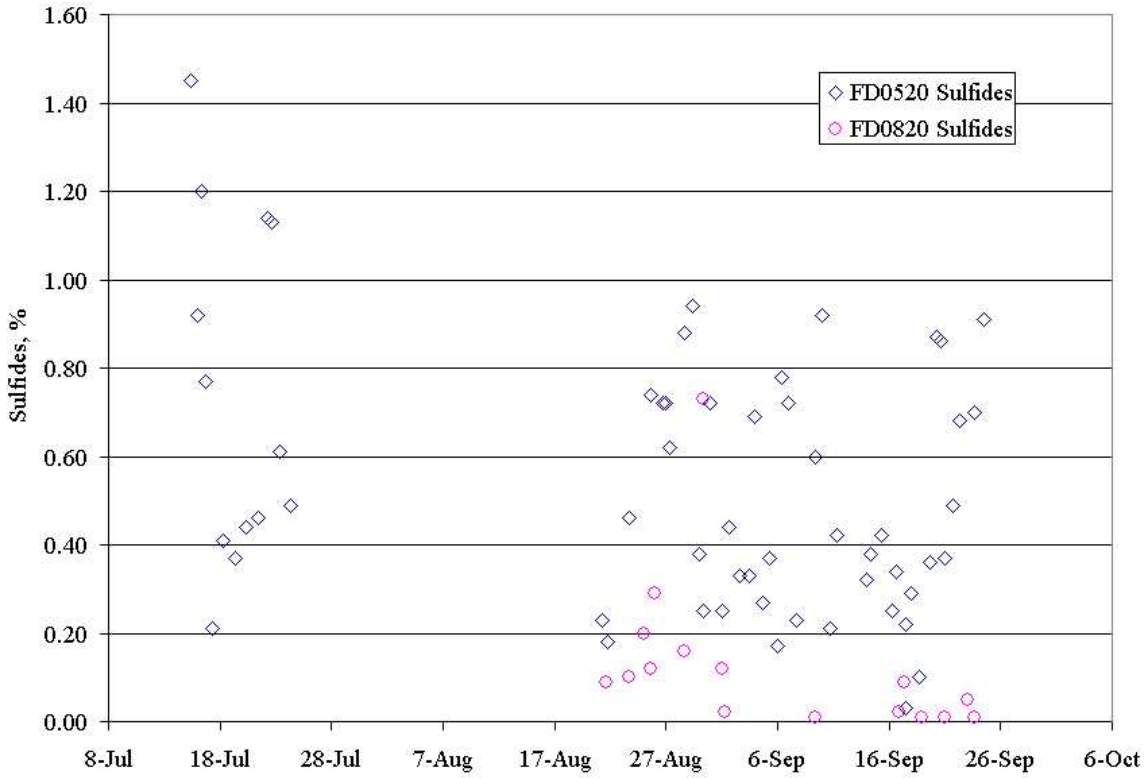

Figure 4.6-2 Sulfides in G-ash (Feed) and Ash

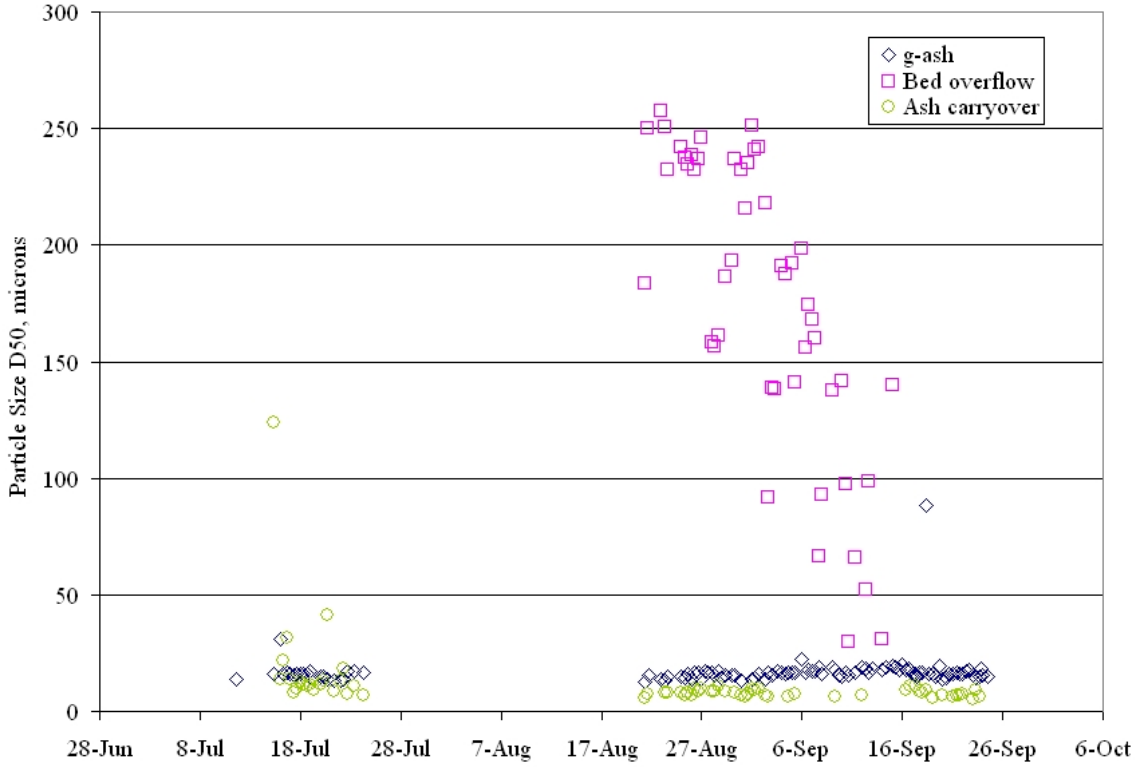

Figure 4.6-3 Particle Size of Feed G-ash, Ash, and Bed

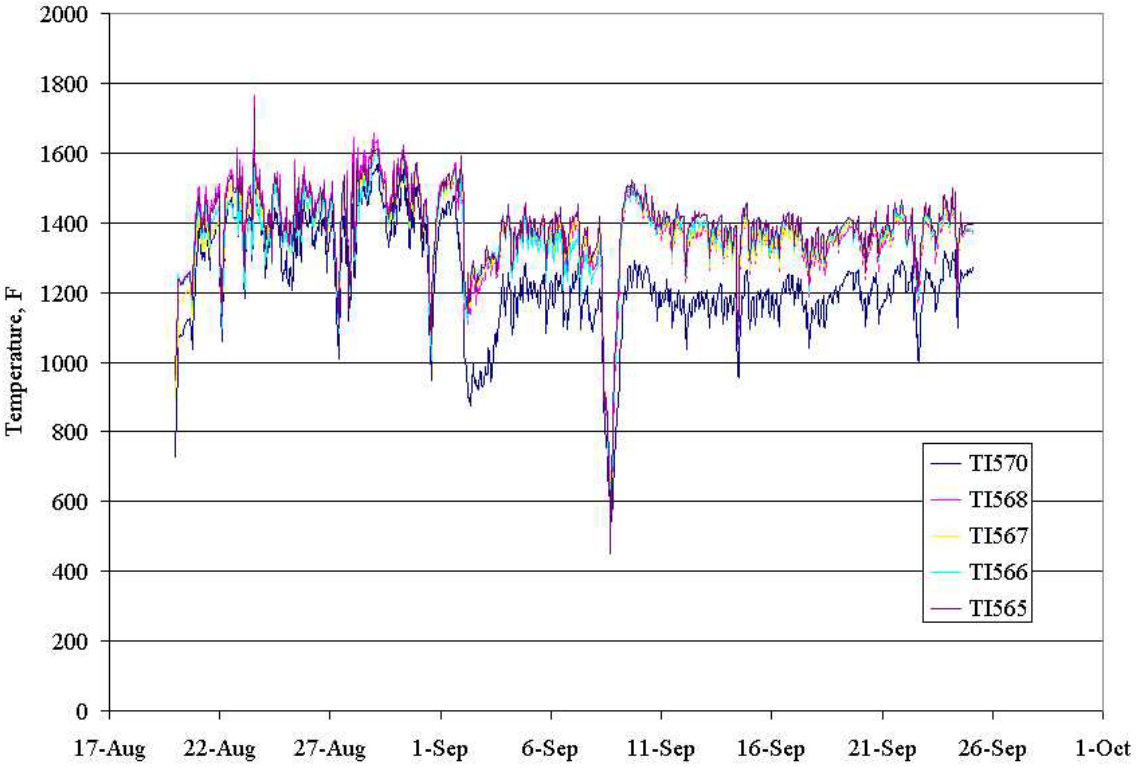

Figure 4.6-4 Temperature Profile of Bed

4.7 PROCESS GAS COOLERS

Heat transfer calculations were done on the primary gas cooler, HX0202, and the secondary gas cooler, HX0402, to determine if their performance had deteriorated during TC06 due to tar or other compounds depositing on the tubes.

The primary gas cooler is between the Transport Reactor cyclone, CY0201, and the Siemens Westinghouse PCD, FL0301. During TC06, HX0202 was not bypassed and took the full gas flow from the Transport Reactor. The primary gas cooler is single-flow heat exchanger with hot gas from the Transport Reactor flowing through the tubes and the shell side operating with the plant steam system. The pertinent equations are:

$$Q = UA\Delta T_{LM} \tag{1}$$

$$Q = c_p M(T_1 - T_2) \tag{2}$$

$$\Delta T_{LM} = \frac{(T_1 - t_2) - (T_2 - t_1)}{\ln \frac{(T_1 - t_2)}{(T_2 - t_1)}} \tag{3}$$

Q = Heat transferred, Btu/hour
U = Heat transfer coefficient, Btu/hr/ft^2/°F
A = Heat exchanger area, ft^2
ΔT_{LM} = Log mean temperature difference, °F
c_p = Gas heat capacity, Btu/lb/°F
M = Mass flow of gas through heat exchanger, lb/hr
T_1 = Gas inlet temperature, °F
T_2 = Gas outlet temperature, °F
t_1 = t_2 = Steam temperature, °F

Using Equations (1) through (3) and the process data, the product of the heat transfer coefficient and the heat exchanger area (UA) can be calculated. The TC06 HX0202 UA is shown on Figure 4.7-1 as 4-hour averages, along with the design UA of 5,200 Btu/hr/°F and the pressure drop across HX0202. If HX0202 is plugging, the UA should decrease and the pressure drop should increase. The UA deterioration is a better indication of heat exchanger plugging because the pressure drop is calculated by the difference of two numbers of about the same size, usually from 150 to 240 psig, resulting in pressure drops of 1 to 3 psi.

The TC06 UA rose up to about 10,500 Btu/hr/°F after about 50 hours of operation, well above the design UA of 5,200 Btu/hr/°F. The UA of about 10,500 Btu/hr/°F was maintained until just after the 4-week break. After the 4-week break the UA slowly rose from 8,500 to 10,300 Btu/hr/°F. There were several periods when the UA rose to above 12,000 Btu/hr/°F (hours

635 to 671, 759, 839, and 883 to 907). These were periods when the HX0202 outlet temperature thermocouple TI440 was malfunctioning. Periods of low UA were during coal trips.

The HX0202 pressure drop trends paralleled those of UA. The pressure drop rose to between 2.0 and 2.5 during the first 50 hours of TC06, then slowly decreased to between 1.6 and 2.2 psi. After the 4-week break, the pressure drop slowly increased from about 1.4 psi to about 2.0 psi at hour 895. The pressure drop then increased to between 2.7 and 3.5 during the high coal-rate operation. There appeared to be no plugging during TC06. This analysis fails to notice the HX0202 steam leak that was discovered after the completion of TC06.

The GCT4 test run had HX0202 UAs at 7,000 to 8,000 Btu/hr/°F (lower than TC06) which were in the range of 9,000 to 10,500 Btu/hr/°F. The pressure drops for GCT4 HX0402 (1.0 to 2.0 psi) were lower than TC06 pressure drops (1.4 to 3.0 psi).

The secondary gas cooler, HX0402, is single-flow heat exchanger with hot gas from the PCD flowing through the tubes and the shell side operating with plant steam system. Some heat transfer and pressure drop calculations were done around HX0402 to determine if there was any plugging or heat exchanger performance deterioration during TC06. HX0402 is not part of the combustion gas turbine commercial flow sheet. In the commercial gas turbine flow sheet, the hot synthesis gas from the PCD would be directly sent to a combustion gas turbine. HX0402 would be used commercially if the synthesis gas was to be used in a fuel cell or as a chemical plant feedstock.

Using Equations (1) through (3) and the process data, the product of the heat transfer coefficient and the heat exchanger area (UA) can be calculated. The UA for TC06 testing is shown in Figure 4.7-2 as 4-hour averages, along with the design UA of 13,100 Btu/hr/°F and the pressure drop across HX0402. If HX0402 is plugging, the UA should decrease and the pressure drop should increase.

The UA was at 17,000 to 18,000 Btu/hr/°F for the first 255 hours of TC06, well above the design UA of 13,100 Btu/hr/°F. After hour 255, the UA was very constant at 16,000 Btu/hr/°F until hour 719, when the coal-feed rate was reduced. The UA decreased to 14,800 Btu/hr/°F until the coal rate was increased at hour at 895. The UA then increased to 16,600 Btu/hr/°F by the end of TC06.

The HX0402 TC06 pressure drop was between at 3.5 and 4.5 psi for the first 255 hours of TC06 operation. After hour 255, the pressure drop decreased to about 3.0 psi. The pressure drop then slowly increased up to 3.8 psi at hour 623. When the coal rate was decreased the pressure drop decreased to 2.5 psi until the coal rate was increased at hour 895. The pressure dropped then increased to 3.5 at the end of TC06. There was no evidence of HX0402 plugging during the first 5 days of operation.

The GCT4 test run had HX0402 UAs at 14,000 to 17,000, which were in the same range as TC06 at 14,500 to 18,000 Btu/hr/°F. The pressure drops for GCT4 HX0402 (1.5 to 3.5 psi) were slightly less than TC06 (2.0 to 4.5 psi).

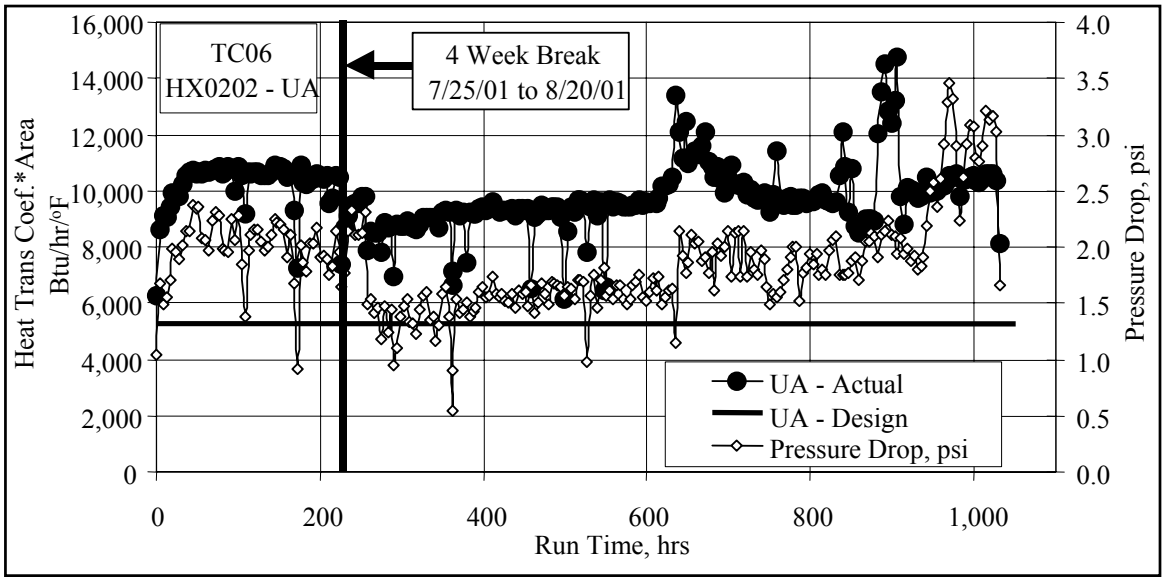

Figure 4.7-1 HX0202 Heat Transfer Coefficient and Pressure Drop

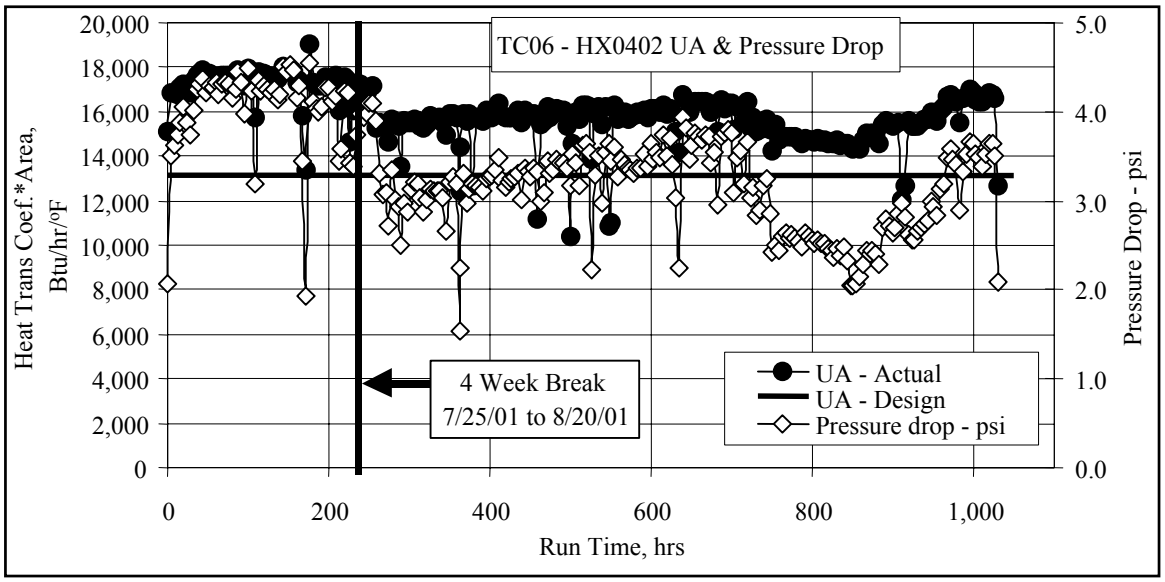

Figure 4.7-2 HX0402 Heat Transfer Coefficient and Pressure Drop

TERMS

Listing of Abbreviations

AAS	Automated Analytical Solutions
ADEM	Alabama Department of Environmental Management
AFBC	Atmospheric Fluidized-Bed Combustor
APC	Alabama Power Company
APFBC	Advance Pressurized Fluidized-Bed Combustion
ASME	American Society of Mechanical Engineers
AW	Application Workstation
BET	Brunauer-Emmett-Teller (nitrogen-adsorption specific surface technique)
BFI	Browning-Ferris Industries
BFW	Boiler Feed Water
BMS	Burner Management System
BOC	BOC Gases
BOP	Balance-of-Plant
BPIR	Ball Pass Inner Race, Frequencies
BPOR	Ball Pass Outer Race, Frequencies
BSF	Ball Spin Frequency
CAD	Computer-Aided Design
CAPTOR	Compressed Ash Permeability Tester
CEM	Continuous Emissions Monitor
CFB	Circulating Fluidized Bed
CFR	Code of Federal Regulations
CHE	Combustor Heat Exchanger
COV	Coefficient of Variation (Standard Deviation/Average)
CPC	Combustion Power Company
CPR	Cardiopulmonary Resuscitation
CTE	Coefficient of Thermal Expansion
DC	Direct Current
DCS	Distributed Control System
DHL	DHL Analytical Laboratory, Inc.
DOE	U.S. Department of Energy
DSRP	Direct Sulfur Recovery Process
E & I	Electrical and Instrumentation
EERC	Energy and Environmental Research Center
EPRI	Electric Power Research Institute
EDS or EDX	Energy-Dispersive X-Ray Spectroscopy
ESCA	Electron Spectroscopy for Chemical Analysis
FCC	Fluidized Catalytic Cracker
FCP	Flow-Compacted Porosity
FFG	Flame Front Generator
FI	Flow Indicator
FIC	Flow Indicator Controller
FOAK	First-of-a-Kind
FTF	Fundamental Train Frequency

FW	Foster Wheeler
GBF	Granular Bed Filter
GC	Gas Chromatograph
GEESI	General Electric Environmental Services, Inc.
HHV	Higher Heating Valve
HP	High Pressure
HRSG	Heat Recovery Steam Generator
HTF	Heat Transfer Fluid
HTHP	High-Temperature, High-Pressure
I/O	Inputs/Outputs
ID	Inside Diameter
IF&P	Industrial Filter & Pump
IGV	Inlet Guide Vanes
IR	Infrared
KBR	Kellogg Brown & Root, Inc.
LAN	Local Area Network
LHV	Lower Heating Valve
LIMS	Laboratory Information Management System
LMZ	Lower Mixing Zone
LOC	Limiting Oxygen Concentration
LOI	Loss on Ignition
LPG	Liquefied Propane Gas
LSLL	Level Switch, Low Level
MAC	Main Air Compressor
MCC	Motor Control Center
MMD	Mass Median Diameter
MS	Microsoft Corporation
NDIR	Nondestructive Infrared
NETL	National Energy Technology Laboratory
NFPA	National Fire Protection Association
NO_X	Nitrogen Oxides
NPDES	National Pollutant Discharge Elimination System
NPS	Nominal Pipe Size
OD	Outside Diameter
ORNL	Oak Ridge National Laboratory
OSHA	Occupational Safety and Health Administration
OSI	OSI Software, Inc.
P&IDs	Piping and Instrumentation Diagrams
PC	Pulverized Coal
PCD	Particulate Control Device
PCME	Pollution Control & Measurement (Europe)
PDI	Pressure Differential Indicator
PDT	Pressure Differential Transmitter
PFBC	Pressurized Fluidized-Bed Combustion
PI	Plant Information
PLC	Programmable Logic Controller
PPE	Personal Protection Equipment

PRB	Powder River Basin
PSD	Particle-Size Distribution
PSDF	Power Systems Development Facility
ΔP or DP or dP	Pressure Drop or Differential Pressure
PT	Pressure Transmitter
RAPTOR	Resuspended Ash Permeability Tester
RFQ	Request for Quotation
RO	Restriction Orifice
RPM	Revolutions Per Minute
RSSE	Reactor Solid Separation Efficiency
RT	Room Temperature
RTI	Research Triangle Institute
SCS	Southern Company Services, Inc.
SEM	Scanning Electron Microscopy
SGC	Synthesis Gas Combustor
SMD	Sauter Mean Diameter
SRI	Southern Research Institute
SUB	Start-up Burner
TCLP	Toxicity Characteristic Leaching Procedure
TR	Transport Reactor
TRDU	Transport Reactor Demonstration Unit
TRS	Total Reduced Sulfur
TSS	Total Suspended Solids
UBP	Uncompacted Bulk Porosity
UMZ	Upper Mixing Zone
UND	University of North Dakota
UPS	Uninterruptible Power Supply
UV	Ultraviolet
VFD	Variable Frequency Drive
VOCs	Volatile Organic Compounds
WGS	Water-Gas Shift
WPC	William's Patent Crusher
XRD	X-Ray Diffraction
XXS	Extra, Extra Strong

Listing of Units

acfm	actual cubic feet per minute
Btu	British thermal units
°C	degrees Celsius or centigrade
°F	degrees Fahrenheit
ft	feet
FPS	feet per second
gpm	gallons per minute
g/cm^3 or g/cc	grams per cubic centimeter
g	grams
GPa	gigapascals
hp	horsepower
hr	hour
in.	inches
inWg (or inWc)	inches, water gauge (inches, water column)
in.-lb	inch pounds
°K	degrees Kelvin
kg	kilograms
kJ	kilojoules
kPa	kilopascals
ksi	thousand pounds per square inch
m	meters
MB	megabytes
min	minute
mm	millimeters
MPa	megapascals
msi	million pounds per square inch
MW	megawatts
m/s	meters per second
MBtu	Million British thermal units
m^2/g	square meters per gram
μ or μm	microns or micrometers
dp_{50}	particle-size distribution at 50 percentile
ppm	parts per million
ppm (v)	parts per million (volume)
ppm (w)	parts per million (weight)
lb	pounds
pph	pounds per hour
psi	pounds per square inch
psia	pounds per square inch absolute
psid	pounds per square inch differential
psig	pounds per square inch gauge
ΔP	pressure drop
rpm	revolutions per minute
s or sec	seconds
scf	standard cubic feet

scfh	standard cubic feet per hour
scfm	standard cubic feet per minute
V	volts
W	watts